ВЕСТНИК ТРАНСПЛАНТОЛОГИИ И ИСКУССТВЕННЫХ ОРГАНОВ

VESTNIK TRANSPLANTOLOGII I ISKUSSTVENNYKH ORGANOV

RUSSIAN JOURNAL OF TRANSPLANTOLOGY AND ARTIFICIAL ORGANS

УЧРЕДИТЕЛИ: ОБЩЕРОССИЙСКАЯ ОБЩЕСТВЕННАЯ ОРГАНИЗАЦИЯ ТРАНСПЛАНТОЛОГОВ «РОССИЙСКОЕ ТРАНСПЛАНТОЛОГИЧЕСКОЕ ОБЩЕСТВО»

ФГБУ «НМИЦ ТИО ИМЕНИ АКАДЕМИКА В.И. ШУМАКОВА» МИНЗДРАВА РОССИИ

ФГАОУ ВО ПЕРВЫЙ МГМУ ИМЕНИ И.М. СЕЧЕНОВА МИНЗДРАВА РОССИИ (СЕЧЕНОВСКИЙ УНИВЕРСИТЕТ)

THE OFFICIAL JOURNAL OF ALL-RUSSIAN PUBLIC ORGANIZATION OF TRANSPLANTOLOGISTS "RUSSIAN TRANSPLANT SOCIETY"

SHUMAKOV NATIONAL MEDICAL RESEARCH CENTER OF TRANSPLANTOLOGY AND ARTIFICIAL ORGANS

I.M. SECHENOV FIRST MOSCOW STATE MEDICAL UNIVERSITY (SECHENOV UNIVERSITY)

2021. Том XXIII. № 4

2021. Vol. XXIII. № 4

Научно-практический журнал основан в 1999 г.
Регистр. № 018616

Scientific and Practical Journal was founded in 1999
Reg. № 018616

Журнал «Вестник трансплантологии и искусственных органов» включен ВАК РФ в перечень российских рецензируемых научных изданий, в которых должны быть опубликованы результаты диссертационных работ

Журнал «Вестник трансплантологии и искусственных органов» включен ФГБУ «НМИЦ ТИО им. ак. В.И. Шумакова» Минздрава России в перечень российских рецензируемых научных изданий, в которых должны быть опубликованы основные результаты исследований в рамках диссертаций, представляемых к защите в диссертационный совет ФГБУ «НМИЦ ТИО им. ак. В.И. Шумакова» Минздрава России

Журнал «Вестник трансплантологии и искусственных органов» индексируется в Scopus и размещен на платформе Web of Science Core Collection: Emerging Science Citation Index

"Russian Journal of Transplantology and Artificial Organs" is included in the list of leading peer-reviewed scientific publication editions, produced in the Russian Federation and is recommended for publication of primary results of dissertation research

"Russian Journal of transplantology and artificial organs" is included by the Federal State Budgetary Institution "Shumakov National Medical Research Center of Transplantology and Artificial Organs" of the Ministry of Health of Russia in the list of Russian peer-reviewed scientific publications in which the main results of research should be published within the framework of dissertations submitted for defense to the dissertation council of Shumakov National Medical Research Center of Transplantology and Artificial Organs

"Russian Journal of Transplantology and Artificial Organs" is indexed in Scopus and in the Emerging Science Citation Index of the Web of Science Core Collection

ISSN 1995-1191

Адрес для корреспонденции:

Россия, 123182, Москва, ул. Щукинская, 1
Тел./факс +7 (499) 193 87 62
E-mail: vestniktranspl@gmail.com
Интернет-сайт журнала: http://journal.transpl.ru
Научная электронная библиотека: http://elibrary.ru

Address for correspondence:

1, Shchukinskaya st., Moscow 123182, Russia
Tel./Fax +7 (499) 193 87 62
E-mail: vestniktranspl@gmail.com
Journal's web site: http://journal.transpl.ru
Scientific eLibrary: http://elibrary.ru

Подписной индекс в каталоге ОАО «АРЗИ» – 80248

СОДЕРЖАНИЕ

CONTENTS

ДВА ГОДА ПАНДЕМИИ: ТРАНСПЛАНТОЛОГИЧЕСКАЯ ПОМОЩЬ В РФ В 2021 ГОДУ

Длительность пандемии новой коронавирусной инфекции COVID-19 составляет уже 2 года, однако оказание трансплантологической помощи в РФ не останавливается, и в 2021 году темп выполнения трансплантаций приблизился к 2019 году – самому успешному в истории отечественной трансплантологии. Невзирая на тот факт, что многие медицинские учреждения в России, как и во всем мире, были перепрофилированы для лечения пациентов с новой коронавирусной инфекцией и проведение пересадок в некоторых из них было временно приостановлено, предпринимались все возможные меры, для того чтобы найти выходы из сложившейся ситуации. Общими усилиями удалось это сделать, и несмотря на сложности, которые создавала пандемия, мы все же добились успехов.

На сегодняшний день трансплантационная программа запущена и успешно развивается в 62 учреждениях по всей стране. Только за период пандемии были выполнены первые трансплантации почки в Туле, Владивостоке и Улан-Удэ, трансплантация сердца в Тюмени. Открыл свои двери для пациентов и Филиал НМИЦ ТИО имени академика В.И. Шумакова в г. Волжский, где пациентам не только оказывается трансплантологическая помощь, но и проводятся диагностика и устранение даже самых сложных сопутствующих диагнозов. Впервые в Военно-медицинской академии им. С.М. Кирова в Санкт-Петербурге выполнили пересадку печени ребенку – до этого такие операции проводились только в столице. В Российской детской клинической больнице была запущена программа родственной трансплантации почки детям, а

TWO YEARS OF COVID-19: TRANSPLANT CARE IN THE RUSSIAN FEDERATION 2021

The novel coronavirus disease (COVID-19) outbreak and pandemic that is ravaging our world, has already lasted two years. However, provision of transplant care in the Russian Federation continues. In 2021, the rate of transplant surgeries approached that of 2019 – the most successful year in the history of Russian transplantology. Even though many medical institutions in Russia, as well as all over the world, have been reassigned to treat COVID-19 patients, and some of these centers have temporarily suspended transplant surgeries, all possible measures have been taken to find a way out of this situation. By our joint efforts, we were able to do this, and despite the challenges posed by the pandemic, we were still able to make progress.

To date, transplantation programs have been launched and are successfully developing in 62 institutions across the country. During the pandemic period alone, kidney transplants were performed for the first time in Tula, Vladivostok and Ulan-Ude, and heart transplantation in Tyumen. The Volzhskiy branch of Shumakov National Medical Research Center of Transplantology and Artificial Organs also opened its doors to patients, where people could receive transplant care, and as well get complex related complications diagnosed and treated. A liver transplant was performed on a child for the first time in Kirov Military Medical Academy in St. Petersburg. Before then, such operations had been performed only in Moscow. The Russian Children's Clinical Hospital launched a related pediatric kidney transplantation program. The first series of liver transplants were performed at the Moscow Clinical Scientific Center.

в Московском клиническом научном центре выполнена первая серия трансплантаций печени.

Все это означает, что ведомственная целевая программа Минздрава России «Донорство и трансплантация органов в Российской Федерации» продолжает успешно реализовываться, и нам удается наращивать объемы оказания помощи, даже с учетом всех сложностей, созданных пандемией.

В 2022 году операции по трансплантации будут выполнять медицинские центры в 40 регионах страны. Сегодня есть все основания рассчитывать на то, что в грядущем году удастся реализовать все задуманное и приумножить перспективы: уже обучены региональные специалисты и обсуждается запуск трансплантационных программ в Хабаровском крае, Республике Крым, Ярославской, Курской, Ивановской областях и в городе Севастополе.

Открытие новых программ, расширение существующих, приумножение числа компетентных кадров позволяет не только увеличивать количество выполняемых операций, но и способствует расширению горизонтов научной отрасли.

С уважением,
академик РАН С.В. Готье

All this makes it crystal clear that departmental special-purpose programme "Organ Donation and Transplantation in the Russian Federation" by the Russian Ministry of Health, continues to be implemented successfully, and we are able to increase the volume of care, even with all the challenges created by the COVID-19 pandemic.

In the coming year 2022, medical centers will be carrying our transplant surgeries in 40 regions across the country. Today there is every reason to expect that in the coming year, we will be able to implement all the plans and considerably increase the prospects. Regional specialists have already been trained and the launch of transplant programs in Khabarovsk Krai, Republic of Crimea, Yaroslavl Oblast, Kursk Oblast, Ivanovo Oblast and Sevastopol is currently being deliberated on.

Launching of new programs, expansion of existing ones, and boosting of the number of highly-skilled personnel would not only increase the number of operations performed, but also expand the horizons and potential of the medical industry.

Sincerely,
Sergey Gautier
Member, Russian Academy of Sciences

DOI: 10.15825/1995-1191-2021-4-8-12

ANALYSIS OF THE ODDS RATIO OF DEVELOPMENTAL DELAY IN CHILDREN WITH BILIARY ATRESIA 12 MONTHS AFTER LIVER TRANSPLANTATION

A.V. Syrkina[1], O.M. Tsirulnikova[1, 2], I.E. Pashkova[1], O.V. Silina[1], E.V. Chekletsova[1], S.Yu. Oleshkevich[1]

[1] Shumakov National Medical Research Center of Transplantology and Artificial Organs, Moscow, Russian Federation

[2] Sechenov University, Moscow, Russian Federation

Background. Liver cirrhosis occurring before 1 year of age can affect a child's development. Liver transplantation is the only radical treatment for decompensated cirrhosis. In biliary atresia, cirrhosis develops during the first months of life. The duration of cirrhosis in biliary atresia may vary from palliative Kasai portoenterostomy (PE) to liver transplantation. Developmental abnormalities in children with biliary atresia have been shown to occur both before and after liver transplantation. Association between duration of liver cirrhosis and psychomotor development of children has been underestimated. **Objective:** to determine the chances of developmental delay in children depending on the cirrhosis persistence duration. **Materials and methods.** The study enrolled 83 children with biliary atresia (47 children underwent palliative Kasai PE, 36 children with liver transplantation did not undergo Kasai PE). All children had their psychomotor development assessed before PE and 12 months after PE using the Griffiths psychomotor developmental scale (translation and adaptation by E.S. Keshishian) for children up to 24 months of age. Statistical analysis was performed by calculating odds ratios with 95% confidence intervals. **Results**. Comparative analysis showed that in the subgroup of children who underwent Kasai PE, cirrhosis persistence before transplantation was 2.6 months longer than in children without Kasai PE ($p = 0.011$). The odds of developmental delay in preparation for liver transplantation were 3.3 times higher in the subgroup of children who underwent Kasai palliative PE compared to children without palliative (95%, CI 1.35–8.31). The odds of developmental delay 12 months after liver transplantation were 4.4 times higher in the subgroup of children who underwent palliative Kasai PE than in children without the palliative care (95% CI 1.54–12.5). **Conclusion**. Children who underwent liver transplantation after palliative surgical treatment had lower levels of psychomotor development than children without palliative Kasai PE both before and 12 months after liver transplantation ($p = 0.0018$, $p = 0.01$ respectively).

Keywords: liver transplantation, biliary atresia, Kasai portoenterostomy, neuropsychiatric development.

INTRODUCTION

Biliary atresia is one of the most common indications for liver transplantation in children under 1 year of age. According to Gautier [1], the annual number of pediatric orthotopic liver transplants (OLTx) in the Russian Federation remains stable at 110–130 operations per year, which corresponds to the identified need of the population for this method of treatment [1]. In 2020, the Shumakov National Medical Research Center of Transplantology and Artificial Organs (Shumakov Center) performed 98 pediatric liver transplantations, of which 85 were related. Among them, 45 liver transplants were performed for cirrhosis as a result of biliary atresia. The Shumakov Center has reported that one- and three-year liver transplant survival rates are 92.1% and 90.9%, respectively [2].

Survival and long-term outcomes continue to improve for most children receiving related liver transplantation. This is due to improvements in surgical technique, perioperative care, and modern immunosuppressive therapy.

Liver cirrhosis, occurring before the age of 1 year, can affect motor and psycho-speech development in children [3]. The persistence time of cirrhosis differs in children with biliary atresia, depending on the palliative stage of Kasai PE. Often complications of cirrhosis (synthetic liver failure, development of portal hypertension, portosystemic shunting) are masked by normal levels of total and direct bilirubin in children who underwent Kasai PE and lead to late diagnosis of decompensated cirrhosis and delayed liver transplantation.

The literature describes developmental disorders in children with cirrhosis as a result of biliary atresia both

Corresponding author: Alla Syrkina. Address: 1, Shchukinskaya str., Moscow, 123182, Russian Federation. Phone: (903) 769-16-08. E-mail: AllaSyrk@gmail.com

in preparation for liver transplantation [4, 5] and after it [6, 7].

The objective of this study was to determine the chances of developmental delay in children depending on the time of cirrhosis persistence.

MATERIALS AND METHODS

To realize this goal, we recruited a group of children with biliary atresia (N = 83) who were admitted at the Shumakov Center, Moscow. Inclusion criteria were: established diagnosis of biliary atresia and liver transplantation before 12 months of life. Exclusion criteria were concomitant neurological diseases, neurotoxic reactions to immunosuppressants after liver transplantation.

The children were divided into subgroups depending on the palliative stage of Kasai PE. 47 children underwent Kasai PE at the age of 1–3 months of life, and 36 children without a palliative stage underwent related liver transplantation immediately. Table presents the characteristics of children in subgroups.

Comparative analysis showed that in the subgroup of children who underwent Kasai PE, liver cirrhosis persisted for 2.6 months longer before transplantation than in children without Kasai PE (p = 0.011).

All the children were assessed before and 12 months after liver transplantation using the Griffiths Psychomotor Development Scale (translation and adaptation by E.S. Keshishian) for children up to 24 months of life.

We carried out a statistical analysis of the odds ratio of developmental delay for children depending on the palliative stage of Kasai PE.

RESULTS

The first measurement was made in preparation for liver transplantation. Thirty-four children showed developmental delay: 14 children without palliative stage and 32 children of the Kasai PE subgroup. The difference in the subgroups was statistically significant (p = 0.0018). Fig. 1 presents the number of children in preparation for liver transplantation with normal and abnormal development depending on the palliative stage of Kasai PE.

We analyzed the presence of developmental delay depending on Kasai PE (Fig. 2).

The odds of developmental delay in preparation for liver transplantation were 3.3 times higher in the subgroup of children who underwent palliative Kasai PE compared to children who did not (95%, CI 1.35–8.31).

The second measurement was performed in children 12 months after liver transplantation. In the group of children without Kasai PE, 6 children (16.7%) had a developmental delay of less than 3 months. In the group of children who underwent palliative Kasai PE, 8 patients

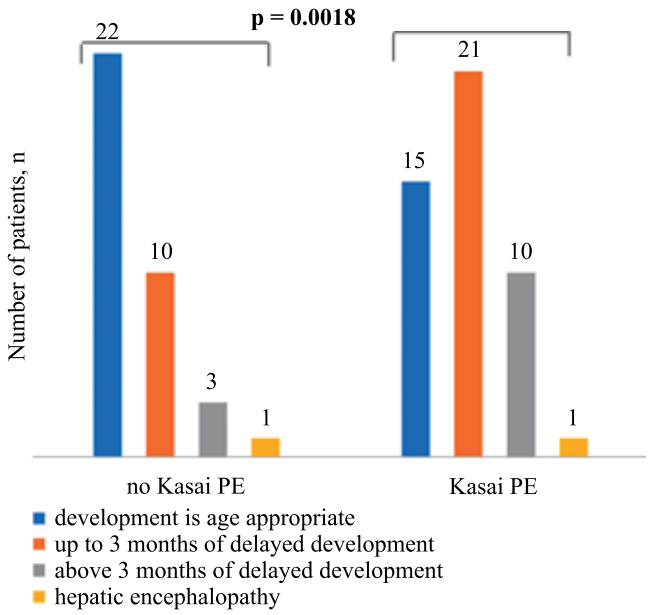

Fig. 1. Developmental levels of children with cirrhosis as a result of biliary atresia at the stage of preparation for transplantation

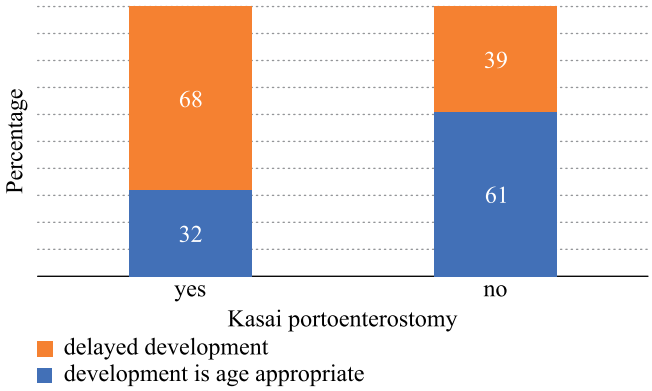

Fig. 2. Analysis of developmental delay depending on palliative Kasai PE

Table

Characteristics of children enrolled in the study

Characteristics	no Kasai PE, n = 36	Kasai PE, n = 47	Significance
Age at liver transplantation, months (min-max)	6.5 (4–15)	9.1 (5–24)	p = 0.011
Number of children with shoulder circumference <3 percentile, n (%)	17 (47)	23 (48)	p = 0.06
PELD mean score (min–max)	23 (13–44)	28.5 (9–34)	p = 0.075
Mean body weight before transplantation, kg (min–max)	6.7 (5.3–9.3)	6.9 (5.0–10.5)	p = 0.34
Hepatic encephalopathy, n (%)	1 (2.8)	1 (2.1)	p = 0.1

showed a developmental delay of more than 3 months, and 14 children had a delay of less than 3 months – a total of 22 children (46.8%). The difference in subgroups with respect to the number of children with developmental delay was statistically significant, p = 0.01 (Fig. 3).

We analyzed the presence of developmental delay in children 12 months after liver transplantation depending on Kasai PE (Fig. 4).

The odds of developmental delay 12 months after liver transplantation were 4.4 times higher in the subgroup of children who underwent Kasai palliative portoenterostomy compared with children without palliative stage (95%, CI 1.54–12.5).

Thus, children with a mean age of 9 months at the time of liver transplantation have a 3.3-fold higher chance of developmental delay before OLTx and 4.4-fold higher chance 12 months after OLTx compared to children who underwent liver transplantation at 6.5 months of age.

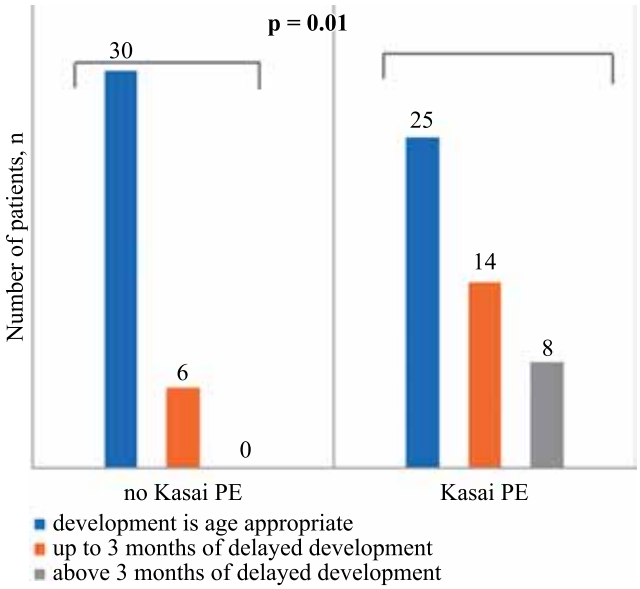

Fig. 3. Developmental levels of children with cirrhosis as a result of biliary atresia 12 months after liver transplantation in subgroups

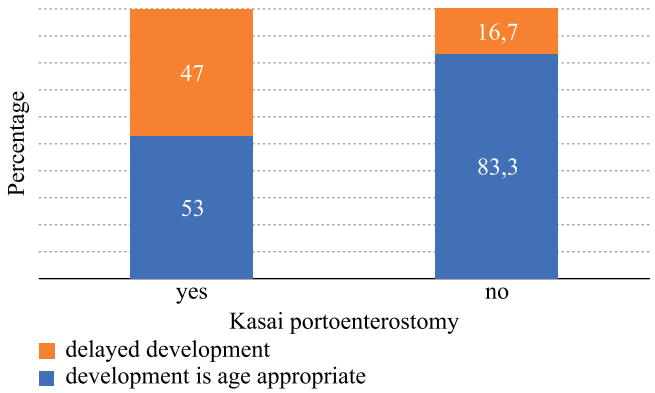

Fig. 4. Analysis of developmental delay depending on palliative Kasai PE

DISCUSSION

The pathogenesis of developmental delay in children with biliary atresia is associated with many processes, such as accumulation of neurotoxic substances affecting the central and peripheral nervous system, catabolic orientation of metabolic processes, insufficient liver synthesis of growth factors, and muscle depletion involved in ammonia detoxification. Increased proinflammatory cytokines IL-6 and IL-18 are shown in patients with cirrhosis [8]. Systemic inflammation means the development of neuroinflammation, which can manifest in different ways. At the level of the central nervous system, it manifests as development of acute conditions: seizures and coma, and chronic neurodegeneration, manifested by developmental and behavioral disorders in children [9–13]. Neuroinflammation at the level of the peripheral nervous system manifests as chronic inflammatory demyelinating polyneuropathy [14, 15] with a clinical picture of muscle weakness, decreased muscle tone and strength, autonomic disorders in patients with biliary cirrhosis [15].

The significance of neuroinflammation is currently being actively studied in the context of various diseases. Whereas, for biliary atresia and decompensated cirrhosis in children, research is required.

Neuroinflammation correlates with cognitive and emotional problems in adults with cirrhosis; in particular, increased levels of tumor necrosis factor alpha are associated with depression and fatigue in chronic liver disease [16]. At the same time, clinical studies devoted to the development of paediatric liver recipients have reported contradictory data. Only some researchers tend to connect developmental disorders of paediatric liver recipients with unsuccessful Kasai PE [17–19].

CONCLUSION

Our study has shown a difference in the developmental level of children with biliary atresia depending on the cirrhosis persistence time. A 2.6-month increase in cirrhosis persistence time increased the odds of developmental delay 3.3-fold before OLTx (95%, CI 1.35–8.31) and 4.4-fold 12 months after OLTx (95%, CI 1.54–12.5). Children who underwent liver transplantation after palliative surgical treatment had lower levels of psychomotor and cognitive development than children without palliative Kasai portoenterostomy both before and 12 months after liver transplantation (p = 0.0018, p = 0.01, respectively).

The authors declare no conflict of interest.

REFERENCES

1. *Gautier SV, Khomyakov SM.* Donorstvo i transplantatsiya organov v Rossiyskoy Federatsii v 2019 godu. XII soobshchenie registra Rossiyskogo transplantologicheskogo

obshchestva. *Vestnik transplantologii i iskusstvennykh organov*. 2020; 22 (2): 8–34.
2. *Monakhov A, Gautier S, Tsiroulnikova O et al*. Living donor left lateral sectionectomy: Should the procedure still be performed open? *Journal of Liver Transplantation.* 2021; 1.
3. *Stewart SM, Uauy R, WallerDA et al*. Mental and motor development correlates in patients with end-stage biliary atresia awaiting liver transplantation. *Pediatrics*. 1987; 79 (6): 882–888.
4. *Sun Y, Jia L, Yu H* et al. The Effect of Pediatric Living Donor Liver Transplantation on Neurocognitive Outcomes in Children. *Ann Transplant.* 2019; 24: 446–453.
5. *Rodijk LH et al*. Early Motor Repertoire in Infants With Biliary Atresia: A Nationwide Prospective Cohort Study. *Journal of Pediatric Gastroenterology and Nutrition*. 2021; 72 (4): 592.
6. *Santos JC* et al. Neuropsychomotor development in children and adolescents with liver diseases: systematic review with meta-analysis. *Arq Gastroenterol*. 2021; 58 (2): 217–226.
7. *Squires JE, Saquetto MB, Gomes M et al.* Neurodevelopmental Outcomes in Preschool and School Aged Children With Biliary Atresia and Their Native Liver. *J Pediatr Gastroenterol Nutr*. 2020; 70 (1): 79–86.
8. *Montoliu C, Piedrafita B, Serra SA et al.* IL-6 and IL-18 in blood may discriminate cirrhotic patients with and without minimal hepatic encephalopathy. *J Clin Gastroenterol.* 2009; 43 (3): 272–279.
9. *Rangroo Thrane V, Thrane AS, Wang F et al*. Ammonia triggers neuronal disinhibition and seizures by impairing astrocyte potassium buffering. *Nat Med*. 2013; 19 (12): 1643–1648.
10. *Tsirul'nikova OM, Syrkina AV, Miloserdov IA i dr.* Ostrye simptomaticheskie sudorozhnye pristupy v rannem posleoperatsionnom periode transplantatsii pecheni, pochki. *Vestnik transplantologii i iskusstvennykh organov*. 2021; 23 (2): 158–166.
11. *Kenston SSF, Song X, Li Z et al.* Mechanistic insight, diagnosis, and treatment of ammonia-induced hepatic encephalopathy. *Journal of Gastroenterology and Hepatology*. 2019; 34 (1): 31–39.
12. *Garcia-Martinez R, Rovira A, Alonso J et al.* Hepatic encephalopathy is associated with posttransplant cognitive function and brain volume. *Liver Transp*l. 2011; 17 (1): 38–46.
13. *Sotil EU, Gottstein J, Ayala E et al.* Impact of preoperative overt hepatic encephalopathy on neurocognitive function after liver transplantation. *Liver Transpl*. 2009; 15 (2): 184–192.
14. *Kharbanda PS, Prabhakar S, Chawla YK et al*. Peripheral neuropathy in liver cirrhosis. *J Gastroenterol Hepatol.* 2003; 18 (8): 922–926.
15. *Murata K, Ishiguchi H, Ando R et al.* Chronic inflammatory demyelinating polyneuropathy associated with primary biliary cirrhosis. *J Clin Neurosci.* 2013; 20 (12): 1799–1801.
16. *Swain MG*. Fatigue in liver disease: pathophysiology and clinical management. *Can J Gastroenterol.* 2006; 20 (3): 181–188.
17. *Caudle SE, Katzenstein JM, Karpen S et al*. Developmental assessment of infants with biliary atresia: differences between boys and girls. *J Pediatr Gastroenterol Nutr*. 2012; 55 (4): 384–389.
18. *Ng VL, Sorensen LG, Alonso EM et al*. Neurodevelopmental Outcome of Young Children with Biliary Atresia and Native Liver: Results from the ChiLDReN Study. *J Pediatr.* 2018; 196: 139–147.e3.
19. *Syrkina AV, Pashkova IE, Monakhov AR i dr.* Osobennosti nervno-psikhicheskogo razvitiya detey s biliarnoy atreziey posle transplantatsii pecheni. *Vestnik transplantologii i iskusstvennykh organov*. 2021; 23 (3): 66–72.

The article was submitted to the journal on 7.09.2021

DOI: 10.15825/1995-1191-2021-4-13-18

EVALUATION OF THE EFFECTIVENESS OF PROPHYLACTIC STRATEGIES FOR CYTOMEGALOVIRUS INFECTION IN PEDIATRIC KIDNEY RECIPIENTS

O.M. Tsirulnikova[1, 2], P.M. Gadzhieva[1], I.A. Miloserdov[1, 2], D.A. Saydulaev[1], I.E. Pashkova[1]

[1] Shumakov National Medical Research Center of Transplantology and Artificial Organs, Moscow, Russian Federation

[2] Sechenov University, Moscow, Russian Federation

Cytomegalovirus (CMV) infection is the most severe viral infection in renal transplant recipients, which can occur in the post-transplant period in both adult and pediatric recipients. Developing and applying an effective prevention and treatment strategy for pediatric renal graft recipients is a priority. **Objective:** to compare the effectiveness of the protocols used for the prevention of CMV infection in pediatric kidney transplant recipients. **Materials and methods.** The study enrolled 118 patients who underwent primary kidney transplantation at Shumakov National Medical Research Center of Transplantology and Artificial Organs. Based on retrospective analysis, all recipients were divided into two groups, depending on the prophylactic strategy after kidney transplantation. The follow-up period for pediatric kidney recipients ranged from 108 to 1803 (623.5 ± 379.5) days. CMV infection activity was monitored by polymerase chain reaction. **Results**. The frequency of CMV infection activation episodes at 3 and 6 months was independent of the prophylaxis strategy used. The recurrence rate of CMV infection one year after surgery was significantly lower ($p = 0.037$) with Strategy 2. No cases of CMV syndrome or CMV disease, graft dysfunction, or chronic rejection associated with CMV infection were reported. Increasing the dose of antiviral drugs in Strategy 1 did not increase the risk of cytotoxicity and nephrotoxicity, which are reversible (creatinine levels were not significantly different in the study groups at 3, 6, 12 months, $p = 0.542$, $p = 0.287$, $p = 0.535$, respectively). The incidence of kidney graft rejection did not increase in patients with lower doses of immunosuppressants in Strategy 2. **Conclusion.** Both prophylactic strategies are effective in pediatric kidney recipients. However, the choice of a strategy depends on the individual characteristics of the patient and requires a personalized approach.

Keywords: cytomegalovirus (CMV) infection, kidney transplantation, universal prophylaxis, pediatrics, nephrology, immunosuppression.

INTRODUCTION

Currently, protocols for prevention and treatment of CMV infection at various transplantation centers vary, but two strategies are acceptable according to international guidelines: universal prophylaxis and preemptive therapy [1]. Universal prophylaxis involves administration of antiviral drugs to all patients or a group of patients at risk. Antiviral drugs are usually started immediately after kidney transplantation for 3 to 6 months [2, 6]. However, under this strategy, there are increasing reports of CMV infection being resistant to therapy in solid organ recipients [3].

Several studies have identified CMV infection as a predictor of graft loss, worsening long-term outcomes, and as a cause of mortality in kidney allograft recipients. Tomas Reischig et al. identified CMV viremia as an independent risk factor for graft loss. The study included 180 transplant recipients: 87 (48%) patients received prophylaxis with valacyclovir and 45 (25%) with valganciclovir; for at least 100 days, 48 (27%) received preventive therapy. At 12 months after CMV transplantation, CMV DNAemia developed in 102 (57%) patients with 36 (20%) having a viral load of ≥2,000 copies/ml. Multivariate Cox analysis identified CMV DNAemia as an independent risk factor for graft loss (hazard ratio 3.42; $p = 0.020$); however, after stratification by viral load, only CMV DNAemia ≥2,000 copies/ml (hazard ratio 7.62; $p < 0.001$) remained significant. Kidney transplant recipients having CMV DNAemia with a higher viral load irrespective of the time to onset are at increased risk for graft loss. Glomerular allograft pathology was associated with chronic humoral rejection (in the absence of donor-specific antibodies in the study recipients) [13].

For preemptive therapy, patients are routinely referred for CMV infection testing, and therapy is initiated as soon as active viral replication becomes apparent. According to the guidelines for preventive therapy, treatment is continued until two consecutive negative antigenemia tests

Corresponding author: Patimat Gadzhieva. Address: 1, Shchukinskaya str., Moscow, 123182, Russian Federation. Phone: (916) 358-16-80. E-mail: gadzhievamd@gmail.com

are obtained. Patients with CMV infection should receive intravenous ganciclovir or oral valganciclovir for at least 14 days until symptoms disappear [2]. Each strategy has its disadvantages and advantages. The disadvantage of preemptive therapy is the condition of high compliance of pediatric recipients and their parents. Universal prophylaxis reduces the number of CMV episodes, the recurrence rate, and the severity of the disease course, but it is associated with nephrotoxicity and cytotoxicity. Clinical reports have demonstrated positive results with universal prophylaxis. However, there are clinical reports of the occurrence of CMV infection in long-term post-transplant recipients who received prophylaxis with valganciclovir [1, 10, 12, 14]. In a study by Andre C. Kalil in evaluating the safety and efficacy of universal valganciclovir prophylaxis among solid organ recipients, one in 25 recipients (n = 1831) had CMV infection with late onset (OR = 8.95, 95% CI 1.07 to 74.83; p = 0.04) [4]. This study also identified the most common side effect of valganciclovir – absolute neutropenia.

A number of other studies have focused on the successful use of proliferative signal inhibitors as part of basic three-component immunosuppressive therapy for the prevention and treatment of cytomegalovirus infection [15]. Patients receiving everolimus (EVR) demonstrated a significant increase in the number of CMV-specific effector CD8+ and CD4+ T cells compared to patients receiving cyclosporine (CsA) and mycophenolate mofetil (MMF) [5]. The efficacy and safety of the combination of tacrolimus (TAC) and EVR was recently confirmed in the TRANSFORM study [5]. The efficacy of this protocol for cytomegalovirus infection is also explained by the possibility of reducing TAC levels when EVR is used, which allows for an increase in the number of effector CMV-specific cells. Taking into account the existing side effects of valganciclovir, risks of adverse immunological events with decreased immunosuppression, risks of preventive therapy in pediatric recipients, due to the impossibility of ensuring a high compliance in this category of patients, the development of an optimal protocol for prevention of CMV infection in pediatric recipients is still open for discussion.

Objective: to conduct a comparative analysis of the effectiveness of the protocols used for prevention of CMV infection in pediatric kidney recipients.

CLINICAL OBSERVATIONS AND STUDY METHODS

The study included 118 patients transplanted from January 2018 to July 2021 at Shumakov National Medical Research Center of Transplantology and Artificial Organs, Moscow. Among them were 63 (53.3%) boys and 55 (46.7%) girls aged 1 to 17 (10.6 ± 5) years, with body weight from 7 to 71 (29.5 ± 14.7) kg, who received a kidney from a deceased (n = 37) and a living related (n = 81) donor. The follow-up period ranged from 108 to 1803 (623.5 ± 379.5) days. The minimum follow-up period was 3 months.

Based on analysis of patient histories and outpatient records, all recipients were divided into two groups, depending on their prophylaxis strategy after kidney transplantation (Strategy 1 and Strategy 2). The Strategy 1 group included 71 pediatric recipients after primary kidney transplantation between 2018 and 2021. The operated children included 30 (42.3%) girls and 41 (57.7%) boys, aged 1 to 17 (10 ± 5) years, with a body weight of 8 to 57 (28 ± 14.7) kg, who received a transplant from a deceased (n = 23) and from a living related (n = 48) donor. The recipients received universal prophylaxis for CMV infection, which was represented by valganciclovir dose according to Asberg method for 6 months; if viral replication was detected, valganciclovir was administered in a therapeutic dose.

The Strategy 2 group included 47 pediatric recipients after primary kidney transplantation between 2018 and 2021. The operated children included 25 (53.2%) girls and 22 (46.8%) boys aged 2 to 17 (11.6 ± 5) years, with a body weight of 7 to 68 (30.9 ± 14.9) kg, who received a transplant from a deceased (n = 14) and from a living related (n = 33) donor. The recipients received universal prophylaxis for CMV infection, which included valganciclovir dose according to Asberg method for 6 months; when viral replication was detected, immunosuppressive therapy was reduced (i.e., reduction in the number of components in the treatment regimen, reduction in immunosuppressant dose, etc).

CMV was monitored by quantitative polymerase chain reaction (PCR) testing of the virus DNA in the blood. In the first month after kidney transplantation, monitoring was performed every week, then every month; 6 months after transplantation, CMV monitoring was performed every 3 months.

The following parameters were evaluated in the study: clinical and demographic characteristics of the recipients, incidence and characteristics of CMV events, incidence of acute allograft rejection, renal function, patient and graft survival, and nephrotoxicity and cytotoxicity of the prophylaxis protocol. Renal function after transplantation was assessed using the Schwartz formula.

Biopsy-confirmed cellular and antibody-mediated rejection were classified according to the Banff-2017 classification.

Statistical analysis was performed using IBM STATISTICS 20 (IBM SPSS Inc., USA) StatTech v. 2.2.0 (developer LLC Stattech, Russia), an application software package for calculations.

RESULTS

Among the observed kidney recipients, Strategy 1 was used in 60% (n = 71) of cases and Strategy 2 was used in 40% (n = 47). A comparative analysis of the

demographic data of the kidney recipients depending on the selected Strategy found that the age of the children in the Strategy 1 group was significantly lower than that in the Strategy 2 group (p = 0.010) (Table 1).

There were no significant differences in sex and body weight in pediatric kidney recipients, which indicates the homogeneity of the studied groups.

Comparative analysis showed no differences between the groups in terms of graft variant, haplotype compatibility, DR locus and number of mismatches (p ≥ 0.05), although the proportion of related grafts compatible by haplotype and DR locus was higher in the Strategy 2 group.

Table 1

Comparative analysis of demographic data of kidney recipients

Indicator	Strategy 1 (n = 71)	Strategy 2 (n = 47)	p
Gender: boys, n (%) girls, n (%)	 41 (57.7%) 30 (42.3%)	 22 (46.8%) 25 (53.2%)	0.256
Age, years	1 to 17 (10 ± 5)	2 to 17 (11.6 ± 5)	**0.010***
Body weight, kg	8 to 57 (28 ± 14.7)	7 to 68 (30.9 ± 14.9)	0.420

* – differences in indicators are statistically significant (p < 0.05).

Table 2

CMV infection activation in pediatric recipients 3 and 6 months after kidney transplantation

Detection time, months	CMV infection, n (%)	Category		p
		Strategy 1	Strategy 2	
3	no replication	34 (54.0%)	29 (46.0%)	0.141
	replication detection	37 (67.3%)	18 (32.7%)	
6	no replication	36 (55.4%)	29 (44.6%)	0.191
	replication detection	26 (68.4%)	12 (31.6%)	

* – differences in indicators are statistically significant (p < 0.05).

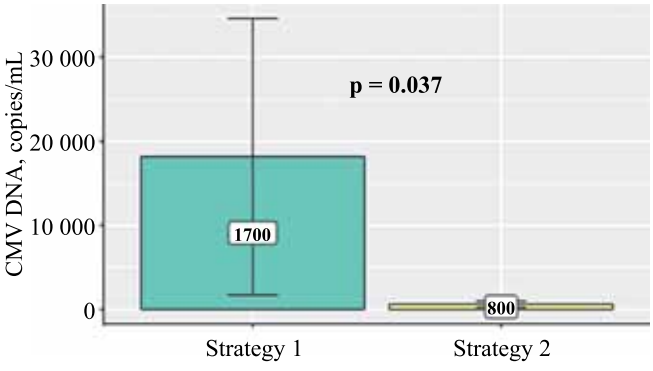

Fig. 1. Comparative analysis of median CMV DNA levels in pediatric kidney recipients with Strategy 1 (n = 71) and Strategy 2 (n = 47) 3 months after transplantation

No clinical manifestations of CMV infection, either as CMV syndrome (0%) or CMV disease (0%), were reported in pediatric kidney recipients when Strategy 1 and Strategy 2 were used for CMV infection prevention.

CMV infection activation in the form of asymptomatic viremia in pediatric recipients 3 months after kidney transplantation in Strategy 1 was detected in 37 (52%) recipients. In Strategy 2, asymptomatic CMV viremia was detected in 18 (38%) recipients 3 months later (Table 2).

Comparative analysis showed no statistical significance in the incidence of CMV infection 3 months after kidney transplantation (p = 0.141). In the Strategy 1 group, the median CMV DNA level was 1700 [600; 11,000] copies/ml, and in the Strategy 2 group, it was 800 [600; 1875] copies/ml. Strategy 1 had a higher median CMV DNA level than Strategy 2 (p = 0.037) (Fig. 1).

Most of the kidney recipients had an episode of active CMV infection in the early postoperative period, i.e., developed within 14 days after kidney transplantation. Comparative analysis showed no statistical significance in CMV infection incidence 3 months after kidney transplantation (p = 0.141).

By the end of the study, 103 recipients had reached a follow-up period of 6 months, which was 87.3% of the total number of patients included in the study. Six months after transplantation in Strategy 1, asymptomatic CMV viremia occurred in 26 (41.9%) of the 62 recipients. In Strategy 2, 12 (29.3%) of 41 recipients also had CMV viremia at 6 months. In the Strategy 1 group, the median CMV DNA level was 0 [0; 615] copies/ml, and in the Strategy 2 group, it was 0 [0; 508] copies/ml (p = 0.178). A comparative analysis of the incidence of CMV infection activation in pediatric recipients six months after kidney transplantation was performed in the study groups. Although the comparative analysis showed no statistically significant differences between the groups (p = 0.191), CMV replication incidence in Strategy 1 group was almost double that in Strategy 2 (Table 2).

By the end of the study, 78 kidney recipients had reached the 12-month follow-up period, which was 66.1% of the total number of patients included in the study. Twelve months after transplantation, 14 (27.5%) of 51 recipients in Strategy 1 developed CMV infection, while 2 (7.4%) of 27 developed same in Strategy 2. The Strategy 1 group had a median CMV level of 0 [0; 600] copies/ml, the Strategy 2 group had 0 [0; 0] copies/ml (p = 0.028). A comparative analysis of the incidence of CMV infection activation in pediatric recipients 12 months after kidney transplantation was performed in the study groups.

The comparative analysis showed that activation of CMV infection in pediatric recipients 12 months after

transplantation occurred more frequently with Strategy 1 (p = 0.037) (Fig. 2).

We analyzed the number of recurrent CMV infection depending on the chosen strategy of CMV infection prevention in children after kidney transplantation for the whole period of observation (Table 3).

No statistically significant difference (p = 0.281) could be found in the number of CMV reactivation episodes between the two strategies. However, as shown in Table 3, the total number of relapses was higher in Strategy 1 recipients.

Evaluation of adverse events

We analyzed the presence of cytopenia (leukopenia, neutropenia, thrombocytopenia) after 3 and 6 months and found no statistically significant differences between the groups (p = 0.396, p = 0.738, respectively). At 12 months after transplantation, cytopenia was not detected in any of the study groups. Serum creatinine levels in kidney recipients did not statistically differ at different times after transplantation (3, 6, 12 months) regardless of the CMV prophylaxis strategy used (p = 0.542, p = 0.287, p = 0.535, respectively).

Assessment of adverse immunological events

There were no cases of graft rejection associated with activation of CMV infection in recipients during prophylaxis.

Fig. 3 shows a comparison of survival without adverse events (mortality, rejection, return to hemodialysis) in kidney recipients depending on the cytomegalovirus infection prophylaxis strategy.

A comparative analysis of one-year survival without adverse events (mortality, rejection, return to hemodialysis) in kidney recipients depending on CMV infection prevention strategy showed no statistical difference (p = 0.537).

DISCUSSION

CMV infection remains one of the most common viral infectious complications in solid organ recipients, affecting the course of the post-transplant period [9, 10, 14]. CMV infection in pediatric kidney recipients has been shown to be associated with indirect effects. CMV infection can cause acute and/or chronic damage, graft rejection, and consequently affect poor graft survival, which are attributed to indirect effects. Any effort to prevent CMV will help improve long-term outcomes. The first milestone in the fight against CMV infection was the advent of antiviral drugs and the use of prophylactic strategies. To this day, they are the CMV prevention cornerstones, but they are not enough to prevent the virus from replicating [11].

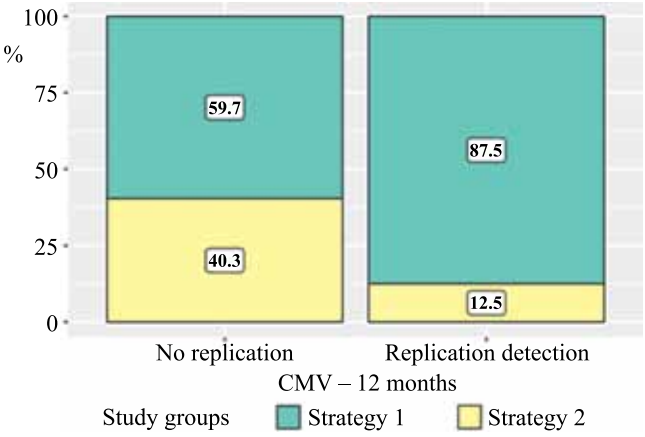

Fig. 2. CMV infection activation in pediatric recipients 12 months after kidney transplantation

Table 3

Analysis of recurrence rates of CMV infection depending on the strategy chosen

Category	Number of recurrent CMV infection, n						p
	0	1	2	3	4	6	
Strategy 1	37	8	6	5	5	1	0.281
Strategy 2	31	6	4	1	0	0	

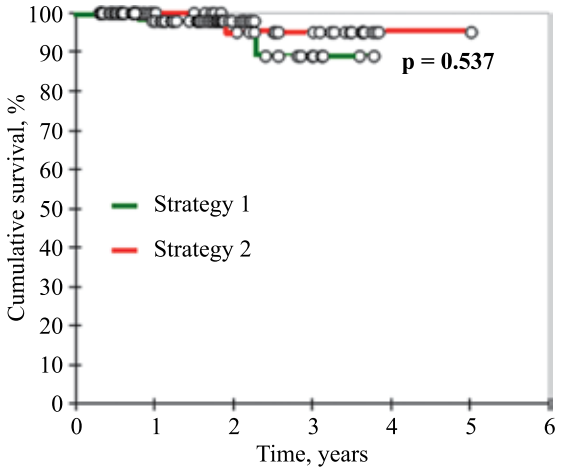

Fig. 3. Comparison of survival without adverse events (mortality, rejection, return to hemodialysis) in kidney recipients depending on the CMV prevention strategy

Over the past two decades, it has become clear that both innate and CMV-specific immunity play a crucial role in controlling CMV, necessitating the optimization of immunosuppressive therapy protocols. The present study conducted a comparative retrospective analysis of the clinical outcomes of kidney transplantation in 118 pediatric kidney recipients in order to develop individualized prophylaxis for cytomegalovirus infection. The results revealed that the viral load differed in the groups only 12 months after transplantation; no differences were detected in other time periods.

Comparative analysis showed that activation of CMV infection one year after transplantation occurred more often with Strategy 1, i.e., when prophylaxis was no longer used. The risk of recurrence was significantly lower with Strategy 2, which is logical against the background of reduced immunosuppression.

However, Strategy 2 must take into account the restrictive criteria for the acceptability of immunosuppressive therapy reduction – reduction of calcineurin inhibitor and the use of mTOR inhibitors – acceptable for recipients with low or moderate immunological risk, thus limiting the widespread use of this approach.

CONCLUSION

The presented experience in CMV prevention in kidney recipients has shown that the algorithms used for diagnosis and prevention of CMV infection and, when appropriate, algorithms for treatment of episodes of active CMV infection, demonstrate good clinical outcomes both in controlling recurrent CMV infection and preventing CMV disease and CMV syndrome, and in reducing the likelihood of developing indirect CMV effects affecting graft function, graft survival, and recipient survival.

The authors declare no conflict of interest.

REFERENCES

1. *Witzke O, Nitschke M, Bartels M et al.* Valganciclovir Prophylaxis Versus Preemptive Therapy in Cytomegalovirus-Positive Renal Allograft Recipients Long-term Results After 7 Years of a Randomized Clinical Trial. *Transplantation*. 2018; 102 (5): 876–882.
2. *Prokopenko EI.* Citomegalovirusnaya infekciya posle transplantacii pochki: real'nye dostizheniya i perspektivy izucheniya patogeneza, profilaktiki i lecheniya. *Vestnik transplantologii i iskusstvennyh organov*. 2019; 21 (3): 151–165.
3. *Fisher CE, Knudsen JL, Lease ED et al.* Risk factors and outcomes of ganciclovir resistant cytomegalovirus infection in solid organ transplant recipients. *Clin Infect Dis*. 2017; 65: 57–63.
4. *Kalil AC, Freifeld AG, Lyden ER, Stoner JA.* Valganciclovir for Cytomegalovirus Prevention in Solid Organ Transplant Patients: An Evidence-Based Reassessment of Safety and Efficacy. *Plos one*. 2009; 4 (5): e5512.
5. *Pascual J, Berger SP, Witzke O et al.* Everolimus with reduced calcineurin inhibitor exposure in renal transplantation. *Journal of the American Society of Nephrology*. 2018; 29 (7): 1979–1991.
6. *Razonable RR, Humar A.* Cytomegalovirus in solid organ transplant recipients-Guidelines of the American Society of Transplantation Infectious Diseases Community of Practice. *Clin Transplan*. 2019; 33 (9): e13512.
7. *Maksimowicz-McKinnon K, Zhou J, Hudy J et al.* Hudy Subclinical CMV viremia is associated with increased nosocomial infections and prolonged hospitalization in patients with systemic autoimmune diseases. *Journal of Clinical virology*. 2021; 140: 104849.
8. *Chemaly RF, Chou S, Einsele H et al.* Definitions of resistant and refractory cytomegalovirus infection and disease in transplant recipients for use in clinical trials. *Clin Infect Dis*. 2019; 68 (8): 1420–1426.
9. *Burgan H, Gosteli G, Giovannini M et al.* Very-late-onset cytomegalovirus disease: a case-report and review of the literature. *BMC Res Notes*. 2017; 10: 210.
10. *Lopez-Oliva MO, Flores J, Madero R et al.* Cytomegalovirus infection after kidney transplantation and long-term graft loss. *Nefrologia*. 2017; 37 (5): 515–525.
11. *Khan SF, Yong MK, Slavin MA et al.* Very late-onset cytomegalovirus disease with ganciclovir resistance >15 years following renal transplantation. *Transpl Infect Dis*. 2021; 23: e13441.
12. *Reischig T, Kacer M, Hruba P et al.* The impact of viral load and time to onset of cytomegalovirus replication on long-term graft survival after kidney transplantation. *Antivir Ther.* 2017; 22 (6): 503–513.
13. *Lollinga WT, Rurenga-Gard L, van Doesum W et al.* High human cytomegalovirus DNAemia early post-transplantation associates with irreversible and progressive loss of renal function – a retrospective study. *Transpl Int*. 2017; 30: 817–826.
14. *Mallat SG, Tanios BY, Itani HS et al.* CMV and BKPyV infections in Renal Transplant recipients Receiving an mTOR Inhibitor-Based regimen: A Systematic Review and Meta-Analysis or Randomized, Controlled Trials. *Clin J Am Soc Nephrol.* 2017; 12 (8): 1321–1326.

The article was submitted to the journal on 7.07.2021

DOI: 10.15825/1995-1191-2021-4-19-25

LUNG CANCER IN SOLID ORGAN TRANSPLANT RECIPIENTS

A.V. Nikulin, I.V. Pashkov, Ya.S. Yakunin

Shumakov National Medical Research Center of Transplantology and Artificial Organs, Moscow, Russian Federation

Lung cancer remains the leading cause of cancer mortality worldwide. Solid organ transplant recipients are at risk of developing malignant tumors, including lung cancer, due to long-term use of immunosuppressive drugs. Development of cancer, including lung cancer, in this patient cohort, has a number of peculiarities. Moreover, malignant tumors in these patients are difficult to treat and have a poorer prognosis. This review presents a study of the issues concerning the mechanisms of lung cancer development, screening methods and treatment in solid organ transplant recipients.

Keywords: solid organ transplant recipients, immunosuppressive therapy, malignant tumors, lung cancer.

INTRODUCTION

Despite recent advances in immunology, genetics, pharmacology and other sciences, lung cancer remains the leading cause of death among all malignancies. As the number of smokers increases in the world, so does the incidence of lung cancer [1].

The International Agency for Research on Cancer estimates that 2,206,771 new cases of lung cancer were identified in 2020, representing 11.4% of all cancers. The mortality rate was 1,796,144, representing 18% of all cancer deaths in 2020. In men, lung cancer ranks first in mortality rate (21.5% of total mortality), and in women it ranks second place after breast cancer (13.7%) [51]. Solid organ transplantation is the only and so far irreplaceable method of treatment of end-stage diseases when other means of treatment are powerless. The number of solid organ transplants is increasing year by year in the world. The year 2020 is an exception due to the Covid-19 pandemic. According to the International Society for Organ Donation and Transplantation, 113,363 solid organ transplants have been performed worldwide. Solid organs recipients are at risk of developing malignancies, including lung cancer, due to long-term use of immunosuppressive drugs. In addition, malignant tumors in solid organ recipients are difficult to treat and have a worse prognosis [2–8, 52].

INCIDENCE

The overall incidence of malignant tumors in solid organ recipients depends on the country of residence, diet, habits, environmental conditions, and other factors. World statistics give different data on the incidence of malignant tumors in solid organ recipients, depending on the group of patients, age and transplanted organ. The average incidence is 2–6% [9, 10]. The most common tumors are lymphoproliferative diseases and skin cancer. The risk of lung cancer in solid organ recipients ranges from 0.3% to 0.85%, which is similar to the incidence in the general population [9, 10]. There is an increased incidence of lung cancer in lung and heart recipients compared to liver and kidney recipients (the ratio was 5.5, 2.9, 2, and 1, respectively). Heart-lung transplant recipients had a 9.3-fold higher risk of developing lung cancer compared to the general population. The authors concluded that this is associated not only with immunosuppressive therapy, but also with age and long-term smoking history [9, 11]. According to A.-M. Noone et al., among 221,962 solid organ transplant recipients, 15,012 developed cancer (6.76%). Lung cancer was the largest contributor to mortality (3.1%), followed by non-Hodgkin lymphoma (1.9%), colorectal cancer (0.7%), and kidney cancer (0.5%). Non-Hodgkin lymphoma was the largest contributor among children (4.1%) and lung cancer was the largest contributor among solid organ recipients aged ≥50 years (3.7–4.3%). The authors concluded that cancer-attributable mortality increases with age and time since transplantation, and therefore cancer deaths will become an increasing burden as recipients live longer [12]. In a study by E. Yanik et al., among 187,384 solid organ recipients, of which kidney recipients constituted 58%, liver recipients 22%, heart recipients 10%, and lung recipients 4%, 9,323 cancers (4.97%) were detected. The most common was lung cancer (n = 1,993 (1.06%)) [13]. D. Pérez-Callejo et al. analyzed 633 lung transplant patients and found that the most common causes for transplantation were idiopathic pulmonary fibrosis (47.8%) and emphysema (43.4%). During follow-up, lung cancer was detected in 23 of them (3.63%). In 5 patients, lung cancer was an incidental finding in the recipient's explanted lung. In 18 patients, cancer developed de novo in single-lung transplant re-

Corresponding author: Andrey Nikulin. Address: 1, Shchukinskaya str., Moscow, 123182, Russian Federation. Phone: (495) 190-35-62. E-mail: nikulin5642@gmail.com

cipients (12 cases in the native lung and 6 cases in the donor lung) [14].

PATHOGENESIS AND RISK FACTORS

There are several mechanisms by which solid organ recipients get lung cancer: de novo in the native lung (in the case of a single-lung transplant), in the donor lung, or as a progression of a pre-existing tumor in the explanted lung. Reports about detection of lung cancer in the recipient's explanted lung are not so rare, which suggests that solid organ recipients should be examined more thoroughly before surgery. For example, in Y. Jun Choi et al., out of 247 lung recipients, 6 (2.4%) were diagnosed with lung cancer as an incidental finding in the explanted lung [15]. The probability of donor-transmitted tumor with donor lung is extremely low, but such transmission mechanism exists and it is imperative to perform computed tomography in a potential donor. This is more relevant to lung transplantation. However, reports have cases of lung cancer transmission, for example, with transplanted liver (in this observation, lung cancer metastasis from an undetected nidus was detected in the liver) [16].

Among lung cancer risk factors, besides smoking, which most authors consider to be the main one, Epstein–Barr virus and progression of post-transplantation lymphoproliferative diseases are also distinguished [14]. In addition, development of lung cancer can be influenced by adverse environmental conditions, such as exposure to silica and asbestos. Some terminal stages of diseases for which lung transplantation is performed, such as chronic obstructive pulmonary disease and pulmonary fibrosis, also suggest increased risk of lung cancer in single-lung versus double-lung transplantation. Most authors say that the risk of lung cancer almost doubles after 60 years of age [8, 14, 17–21].

IMMUNOSUPPRESSIVE THERAPY AS A SPECIFIC FACTOR

Loss of immunological surveillance due to decreased antitumor immunity, especially in patients with pulmonary fibrosis whose risk of lung cancer incidence is approximately 7 times higher than in the population, activation of pro-oncogenic viruses, direct carcinogenic effect of immunosuppressive drugs are all specific risk factors for lung cancer in solid organ recipients in comparison with the population [4–6, 12, 22–27].

SCREENING

The possibility of early detection and timely treatment of malignant tumors in solid organ recipients directly depends on periodic screening examinations [25, 28]. Although early diagnosis of lung cancer can improve treatment outcomes in this category of patients, the position of some authors who express doubts about the expediency of screening in solid organ recipients with life-threatening comorbidities or with life expectancy of less than 5–10 years is puzzling [29]. Current English-language guidelines for screening of cancer of various localizations, including lung cancer, for solid organ recipients are based on extrapolation of the results of screening studies in the general population, as well as on understanding of the high risk of lung cancer in this category of patients [29]. In lung recipients with a long history of smoking, despite quitting smoking, close monitoring is a prerequisite for early diagnosis of lung cancer [9].

A screening program to detect lung cancer in the U.S. population revealed that the use of low-dose multislice computed tomography in comparison with radiography reduces lung cancer mortality by 20% [20, 21]. The use of the Lung Imaging Reporting and Data System (Lung-RADS) to interpret the changes detected during screening allows standardization of CT scan description, as well as development of clear guidelines for determining treatment tactics (Table) [30, 31]. Thus, the use of such a data evaluation system for lung cancer diagnosis in solid organ recipients seems promising.

PREVENTION AND TREATMENT

The fundamental method of lung cancer prevention is "cancer vigilance" at all stages of medical care and dynamic monitoring. Besides total smoking cessation, methods of prevention also include "reasonable" minimization of immunosuppression [13, 25].

Lung cancer treatment in solid organ recipients does not differ from that in the population. Treatment strategy depends on the stage, histological structure of the tumor, and presence of concomitant diseases in the recipient [25, 32]. The peculiarities of this category of patients are the fact that chemotherapy within the framework of complex treatment often cannot be carried out in full due to concomitant diseases and the danger of graft rejection caused by reduced dosage of immunosuppressive drugs [3]. In the English-language literature, there are currently no guidelines on changing the immunosuppressive therapy regimen in solid organ recipients after diagnosed lung cancer, although chemotherapy usually decreases the intensity of immunosuppressive therapy [33, 34]. Immunotherapy is now coming to the fore in a number of cases of different tumor types (high PD-L1 expression and tumor mutational burden). However, interference with the immune system can have disastrous consequences in patients on immunosuppressive therapy, as the issue of simultaneous administration of immuno-oncological and immunosuppressive drugs remains unexplored [35]. Surgery is the gold standard in stage I and II non-small cell lung cancer (NSCLC). At the same time, stereotactic ablative radiotherapy (SABR) is the method of choice in patients with stage I NSCLC who are inoperable due to their somatic status [36–38]. However, the safety of SABR has not been evaluated in solid organ recipients,

which is a major drawback for this method. According to G. Drevet et al., surgical method of treatment is more preferable in treatment of lung cancer of stages II and IIIA in cases of resectable tumor and operability of pa-

Table

Lung-RADS, a system for assessing changes in the lungs detected by MSCT. Treatment tactics and risks of malignancy [31]

Category descriptor	Score	Findings	Tactics	Risk of malignancy	Population prevalence
Incomplete research	0	No data for comparison	Additional MSCT	–	1%
No nodules and definitely benign nodules	1	No lung nodules OR nodule(s) with specific calcifications: complete, central, popcorn, concentric rings and fat containing nodules	MSCT in 12 months	<1%	90%
Benign appearance with a very low likelihood of becoming a clinically active cancer due to size or lack of growth	2	**Perifissural nodule(s)** <10 mm **Solid nodule(s)**: <6 mm new <4 mm **Part solid nodule(s)**: <6 mm **Non-solid nodule(s) (ground-glass nodules, GGN)**: <30 mm OR ≥30 mm and unchanged or slowly growing **Category 3 or 4 nodules unchanged for ≥3 months**			
Probably benign	3	**Solid nodule(s)**: ≥6 to <8 mm OR new 4 mm to <6 mm **Part solid nodule(s)**: ≥6 mm with solid component <6 mm OR new <6 mm **GGN**: ≥30 mm	MSCT in 6 months	1–2%	5%
Suspicious	4A	**Solid nodule(s)**: ≥8 to <15 mm at baseline OR growing <8 mm OR new 6 to <8 mm **Part solid nodule(s)**: ≥6 mm with solid component ≥6 mm to <8 mm OR with a new or growing <4 mm solid component **Endobronchial nodule**	MSCT in 3 months; PET/CT may be used when there is a ≥8 mm solid component	5–15%	2%
Very suspicious	4B	**Solid nodule(s)**: ≥15 mm OR new or growing, and ≥8 mm **Part solid nodule(s)** with: a solid component ≥8 mm OR a new or growing ≥4 mm solid component	MSCT/PET and/or tissue sampling For new large nodules, CT in 1 month to address potentially infectious or inflammatory conditions	>15%	2%
	4X	Category 3 or 4 nodules with additional features or imaging findings that increase the suspicion of malignancy (spiculation, GGN that doubles in size in 1 year, enlarged lymph nodes, etc.)			
Other clinically significant findings (non-lung cancer)	S	May add on to any category	–	–	10%

tients. Traditional radiotherapy and chemotherapy are recommended for treatment of inoperable lung cancer of stage II and locally disseminated lung cancer of stage III. In solid organ recipients, special caution should be exercised when prescribing radiation or chemotherapy due to immunosuppressive therapy, concomitant diseases, frequent presence of renal insufficiency [39].

Video-assisted thoracoscopic surgery (VATS) for anatomical lung resections are increasingly used worldwide to treat various diseases, including primary lung cancer [40]. As surgeons accumulate practical experience and surgical techniques improve, the range of VATS is expanding in various areas of thoracic surgery [40]. The vast majority of thoracic surgeries previously performed traditionally from thoracotomy can be performed using endoscopic equipment from small incisions [41]. In specialized thoracic departments, the number of VATS lobectomies often exceeds the number of open lobectomies performed [41]. The gradual abandonment of thoracotomy in favor of VATS has led to better patients' quality of life while maintaining the same surgical safety [42]. At the time this technology appeared, there were still doubts concerning the radicality of operations performed and long-term survival rate of patients with lung cancer. But now, it is generally accepted that thoracoscopic access for lobectomy for NSCLC does not lead to worse long-term outcomes in patients' survival in comparison with traditional thoracotomy [40]. At the same time, VATS has a number of advantages, namely, a smaller number of complications in early and late postoperative period, and shorter hospital stay [40, 43]. T. Demmy, et al. emphasize that in elderly and debilitated patients, immediate and long-term outcomes of VATS are better than in thoracotomy [41]. According to P. Falcoz et al., early postoperative mortality in VATS lobectomy group in NSCLC patients was twice lower in comparison with open lobectomies [40]. The advantages of VATS are particularly pronounced in elderly patients (over 70 years old), and underweight and predicted low functional scores in the postoperative period (SPH1 <40%) [40]. Reports on the use of VATS in solid organ recipients are rare. M. Al-Ameri et al. comparing immediate and long-term results of uniportal and multiportal VATS accesses in patients with various pathologies of the lungs and mediastinum, came to the conclusion that there are no significant differences in the number of postoperative complications (6% in both groups), and that the 30-day mortality and overall survival at 1 year was 0% and 97% in the uniportal group, and 0.5% and 98% in the multiportal group (P = 0.71). In addition, the author reported faster rehabilitation and shorter hospital stay for uniportal access (76.2% versus 62.1%, P = 0.008) [44]. However, uniportal access is still not widespread according to a survey among members of the European Society of Thoracic Surgeons (ESTS) [45]. J J. Seitlinger et al. note that conversion rate, i.e. conversion from miniaccess to conventional thoracomy, decreases with the improvement of surgical technique and is less than 10% [46]. At the same time, patients undergoing conversion have a higher risk of complications in early and late postoperative period (40.9% versus 16.8%) and mortality (6.8% versus 0.2%) [46]. Meanwhile, open surgery cannot be completely abandoned, because, with all its advantages, VATS is powerless in situations where it is impossible to create adequate working space for safe manipulations inside the thoracic cavity during surgery. (e.g., intolerance to single-lung ventilation) [41]. H. Maeda et al. conducted an interesting study, analyzing 12 cases of VATS in kidney recipients [47]. The authors compared both laboratory parameters, in particular serum creatinine levels, and assessed the glomerular filtration rate before and after surgery and postoperative complications. Operative methods used included VATS wedge resection (n = 4), VATS segmentectomy (n = 4), VATS lobectomy (n = 2), VATS mediastinal tumor resection (n = 1), and VATS chest wall tumor resection (n = 1). All patients received two to three immunosuppressive drugs, and no patients required perioperative hemodialysis. There were no bronchopulmonary complications in the early postoperative period. There were no statistically significant differences between preoperative and postoperative serum creatinine levels and estimated glomerular filtration rate. The authors conclude that such operations are safe in recipients on immunosuppressive therapy [47].

PROGNOSIS

The course of malignant tumors, including lung cancer, is more aggressive in solid organ recipients. Prognosis and life expectancy are determined by the stage of the disease, the presence of N2 status, driver mutations, the degree of pathomorphosis, treatment regimen, etc. [20, 25, 48]. According to G Drevet et al., the 5-year survival rate of resectable lung cancer after surgical treatment was 40.6%, which is comparable with the survival rate in the population (40.7 to 50%) [9]. L. Nora Chen et al. report that the median survival of lung recipients after lung cancer diagnosis was 32 months (IQR, 10–52 months), which is significantly lower compared to the general population [48]. S. Zhang et al. reported a 17.9% overall 5-year survival rate in kidney recipients after lung cancer diagnosis [49]. K. Sigel et al., having investigated 597 cases of lung cancer detection in solid organ recipients, concluded that the survival rate of solid organ recipients, not including lung recipients, is worse in comparison with patients with lung cancer in the population [50]. It is necessary to treat the literature data with caution, since all the above prognostic factors should be considered, first of all, the lesion of regional lymph nodes. Survival rate is also directly affected by the adequacy of lymphodissection performed during surgery. It should also be noted that in some cases, it is difficult to compare the results of different authors, because in

different years, different TNM classification was used to assess tumor spread.

CONCLUSION

Despite conflicting data from various authors, reports suggest an increased risk of lung cancer in solid organ recipients, especially lung and heart-lung recipients. Given the increasing role of malignant tumors, including lung cancer, in the overall mortality of solid organ recipients, as well as increased life expectancy of solid organ recipients, the development of screening and prevention of lung cancer in solid organ recipients is a timely and urgent task. In our opinion, we must be critical of the recommendations of some authors that screening in solid organ recipients with life-threatening comorbidities and a life expectancy of less than 10 years is inappropriate. Creation of an evidence-based screening program aimed at early detection of lung cancer in solid organ recipients (e.g., the Lung-RADS data evaluation system, which has proven to be excellent in the United States), would allow early treatment to be initiated. The choice of optimal treatment tactics for lung cancer in solid organ recipients requires further study. As data accumulates, it will be possible to make a conclusion about the safety of chemotherapy and immunotherapy in this category of patients. Surgical treatment of lung cancer in solid organ recipients does not fundamentally differ from that in the population, and VATS is not inferior to open surgeries, having at the same time a number of advantages. Introduction of minimally invasive methods of surgical treatment of lung cancer in this category of patients will shorten the patient's stay in the hospital, and significantly speed up rehabilitation since there is less pain and less surgical trauma.

The authors declare no conflict of interest.

REFERENCES

1. *Bade BC, Dela Cruz CS.* Lung Cancer 2020: Epidemiology, Etiology and Prevention. *Clin Chest Med Elsevier Inc*. 2020; 41 (1): 1–24. doi: 10.1016/j.ccm.2019.10.001.
2. *Wareham NE et al.* Risk of *de novo* or secondary cancer after solid organ or allogeneic haematopoietic stem cell transplantation. *J Cancer Res Clin Oncol Springer Berlin Heidelberg*. 2019; 145 (12): 3125–3135. doi: 10.1007/s00432-019-03039-2.
3. *Shtraichman O, Ahya VN.* Malignancy after lung transplantation. *Ann Transl Med.* 2020; 8 (6): 416–416. doi: 10.21037/atm.2020.02.126.
4. *Rousseau-Gazaniol C et al.* Lung cancer in renal transplant recipients: A case-control study. *Lung Cancer Elsevier Ireland Ltd*. 2017; 111: 96–100. doi: 10.1016/j.lungcan.2017.07.011.
5. *Acuna SA.* Etiology of increased cancer incidence after solid organ transplantation. *Transplant Rev Elsevier Inc.* 2018; 32 (4): 218–224. doi: 10.1016/j.trre.2018.07.001.
6. *Katabathina VS et al.* Malignancy after solid organ transplantation: Comprehensive imaging review. *Radiographics*. 2016; 36 (5): 1390–1407. doi: 10.1148/rg.2016150175.
7. *Yanik EL et al.* Cancer risk after pediatric solid organ transplantation. *Pediatrics*. 2017; 139 (5). doi: 10.1542/peds.2016-3893.
8. *Potaris K et al.* Lung cancer after heart transplantation: A 17-year experience. *Ann Thorac Surg.* 2005; 79 (3): 980–983. doi: 10.1016/j.athoracsur.2004.05.021.
9. *Drevet G et al.* Lung cancer surgical treatment after solid organ transplantation: A single center 30-year experience. *Lung Cancer Elsevier*. 2020; 139: 55–59. doi: 10.1016/j.lungcan.2019.10.023.
10. *Robbins HY, Arcasoy SM.* Malignancies Following Lung Transplantation. *Clin Chest Med.* 2011; 32 (2): 343–355. doi: 10.1016/j.ccm.2011.02.011.
11. *Olland ABM et al.* Primary lung cancer in lung transplant recipients. *Ann Thorac Surg Elsevier Inc.* 2014; 98 (1): 362–371. doi: 10.1016/j.athoracsur.2014.04.014.
12. *Noone AM et al.* Cancer-attributable mortality among solid organ transplant recipients in the United States: 1987 through 2014. *Cancer.* 2019; 125 (15): 2647–2655. doi: 10.1002/cncr.32136.
13. *Yanik EL et al.* Comparison of cancer diagnoses between the US solid organ transplant registry and linked central cancer registries. *Am J Transplant.* 2016; 16 (10): 2986–2993. doi: 10.1111/ajt.13818.
14. *Pérez-Callejo D et al.* Lung cancer in lung transplantation: Incidence and outcome. *Postgrad Med J.* 2018; 94 (1107): 15–19. doi: 10.1136/postgradmedj-2017-134868.
15. *Choi YJ et al.* Incidental lung cancer of explanted lungs from lung transplant recipients: Incidence, characteristics, and 5-year survival. *Yonsei Med J.* 2020; 61 (11): 958–964. doi: 10.3349/ymj.2020.61.11.958.
16. *Sonbol MB et al.* A Case of Donor-Transmitted Non-Small Cell Lung Cancer After Liver Transplantation: An Unwelcome Guest. *Oncologist*. 2019; 24 (6): 2018–2020. doi: 10.1634/theoncologist.2018-0517.
17. *Chatron E et al.* Lung cancer after lung transplantation: An analysis of 25 years of experience in a single institution. *Clin Transplant.* 2019; 33 (1): 0–2. doi: 10.1111/ctr.13446.
18. *Ekström M, Riise GC, Tanash HA.* Risk of cancer after lung transplantation for COPD. *Int J COPD.* 2017; 12: 2841–2847. doi: 10.2147/COPD.S147065.
19. *Verleden GM, Fisher AJ.* Lung transplantation and lung cancer: Is there a link? *Respiration.* 2011; 81 (6): 441–445. doi: 10.1159/000326934.
20. *Triplette M et al.* HHS Public Access. 2020; 19 (5): 1478–1490. doi: 10.1111/ajt.15181.
21. *Gershman E et al.* Characteristics of lung cancer in idiopathic pulmonary fibrosis with single lung transplant versus non-transplanted patients: A retrospective observational study. *BMJ Open Respir Res.* 2020; 7 (1): 1–6. doi: 10.1136/bmjresp-2020-000566.
22. *Vajdic CM, Van Leeuwen MT.* Cancer incidence and risk factors after solid organ transplantation. *Int J Cancer.* 2009; 125 (8): 1747–1754. doi: 10.1002/ijc.24439.

23. *Asch WS, Perazella MA.* Cancer and Mortality in Solid-Organ Transplantation: Preventable or Inevitable? *Am J Kidney Dis.* 2016; 68 (6): 839–842. doi: 10.1053/j.ajkd.2016.06.009.
24. *Huo Z et al.* Cancer Risks in Solid Organ Transplant Recipients: Results from a Comprehensive Analysis of 72 Cohort Studies. *Oncoimmunology. Taylor & Francis*. 2020; 9 (1). doi: 10.1080/2162402X.2020.1848068.
25. *Brennan DC et al.* Development of malignancy following solid organ transplantation. *UpToDate.* 2016; 10: 1–20.
26. *Endén K et al.* Cancer morbidity and mortality after pediatric solid organ transplantation – a nationwide register study. *Pediatric Nephrology*. 2020; 35 (9): 1719–1728. doi: 10.1007/s00467-020-04546-y.
27. *Fogel AL, Miyar M, Teng JMC.* Cutaneous Malignancies in Pediatric Solid Organ Transplant Recipients. *Pediatr Dermatol.* 2016; 33 (6): 585–593. doi: 10.1111/pde.12941.
28. *Belli EV et al.* Lung cancer following lung transplant: Single institution 10 year experience. Lung Cancer. *Elsevier Ireland Ltd*. 2013; 81 (3): 451–454. doi: 10.1016/j.lungcan.2013.05.018.
29. *Acuna SA et al.* Cancer Screening Recommendations for Solid Organ Transplant Recipients: A Systematic Review of Clinical Practice Guidelines. *Am J Transplant.* 2017; 17 (1): 103–114. doi: 10.1111/ajt.13978.
30. *Godoy MCB et al.* Understanding Lung-RADS 1.0: A Case-Based Review. *Semin Ultrasound, CT MRI Elsevier*. 2018; 39 (3): 260–272. doi: 10.1053/j.sult.2018.03.001.
31. *American College of Radiology.* Lung-RADS® Version 1.1 Assessment Categories. 2019; 3.
32. *Robinson C, Chanchlani R, Kitchlu A.* Malignancies after pediatric solid organ transplantation. *Pediatric Nephrology*. 2020. doi: 10.1007/s00467-020-04790-2.
33. *Wang X, Dong M.* Malignancy After Lung Transplantation: How to Manage Immunosuppression? *Transplant Proc Elsevier Inc.* 2020; 52 (1): 315–320. doi: 10.1016/j.transproceed.2019.09.012.
34. *Engels EA.* Cancer in Solid Organ Transplant Recipients: There Is Still Much to Learn and Do. *Am J Transplant.* 2017; 17 (8): 1967–1969. doi: 10.1111/ajt.14140.
35. *Wong K et al.* Safety and Efficacy of Immune Checkpoint Inhibitors in Patients With Metastatic Cancer Post Solid Organ Transplantation: A Case Report and Review of the Literature. *Transplant Proc Elsevier Inc*. 2019; 51 (9): 3053–3058. doi: 10.1016/j.transproceed.2019.08.002.
36. *Acuna SA et al.* Cancer recurrence after solid organ transplantation: A systematic review and meta-analysis. *Transplant Rev Elsevier Inc*. 2017; 31 (4): 240–248. doi: 10.1016/j.trre.2017.08.
37. *Buxeda A et al.* Gender differences in cancer risk after kidney transplantation. *Oncotarget*. 2019; 10 (33): 3114–3128. doi: 10.18632/oncotarget.26859.
38. *Chen H et al.* Stereotactic ablative radiotherapy for early-stage lung cancer following double lung transplantation. *Radiat Oncol Radiation Oncology*. 2018; 13 (1): 10–14. doi: 10.1186/s13014-018-1089-8.
39. *Drevet G et al.* Lung cancer surgical treatment after solid organ transplantation: a single center 30-year experience. *Lung Cancer*. 2020; 145: 222–224. doi: 10.1016/j.lungcan.2019.10.023.
40. *Falcoz PE et al.* Video-assisted thoracoscopic surgery versus open lobectomy for primary non-small-cell lung cancer: A propensity-matched analysis of outcome from the European Society of Thoracic Surgeon database. *Eur J Cardio-thoracic Surg.* 2016; 49 (2): 602–609. doi: 10.1093/ejcts/ezv154.
41. *Demmy T, Dexter E.* Overview of minimally invasive thoracic surgery. *UpToDate.* 2019; 1–84.
42. *Cheng X et al.* Minimally Invasive Thoracic Surgery 3.0. *Ann Surg.* 2018; 267 (1): 37–38. doi: 10.1097/SLA.0000000000002.
43. *Xia ZN et al.* Laparoscopic-Assisted Resection for Advanced Colorectal Cancer in Solid Organ Transplant Recipients. *J Investig Surg. Taylor & Francis*. 2018; 31 (6): 483–490. doi: 10.1080/08941939.2017.1359707.
44. *Al-Ameri M et al.* Uniportal versus multiportal video-assisted thoracic surgery for lung cancer. *J Thorac Dis.* 2019; 11 (12): 5152–5161. doi: 10.21037/jtd.2019.12.01.
45. *Cao C et al.* European questionnaire on the clinical use of video-assisted thoracoscopic surgery. *Interact Cardiovasc Thorac Surg.* 2018; 27 (3): 379–383. doi: 10.1093/icvts/ivy062.
46. *Seitlinger J et al.* Conversion from video-assisted thoracic surgery (VATS) to thoracotomy during major lung resection: how does it affect perioperative outcomes? *Interact Cardiovasc Thorac Surg.* 2021; 32 (1): 55–63. doi: 10.1093/icvts/ivaa220.
47. *Maeda H et al.* Video-assisted thoracoscopic surgery after renal transplantation: A single-institution experience. *Asian J Endosc Surg.* 2016; 9 (1): 37–43. doi: 10.1111/ases.12248.
48. *Chen LN et al.* Characteristics and outcomes of lung cancer in solid organ transplant recipients. *Lung Cancer Elsevier*. 2020; 146: 297–302. doi: 10.1016/j.lungcan.2020.06.018.
49. *Zhang SX, Liu Y.* Primary lung cancer in Chinese renal transplant recipients: a single-center analysis. *Nan Fang Yi Ke Da Xue Xue Bao*. 2017; 37 (6): 715–720. doi: 10.3969/j.issn.1673-4254.2017.06.01.
50. *Sigel K et al.* Lung cancer prognosis in elderly solid organ transplant recipients. *Transplantation.* 2015; 99 (10): 2181–2189. doi: 10.1097/TP.0000000000000715.
51. https://gco.iarc.fr [Internet]. International Agency for Research on Cancer. Available from: https://gco.iarc.fr.
52. http://www.transplant-observatory.org [Internet]. Global Observatory on Donation and Transplantation. Available from: http://www.transplant-observatory.org.

The article was submitted to the journal on 19.08.2021

DOI: 10.15825/1995-1191-2021-4-26-31

THE INCIDENCE AND RISK FACTORS OF CHRONIC REJECTION IN ACUTELY REJECTED PEDIATRIC LIVER TRANSPLANTATION

S.M. Dehghani[1], I. Shahramian[2], M. Ayatollahi[1], F. Parooie[2], M. Salarzaei[2], M. Bahmanyar[3], A. Sargazi[2], M. Delaramnasab[2]

[1] Shiraz Organ Transplantation Center, Nemazee Hospital, Shiraz University of Medical Sciences, Shiraz, Iran

[2] Pediatric Gastroenterology and Hepatology Research Center, Zabol University of Medical Science, Zabol, Iran

[3] Fasa University of Medical Science, Fasa, Iran

Background. Chronic graft rejection (CR) represents an increasing concern in pediatric liver transplantation (LT). Risk factors of CR in this population are uncertain. In present study, we aimed to ascertain if clinical parameters could predict the occurrence of CR in LT children. **Methods.** We retrospectively analyzed the results from 47 children who had experienced acute hepatic rejection in Namazee hospital, Shiraz, Iran during 2007–2017. **Results.** Out of 47 children, 22 (46.8%) and 25 (53.2%) were boys and girls respectively. Ascites, gastrointestinal bleeding, and spontaneous bacterial peritonitis were observed in 20 (44.4%), 14 (31.1%), and 4 (9.1%) respectively. Post-transplant vascular and biliary complications were observed in 3 (7%) and 4 (9.3%) cases respectively. The mean time from LT to normalization of liver enzymes was 14.2 ± 7.5 days. The mean of acute rejection episodes was 1.4 ± 0.6 (median = 1 (22, 46.8%), range of 1–3). Six (12.7%) patients experienced CR. The mean time from LT to CR was 75 ± 28.4 days. A significant association was found between CR and patients' condition (being inpatient or outpatient) before surgery (P = 0.03). No significant relationship was found between CR and post-transplant parameters except for biliary complications (P = 0.01). Both biliary complication (RR = 33.7, 95% CI: 2.2–511, P = 0.01) and inpatient status (RR = 10.9, 95% CI: 1.1–102.5, P = 0.03) significantly increased the risk of CR. **Conclusion.** Being hospitalized at the time of LT, and development of biliary complications might predict risk factors for development of CR in LT children.

Keyword: Liver transplantation, Graft rejection, Host vs Graft Reaction.

INTRODUCTION

In the courtesy of substantial improvements in pre- and post-transplant care, patients who are organ transplanted now encounter lower rate of early complications after surgery. However, patients are still at risk of long-term complications and in particular, chronic graft rejection (CR). Accordingly, CR is the most debating and concerning survival-limiting complication in liver transplanted patients and is encountered in 2–20% of the patients [1, 2]. CR is generally defined by foamy changes in sinusoidal and vascular beds as well as the loss of >50% of portal bile ducts [3, 4]. The most identifiable feature in biopsy specimens, however, is the loss of bile ducts as foamy changes which are usually restricted to large arteries. Nevertheless, the loss of bile ducts is considered as a late feature of CR [3]. Immunosuppressive therapies have had the least impacts in progression of tissue degeneration in advanced CR. The majority of patients affected with advanced CR are required to be re-transplanted [5]. In accordance, CR is the main reason for graft failure in pediatric population [6]. After nearly five decades experience on pediatric LT, survival rate for patients hits 90% in 1-year post transplant [7]. This survival rate could particularly be attributed to improvements in preoperative managements, optimizing donor selection strategies, and developing proficient surgical methods. The majority of these advancements, however, contribute to lower acute and short-term complications while long-term complications, and in particular, CR, is still relatively common encountered feature. Compared to adult LT (2–5%), CR is encountered in higher ratios (8–12%) in pediatric patients [6]. Parameters associated CR are not well known in pediatric LT. Based on this, studying risk factors related to incidence of CR is of crucial importance to early identify CR in pediatric LT.

METHODS

This was a retrospective study performed in Organ transplant center of Nemazi Hospital, Shiraz, Iran. Data on CR was gathered from 47 pediatric patients who had

Corresponding author: Iraj Shahramian, Full Professor of Pediatric Gastroenterology and Hepatology, Zabol University of Medical Science, Zabol, Iran.
Tel/fax: +985432239031. E-mail: ir_buper@yahoo.com

experienced acute rejections. A comprehensive view on these patients has been reported earlier by ours. These patients had biopsy diagnosed acute rejection. Chronic rejection was diagnosed in these patients based on the loss of >50% of portal bile ducts. Statistical analysis was performed in SPSS 19 software using appropriate descriptive and analytical tests.

RESULTS

From 47 children, 22 (46.8%) and 25 (53.2) were boys and girls respectively. Family history of liver disease was noted in 9 (19.1%) of the patients. None of the patients had renal insufficiency, cyanosis or hepatopulmonary syndromes pre-transplant. However, ascites, gastrointestinal bleeding, and spontaneous bacterial periodontitis (SBP) were observed in 20 (44.4%), 14 (31.1%), and 4 (9.1%) of patients respectively.

Only 6 (13%) of the patients had been hospitalized at the time of transplantation. Cadaveric transplants were done in 33 (71.7%), while the grafts came from either fathers or mothers in 4 (6.5%) and 10 (21.7%) cases respectively. The means for the numbers of transfused FFP, whole blood, and packed cell units before LT were 1 ± 1.7, 0.4 ± 1.4, 0.6 ± 1.5 respectively. basic clinical features of the patients have been noted in table 1.

One (2.2%) patient developed diabetes, and 1 (2.2%) developed renal insufficiency after transplantation. Serological tests for cytomegalovirus (CMV) was positive for 1 (2.2%) case after transplantation. Bayloma was noted in 6 (14%) of the patients after the surgery. Post-transplant vascular and biliary complications were observed in 3 (7%) and 4 (9.3%) of the cases respectively. No cases developed post-transplant lymphoproliferative disorder (PTLD) following LT.

The mean time from LT to normalization of liver enzymes was 14.2 ± 7.5 days. The mean of acute rejection episodes was 1.4 ± 0.6 (median = 1 (22, 46.8%), range of 1–3). Six (12.7%) patients experienced chronic rejections. The mean time from transplantation to CR was 75 ± 28.4 days. Table 2 represents features of the six patients who developed CR.

No association was identified between CR and sex, blood group, child class, pre-transplant complications (SBP, GI bleeding, ascites, hepatopulmonary syndrome, cyanosis, renal insufficiency), and graft origin (cadaveric, parental). However, fisher exact test revealed a significant association between CR condition (being inpatient of outpatient) of the patients before surgery (P = 0.03). Beside biliary complications (P = 0.01, table 3), no significant relationship was found between CR and post-transplant parameters (diabetes, renal insufficiency, CMV infection, and vascular complications). In regres-

Table 1

Basic clinical features in 47 liver transplanted children

Parameter		Amount
Blood groups	A+	17 (36.2)
	B+	8 (17)
	B–	2 (4.3)
	O+	17 (36.2)
	O–	2 (4.3)
	AB+	1 (2.1)
Child class	A	12 (22.2)
	B	24 (58.3)
	C	11 (19.4)
Age at transplant (years)		9.6 ± 9.5
Weight at transplant (Kg)		23.7 ± 13.4
PELD/MELD score		18.7 ± 10.5
Child Score		7.6 ± 2.3
Hospitalization episodes		2.5 ± 2
Bleeding volume (ml)		327.6 ± 420.3
Surgery time (hours)		192.8 ± 109.6
ICU stay after transplantation (days)		10.7 ± 5.1
Hospital stay after transplantation (days)		14.2 ± 5.9

Table 2

Features of six children who developed chronic graft rejection after liver transplantation

Features	P 1	P 2	P 3	P 4	P 5	P 6
Gender	M	F	M	M	M	F
Age at transplant (years)	6	3	2.5	10	11	2
PELD/MELD score	24	16	28	40	14	18
Child Score	6	11	8	12	6	7
Time to liver enzyme normalization (days)	17	8	28	17	10	12
Acute rejection episodes	1	1	1	2	2	2
Time to chronic rejection (days)	102	94	89	43	87	35
Status before transplant	inpatient	inpatient	outpatient	inpatient	outpatient	outpatient
Type of transplant	Mother	Mother	Cadaver	Cadaver	Cadaver	Cadaver
Biliary complications	Yes	No	No	No	No	Yes

Note. P – patient; M – male; F – female.

sion analysis, both biliary complication and inpatient status increased the risk of CR significantly (table 4).

DISCUSSION

Graft failure due to CR is a growing concern in pediatric LT. Mechanisms behind CR are of great interest for researchers in order to make progress on patient and graft outcome. In respective to the adults, LT in children offers a superior prognosis. This is governed by a variety of factors such as graft quality and viability (source, harvesting, preserving and transporting) as well as efficiency of surgical techniques and inter-individual patients' related factors.

In our study, 6 (12.7%) patients encountered CR. The mean time from LT to CR was 75 ± 28.4 ranging from 35–102 days. It has been noted that graft failure is mostly encountered within three months after LT, while 85% of rejections occurred within six months [8]. In a study in Brazil on 537 LT children, 29 (5.4%) developed CR [6]. In another report in 22 pediatric LT, 2 (9%) encountered CR [9]. In a study by Dattani et al., 2% of 46 LT children developed CR [10]. CR development is a multifactorial phenomenon. This could be provoked in grafts from unrelated donors as CR was reported in 14.7% of patients transplanted with unrelated while in 7% of related allografts [11]. Overall, CR is a relatively common feature in pediatric LT, however, its risk factors and underlying pathological and immunological mechanisms need to be more elucidated.

In our patients, neither of recipients' age, weight, PELD/PELD or child scores, and nor acute rejection episodes, hospitalization period, time laps for normalization of liver enzymes, and receiving blood components or bleeding during surgery were associated with occurrence of CR. Nevertheless, status of the patients at the time of LT (i.e. inpatient or outpatient), the ICU stay duration, and post-transplant biliary compilations were significantly associated with CR. Among risk factors of CR in LT are recurrent acute rejections [3, 6, 12], viral infections [13–16], low-dose immunosuppression ther-

Table 3

Univariate analysis for association of clinical characteristics pre and post liver transplantation with occurrence of chronic graft rejection

Parameters		Chronic rejection		p
		Yes (n = 6)	No (n = 41)	
Biliary	Yes	2	3	0.01*
	No	4	38	
Status	Inpatient	2	3	0.03*
	Outpatient	4	37	
Age at trans		15.5 ± 2.7	8.7 ± 4.3	0.11
Weight at trans		27 ± 18.1	23.1 ± 12.6	0.74
PELD/MELD score		22.7 ± 11.7	18.1 ± 10.5	0.40
Child score		8 ± 2.7	7.5 ± 2.3	0.61
FFP units		1.2 ± 1.4	1 ± 1.8	0.38
Whole blood units		0.25 ± 0.5	0.52 ± 1.5	0.89
Hospitalization before		1.5 ± 0.5	2.7 ± 2.1	0.16
Bleeding volume at surgery		568 ± 567.5	296 ± 396.1	0.18
ICU stays after transplant		5.5 ± 3.9	11.5 ± 4.8	0.007**
Surgery time		230 ± 62.4	189.7 ± 112.8	0.84
Hospital stay after transplant		13 ± 6	14.5 ± 5.9	0.93
Days to normalization of liver enzymes		14.8 ± 6.6	14.1 ± 7.8	0.56
Acute rejection episodes		1.4 ± 0.5	1.4 ± 0.6	0.84

Note. * – Fisher exact test; ** – Mann Whitney U test.

Table 4

Logistic regression analysis for selected variables and risk of chronic rejection in pediatric liver transplantation

Parameters		RR	95%CI	p	Adjusted RR	95%CI	p
Status	Outpatient	Ref			Ref		
	Inpatient	9	1.3–60.4	0.02	10.9	1.1–102.5	0.03
Biliary complications	No	Ref					
	Yes	26.2	2.1–316	0.01	33.7	2.2–511	0.01

apy, anti-viral therapy [2], underlying liver disease [17, 18], human leukocyte antigen (HLA) mismatch [18–20], ABO-incompatible graft [21, 22], donor-specific antibodies (DSA) against HLA or other immune determinants (i.e. complement system) [23–25], and post-transplant complications (i.e. vasculopathies and sinusoidal fibrosis [16]. In another study, however, none of 36 patients who received long-term low dose immunosuppressive therapy developed CR [26]. In fact, tacrolimus based immunosuppressive treatment has been reported as an effective factor for preventing CR [4, 27], however, other studies suggested that immunosuppression regimes could not be definitive determinants in prevention of CR [6, 26]. DSAs which have been mainly against HLA II and C3d component of complement system are seen in increasing frequencies with the time after transplantation (8% within 5 years while 50% in >15 years of LT) [23]. Nevertheless, DSAs may not be specific for detection of CR as they have also been described in as high as 56% of patients without any evidences of CR [25]. Allografts In patients positive for CMV infection have shown more pronounced fibrotic and vasculopathy, as well as necrotic changes [13]. This has been attributed to higher expression of vascular growth factors (such as platelet derived growth factor and fibroblast growth factor; i.e. PDGF and FGF) [13]. On the other hand, chronic stimulation of inflammatory cytokines has been suggested as a possible contributor to the aggravation of hepatic inflammation and CR [13]. Some other risk factors have also been described for CR. Of these are recipient general health and absence of autoimmune disorders, as well as recipient age and gender [12, 22]. These implications are mainly acknowledged from adult studies, and on the other hand, these risk factors have been inconsistent among different populations.

In the study of Tannuri et al., CR was not asscoiated with neither of the age or gender of recipients, nor with graft origin, unerlying liver disease, acute rejection episodes, viral infections (CMV and EBV), immunosuppressive treatement, and post transplant complications (i.e. PTLD, vascular, and biliary complications) [6]. Instead, ductopenia was noted as the sole predictor of CR in the recent reprot [6]. Here we found that billiary complications afetr LT signfiicantly increased the risk of CR (Adjusted relative risk = 33.7, 95% CI: 2.2–511). Biliary complication is a respectively common sequala after LT [28, 29]. Some factors that may contribute to the development of biliary defects have been noted as high serum bilirubin, advanced donor age, MELD score, acute rejections and biliary structural defects following LT [29]. Furthermore, patients with primary biliary cirrhosis had higher risk for occurrence of biliary complications after LT [29]. Recently by proposing a chronic antibody-mediated rejection (cAMR) score based on a variety of serological, histological and clinical parameters, it was possible to predict a risk-stratification for graft failure following 10 years of LT [16]. Overall, many inter and intra individual, as well as procedural factors are important in development of CR in LT.

In addition to clinical parameters, lights have also been shed on the molecular and cellular mechanisms involved in hepatic CR. In study of Wei et al. in animal model of CR, it was found that the expression of at least sixty two proteins were modulated in the face of CR development [30]. Among these, CLU (clusterin), a widely expressed secretory glycoprotein with proposed roles in protein hemostasis, graft survival, apoptosis, immune tolerance and tumorigenesis was suggested as a reliable early indicator of CR [30–32]. Two other possible early indicators of CR proposed by Wei et al. included keratin type I cytoskeletal 19 (Krt19) and lipocalin 2, a neutrophilic gelatinase with respective roles in regulating bile duct biogenesis and immune system [30]. In addition, Th2 lymphocytes seems to contribute in hepatic CR by production of IL-10 and promoting humoral and inflammatory responses [33]. Through balancing Th1/Th2 responses, invariant natural killer T cells (iNKT) may execute a substantial role in inducing immune tolerance toward liver allografts [34]. New evidences have suggested a role for hepatic mast cells in augmenting immune tolerance and graft preservation [35]. From other early molecular indicators of CR has been proposed increased expression of apoptotic receptor (i.e. FasL) on Kupfer cells and antigen presenting cells (APCs) within hepatic allografts [36]. Decreased expression of serine/threonine kinase; STK17A, with suggested roles in biliary biogenesis in liver allograft may also be an early predictor of hepatic CR [37]. More studies are necessary to unravel molecular adaptors responsible for CR in LT.

CONCLUSION

The only rescuing option in patients afflicted with CR may be re-transplantation. Considering this, and also potential reversibility of CR in early phases, accurate and timely diagnosis of CR in initial stages is of paramount importance. This necessitates identifying and monitoring at risk patients for CR. Our findings suggest that being hospitalized at the time of LT, and development of biliary complications might predict such high risk conditions.

The authors declare no conflict of interest.

REFERENCES

1. *Pfitzmann R, Nüssler NC, Hippler-Benscheidt M, Neuhaus R, Neuhaus P.* Long-term results after liver transplantation. *Transplant International*. 2008; 21 (3): 234–246.
2. *Ueda Y, Kaido T, Ito T, Ogawa K, Yoshizawa A, Fujimoto Y et al.* Chronic rejection associated with antiviral therapy for recurrent hepatitis C after living-donor liver transplantation. *Transplantation*. 2014; 97 (3): 344–350.

3. *Neil DA, Hubscher SG.* Histologic and biochemical changes during the evolution of chronic rejection of liver allografts. *Hepatology (Baltimore, Md)*. 2002; 35 (3): 639–651.
4. *Jain A, Mazariegos G, Pokharna R, Parizhskaya M, Kashyap R, Kosmach-Park B et al.* The absence of chronic rejection in pediatric primary liver transplant patients who are maintained on tacrolimus-based immunosuppression: a long-term analysis. *Transplantation*. 2003; 75 (7): 1020–1025.
5. *O'Leary J, Kaneku H, Susskind B, Jennings L, Neri M, Davis G et al.* High mean fluorescence intensity donor-specific anti-HLA antibodies associated with chronic rejection postliver transplant. *American Journal of Transplantation*. 2011; 11 (9): 1868–1876.
6. *Tannuri AC, Lima F, Mello ES, Tanigawa RY, Tannuri U.* Prognostic factors for the evolution and reversibility of chronic rejection in pediatric liver transplantation. *Clinics (Sao Paulo, Brazil)*. 2016; 71 (4): 216–220.
7. *McLin VA, Allen U, Boyer O, Bucuvalas J, Colledan M, Cuturi MC et al.* Early and Late Factors Impacting Patient and Graft Outcome in Pediatric Liver Transplantation: Summary of an ESPGHAN Monothematic Conference. *Journal of pediatric gastroenterology and nutrition*. 2017; 65 (3): e53–e59.
8. *Neil D, Adams D, Gunson B, Hubscher S.* Is chronic rejection of liver transplants different to graft arteriosclerosis (chronic rejection) of kidney and heart transplants. *Transplantation proceedings*. 1997; 29: 2533–2534.
9. *Akdur A, Kirnap M, Ayvazoglu Soy EH, Ozcay F, Moray G, Arslan G et al.* Unusual Indications for a Liver Transplant: A Single-Center Experience. *Experimental and clinical transplantation: official journal of the Middle East Society for Organ Transplantation*. 2017; 15 (Suppl 1): 128–132.
10. *Dattani N, Baker A, Quaglia A, Melendez HV, Rela M, Heaton N.* Clinical and histological outcomes following living-related liver transplantation in children. *Clinics and research in hepatology and gastroenterology*. 2014; 38 (2): 164–171.
11. *Ali MA, Elshobari MM, Salah T, Kandeel AR, Sultan AM, Elghawalby AN et al.* Impact of donor-recipient genetic relationship on outcome of living donor liver transplantation. *Liver Transpl*. 2017; 23 (1): 43–49.
12. *Neuberger J.* Incidence, timing, and risk factors for acute and chronic rejection. *Liver transplantation and surgery: official publication of the American Association for the Study of Liver Diseases and the International Liver Transplantation Society*. 1999; 5 (4 Suppl 1): S30–S36.
13. *Gao LH, Zeng LX, Chen HM, Wan RH.* Cytomegalovirus infection accelerates the process of chronic rejection in rat liver transplantation. *Transplantation proceedings*. 2013; 45 (6): 2536–2538.
14. *Guardia-Silva AC, Stucchi RS, Sampaio AM, Milan A, Costa SC, Boin IF.* Detection of cytomegalovirus and human herpesvirus-6 DNA in liver biopsy specimens and their correlation with rejection after liver transplantation. *Transplantation proceedings*. 2012; 44 (8): 2441–2444.
15. *Gao LH, Zheng SS.* Cytomegalovirus and chronic allograft rejection in liver transplantation. *World journal of gastroenterology*. 2004; 10 (13): 1857–1861.
16. *O'Leary JG, Cai J, Freeman R, Banuelos N, Hart B, Johnson M et al.* Proposed Diagnostic Criteria for Chronic Antibody-Mediated Rejection in Liver Allografts. *American journal of transplantation: official journal of the American Society of Transplantation and the American Society of Transplant Surgeons*. 2016; 16 (2): 603–614.
17. *Ruth ND, Kelly D, Sharif K, Morland B, Lloyd C, McKiernan PJ.* Rejection is less common in children undergoing liver transplantation for hepatoblastoma. *Pediatric transplantation*. 2014; 18 (1): 52–57.
18. *Harimoto N, Ikegami T, Nakagawara H, Yamashita YI, Yoshizumi T, Uchiyama H et al.* Chronic immune-mediated reaction syndrome as the cause of late graft mortality in living-donor liver transplantation for primary biliary cirrhosis. *Transplantation proceedings*. 2014; 46 (5): 1438–1443.
19. *Uchiyama H, Kayashima H, Matono R, Shirabe K, Yoshizumi T, Ikegami T et al.* Relevance of HLA compatibility in living donor liver transplantation: the double-edged sword associated with the patient outcome. *Clinical transplantation*. 2012; 26 (5): E522–E529.
20. *Muro M, Lopez-Alvarez MR, Campillo JA, Marin L, Moya-Quiles MR, Bolarin JM et al.* Influence of human leukocyte antigen mismatching on rejection development and allograft survival in liver transplantation: is the relevance of HLA-A locus matching being underestimated? *Transplant immunology*. 2012; 26 (2–3): 88–93.
21. *Lee EC, Kim SH, Park SJ.* Outcomes after liver transplantation in accordance with ABO compatibility: A systematic review and meta-analysis. *World journal of gastroenterology*. 2017; 23 (35): 6516–6533.
22. *Gupta P, Hart J, Cronin D, Kelly S, Millis JM, Brady L.* Risk factors for chronic rejection after pediatric liver transplantation. *Transplantation*. 2001; 72 (6): 1098–1102.
23. *Couchonnal E, Rivet C, Ducreux S, Dumortier J, Bosch A, Boillot O et al.* Deleterious impact of C3d-binding donor-specific anti-HLA antibodies after pediatric liver transplantation. *Transplant immunology*. 2017; 45: 8–14.
24. *Muro M, Moya-Quiles MR, Mrowiec A.* Humoral Response in Liver Allograft Transplantation: A Review of the Role of Anti-Human Leukocyte Antigen (HLA) Antibodies. *Current protein & peptide science*. 2016; 17 (8): 776–784.
25. *Kaneku H, O'Leary JG, Taniguchi M, Susskind BM, Terasaki PI, Klintmalm GB.* Donor-specific human leukocyte antigen antibodies of the immunoglobulin G3 subclass are associated with chronic rejection and graft loss after liver transplantation. *Liver transplantation: official publication of the American Association for the Study of Liver Diseases and the International Liver Transplantation Society*. 2012; 18 (8): 984–992.
26. *Barbier L, Garcia S, Cros J, Borentain P, Botta-Fridlund D, Paradis V et al.* Assessment of chronic rejection in liver graft recipients receiving immunosuppression

with low-dose calcineurin inhibitors. *Journal of hepatology*. 2013; 59 (6): 1223–1230.
27. *Jain A, Mazariegos G, Pokharna R, Parizhskaya M, Kashyap R, Kosmach-Park B et al.* The absence of chronic rejection in pediatric primary liver transplant patients who are maintained on tacrolimus-based immunosuppression: a long-term analysis1. *Transplantation*. 2003; 75 (7): 1020–1025.
28. *Santos O, Londono M, Marin J, Munoz O, Mena A, Guzman C et al.* An experience of liver transplantation in Latin America: a medical center in Colombia. *Colombia medica (Cali, Colombia)*. 2015; 46 (1): 8–13.
29. *Mocchegiani F, Vincenzi P, Lanari J, Montalti R, Nicolini D, Svegliati Baroni G et al.* Immunological risk factors in biliary strictures after liver transplantation. *Annals of transplantation*. 2015; 20: 218–224.
30. *Wei W, Huang XH, Liang D, Zeng YY, Ma C, Wu YB et al.* A proteomic analysis of transplanted liver in a rat model of chronic rejection. *Clinics and research in hepatology and gastroenterology*. 2015; 39 (3): 340–350.
31. *Chiang K, Goto S, Chen C, Lin C, Lin Y, Pan T et al.* Clusterin may be involved in rat liver allograft tolerance. *Transplant immunology*. 2000; 8 (2): 95–99.
32. *Li S, Guan Q, Chen Z, Gleave ME, Nguan CY, Du C.* Reduction of cold ischemia–reperfusion injury by graft-expressing clusterin in heart transplantation. *The Journal of Heart and Lung Transplantation*. 2011; 30 (7): 819–826.
33. *Wan R, Tang L, Shan R, Zeng L, Chen H, Gao L.* Humoral immunity-mediated chronic rejection in liver transplantation is associated with predominant IL-10 expression. *Frontiers in bioscience (Elite edition)*. 2012; 4: 2121–2130.
34. *Liu Y, Luan X, Li J, He Y, Li M.* The role of invariant NKT cells in liver transplant tolerance in rats. *Transplantation proceedings*. 2012; 44 (4): 1041–1044.
35. *Nakano T, Lai CY, Goto S, Hsu LW, Kawamoto S, Ono K et al.* Immunological and regenerative aspects of hepatic mast cells in liver allograft rejection and tolerance. *PloS one*. 2012; 7 (5): e37202.
36. *Miyagawa-Hayashino A, Tsuruyama T, Egawa H, Haga H, Sakashita H, Okuno T et al.* FasL expression in hepatic antigen-presenting cells and phagocytosis of apoptotic T cells by FasL+ Kupffer cells are indicators of rejection activity in human liver allografts. *The American journal of pathology*. 2007; 171 (5): 1499–1508.
37. *Ozeki M, Salah A, Aini W, Tamaki K, Haga H, Miyagawa-Hayashino A*. Abnormal Localization of STK17A in Bile Canaliculi in Liver Allografts: An Early Sign of Chronic Rejection. *PloS one*. 2015; 10 (8): e0136381.

The article was submitted to the journal on 13.02.2020

DOI: 10.15825/1995-1191-2021-4-32-41

CHANGES IN GLOMERULAR FILTRATION RATE IN LIVER RECIPIENTS AFTER REDUCED EXPOSURE TO CALCINEURIN INHIBITORS WITH CONCOMITANT EVEROLIMUS ADMINISTRATION WITHIN THE FIRST YEAR AFTER IMMUNOSUPPRESSION CONVERSION

V.E. Syutkin, A.A. Salienko, S.V. Zhuravel, M.S. Novruzbekov
Sklifosovsky Research Institute of Emergency Care, Moscow, Russian Federation

Objective: to compare changes in estimated glomerular filtration rate (eGFR) in liver recipients with initially normal and impaired eGFR within the first year after immunosuppression conversion. **Materials and methods.** Enrolled in the study were 215 recipients of deceased-donor livers from February 2009 to February 2020, who received everolimus with dose reduction or complete withdrawal of calcineurin inhibitors (immunosuppression conversion, ISxC) for varying periods of time. GFR was measured using the MDRD-4 formula immediately before ISxC, then 3, 6, and 12 months after orthotopic liver transplantation (LTx). One month was considered an acceptable temporary deviation from the corresponding point. **Results.** At the time of ISxC, 32 (15%) of 215 recipients had normal renal function. Chronic kidney disease (CKD) increased in 60% of the recipients with normal eGFR by the end of the first year following ISxC; the fall in eGFR was particularly pronounced in older recipients. In the group with a baseline eGFR of 60–89 mL/min/1.73 m^2, eGFR normalized in 62% of cases within 12 months; 28% of cases had no changes in renal function. In the subgroup with a pronounced decrease in eGFR at the time of ISxC, increased eGFR was observed as early as 1 month after ISxC, and the maximum was recorded after 3–6 months. The mean eGFR relative to baseline by month 3 after eGFR were higher for ISxC that was done in the first 2 months after LTx (19.7 ± 15.7 ml/minute/1.73 m^2) than for ISxC done in the long-term period after LTx (10.1 ± 8.7 ml/minute/1.73 m^2, $p < 0.05$). **Conclusion.** Changes in eGFR in liver recipients receiving EVR plus low-dose calcineurin inhibitor (CNI) depend on baseline eGFR and are multidirectional. The use of ISxC in the early post-LTx period led to a more pronounced improvement in eGFR. Maximal changes in eGFR were observed by 3–6 months after ISxC.

Keywords: liver transplantation, immunosuppressive therapy, calcineurin inhibitor nephrotoxicity, everolimus.

Chronic kidney disease (CKD) is a common complication following liver transplantation (LTx). End-stage CKD (eGFR ≤29 mL/min/1.73 m^2 by MDRD formula) occurs in 8% at 1 year and in 18% at 5 years after LTx [1]. The most significant reason for deterioration of renal function in liver recipients is the use of calcineurin inhibitors (CIs) – cyclosporine (CsA) and tacrolimus (TAC) – as the main component of immunosuppressive therapy (IST). Nephrotoxicity of CI is well studied and described in detail [2, 3]. Accordingly, minimizing the exposure (area under the concentration-time curve) to CIs is necessary to slow down CKD progression and preserve kidney function in liver recipients.

A possible way to reduce CI exposure without simultaneously increasing the risk of rejection is to compensate for the IST action by prescribing drugs with a different mechanism of action. One of such drugs is proliferative signal inhibitor, everolimus (EVR). IST efficacy and safety – with respect to progression of CKD in liver recipients – based on EVR combination with simultaneous minimization of TAC exposure has been demonstrated in the CRAD2304 and CRAD2307 clinical trials [4, 5]. In both trials, recipients had relatively high GFR (80 and 90 mL/min/1.73 m^2) at the time of randomization. The effectiveness of GFR restoration after IST conversion (EVR combined with reduced CI dose (ISxC)) in liver recipients with reduced baseline GFR has not been sufficiently studied.

Objective: To compare changes in GFR in liver recipients with normal baseline and impaired GFR within the first year after ISxC.

PATIENTS AND RESEARCH METHODS

We retrospectively analyzed changes in eGFR in 215 recipients who received LTx from a deceased donor between February 2009 and February 2020 and who re-

Corresponding author: Anastasiia Salienko. Address: 3, Bolshaya Sukharevskaya Ploshchad, Moscow, 129090, Russian Federation. Phone: (926) 689-15-45. E-mail: SalienkoAA@sklif.mos.ru

ceived one or more EVR doses as part of routine clinical practice. At the time of the analysis, 169 patients were alive and remained patients at the liver transplant center, 27 had died, and 19 had dropped out of hospital care at various times. Of the 169 recipients who were alive at the time of analysis and continued to be seen at the transplant center, EVR was withdrawn in 51 cases, and 118 recipients continued to receive therapy.

Before ISxC, 102 recipients received CIs as the main component of maintenance IST, in 113 cases EVR was administered simultaneously with CIs in the first two weeks after LTx. Cyclosporine (initial dose of 5–6 mg/kg per day) was given to 34 (15.8%) recipients. Target CsA blood concentrations, determined 30 minutes before drug administration (C_0) in the first months after LTx, were 150–250 ng/mL, thereafter 100–150 ng/mL. 181 (84.1%) recipients received TAC (initial daily dose of 0.05–0.075 mg/kg). Target TAC blood concentrations determined 30 minutes before drug administration (C_0): month 1–3, 8–10 ng/mL; thereafter, 6–8 ng/mL.

Mycophenolate mofetil (MMF) drugs were administered to 131 patients, of whom 93 patients received mycophenolic acid; 38 patients received mycophenolate mofetil. MMF drugs were withdrawn in all but one recipient at different times during the postoperative period. No glucocorticoids were administered to 171 recipients in the postoperative period. In 14 recipients, prednisone was discontinued within the first 3–4 months after OLTx. Nineteen recipients were treated at a later stage. Eleven recipients continued to receive low (5 mg/day) doses of prednisolone.

Indications for EVR were: renal failure in 85 recipients (39.5%), presence of hepatocellular carcinoma (HCC) as one of the indications for LTx – in 79 recipients (36.7%). Twenty-three recipients (11%) were prescribed EVR due to renal failure and the presence of HCC prior to LTx; 7 (3%) recipients were prescribed EVR due to HCC progression in the postoperative period. In 4 (2%) cases, EVR was prescribed due to neurological complications while taking CIs. Eight (3.7%) recipients received EVR as part of the CRAD2304 clinical trial [5]. Other indications for EVR were tumors (non-HCC, n = 5), lymphoma (n = 2), and liver transplantation (n = 2).

After ISxC, EVR was administered at 1 to 2 mg per day (0.01 to 0.04 mg/kg) in two doses. The target EVR blood concentration 30 minutes before drug administration (C_0) was 3–5 ng/ml. The CI dose was reduced simultaneously with EVR administration; the target TAC levels in the two-component therapy regimen were 3–5 ng/mL, and the target CsA level was 50–75 ng/mL. In 16 cases, CIs were canceled entirely.

The studied population included 150 men and 65 women aged 53 (50.3; 53.1) years (M (95% CI), with a mean body weight of 76 (74.3; 79) kg. Surgery for end-stage cirrhosis was performed in 199 (92.5%) patients with chronic diffuse liver disease, of which 102 (51.3%) cases were combined with HCC; 12 (5.5%) patients with primary liver tumors without cirrhosis; 4 (1.9%) – for other reasons. Seven recipients underwent combined liver–kidney allotransplantation.

The eGFR was calculated using the MDRD-4 formula immediately before immunosuppression conversion, 3, 6, and 12 months after OLTx [6]. One month was considered an acceptable time deviation from the corresponding point.

Statistical processing of numerical values was performed using the Statistica 7.0 software. Statistical significance of differences between compared parameters was established using Wilcoxon signed-rank test for paired comparisons of dependent variables and Kolmogorov–Smirnov test for comparisons of independent variables. Differences between compared parameters were considered statistically significant if the probability of error was less than 0.05 ($p < 0.05$).

RESULTS

Dependence of change in renal function during the first year of follow-up after IST conversion on baseline eGFR

The majority of recipients at the time of ISxC had eGFR below normal; only 32 (15%) of 215 recipients had normal renal function. Table 2 shows that after ISxC, the proportion of recipients with severe renal impairment (eGFR <30 mL/min/1.73 m^2) gradually decreased, the proportion of recipients with moderate-to-severe renal impairment (eGFR 30 to 44 mL/min/1.73 m^2) remained the same (about 20% of total recipients), whereas the proportion of recipients with mild to moderately mild renal impairment (eGFR 45 to 89 mL/min/1.73 m^2) increased. Despite ISxC, the proportion of recipients with normal eGFR decreased during the first year after LTx.

To identify the effect of baseline renal dysfunction on eGFR dynamics after ISxC, we analyzed the pattern of changes in CKD degree depending on baseline eGFR.

Normal eGFR levels after 12 months of follow-up were preserved only in 40% of liver recipients with normal baseline eGFR (>90 mL/min/1.73 m^2). In the

Table 1

Degree of renal dysfunction at the time of immunosuppression conversion

eGFR range (mL/min/1.73 m^2)	n	eGFR (MDRD4), M (CI)
>90	32	109.2 (103.1; 115.4)
60–89	52	73.0 (70.7; 75.3)
45–59	35	52.6 (51.1; 54.2)
30–44	45	36.6 (35.4; 37.8)
15–29	44	23.2 (21.9; 24.5)
<15	7	10.9 (8.2; 13.7)

rest, eGFR deteriorated, but was not pronounced (eGFR remained more than 60 mL/min/1.73 m^2) in the vast majority of cases (50%) it.

ISxC in the group of patients with a mild decrease in baseline eGFR (60–89 mL/min/1.73 m^2) in 62% of recipients within 12 months led to eGFR normalization. In 28% of these recipients, no change in renal function was observed at follow-up within the first year of ISxC. And only 10% of recipients at 12 months after ISxC had eGFR fall to levels consistent with stage 3 CKD.

In half (45–50%) of the liver recipients who underwent ISxC with moderate renal dysfunction (eGFR correlated with stages 3A and 3B CKD), eGFR remained at the same level during the first 12 months of follow-up. Forty-two percent of recipients with baseline eGFR of 45–59 mL/min/1.73 m^2 and 55% of recipients with baseline eGFR of 30–44 mL/min/1.73 m^2 showed better renal function one year after ISxC, up to complete normalization in 5–17% of recipients.

In the subgroup of recipients who underwent ISxC with baseline severe renal impairment (eGFR 15–29 mL/min/1.73 m^2), as early as one month after ISxC, 70% had increased eGFR, with 12% to levels above 60 mL/min/1.73 m^2; 12 months later, eGFR corresponding to stage 4 CKD, was retained in only 25% of recipients.

In all 7 recipients with baseline eGFR <15 mL/min/1.73 m^2 after ISxC, eGFR increased after 1 month of follow-up, and in 4 of them – to levels >30 mL/min/1.73 m^2. The results of our analysis are shown graphically in Figs. 1 and 2.

The dynamics of median eGFR as a function of baseline eGFR during the first 12 months of follow-up are shown in Figs. 3, 4 and Table 3.

Table 2

Proportion of recipients with different CKD stages depending on eGFR at the time of ISxC in recipients within the first year after LTx

eGFR range (mL/min/1.73 m^2)	ISxC	Month 1	Month 3	Month 6	Month 12
>90	14.9%	14.6%	10.5%	10.1%	8.1%
60–89	24.2%	28.1%	39.0%	42.4%	34.3%
45–59	16.3%	26.5%	27.9%	27.3%	27.3%
30–44	20.9%	21.6%	20.3%	18.7%	23.2%
15–29	20.5%	9.2%	2.3%	1.4%	7.1%
<15	3.3%	0	0	0	0
Number of recipients with known eGFR	215	185	172	139	99

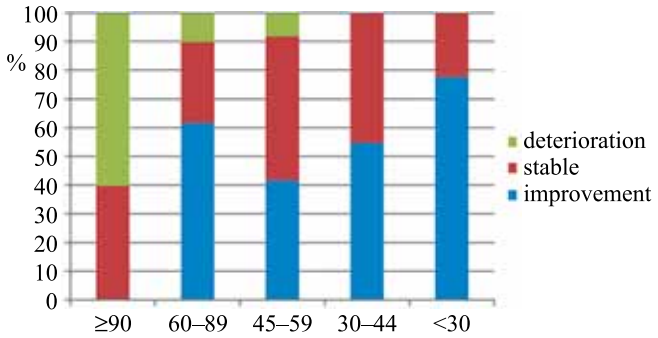

Fig. 1. Changes in renal function 12 months after ISxC

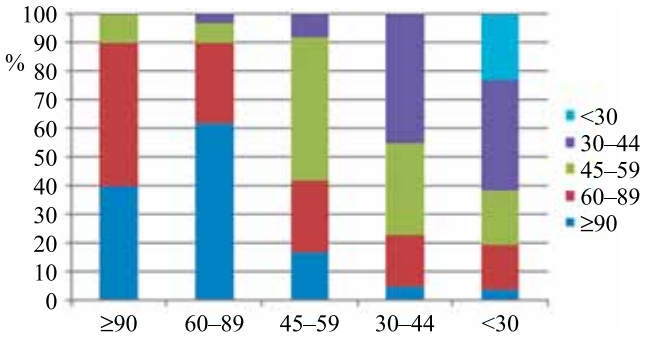

Fig. 2. Changes in eGFR (by CKD stages) 12 months after ISxC

Table 3

Change in median eGFR in the first 12 months of follow-up after ISxC (Me (Q25; Q75), mL/min/1.73 m^2)

Group (by baseline gGFR)	Baseline eGFR	Month 1	Month 3	Month 6	Month 12
>90	103.1 (97.1; 125.5)	89.5 (73.1; 100.4)‡	84.1 (71.6; 94.4)‡	87.0 (70.5; 95.1)‡	82.7 (72.2; 95.5)‡
60–89	73.3 (65.0; 79.2)	71.2 (57.1; 84.2)	64.9 (56.9; 82.0)	68.3 (58.1; 81.5)	69.4 (54.7; 78.6)
<60	34.4 (24.5; 46.3)	46.2 (34.7; 56.9)†	52.2 (41.7; 62.3)†	52.5 (42.5; 64.9)†	48.6 (39.1; 59.7)†

Compared to baseline eGFR: ‡ – $p < 0.01$, † – $p < 0.001$.

Thus, eGFR dynamics depended on the presence and severity of renal failure at the time of ISxC. Analysis of the presented eGFR changes during the first year after ISxC allows us to distinguish three subgroups of recipients. In the subgroup of recipients with normal baseline eGFR, 60% of liver recipients tended to have worsening renal function despite ISxC. In the remaining 40% of recipients, ISxC prevented a decline in eGFR during the one-year follow-up. Overall, in the subgroup, the median eGFR at 12 months after ISxC was 82.7 mL/min/1.73 m^2, a decrease of 19.8% from baseline.

The other subgroup consists of recipients with a mild to moderate decrease in eGFR at the time of ISxC (eGFR 45–89 mL/min/1.73 m^2). During the first year of follow-up, eGFR remained unchanged in 28–50% of recipients in this subgroup. In recipients with a slight initial decrease in eGFR (60–89 mL/min/1.73 m^2), 62% of cases showed eGFR normalization after 12 months. In the subgroup of recipients with a more severe decrease in baseline eGFR (45–59 mL/min/1.73 m^2) one year after ISxC, CKD worsened in only 8% of cases and improved in 42%. On average, eGFR scores in this subgroup of recipients remained stable during the first year after ISxC, with no clear trend toward improvement or deterioration in renal function (Figs. 3 and 4).

Recipients with significantly reduced renal function (eGFR <45 mL/min/1.73 m^2), who formed the third subgroup, showed a clear improvement in renal function after ISxC, with the eGFR increase being more significant the more severe the baseline renal dysfunction. At baseline eGFR 30–49 mL/min/1.73 m^2, 55% of recipients showed improvement in CKD stage after one year of follow-up, with 45% of CKD stage remaining the same. No recipient in the subgroup had a deterioration in CKD stage after 12 months of follow-up.

It should be noted that the increase in eGFR was rapid, reaching the level of statistical significance as early as 1 month after ISxC, and peaked after 3–6 months (Table 3; Fig. 3, 4). The fall in median eGFR by 3 months of follow-up was 13.9% in recipients with baseline eGFR 45–59 mL/min/1.73 m^2, 43.2% in recipients with baseline eGFR 30–44 mL/min/1.73 m^2, and 115% in recipients with baseline eGFR <30 mL/min/1.73 m^2 (!).

Dependence of changes in eGFR on ISxC timing

We compared changes in eGFR in the first 12 months of follow-up after ISxC in recipients with significantly reduced baseline renal function (eGFR <60 mL/min/1.73 m^2) as a function of ISxC timing.

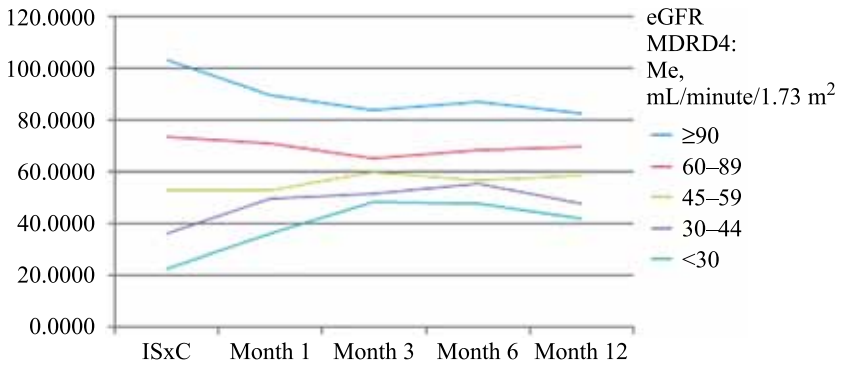

Fig. 3. Changes in median eGFR in the first 12 months of follow-up after ISxC (Me, mL/min/1.73 m^2) depending on baseline eGFR (by CKD stages)

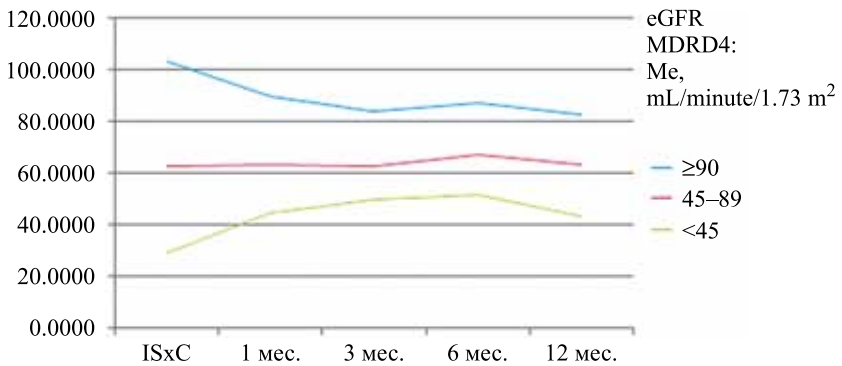

Fig. 4. Changes in median eGFR in the first 12 months of follow-up after ISxC (Me, mL/min/1.73 m^2) depending on baseline eGFR

Most recipients with a significantly reduced baseline eGFR (<60 mL/min/1.73 m^2) underwent ISxC in the first 12 months after LTx. The mean baseline eGFR was lower in this subgroup of recipients than in the subgroup of recipients who underwent ISxC at a later date (Table 4). The mean eGFR when assessed at 1 month, 3 months, 6 months, and 12 months after ISxC between the subgroups of recipients with early and late ISxC were comparable.

However, in the months after ISxC in which the maximum increase in eGFR was observed (months 3 and 6, see Fig. 3), the mean increases in eGFR relative to baseline were higher for early ISxC than for ISxC performed at a later time after LTx (Table 5).

Influence of gender, recipient age, and calcineurin inhibitor on eGFR changes

At the time of ISxC, mean eGFR were comparable in men and women in both the entire recipient population (56.7 ± 30.6 and 49.7 ± 29.0 mL/min/1.73 m^2, respectively) and in the subgroup of recipients with significantly reduced eGFR (34.5 ± 12.6 and 33.7 ± 15.5 mL/min/1.73 m^2). Baseline eGFR were also independent of the CIs variant that the recipients received before ISxC. In the TAC subgroup, eGFR was 55.0 ± 30.3 mL/min/1.73 m^2, and in the CsA subgroup, it was 55.0 ± 30.9 mL/min/1.73 m^2. Comparable results for both baseline eGFR and its dynamics during follow-up after ISxC were also obtained when analyzed based on recipient age. The median age of recipients was 53 years. Table 6 presents the eGFR dynamics as a function of recipient age. Since the eGFR dynamics in recipients with normal baseline eGFR and significantly decreased eGFR were multidirectional, we considered it right to present it separately.

We see that the mean baseline eGFR in younger and older recipients were very similar. After ISxC, eGFR decreased more markedly in older than in younger recipients with baseline eGFR ≥60 mL/min/1.73 m^2. The differences between the subgroups reached statistical

Table 4

Mean eGFR depending on ISxC timing

Months after ISxC	Early conversion (<12 months after OLTx)		Late conversion (>12 months after OLTx)		p
	n	M (SD), mL/min/1.73 m^2	n	M (SD), mL/min/1.73 m^2	
Baseline eGFR	**114**	**34.0 (13.5)**	**17**	**41.4 (11.1)**	**0.03**
Month 1	101	49.0 (19.3)	10	44.7 (12.8)	>0.05
Month 3	87	55.0 (18.1)	13	50.9 (11.2)	>0.05
Month 6	67	54.8 (16.7)	12	52.6 (13.3)	>0.05
Month 12	50	50.3 (17.5)	10	53.7 (20.4)	>0.05

Table 5

Mean increase in eGFR from baseline depending on ISxC timing

Increase by months after ISxC	Early conversion (<2 months after LTx)		Mean conversion (2–12 months after LTx)		Late conversion (>12 months after LTx)		P (between early and late ISxC)
	n	M (SD), mL/min/1.73 m^2	n	M (SD), mL/min/1.73 m^2	n	M (SD), mL/min/1.73 m^2	
By month 1	82	15.9 (20.2)	19	11.9 (10.3)†	10	7.3 (8.0)	>0.1
By month 3	**71**	**22.3 (20.6)**	16	19.7 (15.7)†	**13**	**10.1 (8.7)**	**0.039**
By month 6	**53**	**23.5 (20.0)**	14	13.0 (11.5)†	**12**	**10.4 (8.1)**	**0.03**
By month 12	39	19.0 (18.6)	11	12.1 (18.6)†	10	12.8 (15.0)	>0.1

† – differences between groups are insignificant (P > 0.01).

Table 6

Mean eGFR at the time of ISxC and increase in eGFR from baseline, depending on recipient age

eGFR, M (SD), mL/min/1.73 m^2	Baseline eGFR ≥60 mL/min/1.73 m^2			Baseline eGFR <60 mL/min/1.73 m^2		
	Age		p	Age		p
	≤53 лет	>53 лет		≤53 years	>53 years	
Baseline eGFR	88.7 (23.9)	84.3 (18.4)	>0.1	36.3 (13.6)	33.8 (13.2)	>0.1
Increase by month 1	–1.8 (24.6)	–14.3 (20.6)	>0.05	15.2 (17.7)	13.6 (18.8)	>0.1
Increase by month 3	**–6.0 (22.2)**	**–15.1 (18.7)**	**<0.05**	24.3 (22.5)	16.2 (13.8)	>0.05
Increase by month 6	–6.1 (22.5)	–12.9 (16.6)	>0.05	22.9 (21.6)	16.7 (14.0)	>0.1
Increase by month 12	–12.4 (17.8)	–11.0 (20.9)	>0.1	17.6 (19.1)	15.9 (14.8)	>0.05

significance at month 3 after ISxC. At the same time, the subgroup with baseline eGFR <60 mL/min/1.73 m^2 also showed a trend toward more significant improvement in eGFR in the younger recipient subgroup, but differences between subgroups did not reach statistical significance at all assessment points. Maximum differences between the subgroups of younger and older recipients are also detected at month 3 after ISxC.

DISCUSSION

At the Moscow Liver Transplantation Center, EVR has been used as one of the components of maintenance IST since 2009 as part of the CRAD2304 protocol and since 2010 as part of routine clinical practice. The experience in the use of EVR in liver recipients in our Center is the largest in Russia. Our first publications showed that kidney function in liver recipients who received EVR while minimizing exposure to CIs can be improved [7, 8]. In these works, 10–24 recipients were analyzed. This present paper retrospectively analyzed 215 liver recipients who received EVR as one of the components of maintenance IST. At the time of writing, over 20 recipients have continuously received EVR for more than 5 years (maximum 11 years). However, given the format of the paper, we decided to limit the analysis to changes in GFR in the first year after ISxC.

Direct methods of measuring GFR are difficult to apply in everyday clinical practice. Several formulas have been developed to estimate GFR in CKD patients, such as the Cockcroft–Gault formula [9] and formulas derived from the Modification of Diet in Renal Disease (MDRD) study [6, 10]. The Cockcroft–Gault and MDRD formulas have been shown to be applicable in calculating GFR in a large cohort of liver recipients, with the MDRD formula (including only 4 variables) proving more accurate than the Cockcroft–Gault formula [11].

The most common indications for including EVR in a maintenance IST regimen in liver recipients are impaired renal function and prevention of recurrent HCC (or an attempt to improve the course of recurrent HCC after LTx). Accordingly, a proportion of recipients have normal eGFR at the time of ISxC. As part of routine clinical practice, we have noted that eGFR changes in recipients with normal baseline and impaired renal function after ISxC are multidirectional in nature. Therefore, combining these recipients into one group for analysis results in leveling out eGFR changes. Our analysis not only confirmed this hypothesis but also revealed a number of patterns.

To date, the world has accumulated considerable experience in the use of EVR in liver recipients, and a large number of papers have been published, retrospectively evaluating the results of routine clinical practice. To discuss our results, we have chosen several publications with the least, in our opinion, possibility of systematic errors. One such work is the article by Lee et al. (2020), who analyzed a pool of liver recipients (n = 772) enrolled in clinical trials CRAD2304 and CRAD2307 [12]. The authors report the results of their analysis at 24 months after randomization. Our analysis is limited to 12 months. In addition, Lee et al. combine recipients with baseline eGFR >90 and 60–89 mL/min/1.73 m^2 into one subgroup, treating eGFR >60 mL/min/1.73 m^2 as normal. In our study, eGFR changes in these subgroups differed in the first 12 months after ISxC.

We have shown that recipients with normal baseline renal function have decreased eGFR one year after ISxC, as in the general population of liver recipients receiving standard doses of CIs. Lee et al. reported that of 229 recipients with baseline eGFR ≥60 mL/min/1.73 m^2 receiving EVR against reduced TAC exposure, eGFR ≥60 mL/min/1.73 m^2 was maintained in 189 (82.5%) recipients 24 months after randomization. These results correlate well with ours. At 12 months after ISxC, eGFR ≥60 mL/min/1.73 m^2 was preserved in 90% of our recipients with baseline eGFR corresponding to CKD stages 1/2.

According to Lee et al, eGFR fell in both the group of recipients receiving standard TAC doses and in the group of recipients after ISxC. However, in the subgroup of recipients with normal baseline eGFR and mildly impaired eGFR (≥60 mL/min/1.73 m^2) receiving EVR, the decrease in mean eGFR at month 24 after randomization was less pronounced compared with the same subgroup of recipients receiving standard TAC doses (–12.82 and –17.67 mL/min/1.73 m^2, P = 0.009). The reduction in eGFR in our recipients with normal baseline eGFR at month 12 after ISxC was –20.4 mL/min/1.73 m^2 (Table 3). However, when combined with recipients with baseline eGFR in the 60–89 mL/min/1.73 m^2 range, the difference between medians was –8.6 mL/min/1.73 m^2, which was comparable to the results reported by Lee (–12.82 mL/min/1.73 m^2) [12].

In contrast to Lee et al., who identified and analyzed a subgroup of recipients with GFR ≥60 mL/min/1.73 m^2, we analyzed the subgroups of recipients with eGFR >90 mL/min/1.73 m^2 and 60–89 mL/min/1.73 m^2 separately. We found that after ISxC, the pattern of changes in renal function differed in these subgroups of recipients. In the subgroup of recipients with baseline CKD stage 2, eGFR was essentially unchanged at month 12 after ISxC. We observed similar changes in eGFR in a subgroup of 35 recipients with baseline eGFR of 45–59 mL/min/1.73 m^2 (Figs. 3, 4). In 42% of recipients with baseline CKD stage 3A, there was improved renal function one year after ISxC, up to complete normalization in 17% of recipients. Lee et al. also reported an increase in eGFR to levels >60 mL/min/1.73 m^2 in 25 (51%) of 49 recipients analyzed, who received EVR and whose baseline GFR was consistent with CKD-3A, which correlates well with our results.

We observed the most significant improvement in median eGFR in patients with significantly impaired renal function (CKD-3–5). It was found that the lower the eGFR at the time of ISxC, the higher the increase in median eGFR by month 12 of follow-up. In distinguishing this subgroup, we experienced some difficulty in determining the cutoff threshold (60 or 45 mL/min/1.73 m^2) at which the positive eGFR trend becomes clearly evident (compare Table 3 – cutoff threshold 60 mL/min/1.73 m^2; and Fig. 4 – cutoff threshold 45 mL/min/1.73 m^2). In the subgroup of recipients with baseline eGFR of 45–59 mL/min/1.73 m^2, there was a trend toward increased median eGFR; changes reached the level of statistical significance by month 3 after ISxC (52.7 mL/min/1.73 m^2 and 60.0 mL/min/1.73 m^2, respectively, $p < 0.01$), but after 12 months of follow-up, median eGFR decreased slightly again (58.8 mL/min/1.73 m^2, $p > 0.05$).

We found that sex and nature of CIs had no effect on eGFR changes in our recipient population. Lee et al. included significantly more characteristics (organ from living and deceased donor, cause of LTx, race, presence of diabetes mellitus, donor sex and age) in their analysis. However, as in our case, only two factors had a statistically significant effect on eGFR increase: baseline eGFR and recipient age.

Renal failure develops in liver transplant recipients at different times. According to the TRY study, as early as one month after LTx, the eGFR remained within normal values in only 29.3% of recipients with baseline eGFR >90 mL/min/1.73 m^2 [13]. At longer follow-up, the proportion of such recipients continued to fall, being 14.3% at year 1 and only 10.5% of recipients with normal baseline eGFR at year 5 after LTx.

We showed that ISxC early after LTx resulted in a more pronounced improvement in eGFR. Moreover, the differences in eGFR increase between the subgroups of recipients who underwent ISxC in the first 2 months after LTx and 12 months after LTx were particularly pronounced at months 3–6 after ISxC. Bilbao et al. (2015) also reported that in recipients with impaired renal function who started EVR at a later date (one year after LTx), there was no improvement in GFR, or, having improved at months 3–6, GFR deteriorated again by month 12 after ISxC. When ISxC was performed in the first 12 months after LTx, GFR improvement was greater [14]. We, like the group of researchers from Spain, could not find any differences between particularly early ISxC (first 3 months after LTx) compared to ISxC done at a more distant time (within the next 9 months). Interestingly, the Spanish authors also provide maximal eGFR 3–6 months after ISxC [15]. We have not been able to find a possible explanation for this trend in eGFR after ISxC, but it has been reported by other investigators. In registration clinical trial 2304, differences in GFR between groups were detected very quickly, as early as one month after randomization, with complete distinction between groups achieved by month 4 of therapy. The maximum eGFR in the ISxC group falls within the same time period [5].

FINDINGS

1. Changes in eGFR in liver recipients who receive EVR in combination with reduced CI dose depend on baseline eGFR levels and are multidirectional in nature.
2. 60% of recipients with normal baseline eGFR show worsening CKD by the end of the first year after ISxC; the decline in eGFR is particularly pronounced in older recipients.
3. The median eGFR in the subgroup of recipients with baseline CKD stages 2 and 3A does not change significantly by the end of the first year after ISxC. Deterioration of CKD is observed in no more than 10% of recipients, and improvement in 40–62% of cases.
4. The subgroup of recipients with severely reduced eGFR at the time of ISxC showed rapid (within a month) improvement in renal function at month 12; the increase in median eGFR was the more significant the more severely impaired renal function was at baseline.
5. Performing ISxC early after LTx resulted in a more pronounced improvement in eGFR. Maximum eGFR changes were observed at months 3–6 after ISxC.

The authors declare no conflict of interest.

REFERENCES

1. *Ojo AO et al.* Chronic renal failure after transplantation of a nonrenal organ. *The New England journal of medicine*. 2003; 349 (10): 931–940.
2. *Gijsen VM et al.* Tacrolimus-induced nephrotoxicity and genetic variability: a review. *Ann Transplant.* 2012; 17 (2): 111–121.
3. *Ader JL, Rostaing L.* Cyclosporin nephrotoxicity: pathophysiology and comparison with FK-506. *Curr Opin Nephrol Hypertens.* 1998; 7 (5): 539–545.
4. *Jeng LB et al.* Efficacy and safety of everolimus with reduced tacrolimus in living-donor liver transplant recipients: 12-month results of a randomized multicenter study. *Am J Transplant*. 2018; 18 (6): 1435–1446.
5. *Saliba F et al.* Renal function at two years in liver transplant patients receiving everolimus: results of a randomized, multicenter study. *Am J Transplant*. 2013; 13 (7): 1734–1745.
6. *Levey AS et al.* Using standardized serum creatinine values in the modification of diet in renal disease study equation for estimating glomerular filtration rate. Ann Intern Med. 2006; 145 (4): 247–254.
7. *Khubutiya MSh i dr.* Dlitel'noe primenenie everolimusa v kachestve odnogo iz komponentov immunosupressivnoy terapii u retsipientov pecheni. *Transplantologiya*. 2013 (2): 23–27.

8. *Syutkin VE i dr.* Opyt primeneniya Everolimusa u bol'nykh, perenesshikh ortotopicheskuyu transplantatsiyu pecheni. *Transplantologiya*. 2012 (1–2): 10–14.
9. *Cockcroft DW, Gault MH.* Prediction of creatinine clearance from serum creatinine. *Nephron*. 1976; 16 (1): 31–41.
10. *Levey AS et al.* A more accurate method to estimate glomerular filtration rate from serum creatinine: a new prediction equation. Modification of Diet in Renal Disease Study Group. *Ann Intern Med*. 1999; 130 (6): 461–470.
11. *Gonwa TA et al.* Estimation of glomerular filtration rates before and after orthotopic liver transplantation: evaluation of current equations. *Liver Transpl*. 2004; 10 (2): 301–309.
12. *Lee SG et al.* Efficacy and Safety of Everolimus With Reduced Tacrolimus in Liver Transplant Recipients: 24-month Results From the Pooled Analysis of Two Randomized Controlled Trials. *Transplantation*. 2020.
13. *Karie-Guigues S et al.* Long-term renal function in liver transplant recipients and impact of immunosuppressive regimens (calcineurin inhibitors alone or in combination with mycophenolate mofetil): the TRY study. *Liver transplantation: official publication of the American Association for the Study of Liver Diseases and the International Liver Transplantation Society*. 2009; 15 (9): 1083–1091.
14. *Bilbao I et al.* Renal function improvement in liver transplant recipients after early everolimus conversion: A clinical practice cohort study in Spain. *Liver Transpl*. 2015; 21 (8): 1056–1065.
15. *Nogueras Lopez F et al.* Impact of Everolimus-based Immunosuppression on Renal Function in Liver Transplant Recipients. *Transplant Proc*. 2020; 52 (2): 556–558.

The article was submitted to the journal on 25.08.2021

DOI: 10.15825/1995-1191-2021-4-42-46

PATTERN OF MENSTRUAL CYCLE AFTER KIDNEY TRANSPLANT IN REPRODUCTIVE WOMEN

M.T. Khan[1], R. Hamid[1], Sh. Rashid[2], E. Jahan[2], N. Lal[1], R. Ishtiaq[1]

[1] Renal Transplant Unit, National Institute of Solid Organ and Tissue Transplantation, Dow University Hospital, Karachi, Pakistan

[2] Karachi Medical and Dental College, Karachi, Pakistan

Background. In reproductive women, transplant disturbs the menstrual cycle pattern. The two major conditions usually encountered are amenorrhea and menorrhagia. The objective of the study was to assess the pattern of menstrual cycle after kidney transplant in reproductive women. **Materials and methods.** This cross-sectional study was carried out in a public sector hospital of Karachi, Pakistan. A total 69 patients of reproductive age were included who underwent living kidney donor transplant for more than a year ago. Women having genital tract infection, using hormonal treatment, organic cause of genital tract, clotting disorder and severe cardiac and/or peripheral vascular disease were excluded. Frequency and percentages were calculated for demographic characteristics. Correlation and association analysis was calculated for type of menstruation with menstrual cycle pattern. A P-value less than 0.05 was considered statistically significant. **Results.** Majority of female included in the study aged between 35–39 years (36, 52.2%). The most frequent menstrual disturbance observed was heavy menstrual bleeding (22, 31.9%) and amenorrhea (21, 30.4%). Only 2.9% cases showed normal menstrual pattern. The cross tabulation indicated that 26.1% patients had amenorrhea, 24.6% had oligomenorrhea and 31.9% had menorrhagia. The Durbin–Watson value of 0.656 indicated a strong positive relationship between menstruation cycle pattern (dependent variable) and type of menstruation, marital status, donor's age, children and living location of the patients (independent variables). **Conclusion.** From the result of the present study, it is concluded that the reproductive age women have shown a disturbed pattern of menstrual cycle after kidney transplant. The major observation was that such patients reported amenorrhea, menorrhagia, oligomenorrhea and hypomenorrhea.

Keywords: Reproductive Women, Amenorrhea, Oligomenorrhea, Menorrhagia, Renal Transplant.

INTRODUCTION

Chronic kidney disease (CKD) is a major global health problem in about 11–17% [1]. Globally, about 37% of the CKD patients get kidney transplantation [2]. In CKD, other organ functions are also highly affected. In females, irregular pattern of menstruation has been reported in 66% to 80% of the women, leading to either amenorrhea, polymenorrhea, oligomenorrhea or heavy menstrual bleeding [3–6]. In the end stage renal disease (ESRD), the pulsatile secretion of gonadotropin releasing hormone (GnRH) is affected, eventually results in loss of release of luteinizing hormone (LH) and causing anovulation [7–9]. After kidney transplant, immunosuppressive therapy resumes ovarian function in approximately 73.9% in about one year time [10, 11]. There is little information in the literature about changing menstrual patterns after kidney transplantation. The aim of this study was to observe the post-transplant menstrual pattern in women in our local population.

MATERIALS AND METHODS

This cross-sectional study was carried out in a public sector hospital of Karachi, Pakistan during January 2018 to April 2021. Ethical considerations were followed according to Helsinki Declaration. Patients were enrolled using convenient sampling after their written informed consent. They were properly briefed about the study and were assured that their identity will remain confidential to all other than the researchers themselves. A total 69 patients of reproductive age were included who underwent living kidney donor transplant for more than a year ago. Women having genital tract infection, using hormonal treatment, organic cause of genital tract, clotting disorder and severe cardiac and/or peripheral vascular disease were excluded. A standardized proforma for data collection was developed. Data including age, marital status, number of children, living location of the patients and types of menstruation and menstruation cycle pattern were recorded via face to face interview by a research personnel. Types of menstruation was set as

Corresponding author: Muhammad Tassaduq Khan. Renal Transplant Unit, National Institute of Solid Organ and Tissue Transplantation, Dow University Hospital, Karachi, Pakistan.
Cell: +92 335 2797755. E-mail: muhammad.tassaduq@duhs.edu.pk

independent variables, while menstruation cycle pattern was defined as dependent variable. Menstrual pattern were classified into polymenorrhea <21 days, normal (22–35 days) and oligomenorrhea >35 days. Data was entered and analyzed using Statistical Package for Social Sciences (SPSS) version 20. Frequency and percentages were calculated for demographic characteristics. Correlation and association analysis was calculated for type of menstruation with menstrual cycle pattern. A *P*-value less than 0.05 was considered statistically significant.

RESULT

The demographic characteristics of study participants are shown in Table 1. Majority of female included in the study aged between 35–39 years (36, 52.2%). The menstrual cycle pattern is shown in Table 2. The most frequent menstrual disturbance observed was heavy menstrual bleeding (22, 31.9%) and amenorrhea (21, 30.4%). Only 2.9% cases showed normal menstrual pattern. The cross tabulation indicated that 26.1% patients had amenorrhea, 24.6% had oligomenorrhea and 31.9% had menorrhagia. The Durbin–Watson value of 0.656 indicated a strong positive relationship between menstruation cycle pattern (dependent variable) and type of menstruation, marital status, donor's age, children and living location of the patients (independent variables).

DISCUSSION

Kidney transplant is the best kidney replacement treatment for ESRD and poor quality of life. Usually, kidney transplant is recommended when the glomerular filtration rate (GFR) is less than 15 ml/min/1.73 cm^2. Furthermore, in other words, the kidney transplant is needed when kidney's functional ability is lost about 90%. At this stage, the body's response to medicines is nearly 10% along with further emergence of other diseases. The liver and the reproductive organ are significantly damaged by kidney failure due to high imbalance of electrolytes, fluid retention, occasional urinary output and edema. Edema occurs due to high sodium in circulation with high fluid retention, less vessel filtration leading to development of pressure on heart and brain as well [12].

The peered articles documented that in kidney transplant recipients' anovulation can be completely reversed through a series of medications and the patients can conceive and give birth in a healthy and normal manner. Moreover, start of menstruation cycle is considered as one of the major advantages of kidney transplant women of reproductive age. Patients with stable creatinine level are even more likely to attain normal menstruation cycle within six months [6].

On the other hand, high creatinine level takes time, either a year or two to restore normal ovulation. Furthermore, in women of reproductive age, the kidney disease primarily cause abnormal ovarian function. The

Table 1

Demographic Characteristics of Study Subjects

S. No	Variables	Frequency (n)	Percentage (%)
1.	**Age (Years)**		
	20–24	01	1.4
	25–29	05	7.2
	30–34	24	34.8
	35–39	36	52.2
	40 years and above	03	4.3
2.	**Marital Status**		
	Unmarried	02	2.9
	Married	57	82.6
	Separated / Divorced	10	14.5
3.	**Parity**		
	Nulliparous	09	13.0
	1–2	39	56.5
	3–4	18	26.1
	>4	03	4.3
4.	**Residence**		
	Karachi	27	39.1
	Sindh	21	30.4
	Punjab	07	10.1
	KPK	12	17.4
	Baluchistan	02	2.9
5.	**Duration of Menses**		
	>21 days	03	4.3
	21–45 days	48	69.6
	<45 days	18	26.1
6.	**Menstrual Pattern**		
	Normal	02	2.9
	Amenorrhea	21	30.4
	Oligomenorrhea	17	24.6
	Hypomenorrhea	07	10.1
	Menorrhagia	22	31.9

Table 2

Association between Menstrual Pattern and Type of Menstruation (P-value <0.0001)

S. No	Menstrual Pattern	Amenorrhea	Hypomenorrhea	Normal	Oligomenorrhea	Menorrhagia
1.	Normal (21–35 days)	3 (4.3%)	0	0	0	0
2.	Short cycle (>21 days)	18 (26.1%)	7 (10.1%)	2 (2.9%)	17 (24.6%)	4 (5.8%)
3.	Longer (<35 days)	0	0	0	0	18 (26.1%)
Total		21 (30.4%)	7 (10.1%)	2 (2.9%)	17 (24.6%)	22 (31.9%)

level of irregularity of normal hypothalamus pituitary gonadal axis is dependent on the magnitude of kidney disorder [13].

In normal health condition, the LH and follicle stimulating hormone (FSH) are metabolized by liver and kidneys. But, in case of renal disease, primarily at last stage, these hormones get raised in the bloodstream. The kidney transplantation improves metabolism of LH and FSH. Furthermore, at post kidney transplantation, usually Rapamycin inhibitors are given that assist in normalizing these reproductive hormones to restore the ovulation cycle [14].

The most frequent menstrual disturbance observed in present study was oligomenorrhea and amenorrhea. It could be due to hormonal imbalance in pre-kidney transplant phase in reproductive women. This elevated hormone prolactin occurs due to incrimination of urine wastes in blood. The kidney transplantation improves the GFR, restoring prolactin metabolism and safely eliminating the end product through urine. It has also been found that prolactin secretion is highly sensitive and is largely affected by the daily life stresses. Besides, the restoration of prolactin and testosterone level also gets normal in post-transplant phase [15].

Though menstruation is a part of normal reproductive cycle of female, it plays a significant role in women's health and easily disturbed by disease processes. It can affect both physical and psychological health. Menstrual pattern variation is frequently observed among female with CKD and after kidney transplant. The pattern of menstrual periods after kidney transplant is irregular and women experience bleeding mostly after 16 days with more than 20 ml of bleeding. Due to decreased progesterone level with high level of FSH, LH and estrogen, this condition is usually experienced by women mostly after 16 days. Our study results correlates with this finding. The hormonal irregularities shortens the luteal phase. The cycle is continued for more than 7 days. The overall prevalence of menstrual disturbances in reproductive women in CKD is reportedly 64.2% [16]. In our study, overall menstrual disturbances was found to be 69.6%. Our findings are different from others. One study showed no difference between bleeding pattern before and after transplantation [17]. Another case-control study showed regular menstrual cycle in 72.7%. This result did not correlate with our findings and this might be due to data collection which was done after 1–5 years post-transplantation. Thus, the duration was long as compared to our study [18].

Usually, after six months of kidney transplantation, the normal ovarian cycle restoration occurs. The hormonal therapy reduces the thickness of endometrium with ameliorating the FSH, LH, estrogen and progesterone. The inhibin hormone causes to stop the cycle with 7 days of bleeding of less than 10 ml. Furthermore, it also improves the ovulatory phase that assists in normal formation of endometrium [19]. The cycle is repeated after 24 to 31 days with normal releasing and inhibin pattern. The 5 days of menstruation is with 5 ml to 8 ml blood [20]. The result on cycle length shows 69.6% of the females reported menstrual cycle shorter than 21 days and 26.1% had menstrual cycle longer than 35 days. Earlier studies did show variable results regarding cycle length. The result of the present study showed a significant association between menstrual pattern and type of menstruation (P-value <0.0001).

The findings of our study showed higher incidence of menstrual pattern disturbance. However, our study findings are limited by studying of only clinical symptoms and their relations. Further exploratory research in this regard is needed.

CONCLUSION

From the result of the present study, it is concluded that the reproductive age women have shown a disturbed pattern of menstrual cycle after kidney transplant. The major observation was that such patients reported amenorrhea, menorrhagia, oligomenorrhea and hypomenorrhea. Adopting healthy life style is of utmost importance and can significantly reduce the number of affected individuals and burden of this underestimated disease.

We thank to all patients participating in the study, without whom this study would not have been possible.

The authors declare no conflict of interest.

REFERENCES

1. *Sarada SG, Ramalakshmi S.* Menstrual disorders in chronic kidney disease: causes and management. *Int J of Clinic Obstet and Gynaecol*. 2020; 4 (2): 353–358.
2. *Nastasi AJ, McAdams-DeMarco MA, Schrack J, Ying H, Olorundare I, Warsame F et al*. Pre-kidney transplant lower extremity impairment and post-kidney transplant mortality. *American Journal of Transplantation*. 2018 Jan; 18 (1): 189–196. https://onlinelibrary.wiley.com/doi/abs/10.1111/ajt.14430.
3. *Lin C-T, Liu X-N, Xu H-L, Sui H-Y.* Menstrual Disturbances in Premenopausal Women with End-Stage Renal Disease: A Cross-Sectional Study. *Med Princ Pract*. 2016; 25: 260–265. doi: 10.1159/000444879.
4. *Fayed A, Soliman A, Naguib M, Soliman M, Salaheldin M.* Ovarian reserve in an Egyptian cohort with end-stage kidney disease on hemodialysis and after successful kidney transplantation: a prospective study. *International urology and nephrology*. 2019 Apr; 51 (4): 737–743. https://link.springer.com/article/10.1007/s11255-019-02089-2.
5. *Sikora-Grabka E, Adamczak M, Kuczera P, Wiecek A*. Serum sex hormones concentrations in young women in the early period after successful kidney transplantation. *Endokrynologia Polska*. 2018; 69 (2): 150–155. https://

journals.viamedica.pl/endokrynologia_polska/article/view/51921.

6. *Schmidt E, Pachtman SL, Diedrich JT*. Contraception in Chronic Kidney Disease and Renal Transplantation. In Obstetric and Gynecologic Nephrology 2020 (pp. 225–243). *Springer, Cham*. https://link.springer.com/chapter/10.1007/978-3-030-25324-0_16.
7. *Sarkar M, Bramham K, Moritz MJ, Coscia L*. Reproductive health in women following abdominal organ transplant. *American Journal of Transplantation*. 2018 May; 18 (5): 1068–1076. https://onlinelibrary.wiley.com/doi/abs/10.1111/ajt.14697.
8. *Wiles KS, Nelson-Piercy C, Bramham K*. Reproductive health and pregnancy in women with chronic kidney disease. *Nature Reviews Nephrology*. 2018 Mar; 14 (3): 165. https://www.nature.com/articles/nrneph.2017.187.pdf?origin=ppub.
9. *Serret-Montaya J, Zurita-Cruz JN, Villasís-Keever MA, Aguilar-Kitsu A, del Carmen Zepeda-Martinez C, Cruz-Anleu I et al*. Hyperprolactinemia as a prognostic factor for menstrual disorders in female adolescents with advanced chronic kidney disease. *Pediatric Nephrology*. 2020 Jun; 35 (6): 1041–1049. https://link.springer.com/article/10.1007/s00467-020-04494-7.
10. *Ashuntantang GE, Garovic VD, Heilberg IP, Lightstone L.* Kidneys and women's health: key challenges and considerations. *Nature reviews Nephrology*. 2018 Mar; 14 (3): 203. https://www.nature.com/articles/nrneph.2017.188.pdf?origin=ppub.
11. *Chandra A, Midtvedt K, Åsberg A, Eide IA*. Immunosuppression and reproductive health after kidney transplantation. *Transplantation*. 2019 Nov 1; 103 (11): e325–e333. https://journals.lww.com/transplantjournal/FullText/2019/11000/Immunosuppression_and_Reproductive_Health_After.9.aspx.
12. *Piotti G, Gandolfini I, Palmisano A, Maggiore U.* Metabolic risk profile in kidney transplant candidates and recipients. *Nephrology Dialysis Transplantation*. 2019 Mar 1; 34 (3): 388–400. https://academic.oup.com/ndt/article-abstract/34/3/388/5003174.
13. *Bonthuis M, Groothoff JW, Ariceta G, Baiko S, Battelino N, Bjerre A et al*. Growth patterns after kidney transplantation in European children over the past 25 years: an ESPN/ERA-EDTA registry study. *Transplantation*. 2020 Jan 1; 104 (1): 137–144. https://journals.lww.com/transplantjournal/fulltext/2020/01000/Growth_Patterns_After_Kidney_Transplantation_in.27.aspx.
14. *Schmitz R, Fitch ZW, Xu H, Ghali A, Mehta AK, Guasch A, Kirk AD.* Kidney transplantation using alemtuzumab, belatacept, and sirolimus: Five-year follow-up. *American Journal of Transplantation*. 2020 Dec; 20 (12): 3609–3619. https://onlinelibrary.wiley.com/doi/abs/10.1111/ajt.16121.
15. *Lin C-T, Liu X-N, Xu H-L, Sui H-Y.* Menstrual Disturbances in Premenopausal Women with End-Stage Renal Disease: A Cross-Sectional Study. *Med Princ Pract.* 2016; 25: 260–265. doi: 10.1159/000444879.
16. *Kudrytskaya A, Doronina O, Kalachik O.* Aspects of reproductive state in women after kidney transplantation. In 22nd European Congress of Endocrinology. 2020 Aug 21 (Vol. 70). BioScientifica. https://www.endocrine-abstracts.org/ea/0070/ea0070ep403.
17. *Karyalcin R, Genc V, Oztuna D, Huseynova N, Ercoz S.* Gynecologic symptoms and sexual function in female kidney allograft recipients. *Transplant proc*. 2010 Sep; 42 (7): 2551–2555.
18. *Pietrrzak B, Wielogos M, Kamniski P, Jabiry-Zieirwicz Z, Bobrowska K.* Menstural cycle and sex hormone profile in kidney transplanted women. *NeuroEndorinol Lett*. 2006 Feb-Apr; 27 (1–2).
19. *Laguerre M, Bouvier N, Guleryuz K, Doerfler A, Parienti JJ, Ait Said K, Tillou X.* Sexual Dysfunction Improvement after Kidney Transplantation: A Prospective Study in Men and Women. *International Journal of Sexual Health*. 2020 Nov 13: 18 https://www.tandfonline.com/doi/abs/10.1080/19317611.2020.1842575.
20. *Serret-Montaya J, Zurita-Cruz JN, Villasís-Keever MA, Aguilar-Kitsu A, del Carmen Zepeda-Martinez C, Cruz-Anleu I et al*. Hyperprolactinemia as a prognostic factor for menstrual disorders in female adolescents with advanced chronic kidney disease. *Pediatric Nephrology*. 2020 Jun; 35 (6): 1041–1049. https://link.springer.com/article/10.1007/s00467-020-04494-7.

The article was submitted to the journal on 7.08.2021

DOI: 10.15825/1995-1191-2021-4-47-61

ANTIBODY-MEDIATED REJECTION IN HEART TRANSPLANTATION

V.S. Kvan[1], N.N. Koloskova[1], Yu.A. Kachanova[1], N.N. Sayfullina[1], A.Yu. Goncharova[1], L.B. Krugly[1], A.O. Shevchenko[1–3]

[1] Shumakov National Medical Research Center of Transplantology and Artificial Organs, Moscow, Russian Federation

[2] Sechenov University, Moscow, Russian Federation

[3] Pirogov Russian National Research Medical University, Moscow, Russian Federation

The role of antibody-mediated rejection in predicting survival among heart recipients has been studied in clinical transplantology for over 20 years. This condition is a significant risk factor for heart failure and graft vasculopathy. Antibody-mediated rejection results from activation of the humoral immune system and production of donor-specific antibodies that cause myocardial injury through the complement system. The presence of donor-specific antibodies is associated with lower allograft survival. Treatment of antibody-mediated rejection should take into account the rejection category and the presence or absence of graft dysfunction. The main principle of treatment is to suppress humoral immunity at different levels. World clinical practice has made significant inroads into the study of this issue. However, further research is required to identify and develop optimal treatment regimens for patients with humoral rejection in cardiac transplantation.

Keywords: antibody-mediated (humoral) rejection, graft dysfunction, donor-specific antibodies, heart transplantation.

INTRODUCTION

It took about 25 years to recognize antibody-mediated rejection (AMR), also known as humoral rejection, as an independent disease, develop diagnostic criteria and treatment regimens [1]. The first reports on this new type of heart transplant rejection in the absence of lymphocytic infiltration in biopsy specimens appeared in the late 1980s [2]. Moreover, it was only in 2003 that the first conference dedicated to this issue was held at the National Institute of Health [3]. Over time, the role of complement component deposition in tissues and immune damage to the heart graft has been increasing [4].

In 2010, an international consensus conference was held by the International Society for Heart and Lung Transplantation (ISHLT) to discuss the current status of AMR in heart transplantation. The conference included 67 heart transplant centers defined the criteria for a preliminary pathological diagnosis of AMR and introduced the concept of asymptomatic humoral rejection, which has an impact on patient and allograft survival. Guidelines were made for the timing for specific staining of endomyocardial biopsy specimens. Guidelines for management and future clinical trials were also provided [5]. In 2013, under the leadership of Kobashigawa J.A., director of the severe heart disease department at Cedars-Sinai Medical Center, Los Angeles, the pathological criteria for antibody-mediated heart graft rejection were standardized [1], under which AMR began to be considered as a pathologic diagnosis regardless of the presence or absence of graft dysfunction. The paper also outlined the timing of routine monitoring of donor-specific antibodies (DSA).

Endomyocardial biopsy (EMB) with histological examination of biopsy specimens, immunoperoxidase test and immunofluorescence reaction for complement component C4d performed 2 weeks, 1, 3, 6 and 12 months after transplantation were required for diagnosis of humoral rejection. The presence of complement deposits suggested the presence of AMR. Circulating DSA were monitored by solid-phase analysis also at 2 weeks, 1, 3, 6, and 12 months after transplantation [1].

Circulating antibodies may not always be detected in patients with clinical and pathological signs of AMR, but they can be detected in asymptomatic patients [6]. AMR diagnosis requires clinical manifestations of graft dysfunction, morphological changes in EMB in the form of microvascular damage due mainly to deposition of complement component C4d, and the presence of circulating DSA. Despite the prognostic importance of each of these three criteria [7], once at least two of them are detected, specific treatment should be initiated [8].

Initial AMR therapies included pulse therapy with glucocorticoids, plasmapheresis, and intravenous (IVIg) immunoglobulin infusion. Later these methods were supplemented with rituximab, bortezomib, and complement component antibodies [3]. The use of basic immunosuppressive therapy with tacrolimus and microphenolate mofetil has been shown to be most effective in preventing AMR with the fewest side effects [9].

Corresponding author: Vera Kvan. Address: 1, Shchukinskaya str., Moscow, 123182, Russian Federation.
Phone: (966) 326-28-24. E-mail: vergy2008@mail.ru

AMR classification

According to current diagnostic criteria, routine EMB remains the criterion standard for diagnosing AMR. It is classified into antibody-mediated rejection (pAMR) grades 0–3 depending on the presence of specific histological and immunopathological changes that are either present in isolation pAMR-1 (suspected humoral rejection), or in combination pAMR-2 (confirmed humoral rejection), and pAMR-3 (severe humoral rejection) [8]. The classification is presented in Table 1.

Prevalence

Due to the large number of constantly changing diagnostic criteria for AMR (which included both histopathological changes in EMB and presence/absence of clinical manifestations), as well as the varying frequency of screening studies performed, the prevalence of AMR detected by biopsy varied considerably between 3% and 85% in different sources (starting from 1986) [10].

According to Kfoury et al, prevalence of humoral rejection by 100 days after heart transplantation (HTx) was 85%, using as diagnostic criteria histological changes and immunofluorescence data obtained from routine endomyocardial biopsy in 870 heart recipients [11].

The Michaels et al. study of humoral heart transplant rejection enrolled 600 patients. During the follow-up period from July 1997 to January 2001, AMR was detected in 56 recipients, who underwent a total of 116 biopsies. Of this group of patients, a total of 44 patients (4 to 74 years old, 77 EMBs) showed evidence of isolated AMR, 12 patients had mixed AMR and cellular rejection. AMR was diagnosed by immunofluorescence (presence of immunoglobulin, deposition of complement components C1q and C3 in capillaries, or presence of CD58+ cells in immunoperoxidase assay) as well as by histological criteria (interstitial edema, microthrombosis). It should be noted that although females comprised only 26% of the studied cohort, 23 out of the 44 patients (52%) with humoral rejection were female. Moreover, women had a higher prevalence of heart transplant dysfunction (65%) [12].

Crespo-Leiro et al [13] reported an AMR prevalence of <3%, when using the criteria of graft dysfunction and complement component C4d deposition in capillaries. Using the 2004 and 2006 ISHLT criteria, which included, among others, graft dysfunction, serologic evidence of DSA, and evidence of complement component deposition in capillaries in EMB, AMR incidence was 3% and 5%, respectively [14].

Table 1

ISHLT AMR grading scale (2011)

Grade	Pathological signs
pAMR 0 No AMR	No histologic or immunologic signs of AMR, no DSA detected.
pAMR 1 (H+) Histopathologic AMR	Only histologic changes, no DSA.
pAMR 1 (I+) Immunohistochemical AMR	High titer of DSA in blood plasma as well as products of activation of complement components, fibrin and its degradation products are detected.
pAMR 2 Positive AMR	Both histological and immunopathological signs of AMR.
pAMR 3 Severe AMR	Interstitial hemorrhages, capillary edema and fragmentation, necrotizing vasculitis, myocardial mononuclear infiltration, pycnosis of nuclei and karyorexis. Heart failure increases rapidly and there is a high risk of graft loss.

AMR, antibody-mediated rejection; pAMR, pathological antibody-mediated rejection category; DSA, donor-specific antibody.

Table 2

AMR risk factors [10, 12, 15]

1. Female gender
2. Presence of DSA
3. High panel-reactive antibody index (PRA)
4. Presence of cytomegalovirus infection according to serological study
5. A history of mechanical circulatory support
6. Use of muromonab-CD3 as induction therapy and development of murine monoclonal antibodies
7. Heart retransplantation
8. Number of pregnancies
9. Positive cross-match test

Risk factors for humoral rejection

AMR risk factors are presented in Table 2.

It should be noted that AMR is significantly more common in women than in men, and its prevalence reaches 50% of the total number of heart recipients (despite the fact that women undergo heart transplantation much less frequently than men. Currently, the presence of circulating anti-human leukocyte antigen antibodies (anti-HLA antibodies) and histological signs of AMR has been found to have a strong correlation [16, 17].

AMR pathogenesis

The development of AMR is due to the recipient's immune response consisting in the production of DSA directed against HLA and other non-HLA antibodies that may be expressed on the vascular endothelium of the allograft [18].

The pathological process initiated by the antigen-antibody reaction is localized mainly on the vascular endothelium of the allograft. In some cases, the graft may develop resistance to antibody-mediated reactions, and in others ischemic damage occurs, which is accompanied by diffuse myocardial damage, graft dysfunction with development of heart failure, and cardiac allograft vasculopathy (CAV) [4].

DSA-induced damage can occur without the involvement of the complement system. The most potent complement activators are IgG3, but IgG4 may also be involved and often bind to IgG2 in a "non-complement-fixing complex" [19].

It should be noted that a polyclonal immune reaction usually occurs against HLA epitopes, in which several IgG subclasses are involved, leading to different allograft damage mechanisms. Thus, the relationship between AMR and the complement system, previously considered a must, is now becoming a subject of debate, since AMR may develop even in the absence of deposition of complement components in the capillaries [18].

Prognosis

Humoral rejection can lead to graft dysfunction and increased mortality in cardiac recipients, as well as increased incidence of CAV [20].

Clerkin K.J. et al. at Columbia University Medical Center, USA, conducted a single-center retrospective cohort study that included 689 patients with humoral rejection detected at different times after heart transplantation. More than one-third of patients were diagnosed with AMR late after surgery (mean 1,084 days), with the remaining recipients having a median AMR of 23 days. Graft dysfunction was less common with early rejection (25.6); further survival prognosis in this group of patients did not differ from the non-AMR recipients. In contrast, more than half of patients with late AMR (56%) had graft dysfunction. In addition, late AMR correlated with a higher incidence of CAV (50% at 1 year) and higher mortality. The authors suggest that antibody-mediated endothelial damage and the development of microvascular inflammation lead to the development of CAV [21].

In the Michaels et al. study, hemodynamic abnormalities were detected in 47% of recipients. One year after transplantation, AMR patients had a higher CAV prevalence than the controls (15% vs. 5%, $p = 0.09$). After 5 years, 86% of AMR patients had CAV, compared with 22% of controls) [12, 20].

Detection of antibody-mediated allograft rejection within 1 year after transplantation, late diagnosis of chronic AMR combined with graft dysfunction is associated with 50–60% mortality [22].

DONOR-SPECIFIC ANTIBODIES

A study by Manfredini V. et al. showed that the detection of donor-specific antibodies serves as an accurate prognostic marker of antibody-mediated rejection, but nevertheless may not have clinical significance. To stratify the risk of AMR complications and develop a treatment strategy, it is necessary to determine the DSA subclasses and complement binding activity [18].

Pre-HTx DSA is a known risk factor for poor allograft and recipient survival, especially in the first year after surgery [23].

The presence of HLA antibodies in the blood of heart recipients ("humoral sensitization") has been shown to be accompanied by increased incidence of acute graft rejection and poorer patient survival [24].

CAV is the main cause of graft dysfunction in the long-term period (5–7 years) after surgery. CAV is multifactorial in nature, involving both immune and non-immune mechanisms. HLA antigen mismatches are often noted in heart transplantation, which implies that DSA production after transplantation may contribute to the progression of this disease [23].

In global clinical practice, de novo donor-specific antibodies (dnDSA) are detected using a Luminex-based solid-phase crossmatch assay. A noninvasive biomarker is used to identify patients at increased risk of AMR. The versatility of Luminex-based solid-phase analysis lies not only in the risk stratification and prediction of allograft rejection before transplantation, but also in the possibility of performing screening studies in order to monitor the effectiveness of the therapy in the perioperative period [25].

Detection of HLA antigens A, B and DR and measurement of sensitization to them play an important role in the examination of cardiac recipients. Besides, blood testing of potential cardiac recipients for circulating HLA antibodies to determine the panel-reactive antibody index (PRA) is generally accepted. PRA test result is usually presented as a percentage of panel reactivity (that is, the ratio of the number of wells with positive reactivity to the total number of wells ×100). If there is a significant increase in PRA, a targeted test of the recipient's blood against the lymphocytes of the potential donor – a crossmatch reaction – is required.

Indications for treatment of sensitized patients before heart transplantation vary considerably. Betkowski et al. of St. Louis University Medical Center, Missouri, interviewed the heads of 65 centers involved in organ transplantation in the United States about the use of PRA study protocols and treatment of sensitized patients at these centers. Such treatment was provided at 39 of the

65 centers surveyed. Treatment programs included intravenous immunoglobulin (IVIg) infusion (21 of 39, 53.8%), plasmapheresis (17 of 39, 43.6%), administration of cyclophosphamide (11 of 29, 28.2%), mycophenolate mofetil (9 of 39, 23.1%) and azathioprine (1 of 39, 2.6%).

In some of the protocols, treatment was given before transplantation regardless of PRA index (9 of 39, 23.1%) or immediately before surgery (6 of 39, 15.4%), and 4 centers used an individualized approach to recipient management (4 of 39, 10.2%). In five programs, therapy was given only to sensitized patients on mechanical circulatory support (MSC).

Similarly, another single-center study suggested that heart recipients with pre-existing T and B lymphocyte PRA = 10%, despite a negative crossmatch reaction by the time of transplantation, have earlier and more severe rejection episodes with significantly lower survival rates [26].

A retrospective analysis of data from 19,443 cardiac recipients from the UNOS registry between October 1987 and December 1996 showed that an elevated PRA (20%) correlates with a significantly higher risk of mortality. The risk progressively increases in parallel with the PRA index and higher in MCS patients [24].

The cross-match reaction in cardiac recipients is usually performed in the presence of an elevated pretransplant PRA. Humoral sensitization can occur due to previous hemotransfusions, pregnancies, and the use of MCS as a "bridge" to transplantation.

In a retrospective cohort study conducted by Nwakanma et al, the association between post-transplant PRA index and three primary end points, patient survival, allograft survival, and development of rejection within 1 year of transplantation were analyzed in primary heart recipients (all patients who underwent heart transplantation were excluded) from January 1, 2000 to December 31, 2004.

PRA testing prior to heart transplantation was performed in a total of 8,160 primary heart recipients. All patients were divided into 4 groups: PRA was 0% in 6,481 (79.4%) patients (group 1), 1% to 10% in 930 (11.4%) patients (group 2), 11% to 25% in 309 (3.8%) patients (group 3), and >25% in 440 (5.4%) patients (group 4).

The groups of patients with an elevated PRA were distinguished by their younger age, higher proportion of women, and lower body mass index. These groups also included a greater number of patients with a history of hemotransfusion before transplantation or who had a congenital heart defect or were on the waiting list for a long time.

Patients with a PRA >25% had a statistically significant increase in the risk of rejection within 1 year.

In a study by Loh et al. including 125 heart recipients, it was found that increased PRA (>25%) by the time of transplantation may be a risk factor for poor long-term survival [27].

Lavee et al., conducted a cohort study of 463 heart recipients and found that a PRA >10% serves as a risk factor for rejection and related complications, and a negative lymphocytotoxic cross-match test in patients with elevated PRA does not reduce the risk of death from acute and chronic rejection. In addition, PRA and duration of acute rejection episodes in the first 3 months after transplantation were found to have a positive linear relationship [28].

These findings were supported by Kobashigawa et al, who also found that patients with a PRA >11% at the time of transplantation had more severe rejection episodes with significantly lower post-transplant survival despite a negative cross-match response [26]. In addition, the proportion of sensitized patients increased with increasing frequency of MCS as a "bridge" to transplantation [29].

Sensitized patients with PRA >25% had a statistically significant increase in the risk of rejection compared to patients with PRA of 0%.

Patients with PRA >0% had a poorer post-transplant prognosis compared to patients without PRA; so, their careful evaluation before transplantation is required. Patients with PRA >25% have a particularly high risk of rejection, so they are advised to perform a cross-match reaction [30].

Anti-HLA to donor lymphocytes are detected in 3–11% of patients at the time of heart transplantation, while dnDSA (predominantly anti-HLA class II) develops after transplantation in 10–30% of patients. Although, isolated detection of DSA in heart recipients is not considered a histologic criterion for diagnosis of humoral rejection, circulating DSA is found in almost all AMR cases. The treatment of patients with DSA before and after heart transplantation varies, but most centers treat this case with plasmapheresis or immunoadsorption with intravenous infusion of rituximab and/or immunoglobulin.

In recent years, there has been a significant decrease in the incidence of early allograft rejection after orthotopic heart transplantation (OHT). Currently, only 12% of heart recipients require rejection treatment within the first year after transplantation. The goal of treatment is increasingly becoming to prevent AMR, a major risk factor for mortality, leading to 35–40% mortality within 5 years after heart transplantation [31]. Chronic AMR, often combined with rapidly progressing CAV, plays an important role in the development of graft dysfunction [32]. There is a growing body of evidence indicating that DSA are involved in speeding up CAV development [7].

DSA and survival outcomes after heart transplantation

There is strong evidence of a significant increase in the risk of graft loss and mortality in heart recipients with DSA [33]. In a study involving 213 adult patients (mean follow-up at antibody measurements was 7 years), the overall survival of DSA-positive patients after 5, 10, and 15 years were 89.3%, 80.3%, and 53.6%, respectively, compared with 98.4% after 5 years and 97.3% after 10 and 15 years for a control group of non-DSA patients (only long-term survivors were examined during routine follow-up visits) [34]. This study did not distinguish between pre-transplantation DSA and de novo DSA rates, but there is a clear difference in survival in patients with pre-existing DSA or dnDSA.

Reinsmoen et al. evaluated outcomes in 295 adult heart recipients, 14 of whom had DSA at the time of transplantation and persisted after surgery, and 32 developed dnDSA [33]. At 2 years after transplantation, persisting pre-existing DSA group had 100% graft survival compared with 73% survival in the dnDSA group.

Clerkin et al. had similar results in a cohort study of 221 consecutively enrolled adult patients with a mean follow-up of 3.5 years [6]. Patients who died within the first 30 days were not included in the study. The highest survival rate was seen in patients with pre-existing DSA, and was higher than in patients without DSA. In contrast, 69 patients with dnDSA had a significantly lower survival rate than patients who did not have DSA (p = 0.027) (Fig. 1).

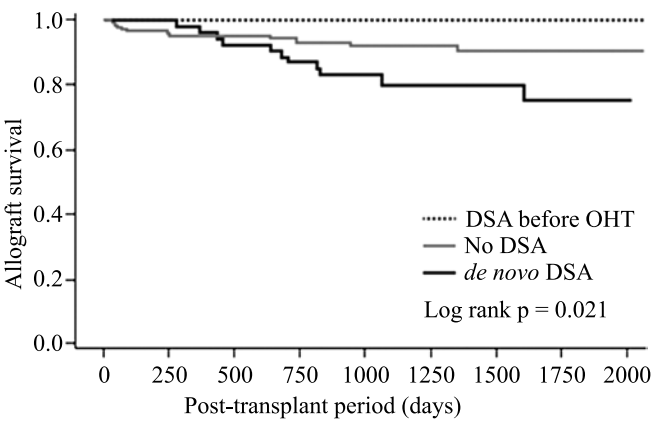

Fig. 1. Allograft survival without adverse events in heart recipients included in the study. DSA, donor-specific antibody; OHT, orthotopic heart transplantation

Table 3

Multivariate analysis of the association between persistent de novo DSA (n = 48) and mortality risk in 243 adult heart recipients in a single-center study. Anti-HLA were measured annually (maximum follow-up was 13 years) [31]

Indicator	Risk ratio	CI 95%	P
Persistent DSA de novo	4.33	1.92, 9.76	**<0.001**
HLA-DR miss-match	2.33	1.08, 5.05	0.032
Donor's age	1.03	1.00, 1.08	0.26
Hemodynamic compromise	0.36	1.00, 5.58	0.050
Treatment of rejection by 1 year after OHT	0.42	1.83, 0.95	0.038

HLA, human leukocyte antigens; DSA, donor-specific antibody; OHT, orthotopic heart transplantation.

De novo DSA

Smith et al. analyzed 243 adult heart recipients with a follow-up period of 13 years. It was found that dnDSA had a significant effect on the risk of adverse events: the hazard ratio (HR) was 3.067 for dnDSA (n = 57) compared with patients who had no HLA antibodies (n = 116). According to multivariate analysis, dnDSA increased the risk of mortality more than any other factor in both adult and pediatric recipients (Table 3) [23]. In a study by Tran et al, 5-year graft survival was 21% in dnDSA patients compared with 72% in patients who had no DSA in a cohort of 105 pediatric heart recipients (p < 0.001%) [7].

There are limited data on the effect of the timing of dnDSA in transplanted heart patients. Ho et al. examined HLA antibodies in 799 heart recipients based on analysis of routine biopsies performed within 15 years of heart transplantation [35]. There was no difference between DSA and non-DSA anti-HLA; however, there was a clear difference in long-term survival between patients who developed DSA before 1 year after transplantation (n = 221) compared with DSA arising at a later date (n = 118). Survival rates were 52% and 40%, respectively, compared with 70% in patients who had no antibodies (p < 0.05 and p < 0.001, respectively).

DSA and cardiac transplant vasculopathy

AMR is common in patients with CAV. Late onset of AMR or asymptomatic AMR is accompanied by a higher risk of developing CAV [36]. There is a possibility that DSA occurring in humoral rejection are involved in CAV development. Moreover, isolated DSA can cause direct damage to endothelial cells by activation and fixation of complement component C4d or acting on natural killer cells (NK-cells) and macrophages, potentially contributing to accelerated progression of atherosclerosis [37].

In a retrospective analysis of 213 patients, Kaczmarek et al. proved that CAV is significantly more common with long-term follow-up in patients with pre-existing or de novo DSA. Significant differences with patients without DSA appeared approximately six years after heart transplantation, reflecting the progressive nature of this disease [34]. The time interval between development of DSA and graft dysfunction due to vasculopathy can be

many months or even years due to slow progression of stenotic arterial disease [38].

Presence of DSA in sensitized patients

Sensitized patients awaiting heart transplantation have a high waitlist mortality because of the difficulty in matching a transplant with a cross-match reaction. Therefore, treatment strategies for patients with anti-HLA should be used. Several studies indicate comparable survival rates in both sensitized adults and children with a positive cross-match reaction compared to patients with negative test results [39, 40]. Various treatment regimens have been studied, including plasmapheresis with or without rituximab, therapy with IVIg [41], CD52 monoclonal antibodies (alemtuzumab), proteosome inhibitors (bortezomib) or complement inhibitors (eculizumab) [42]. Nevertheless, the choice of optimal pre-transplant treatment aimed at improving immunological compliance remains a matter of debate due to low-quality studies involving small cohorts of patients with a short follow-up period [42].

It remains unclear when anti-HLA treatment should be initiated. The timing of transplantation cannot be predicted, so delaying treatment until a donor heart is available would require a very short protocol. On the other hand, preventive intervention while on the waiting list puts patients at increased risk of infection and also creates the possibility of anti-HLA reappearance before transplantation.

As one would expect, sensitizing factors such as re-transplantation, pregnancy, hemotransfusion, or acute rejection (an indicator of a high immunological response) are also associated with the development of high dnDSA levels. Godown et al, directly examined risk factors for dnDSA in a cohort of 121 pediatric heart recipients, 40 of whom developed dnDSA at a mean follow-up of 4.1 years. In a multivariate analysis, only mechanical circulatory support during transplantation, the Negroid race, and donor death from gunshot wounds showed a clear correlation with development of DSA [43].

Rafiei et al. conducted a retrospective study of 196 nonsensitized patients evaluating the effect of immunosuppression on antibody production after heart transplantation. On induction therapy with rabbit antithymocyte globulin (rATG), the proportion of patients who did not develop de novo antibodies one year after surgery was significantly higher (total dose 4.5–7.5 mg/kg) compared to patients without cATG (89% vs 71%, $p = 0.043$) [44]. It is assumed that the mechanism of action of rATG lies in inhibition of pre-existing memory T cells responding to donor antigens and, possibly, apoptosis of DSA-producing plasma cells [45].

Treatment tactics for recipients with DSA in world practice

Barten M.J. et al. collected current information on the diagnosis and management strategies for DSA recipients at 15 centers in Germany, Austria, and Switzerland (including one pediatric specialty center) (Table 4). Between 2006 and 2016, 3,456 heart transplants were performed at these centers. Routine DSA monitoring after HTx was performed in 80% of the centers. The first study of DSA levels was performed between 0 and 90 days after surgery, followed by monitoring at 3, 6, and 12 months. One year after transplantation, anti-HLA levels were screened less frequently (every 3–12 months). All centers examined DSA levels in cases of primary or idiopathic graft dysfunction; in most centers, the presence of DSA was evaluated when acute rejection or allograft vasculopathy developed. Luminex-based solid-phase analysis was universally used; C1q monitoring, complement-dependent cytotoxicity, and flow cytometry were used less frequently. Two-thirds of the centers considered thresholds of mean immunofluorescence intensity (1000–3000) of dnDSA against HLA classes I or II when deciding whether to initiate treatment or not [22].

TREATMENT TACTICS

To date, there is no unified standard for the treatment of humoral heart transplant rejection. Treatment tactics vary considerably from country to country, due to the lack of optimal screening and treatment protocols [22].

The basic immunosuppression protocol includes various combinations of calcineurin inhibitors (cyclosporine or tacrolimus), antimetabolites (mycophenolic acid preparations, azathioprine), proliferative signal inhibitors (sirolimus or everolimus) and corticosteroids (prednisolone, methylprednisolone) [46].

In the United States, Kobashigawa et al. conducted a randomized trial evaluating the efficacy of three different immunosuppressive regimens: (1) cyclosporine, mycophenolate mofetil and corticosteroids; (2) tacrolimus, mycophenolate mofetil and corticosteroids; (3) tacrolimus, sirolimus and corticosteroids. The study included 334 patients over 18 years of age. The end point was either 2R cellular rejection or humoral rejection of the graft with impaired hemodynamics. The follow-up period was one year. The result of the study showed a significant reduction in rejection incidence with both tacrolimus/sirolimus (35.1%) and tacrolimus/mycophenolate mofetil (42.1%) compared with cyclosporine/mycophenolate mofetil (59.6%) [5].

However, a study by Nguyen V.P. et al. showed different results. According to the 2020 publication, adequately chosen induction and immunosuppressive therapy can reduce AMR risk. Stable patients with high risk of

AMR can be transferred to proliferative signal inhibitors (sirolimus, everolimus), which will reduce the incidence of graft rejection [47].

Principles of treatment for humoral rejection include removal of circulating antibodies, reduction of additional alloantibody production, and suppression of T cell and

Table 4

Diagnosis and treatment in DSA detection: key criteria according to a 2017 study from 15 heart transplant centers in Germany, Austria, and Switzerland. Data for each section do not fully converge depending on center

Number of heart transplants	3,456 in all 15 centers from 2006 to 2016. Adults and children Average number of transactions per year: 21
Pre-transplant HLA antibody treatment (a)	Plasmapheresis (pre- and perioperative): 100% Immunoadsorption: 53% Immunoglobulin treatment (pre- and perioperative): 100% Rituximab – 73% Bortezomib – 33% rATG (perioperative): 67% (8/10 thymoglobulin, 2/10 neovil)
Baseline immunosuppression in sensitized patients	Tacrolimus: 87% Cyclosporine: 40% Mycophenolic acid: 100% Everolimus: 13% GCs: 100%
Standard DSA monitoring after transplantation	Conducted in 80% of centers. 6/12 started at month 1, 4/12 at month 3, 1 at day 0, 1 on the day of inclusion in the waiting list. After 3 months, monitoring every 3–6 months until 1 year in all 12 centers where routine monitoring was performed. 7/12 centers continued screening at least once a year after 12 months.
Monitoring of DSA levels after cardiac transplantation in clinical manifestations	The centers conducted a DSA study for the following events: Acute rejection: 93% Graft vasculopathy: 67% Primary graft dysfunction: 100% Idiopathic graft dysfunction: 100%
DSA detection methods	Luminex: 100% C1q: 33% pre-transplant, 20% post-transplant Complement-dependent cytotoxicity: 53% before and 73% after transplantation Flow cytometry: 20%
Mean immunofluorescence intensity threshold at which treatment for DSA was considered	Treatment was conducted in 40% Among the 4 centers, thresholds were: HLA DSA I: 1000–1500 in 3/4 centers, 3000 in 1/4 center HLA DSA II: 1000–1500 in 3/4 centers, 3000 in 1/4 center
Criteria for initiation of treatment for dnDSA	dnDSA alone: 60% dnDSA + echocardiographic signs of graft dysfunction: 100% dnDSA + AMR: 100% dnDSA + allograft dysfunction: 73%
DSA treatment	Immunoglobulins: 79% Rituximab: 79% Immunoadsorption: 50% rATG: 50% (4/7 thymoglobulin, 3/7 Neovia) Plasmapheresis: 43% Extracorporeal photopheresis: 29% Basiliximab: 14% Bortezomib: 7%
Changes in immunosuppressive therapy when dnDSA is detected	Conducted: 64% 7 centers provided information: Tacrolimus dose escalation: 2/7 Replacing cyclosporine with tacrolimus: 1/7 Replacing mycophenolate mofetil with everolimus: 3/7 rATG: 1/7 (thymoglobulin)

HLA, human leukocyte antigens; dnDSA, de novo donor-specific antibodies; GCs, glucocorticoids; DSA, donor-specific antibody; rATG, rabbit anti-thymocyte globulin.

B cell responses. The ISHLT guidelines for AMR treatment are based on the current consensus and have the C evidence level [20].

Methods of treatment of humoral rejection are based on the following principles:

– Suppression of T cell response;
– Elimination of circulating antibodies;
– Inhibition of residual antibodies;
– Suppression or depletion of B cells;
– Suppression or depletion of plasma cells;
– Complement inhibition.

Fig. 2 shows the use of specific treatments for different clinical scenarios, taking into account the degree of humoral rejection, the presence or absence of DSA and graft dysfunction. The algorithm was developed by Chin S. et al. based on an online survey of 184 ISHLT members, with participation mainly from transplant centers in North America and Europe [8].

The ISHLT guidelines for the treatment of antibody-mediated heart transplant rejection recommend high-dose intravenous glucocorticoid infusion and cytolytic drugs. Plasmapheresis or IVIg infusion is used to eliminate or inactivate autoantibodies. In hemodynamic disorders, inotropic and vasopressor drugs may be required to maintain graft function. Systemic anticoagulant therapy can reduce the risk of intravascular thrombosis. Control endomyocardial biopsy should be performed several weeks after treatment had been initiated and should be performed dynamically until complete regression of immunopathological signs. In refractory humoral rejection, monoclonal antibodies have proven effective against common B cell marker (rituximab). If the treatment is ineffective, cardiac retransplantation should be considered [48].

One type of treatment for humoral rejection is the use of therapeutic plasmapheresis. The purpose of this method is mechanical removal of circulating antibodies [49]. Using membrane filtration or centrifugation, extracorporeal separation of plasma from cellular blood components takes place. The removed volume of fluid is replenished with the help of replacement solutions.

There have been no studies investigating therapeutic plasmapheresis (TP) as a monotherapy for AMR.

The use of glucocorticoids is widely used as basic therapy not only for the treatment of cellular rejection, but also in humoral rejection of a heart transplant [49].

Steroids have potent immunosuppressive and anti-inflammatory effects that affect the number, distribution and function of all types of white blood cells and endothelial cells [50]. The use of glucocorticoids is included in the regimen in all clinical trials describing various treatments for humoral rejection.

In addition, anti-lymphocyte globulins, which are antibodies directed against T cell lymphocytes or thymocytes, are widely used. There are two types of antibodies: monoclonal (muromonab-CD3, rituximab) and polyclonal (the best known are rabbit and equine antithymocyte globulins). Antithymocyte globulins are used to treat humoral rejection, but there have been no studies on their role in the treatment of AMR [51].

Rituximab is a genetically engineered, chimeric mouse and human monoclonal antibody directed against the B-cell lineage specific CD20 antigen. For the treatment of humoral rejection or as a desensitizing therapy, rituximab is usually used in combination with other therapies. That is why is it difficult to evaluate its efficacy as a stand-alone drug. There are much evidence of the effectiveness of in the treatment of refractory antibody-mediated rejection (when combined therapy with cytolytic antibodies, corticosteroids, plasmapheresis and cyclophosphamide is not effective) [52]. When using rituximab, there was reduced PRA index in sensitized patients who were refractory to therapy with IVIg, plasmapheresis and mycophenolate mofetil [53].

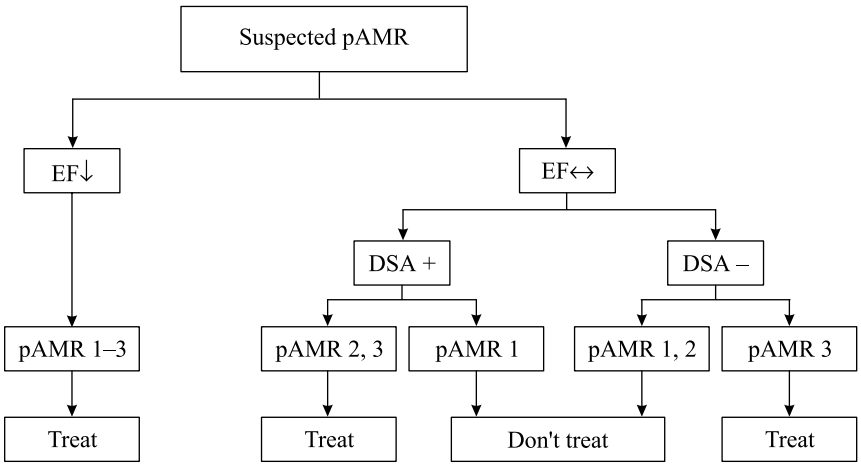

Fig. 2. Treatment modalities for different clinical scenarios, taking into account the humoral rejection category. pAMR, pathological antibody-mediated rejection category; DSA, donor-specific antibody; EF, ejection fraction

Most of the above treatments are usually used in combination, either simultaneously or consecutively [49].

Although plasmapheresis, IVIg, rituximab, and high-dose cyclophosphamide have been successful in reducing circulating antibody levels in sensitized patients prior to heart transplantation, there are large numbers of patients who are immune to these therapies. Patel J. et al. from Los Angeles conducted a pilot study to determine the effectiveness of bortezomib-based desensitization in patients resistant to IVIg, rituximab, and plasmapheresis. Bortezomib is an inhibitor of the 26S proteasome that has a pro-apoptotic effect on plasma cells and reduces antibody production. Seven patients awaiting heart transplantation with a 50% PRA were included in the study. The mean baseline PRA was 62%, which decreased to a mean of 35% after treatment. The study showed that bortezomib reduced PRA in patients who were immune to desensitization with IVIg, rituximab, and plasmapheresis [5].

The need to treat asymptomatic AMR has long been discussed [48].

The feasibility of treating milder forms of humoral rejection, such as pAMR1 (including pAMR1-H and pAMR1-I) and pAMR2 (with or without clinical signs) is in doubt, since the effectiveness of the current therapy for subclinical AMR has not been established.

The decision to treat pAMR 0–2 is based on clinical signs of rejection, such as appearance of heart failure symptoms, presence of graft dysfunction, and immunologic findings (increased existing or de novo DSA).

In asymptomatic humoral rejection, optimization of basic immunosuppressive therapy may be advisable [20].

However, due to increased risks of graft vasculopathy and death in asymptomatic rejection, it may be prudent to treat when all cases of humoral rejection are detected [48].

DSA detection is considered an important prognostic factor for the development of humoral rejection after heart transplantation, but their presence alone is not sufficient to make a diagnosis of AMR and initiate specific therapy. Nevertheless, the appearance of DSA should not be ignored. That's why Manfredini V. et al. developed an algorithm of actions that takes into account the correlation of DSA with symptoms and pathological signs of AMR, the time of their detection and the ability to bind complement (Fig. 3). When DSA is present early after transplantation, there is a clearer association with the development of acute humoral rejection, which responds well to treatment. Occurrence of DSA in the late post-transplant period can lead to chronic allograft damage and development of vasculopathy if not diagnosed on time. Association of DSA with the development of AMR justifies the initiation of specific treatment, especially in the presence of signs of graft dysfunction [18].

Table 5 presents a list of protocols used by several centers of excellence [20].

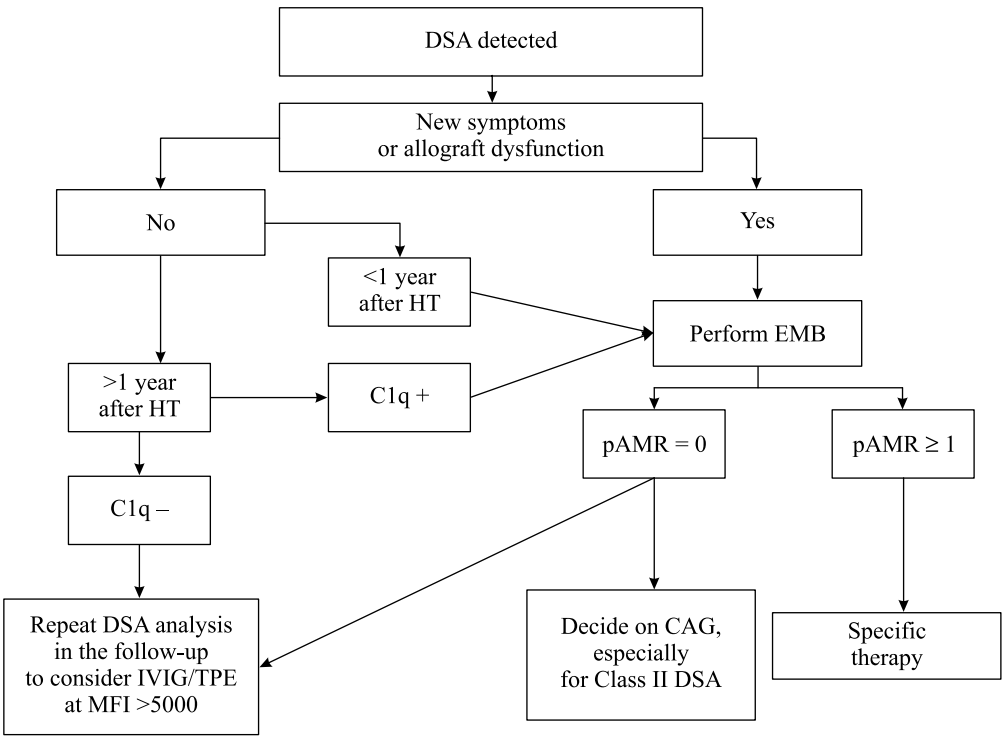

Fig. 3. Algorithm of action when DSA is detected. DSA, donor-specific antibody; HT, heart transplant; EMB, endomyocardial biopsy; C1q, complement binding activity; MFI, mean fluorescence intensity; pAMR, pathological antibody-mediated rejection category

AMR treatment in children

Prevention and treatment of humoral rejection in children is prescribed empirically and encompasses the full range of treatments that are described in adult patients. Diagnostic criteria do not differ from those for adult heart transplantation, and are based on histopathologic and immunopathologic changes. The presence of DSA, pretransplant and post-transplant anti-HLA class I antibodies negatively affects the long-term survival of patients. Therapies aimed at removing circulating antibodies include IVIg or cyclophosphamide before transplantation, intraoperative plasma exchange, and postoperative use of IVIg, therapeutic plasmapheresis, rituximab, or cyclophosphamide [20].

Treatment of sensitized patients awaiting heart transplant

For highly sensitized waitlisted patients, preoperative plasmapheresis is used to reduce circulating antibody levels, which can greatly increase the chances of obtaining a negative cross-match with the donor.

Also, a chimeric high-affinity monoclonal antibody, rituximab, which binds to CD20 lymphocyte receptors that inhibit B cell activation and differentiation, is used as desensitization in highly susceptible patients. The drug dosage is based on the patient's body surface area (375 mg/m^2). An intravenous infusion once a week is recommended, with a treatment duration of up to 4 weeks [5].

Table 5

AMR treatment strategies for adult heart transplant recipients

Center	AMR treatment
University of Utah	Subclinical pAMR-1: No treatment; consider gradual reduction of corticosteroid dose if early after transplantation; pAMR-2 without graft dysfunction or DSA: pulse steroids only; pAMR-2 with graft dysfunction and/or DSA: pulse steroids, IVIg, plasmapheresis, rituximab/bortezomib; pAMR-3: pulse steroids, IVIg, plasmapheresis, rituximab/bortezomib (plus rATG if hemodynamically compromised).
Cedars-Sinai Medical Center	Methylprednisolone 500 mg/d for 3 days; rATG; Plasmapheresis for hemodynamic compromise; IVIg 2 g/kg on days 1 and 30 (day 1 after completion of rATG treatment); Rituximab 1 g (375 mg/m^2 for smaller patients) on days 7 and 21; Refractory patients: add bortezomib 1.3 mg/m^2 on days 1, 4, 7, and 10.
Cleveland Clinic	Methylprednisolone 1 g/d for 3 days; Plasmapheresis 4–5 times over a week, then as needed; Unresolved: consider the following: – IVIg 2 g/kg; – Rituximab 375 mg/m^2 (up to 4 doses); – Bortezomib 1.3 mg/m^2 IV for 4 doses over 2 weeks; – Continue plasmapheresis; Refractory: consider photopheresis or total lymphoid irradiation.
Columbia University	Methylprednisolone; Plasmapheresis 5–6 cycles over 10–14 days; Cyclophosphamide 0.5–1 g/m^2 every 3 weeks for 4–6 months.
Stanford University	Low-risk patients: no treatment or augmentation of baseline immunosuppression with follow-up EMB; High-risk patients (positive DSA, allosensitization): IVIg or rituximab infusion; Hemodynamic compromise: – Any patient presenting with unexplained graft dysfunction is presumptively treated with methylprednisolone sodium succinate IV 500 mg/d to 1000 mg/d for 3 days; – Plasmapheresis daily or every other day (at least 5 sessions); – IVIg immediately after plasmapheresis 2 g/kg divided into 2 doses over 2 consecutive days (not to exceed 140 g) on days 1 and 2 and days 29 and 30. Repeat if there is no effect; – Consider rATG 1.5 mg/kg per day for 3 consecutive days with plasmapheresis in severe hemodynamic compromise; – Rituximab 1 g/d on days 7 and 22; Alternate modalities: – Augmentation of baseline immunosuppression; – Change from cyclosporine to tacrolimus and/or addition of cyclophosphamide 1.5 mg/kg per day; – Bortezomib 1.3 mg/m^2 per day on days 1, 4, 8, and 11

pAMR, pathological antibody-mediated rejection category; IVIg, intravenous immunoglobulin; DSA, donor-specific antibody; rATG, rabbit anti-thymocyte globulin.

IVIg are immunoglobulins, mainly of the IgG class, isolated from donor plasma. This drug reduces antibody levels in sensitized patients prior to heart transplantation. IVIg suppresses anti-HLA in vitro and in vivo. Polyclonal preparations of human immunoglobulin have activity against HLA class I and II molecules, cytokines and their receptors, and T cell receptors. The main immune effects of IVIg can be explained by blockade of Fc-γ receptors, inhibition of complement system, neutralization of autoantibodies and cytokines, and suppression of B-cell receptors [20].

Antibody drugs, especially rATG in combination with IVIg infusion, plasmapheresis and rituximab are used as induction therapy in sensitized patients. Currently, regimens that include polyclonal antibodies are preferable [20].

CONCLUSION

The primary goal of post-heart transplant patient management is to improve long-term survival. Antibody-mediated heart transplant rejection is the leading cause of early morbidity and mortality after surgery. Despite the various treatment options for humoral rejection, to date, there is no single standard of therapy, thereby requiring an individualized approach to each case. Currently, additional randomized clinical trials are required to determine a more precise management tactics for patients with AMR.

The authors declare no conflict of interest.

REFERENCES

1. *Berry GJ, Burke MM, Andersen C et al.* The 2013 International Society for Heart and Lung Transplantation Working Formulation for Standardization of nomenclature in the pathologic diagnosis of antibody-mediated rejection in heart transplantation. *J Heart Lung Transplant.* 2013; 32: 1147–1162.
2. *Hammond EH, Yowell RL, Nunoda S et al.* Vascular (humoral) rejection in heart transplantation: pathologic observations and clinical implications. *J Heart transplant.* 1989; 8: 430–443.
3. *Takemoto SK, Zeevi A, Feng S et al.* National conference to assess antibodymediated rejection in solid organ transplantation. *Am J Transplant.* 2004; 4: 1033–1041.
4. *Kfoury AG, Miller DV.* The impact of asymptomatic antibody-mediated rejection on outcome after heart transplantation. *Current Opinion in Organ Transplantation.* 2019; 24 (3): 259–264. doi: 10.1097/mot.0000000000000640.
5. *Kobashigawa J, Crespo-Leiro MG, Eisminger SM et al.* Report from a consensus conference on antibody-mediated rejection in heart transplantation. *J Heart Lung Transplant.* 2011; 30: 252–269. doi: 10.1016/j.healun.2010.11.003.
6. *Clerkin KJ, Farr MA, Restaino SW et al.* Donor-specific anti-HLA antibodies with antibody-mediated rejection and long-term outcomes following heart transplantation. *J Heart Lung Transplant.* 2017; 36: 540–545.
7. *Tran A, Fixler D, Huang R et al.* Donor-specific HLA alloantibodies: impact on cardiac allograft vasculopathy, rejection, and survival after pediatric heart transplantation. *J Heart Lung Transplant.* 2016; 35: 87–91.
8. *Chih S, Tinckam KJ, Ross HJ.* A survey of current practice for antibodymediated rejection in heart transplantation. *Am J Transplant.* 2013; 13: 1069–1074. doi: 10.1111/ajt.12162.
9. *Stewart S, Winters G, Fishbein M et al.* Revision of the 1990 working formulation for the standardization of nomenclature in the diagnosis of heart rejection. *J Heart Lung Transplant.* 2005; 24: 1710–1720.
10. *Reed EF, Demetris AJ, Hammond E et al.* International Society for Heart and Lung Transplantation. Acute antibody-mediated rejection of cardiac transplants. *J Heart Lung Transplant.* 2006; 25: 153–159.
11. *Kfoury A, Hammond M, Snow G et al.* Cardiovascular mortality among heart transplant recipients with asymptomatic antibody-mediated or stable mixed cellular and antibody-mediated rejection. *J Heart Lung Transplant.* 2009; 28: 781–784.
12. *Michaels P, Espejo M, Kobashigawa J et al.* Humoral rejection in cardiac transplantation: risk factors, hemodynamic consequences and relationship to transplant coronary artery disease. *J Heart Lung Transplant.* 2003; 22: 58–69.
13. *Crespo-Leiro MG, Veiga-Barreiro A, Doménech N et al.* Humoral heart rejection (severe allograft dysfunction with no signs of cellular rejection or ischemia): incidence, management, and the value of C4d for diagnosis. *Am J Transplant.* 2005; 5 (10): 2560–2564. doi: 10.1111/j.1600-6143.2005.01039.x.
14. *Tan CD, Sokos GG, Pidwell DJ et al.* Correlation of donor-specific antibodies, complement and its regulators with graft dysfunction in cardiac antibody-mediated rejection. *Am J Transplant.* 2009; 9: 2075–2084.
15. *Hammond EH, Wittwer CT, Greenwood J et al.* Relationship of OKT3 sensitization and vascular rejection in cardiac transplant patients receiving OKT3 rejection prophylaxis. *Transplantation.* 1990; 50: 776–782.
16. *Rodriguez E, Skojec D, Tan C et al.* Antibody-mediated rejection in human cardiac allografts: evaluation of immunoglobulins and complement activation products C4d and C3d as markers. *Am J Transplant.* 2005; 5: 2778–2785.
17. *Cherry R, Nielsen H, Reed E et al.* Vascular (humoral) rejection in human cardiac allograft biopsies: relation to circulating anti-HLA antibodies. *J Heart Lung Transplant.* 1992; 11: 24–29.
18. *Manfredini V, Leone O, Agostini V et al.* Antibody-mediated rejection in heart transplantation. *Current Opinion in Organ Transplantation.* 2017; 22 (3): 207–214. doi: 10.1097/MOT.0000000000000407.
19. *Thomas KA, Valenzuela NM, Reed EF.* The perfect storm: HLA antibodies, complement, FcgammaRs, and

endothelium in transplant rejection. *Trends Mol Med.* 2015; 21: 319–329.
20. *Colvin MM, Cook JL, Chang P et al.* Antibody-Mediated Rejection in Cardiac Transplantation: Emerging Knowledge in Diagnosis and Management. *Circulation.* 2015; 131 (18): 1608–1639. doi: 10.1161/CIR.0000000000000093.
21. *Clerkin KJ, Restaino SW, Zorn E et al.* The impact of timing and graft dysfunction on survival and cardiac allograft vasculopathy in antibody mediated rejection. *J Heart Lung Transplant*. 2016; 35: 1059–1066.
22. *Barten MJ, Schulz U, Beiras-Fernandez A et al.* The clinical impact of donor-specific antibodies in heart transplantation. *Transplantation Reviews.* 2018; 32 (4): 207–217. doi: 10.1016/j.trre.2018.05.002.
23. *Smith JD, Banner NR, Hamour IM et al. De novo* donor HLA-specific antibodies after heart transplantation are an independent predictor of poor patient survival. *Am J Transplant.* 2011; 11: 312–319. doi: 10.1111/j.1600-6143.2010.03383.x.
24. *Betkowski AS, Graff R, Chen JJ et al.* Panel-reactive antibody screening practices prior to heart transplantation. *J Heart Lung Transplant.* 2002; 21 (6): 644–650. doi: 10.1016/s1053-2498(01)00422-3.
25. *Lachmann N, Todorova K, Schulze H et al.* Luminex and Its Applications for Solid Organ Transplantation, Hematopoietic Stem Cell Transplantation, and Transfusion. *Transfusion Medicine and Hemotherapy.* 2013; 40 (3): 182–189. doi: 10.1159/000351459.
26. *Kobashigawa JA, Sabad A, Drinkwater D et al.* Pretransplant panel reactive-antibody screens. Are they truly a marker for a poor outcome after cardiac transplantation? *Circulation.* 1996; 94 (suppl II); 294–297.
27. *Loh E, Bergin JD, Couper GS et al*. Role of panel-reactive antibody cross-reactivity in predicting survival after orthotopic heart transplantation. *J Heart Lung Transplant.* 1994; 13: 194–201.
28. *Lavee J, Kormos RL, Duquesnoy RJ et al*. Influence of panel-reactive antibody and lymphocytotoxic crossmatch on survival after heart transplantation. *J Heart Lung Transplant.* 1991; 10: 921–929.
29. *Gonzalez-Stawinski GV, Atik FA, McCarthy PM et al.* Early and late rejection and HLA sensitization at the time of heart transplantation in patients bridged with left ventricular assist devices. *Transplant Proc.* 2005; 37: 1349–1351.
30. *Nwakanma LU, Williams JA, Weiss ES et al.* Influence of Pretransplant Panel-Reactive Antibody on Outcomes in 8,160 Heart Transplant Recipients in Recent Era. *Ann Thorac Surg.* 2007; 84 (5): 1556–1563. doi: 10.1016/j.athoracsur.2007.05.095.
31. *Lund LH, Edwards LB, Dipchand AI et al.* The Registry of the International Society for Heart and Lung Transplantation: Thirty-third Adult Heart Transplantation Report – 2016; Focus Theme: Primary Diagnostic Indications for Transplant. *J Heart Lung Transplant.* 2016; 35: 1158–1169.
32. *Shahzad K, Aziz QA, Leva JP et al.* New-onset graft dysfunction after heart transplantation – incidence and mechanism-related outcomes. *J Heart Lung Transplant.* 2011; 30: 194–203.
33. *Reinsmoen NL, Patel J, Mirocha J et al.* Optimizing transplantation of sensitized heart candidates using 4 antibody detection assays to prioritize the assignment of unacceptable antigens. *J Heart Lung Transplant.* 2016; 35: 165–172.
34. *Kaczmarek I, Deutsch MA, Kauke T et al.* Donor-specific HLA alloantibodies: long-term impact on cardiac allograft vasculopathy and mortality after heart transplant. *Exp Clin Transplant.* 2008; 3: 229–235.
35. *Ho EK, Vlad G, Vasilescu ER et al.* Pre- and posttransplantation allosensitization in heart allograft recipients: Major impact of *de novo* alloantibody production on allograft survival. *Hum Immunol.* 2011; 72: 5–10.
36. *Wu GW, Kobashigawa JA, Fishbein MC et al.* Asymptomatic antibody-mediated rejection after heart transplantation predicts poor outcomes. *J Heart Lung Transplant.* 2009; 28: 417–422.
37. *Wehner J, Morrell CN, Reynolds T et al.* Antibody and complement in transplant vasculopathy. *Circ Res.* 2007; 100: 191–203.
38. *Terasaki PI, Cai J.* Human leukocyte antigen antibodies and chronic rejection: from association to causation. *Transplantation.* 2008; 86: 377–383.
39. *Feingold B, Park SY, Comer DM et al*. Outcomes after listing with a requirement for a prospective crossmatch in pediatric heart transplantation. *J Heart Lung Transplant.* 2013; 32: 56–62.
40. *Pollock-BarZiv SM, Hollander ND, Ngan BY et al.* Pediatric heart transplantation in human leukocyte antigen-sensitized patients: evolving management and assessment of intermediate-term outcomes in a high-risk population. *Circulation.* 2007; 116 (suppl I): 172–178.
41. *Jordan SC, Toyoda M, Kahwaji J et al.* Clinical aspects of intravenous immunoglobulin use in solid organ transplant recipients. *Am J Transplant*. 2011; 11: 196–202.
42. *Chih S, Patel J.* Desensitization strategies in adult heart transplantation: Will persistence pay off? *J Heart Lung Transplant.* 2016; 35: 962–972.
43. *Godown J, Slaughter JC, Fossey SC et al.* Risk factors for the development of donor-specific antibodies after pediatric heart transplantation. *Pediatr Transplant.* 2015; 19: 906–910.
44. *Rafiei M, Kittleson M, Patel J et al.* Anti-thymocyte gamma-globulin may prevent antibody production after heart transplantation. *Transplant Proc*. 2014; 46: 3570–3574.
45. *Pascual J, Zuckermann A, Djamali A et al.* Rabbit antithymocyte globulin and donor-specific antibodies in kidney transplantation – a review. *Transplant Rev (Orlando)*. 2016; 30: 85–91.
46. *Christie JD, Edwards LB, Aurora P et al.* The Registry of the International Society for Heart and Lung Transplantation: twentysixth official adult lung and heart-lung transplantation report – 2009. *J Heart Lung Transplant.* 2009; 28: 1031–1049.

47. *Nguyen VP, Kobashigawa JA.* Antibody-medicated rejection after heart transplantation. *Current Opinion in Organ Transplantation.* 2020; 25 (3): 248–254. doi: 10.1097/MOT.0000000000000754.
48. *Vega E, Schroder J, Nicoara A.* Chapter 6. Post-Operative Management of Heart Transplantation Patients. *Best Pract Res Clin Anaesthesiol.* 2017; 31 (2): 201–213. doi: 10.1016/j.bpa.2017.06.002.
49. *Taylor D, Meiser B, Webber S et al.* Task Force 2: Immunosuppression and Rejection. In: The International Society of Heart and Lung Transplantation guidelines for the care of heart transplant recipients. *J Heart Lung Transplant.* 2010; 29: 926–933.
50. *Lindenfeld J, Miller G, Shakar S et al.* Drug therapy in the heart transplant recipient: part I: cardiac rejection and immunosuppressive drugs. *Circulation.* 2004; 110: 3734–3740.
51. *Koch CA, Khalpey ZI, Platt JL.* Accommodation: preventing injury in transplantation and disease. *J Immunol.* 2004; 172: 5143–5148.
52. *Kaczmarek I, Deutsch MA, Sadoni S et al.* Successful management of antibody-mediated cardiac allograft rejection with combined immunoadsorption and anti-CD20 monoclonal antibody treatment: case report and literature review. *J Heart Lung Transplant.* 2007; 26: 511–515.
53. *Balfour IC, Fiore A, Graff RJ et al.* Use of rituximab to decrease panel-reactive antibodies. *J Heart Lung Transplant*. 2005; 24: 628–630.

The article was submitted to the journal on 15.10.2021

DOI: 10.15825/1995-1191-2021-4-62-72

RENAL REPLACEMENT THERAPY IN HEART TRANSPLANT RECIPIENTS

I.L. Poz[1], A.G. Strokov[1, 2], Yu.V. Kopylova[1], V.N. Poptsov[1], S.V. Gautier[1, 2]

[1] Shumakov National Medical Research Center of Transplantology and Artificial Organs, Moscow, Russian Federation

[2] Sechenov University, Moscow, Russian Federation

Kidney injury in cardiac transplant recipients is one of the most severe complications affecting both short- and long-term transplant outcomes. The need for renal replacement therapy (RRT) is determined not only and not so much by the degree of renal dysfunction, as by the need for correction of fluid balance and metabolic disorders. These circumstances are associated with the specificity of extracorporeal renal replacement therapy in donor heart recipients. In this review, we discuss the problems of early versus delayed initiation of RRT, anticoagulation and vascular access, advantages and disadvantages of continuous and intermittent techniques. Special attention is paid to chronic kidney injury and peculiarities of kidney transplantation in heart recipients.

Keywords: heart transplantation, acute kidney injury, hemodialysis, kidney transplant after heart transplant.

Heart transplantation (HTx) is currently the most effective treatment for end-stage heart failure. Acute kidney injury (AKI), whose incidence has been increasing in recent years due to liberalization of indications for HTx and the use of organs obtained from expanded criteria donors, is one of the major complications prolonging hospital stay and worsening the prognosis in heart transplant recipients. According to some transplant centers, the need for renal replacement therapy (RRT) reaches 40%. However, the literature data concerning specific problems of RRT use in heart recipients are few, and considering issues, such as optimal timing of RRT initiation, comparison of efficiency of permanent and intermittent techniques, anticoagulation regimens, choice of optimal vascular access and others, we have to focus on the results of studies evaluating RRT use in intensive care units (ICU).

RRT IN CRITICALLY ILL PATIENTS

Timing of RRT initiation: early vs delayed initiation

Despite the significant increase in the frequency of RRT use in AKI or multiple organ failure in ICU, many aspects of such treatment remain a subject of debate. This applies particularly to the timing of RRT initiation. Early initiation allows to manage fluid balance and rapidly correct electrolyte and metabolic disorders. At the same time, RRT itself can cause a number of complications, particularly hemodynamic, metabolic, and hemorrhagic disorders, catheter-associated infection (CAI), unwanted removal of drugs and their metabolites [1]. To date, a large number of studies have been published in favor of both early and late initiation of RRT in AKI [2–6].

Of the randomized clinical trials (RCTs) that found statistically significant improvements in survival and renal function recovery with early vs. late initiation of RRT, ELAIN (Early vs LAte INitiation of RRT) was the most telling. This single-center trial enrolled 231 patients with AKI after surgery. In the early initiation group, RRT was initiated within 8 hours of diagnosis of KDIGO (AKI Kidney Disease: Improving Global Outcomes) stage 2; in the delayed initiation group, within 12 hours of stage 3 AKI or when absolute indications for RRT arose, which included blood urea elevations greater than 100 mg/dL (16.65 mmol/L), hyperkalemia above 6.0 mEq/L, and edema resistant to diuretic therapy. Mortality was significantly lower in the first group than in the second (39.3% vs. 54.7%, p = 0.03). Of the 119 patients randomized to the delayed-initiation group, 11 did not receive RRT due to restoration of renal function [2].

At the same time, multicenter RCT AKIKI (Artificial Kidney Initiation in Kidney Injury) showed no statistically significant differences in patient survival in the early and delayed RRT initiation groups. The study included 620 patients with AKI from 31 ICUs, which were divided into 2 equal groups. In the delayed-initiation group, RRT initiation criteria were oligo or anuria for more than 72 hours, blood urea concentration greater than 40 mmol/L, hyperkalemia greater than 6.0 mmol/L or 5.5 mmol/L after glucose solution infusion with insulin; a pH below 7.15 and acute pulmonary edema due to fluid overload. Sixty-day survival did not differ between the groups; half of those patients who were assigned a

Corresponding author: Iakov Poz. Address: 1, Shchukinskaya str., Moscow, 123182, Russian Federation. Phone: (991) 245-55-61. E-mail: dr.poz@list.ru

delayed strategy did not receive RRT. The mortality rate in both groups was nearly 50%. CAI was less common in the delayed strategy group, which can be attributed to the shorter duration of RRT. The authors conclude that the delayed strategy avoided RRT in a significant number of patients [3].

Most studies have used the AKI KDIGO stages as criteria for patient selection. In practice, however, these criteria are rarely the only basis for initiating RRT, with most AKI patients with KDIGO stage 3 not receiving RRT [7]. Some authors, comparing outcomes among patients with AKI depending on whether they received RRT or not, demonstrate a better survival rate associated with the absence of RRT [8]. For objective results, it is necessary to form beforehand groups of patients for early and delayed initiation of RRT. However, for the patients included in the group of delayed initiation, there is a risk not to receive RRT as a result of an unfavorable outcome. A recent meta-analysis of RCTs, devoted to the timing of RRT initiation in severe AKI, taking into account individual data of patients, has not revealed dependence of mortality on timing of initiation of RRT, provided that delayed initiation of RRT is carried out at close observation of patients and RRT is initiated at occurrence of appropriate clinical indications [9].

Vascular access for RRT

It is advisable to use ultrasound guidance when implanting the RRT central venous catheter (CVC) in an ICU setting. According to results of a meta-analysis by Rabindranath et al., implantation of RRT catheters in the jugular vein allows to avoid installation defects in the vast majority of cases, reduce manipulation time and significantly reduce the complication rate [10]. According to Prabhu et al., this tactic also provides better results for femoral access [11]. According to clinical guidelines [12, 13], placing temporary catheters into subclavian veins should be avoided to avoid stenosis and to preserve the possibility to implant permanent CVC in the event of chronic renal injury. According to a multicenter RCT conducted by Parienti et al., subclavian vein catheterization is associated with a lower risk of CAI and thrombotic complications and a higher incidence of pneumothorax compared with jugular or femoral catheter localization [14].

Another multicenter RCT indicates that with respect to catheter dysfunction or RRT effectiveness, there were no differences for catheter localization in the internal jugular vein and femoral vein. Catheters located in the right internal jugular vein were associated with a significantly lower incidence of dysfunction compared with the left internal jugular vein. While the same 16 cm jugular catheters were used in both positions, the right position provided the shortest route to the superior vena cava. Femoral access was associated with a significantly lower risk of catheter dysfunction compared with the left jugular access. It was recommended for use when there was no possibility to insert the catheter into the right jugular vein and when the patient's body mass index was less than 28.4. This approach allowed to reduce the incidence of catheter dysfunction without increasing the risk of CAI. For optimal RRT efficiency in case of femoral access, it was recommended to use catheters 25 cm long reaching the inferior vena cava. If it is necessary to continue RRT for a long time, the use of tunneled jugular catheters is considered to be preferable [15].

According to Coupez et al., the incidence of dysfunction in catheter replacement by guidewire is significantly higher than that in new catheter placement (37.6% vs. 15.7%, $p < 0.01$), with the risk of infection not significantly different [16]. Chua et al. report similar results, noting that the risk of catheter infection is higher in older and more massive patients, especially in the femoral position [17]. Heparin lock is traditionally used to maintain catheter patency; citrate-based solutions in various concentrations, antibiotics or other drugs with antibacterial properties are used less frequently. Sungur et al. report that "leakage" of catheter-filling solution into the vascular channel can reach 20% and depends on catheter design. This amount may be clinically significant in increasing the risk of bleeding and antibiotic toxicity [18]. According to reports by Correa Barcellos et al., the use of citrate-based solutions does not reduce the risks of infection and dysfunction [19]. Landry et al. indicate that the use of antibacterial solutions as a lock reduces the risk of infection but may contribute to the development of bacterial resistance and should be considered in cases with a high probability of CAI [20]. Since the risk of catheter infection directly correlates with the duration of its stay in the vessel, the need for continued RRT should be assessed daily, and if there is no need, the catheter should be removed [12, 13].

RRT techniques, continuous and intermittent

A number of techniques are used for RRT in an ICU setting, namely intermittent hemodialysis, sustained low-efficiency dialysis (SLED), extended daily dialysis, prolonged intermittent renal replacement therapy (IRRT), and continuous renal replacement therapy (CRRT) techniques (hemofiltration, hemodiafiltration). CRRT and IRRT methods are usually considered to be complementary; neither of them has obvious advantages over the other [21, 22]. As a rule, the choice of the optimum method is made at a certain stage of treatment in the given patient, and also in view of traditions and possibilities of ICU. According to the literature, CRRT and IRRT can achieve correction of metabolic and water-electrolyte disorders. At the same time, the studies did not reveal the advantages of any method in terms of improving patient survival [21–23]. Schneider et al. performed a

meta-analysis of 23 studies (7 randomized and 16 observational studies) to identify the preferred method of treatment. A pooled analysis of the observational studies showed a higher incidence of dialysis dependence among surviving patients initially treated with IRRT compared to CRRT. However, analysis of the results of randomized trials did not confirm these findings [24]. Wald et al. reported that in critical patients with AKI, the use of CRRT, compared to IRRT, was associated with a lower likelihood of chronic dialysis [25]. In contrast, in a retrospective study using data from 1,338 patients receiving RRT at the University of Pittsburgh Medical Center ICU, Liang et al. reported no statistically significant differences in risks of or causes for non-recovery of renal function (death or esCRF) after 90 and 365 days from treatment initiation with IRRT versus CRRT methods [23]. However, in a retrospective study, it can be difficult to determine why a given patient was started on CRRT or IRRT. For example, CRRT to control volemia was initiated in patients with expected hemodynamic instability, and IRRT was initiated in patients with low-dose vasopressors due to electrolyte disturbances without the need for high volume UV. Nash et al. performed a meta-analysis of 21 randomized clinical trials comparing different RRT methods used to treat AKI patients in ICU. The authors found no statistically significant differences in 30-, 90-day, 2-year survival, and the occurrence of dialysis dependence in patients initially treated with CRRT, IRRT, and SLED [26]. The use of different RRT methods in one patient during treatment depending on clinical indications is a common practice, which is one of the main limitations of such analysis. According to KDIGO clinical practice guidelines, "no RRT is ideal for all patients with AKI. Clinicians should be aware of the pros and cons of different RRTs, and tailor RRT on the basis of the individual and potentially changing needs of their patients" [12].

Efficacy of RRT methods

The efficacy of IRRT is traditionally calculated on the basis of urea kinetics. Fractional clearance of urea for 1 procedure is expressed as Kt/V index, which should reach 1.2–1.4, and the number of sessions to 3–7 times a week [27]. In CRRT, due to the high screening ratio for low molecular weight compounds, almost equal to one, the volume purified from substances such as urea is approximately equal to the ultrafiltration volume for CVVH, and also includes the dialysate volume for CVVHD and CVVHDF. The recommended replacement volume for post-dilution is 20–40 ml/hr/kg patient weight [27, 28] and should provide correction of metabolic, electrolyte and acid-base disorders [29]. The adequacy of RRT is not limited to effective elimination of uremic compounds. Treatment should also provide adequate correction of metabolic, electrolyte and acid-base disorders, as well as water balance. According to Sutherland et al. and Teixeira et al., an increase in fluid accumulation of more than 10–20% from ICU admission to RRT is significantly associated with increased risk of death [30, 31]. The main task is to maintain a neutral fluid balance, and in case of hyperhydration, to achieve gradual removal of excess fluid, avoiding related complications [31–33]. Tolerability of ultrafiltration depends on the rate of intravascular volume replenishment from interstitial space. Devices based on non-invasive hematocrit control are effective for UV management to optimize vascular replenishment [33].

Anticoagulation in RRT

Two main methods of anticoagulation are used to prevent extracorporeal thrombosis – systemic administration of unfractionated or low molecular weight heparin and regional citrate anticoagulation (RCA) [34]. According to a meta-analysis of 11 RCTs performed by Bai et al. in CRRT, RCA significantly reduced the risk of extracorporeal thrombosis compared to regional and systemic heparinization. The RCA group had a significantly lower bleeding risk than the systemic heparin group and a similar bleeding risk to the regional heparin group. No significant survival difference was observed between the groups [35].

At the same time, a number of complications can be associated with the use of RCA, in particular calcium loss and citrate accumulation. The calcium citrate complex has a molecular weight of about 300 Da and easily passes through the dialysis membrane. To maintain a neutral calcium balance, calcium must be administered throughout the procedure. When blood calcium levels fall, parathyroid hormone (PTH) levels rise rapidly, mobilizing calcium from bone tissue. According to Klingele et al., such bone demineralization can lead to fractures during prolonged RRT [36]. When citrate metabolism in the liver is impaired, it accumulates in the blood, ionized calcium is not released from the citrate-calcium complex, and the Ca/Ca^{++} ratio exceeds 2.5. Due to citrate accumulation, bicarbonate concentration decreases, and metabolic acidosis develops. In a retrospective study by Khadzhynov et al., 32 patients out of 1070 (2.99%) who received CRRT with RCA had metabolic signs of citrate accumulation against a background of marked hyperlactatemia. Although this complication occurred in a small number of patients, it was associated with 100% mortality [37]. Thus, in patients with metabolic disorders, RCA requires careful laboratory monitoring.

RRT IN HEART RECIPIENTS

The choice of an RRT technique usually depends on the patient's hemodynamic status. Convection-based CRRT techniques avoid rapid changes in blood osmolarity and homeostasis indices, as well as occurrence of

disequilibrium syndrome. Prolonged procedure helps to distribute the necessary volume of UV over a long period of time, thus reducing the intensity of fluid removal and improving hemodynamic tolerance. Continuous methods are used for hemodynamic instability, intermittent methods replace them when the patient's condition stabilizes [38]. This approach corresponds to KDIGO guidelines [12].

Most publications on AKI in cardiac recipients have little or no description of the RRT techniques used [39–43].

The recently published results of a retrospective observational study by Shen et al. provide a detailed description of the approach to RRT in cardiac recipients at Shanghai Zhongshan Hospital [44]. In the process of data analysis, the recipients were divided into 2 groups. In the early targeted RRT group, the indications for RRT were changed from traditional to anticipatory. In group 2 patients, the onset of RRT was determined by traditional indications. There was an agreement between cardiovascular surgeons, intensive care specialists and nephrologists to determine the early onset of RRT. Early initiation of RRT after orthotopic heart transplant often occurred in the absence of traditional indications, such as accumulated fluid overload ≥5%, persistent low cardiac output, high central venous pressure (CVP), arterial hypotension requiring high doses of inotropic support, and initiation of ECMO. Targeted RRT included hemodialysis, hemofiltration, hemodiafiltration, and isolated UV. Target was established by the time RRT was initiated and assessed every 6 hours. The technique, dose, duration, and frequency of RRT sessions were determined according to the patient's need and tolerability to achieve the target. The targeted RRT protocol included the following parameters.

1. RRT method. Hemodialysis was used in the presence of hyperkalemia, metabolic acidosis and persistent azotemia. Hemofiltration or hemodiafiltration was used in the presence of marked signs of inflammation. If the patient had no metabolic and electrolyte disturbances, isolated UV was used.
2. Duration. If the patient was hemodynamically stable and the goal could be achieved within a day, IRRT or extended IRRT was used. If the target could not be achieved during the day, continuous methods were used.
3. Intensity. Intensity depended on the needs for fluid removal, detoxification and hemodynamic stability.

All procedures were performed on IRRT devices, highly permeable polysulfone membranes with 25–30 ml/hr/kg replacement volume and 150–250 ml/min blood flow. Anticoagulation was performed mainly by low heparin doses. When analyzing the data, the authors obtained the following results. After 72 hours from initiation of treatment, the amount of urine and renal perfusion pressure were significantly higher in Group 1 patients, while creatinine and blood lactate levels, degree of fluid overload, CVP and vasoactive drug doses were significantly lower than those in Group 2 patients. In-hospital mortality (39.1% versus 63.3%, $p = 0.039$), ICU length of stay (26 ± 18 versus 38 ± 20 days; $p = 0.008$), and hospitalization (38 ± 33 versus 64 ± 45; $p = 0.005$) were significantly lower in the early- versus late-RRT group. At the same time, the cost of RRT in group 1 patients was significantly lower than in group 2 (0.54 ± 0.10 vs. 0.63 ± 0.11 \$10,000, $p < 0.001$).

Such an approach to RRT seems to be the most appropriate, as it allows not only to optimally use the capabilities of each technique, but also to maximally adapt them to the specific clinical situation.

Chronicity of renal injury in heart recipients

According to the International Society for Heart and Lung Transplantation registry, the incidence of chronic kidney disease (CKD) in heart recipients reaches 50% by 5 years after surgery, and by the 10-year milestone, 6% of patients need RRT, including 3.7% who become kidney recipients [45]. Despite the fact that AKI is a frequent complication and a probable risk factor for chronic renal damage and mortality after non-transplant cardiovascular surgery, reports on short-term and long-term consequences of renal dysfunction after heart transplantation are quite controversial. For instance, according to some authors, the development of AKI in the early period after HTx was not a predictor of esCRF development in the long term [45–47]. Jokinen et al. even showed an improvement in renal function in heart recipients who required RRT in the early postoperative period by the end of year 1 after transplantation [48]. At the same time, according to Ivey-Miranda et al., the need for RRT in the early postoperative period was a predictor of worse long-term survival in heart recipients [46].

Garcia-Gigorro et al. report a trend toward worse survival by 10 years after HTx, which, however, did not reach statistical significance [40]. Other authors suggest that cardiac recipients who required RRT in the early postoperative period and survived within the first 3 months after transplantation did not have a worse prognosis for long-term survival compared to other recipients [47, 49]. At the same time, according to Wang et al. and Fortrie et al., the need for RRT in the early post-HTx period was an independent predictor of esCRF in the long term [42, 50]. However, Fortrie et al. report significantly worse long-term survival in recipients who required RRT early after HTx [50]. In contrast, the results obtained by Wang et al. suggest that recipients who survived within the first 3 months after surgery had no higher risk of death compared to other recipients [42].

One possible explanation for these contradictions is the different approaches to conducting RRT. For example, preventive initiation of RRT and the use of the

most modern techniques are likely to contribute to better outcomes and, consequently, a better long-term prognosis. However, further research is needed to obtain reliable results.

Kidney transplantation to heart recipients

In heart recipients, the risk of developing CKD increases every year after transplantation. Some degree of renal impairment occurs in about half of heart recipients by 5 years postoperatively [51]. End-stage renal failure requiring RRT develops in 5% of patients by 5 years and in up to 12% by 10 years after transplantation [52]. Kidney transplantation significantly improves survival and quality of life in this category of patients.

Between 1995 and 2008, the number of heart recipients on the waiting list for subsequent kidney transplantation increased by 307%. During the same period, the number of primary patients with end-stage CKD on the donor kidney waiting list increased by only 74%, and the number of kidney recipients waiting for retransplantation increased by 70% [53]. According to Cassuto et al., the relative risk of death for heart recipients after kidney transplantation was significantly lower than for heart recipients on the waiting list (HR = 0.73, CI = 0.58–0.93, p = 0.011). At the same time, delisting of heart recipients due to death or deterioration was 15.8% annually for pre-dialysis CKD patients and 20.3% for dialysis patients [54]. Such data suggest the benefit of earlier kidney transplantation in heart recipients with renal failure.

According to Grupper et al., the median long-term survival of heart recipients with stage 5 CKD after renal transplantation was not significantly different from that of heart recipients without renal failure (17.5 versus 17.1 years, p = 0.27) and was significantly higher than that of heart recipients who remained on dialysis (17.5 versus 7.3 years, p < 0.001) [55]. The study by Roest et al. shows similar results. Kidney transplantation contributed to better survival of heart recipients with esCRF compared with those who remained on dialysis and with those who received conservative therapy (median 6.4 years, 2.2 years, and 0.3 years, respectively, p < 0.0001). Significantly better survival was observed in those who received a kidney from a living donor compared with a deceased donor and in those who received a kidney from a related donor compared with an unrelated donor (p = 0.02) [56].

A separate group is represented by patients suffering from a combination of end-stage renal insufficiency and end-stage renal failure who require simultaneous heart and kidney transplant (SHKTx). According to a number of studies, heart and kidney recipients have a lower rate of rejection of both cardiac and renal transplants compared with heart or kidney recipients alone [57, 58]. According to Hermsen et al. data, the time that elapsed before the development of the first cardiac transplant rejection crisis was significantly longer in heart and kidney transplant recipients than in heart recipients only (p = 0.011). A similar trend, though not reaching statistical significance, was observed in heart-kidney transplantation compared to kidney transplantation from living donors. The authors also found a lower incidence of cardiac allograft vasculopathy in SHKTx than in HTx [59]. Lower incidence and severity of rejection crises, as well as greater efficacy in controlling these crises, has been noted in heart-lung transplantation compared with lung transplantation; in simultaneous liver and kidney transplantation [60] compared with liver or kidney transplantation alone [61]. To date, the mechanisms of such immune tolerance remain unclear, but there are several possible explanations for this phenomenon. They are suppression of the immune response associated with chimerism of hematopoietic cells of the donor [62]; a state of anergy resulting from implantation of a large mass of foreign tissue into the recipient's body, as well as "diversion of the immune response" towards another transplanted organ [63].

In the case of SHKTx, there are simultaneous and staged heart and kidney transplants. In this case, organs from the same donor are used. In simultaneous transplantation, both operations are performed simultaneously. In the staged method, after heart transplantation, the patient is sent to the intensive care unit for a period usually not exceeding 24 hours, and after hemodynamic stabilization, the patient returns to the operating room for kidney transplantation [63]. In some cases, subsequent kidney to heart recipient transplantation (SKTx) is used, with considerably longer time between heart and kidney transplantation. To date, there are no recommendations as to when a single-stage or a staged technique should be used. Despite the increased duration of cold ischemia for the renal graft, many authors have advocated two consecutive operations [64, 66]. In this case, having a recovery period for the new transplanted heart allows to optimize the hydration status before kidney transplantation and to reduce the negative influence of such factors as low perfusion pressure and unstable hemodynamic conditions on the kidney graft. In addition, it is believed that warming the patient and hemostasis is more appropriate prior to kidney transplantation (KTx). Several authors have suggested that the indication for SHKTx in a potential heart recipient is a decrease in estimated glomerular filtration rate (eGFR) to <37–40 mL/min [67, 68], while eGFR ≤30 mL/min is considered a relative contraindication for isolated heart transplantation [69].

According to an analysis of the United Network for Organ Sharing (UNOS) Registry, mortality rates did not differ significantly between heart and kidney donor waiting lists, while the 5-year survival rate of kidney heart recipients was higher than that of heart recipients with renal insufficiency, regardless of the need for dialysis prior to transplantation [70]. Similar results are reported

by Kilic et al. and Schaffer et al. They also note that the appropriateness of using two organs from the transplant pool simultaneously for one recipient is justified by the fact that heart recipients with renal failure who are on the kidney waiting list have more than twice the mortality by the end of 3 years after HTx than patients with isolated esCRF (40% versus 14–18%) [71, 72]. At the same time, Melvinsdottir et al. and Gallo et al. report benefits of SKTx over SHKTx [73, 74]. According to an analysis of the UNOS database from 2007 to 2016, the risk of death for SHKTx recipients was 4.7 times higher than for SKTx recipients when calculated from the HTx date and 2.6 times higher when calculated from the KTx date. It was also shown that although the vast majority of patients with end-stage heart failure and stage 4 and 5 CKD received SHKTx, 17% of patients who received SHKTx had an eGFR of 45 ml/min/1.73 m^2, whereas 38% of patients who received SKTx had an eGFR of 45 ml/min/1.73 m^2. The authors consider one of the advantages of SKTx to be the possibility of kidney transplantation from a living donor [73]. These data are at odds with many previously published results reporting that cardiac recipients with postoperative renal failure have a significantly lower survival rate than recipients without renal failure, and SHKTx can offset this difference. Another analysis of the UNOS database (2000–2015), carried out by a group of authors, which aimed to determine the indications for SHKTx or SKTx based on the severity of renal dysfunction of a potential heart recipient, can only partially explain these contradictions. Patients with an eGFR of 30 mL/min/1.73 m^2 who underwent SHKTx were found to have significantly better survival at 5 years post-transplant compared with those who underwent SKTx (75% and 59%, respectively, $p = 0.04$). For patients with eGFR between 30 and 44 ml/min/1.73 m^2, the differences in survival did not reach statistical significance [74].

Despite the increasing number of simultaneous heart and kidney transplants, to date, there are no guidelines on when to choose a single-stage, staged or subsequent approach. It is clear that if the recipient has systemic hemodynamic disorders and cardiac graft dysfunction, it is advisable to perform kidney transplantation after the clinical condition has been stabilized, which is confirmed by reports from Shumakov National Medical Research Center of Transplantology and Artificial Organs, Moscow [75, 76].

Thus, all varieties of renal replacement therapy, including kidney transplantation, are widely used in heart transplant recipients. Given the complexity and versatility of pathological processes that lead to the need for RRT at all stages of heart transplantation and the heterogeneity of the literature devoted to this problem, it is difficult to expect the appearance of clinical guidelines clearly regulating the tactics of this type of treatment in heart recipients. Timely initiation, careful selection of optimal RRT method taking into account prevailing pathogenetic mechanisms, and assessment of risks of complications are the factors that make it possible to achieve optimal treatment outcomes in this patient cohort.

The authors declare no conflict of interest.

REFERENCES

1. *Sigwalt F, Bouteleux A, Dambricourt F, Asselborn T, Moriceau F, Rimmelé T.* Clinical Complications of Continuous Renal Replacement Therapy. Bellomo R, Kellum JA, La Manna G, Ronco C. (eds): 40 Years of Continuous Renal Replacement Therapy. *Contrib Nephrol.* Basel, Karger, 2018; 194: 109–117. doi: 10.1159/000485608.
2. *Zarbock A, Kellum JA, Schmidt C, Van Aken H, Wempe C, Pavenstadt H et al*. Effect of early vs delayed initiation of renal replacement therapy on mortality in critically ill patients with acute kidney injury: the ELAIN randomized clinical trial. *JAMA*. 2016; 315: 2190–2199. doi: 10.1001/jama.2016.5828.
3. *Gaudry S, Hajage D, Schortgen F, Martin-Lefevre L, Pons B, Boulet E et al.* Initiation strategies for renal-replacement therapy in the intensive care unit. *N Engl J Med.* 2016; 375: 122–133. doi: 10.1056/NEJMoa1603017.
4. *Combes A, Brechot N, Amour J, Cozic N, Lebreton G, Guidon C et al.* Early high-volume hemofiltration versus standard care for post-cardiac surgery shock. The HEROICS study. *Am J Respir Crit Care Med.* 2015; 192: 1179–1190. doi: 10.1164/rccm.201503-0516OC.
5. *Wald R, Adhikari NK, Smith OM, Weir MA, Pope K, Cohen A et al.* Comparison of standard and accelerated initiation of renal replacement therapy in acute kidney injury. *Kidney Int.* 2015; 88: 897–904. doi: 10.1038/ki.2015.184.
6. *Jamale TE, Hase NK, Kulkarni M, Pradeep KJ, Keskar V, Jawale S, Mahajan D.* Earlier-start versus usual-start dialysis in patients with community acquired acute kidney injury: a randomized controlled trial. *Am J Kidney Dis.* 2013; 62: 1116–1121. doi: 10.1053/j.ajkd.2013.06.012.
7. *Hoste EA, Bagshaw SM, Bellomo R, Cely CM, Colman R, Cruz DN et al.* Epidemiology of acute kidney injury in critically ill patients: the multinational AKI-EPI study. *Intensive Care Med*. 2015; 41: 1411–1423. doi: 10.1007/s00134-015-3934-7.
8. *Gaudry S, Ricard JD, Leclaire C, Rafat C, Messika J, Bedet A et al*. Acute kidney injury in critical care: experience of a conservative strategy. *J Crit Care.* 2014; 29: 1022–1027. doi: 10.1016/j.jcrc.2014.07.014.
9. *Gaudry S, Hajage D, Benichou N, Chaïbi K, Barbar S, Zarbock A et al.* Delayed versus early initiation of renal replacement therapy for severe acute kidney injury: a systematic review and individual patient data meta-analysis of randomised clinical trials. *Lancet.* 2020; 395 (10235): 1506–1515. doi: 10.1016/S0140-6736(20)30531-6.
10. *Rabindranath KS, Kumar E, Shail R, Vaux E*. Use of real-time ultrasound guidance for the placement of hemodialysis catheters: a systematic review and meta-analysis of randomized controlled trials. *Am J Kidney Dis.* 2011; 158: 964–970. doi: 10.1053/j.ajkd.2011.07.025.

11. *Prabhu MV, Juneja D, Gopal PB, Sathyanarayanan M, Subhramanyam S, Gandhe S, Nayak KS.* Ultrasound-guided femoral dialysis access placement: a single-center randomized trial. *Clin J Am Soc Nephrol*. 2010; 5: 235–239. doi: 10.2215/CJN.04920709.
12. Kidney disease: Improving Global Outcomes (KDIGO) Acute Kidney Injury Work Group: KDIGO Clinical Practice Guideline for Acute Kidney Injury. *Kidney Inter Suppl*. 2012; 2: 1–138. doi: 10.1038/kisup.2012.1.
13. *Vinsonneau C, Allain-Launay E, Blayau C, Darmon M, Ducheyron D, Gaillot T et al.* Renal replacement therapy in adult and pediatric intensive care: recommendations by an expert panel from the French Intensive Care Society (SRLF) with the French Society of Anesthesia Intensive Care (SFAR) French Group for Pediatric Intensive Care Emergencies (GFRUP) the French Dialysis Society (SFD). *Ann Intensive Care.* 2015; 5: 58. doi: 10.1186/s13613-015-0093-5.
14. *Parienti JJ, Mongardon N, Megarbane B, Mira JP, Kalfon P, Gros A et al.* Intravascular complications of central venous catheterization by insertion site. *N Engl J Med.* 2015; 373 (13): 1220–1229. doi: 10.1056/NEJMoa1500964.
15. *Parienti JJ, Megarbane B, Fischer MO, Lautrette A, Gazui N, Marin N et al.* Catheter dysfunction and dialysis performance according to vascular access among 736 critically ill adults requiring renal replacement therapy: a randomized controlled study. *Crit Care Med.* 2010; 38: 1118–1125. doi: 10.1097/CCM.0b013e3181d454b3.
16. *Coupez E, Timsit JF, Ruckly S, Schwebel C, Gruson D, Canet E et al.* Guidewire exchange vs new site placement for temporary dialysis catheter insertion in ICU patients: is there a greater risk of colonization or dysfunction? *Crit Care.* 2016; 20: 230. doi: 10.1186/s13054-016-1402-6.
17. *Chua HR, Schneider AG, Sherry NL, Lotfy N, Chan MJ, Galtieri J et al*. Initial and extended use of femoral versus nonfemoral double-lumen vascular catheters and catheter-related infection during continuous renal replacement therapy. *Am J Kidney Dis.* 2014; 64: 909–917. doi: 10.1053/j.ajkd.2014.04.022.
18. *Sungur M, Eryuksel E, Yavas S, Bihorac A, Layon AJ, Caruso L.* Exit of catheter lock solutions from double lumen acute haemodialysis catheters – an *in vitro* study. *Nephrol Dial Transplant.* 2007; 22: 3533–3537. doi: 10.1093/ndt/gfm452.
19. *Correa Barcellos F, Pereira Nunes B, Jorge Valle L, Lopes T, Orlando B, Scherer C et al*. Comparative effectiveness of 30% trisodium citrate and heparin lock solution in preventing infection and dysfunction of hemodialysis catheters: a randomized controlled trial (CITRIM trial). *Infection.* 2017; 45 (2): 139–145. doi: 10.1007/s15010-016-0929-4.
20. *Landry DL, Braden GL, Gobeille SL, Haessler SD, Vaidya CK, Sweet SJ.* Emergence of gentamicin-resistant bacteremia in hemodialysis patients receiving gentamicin lock catheter prophylaxis. *Clin J Am Soc Nephrol*. 2010; 5: 1799–1804. doi: 10.2215/CJN.01270210.
21. *Bagshaw SM, Berthiaume LR, Delaney A, Bellomo R.* Continuous versus intermittent renal replacement therapy for critically ill patients with acute kidney injury: a meta-analysis. *Crit Care Med*. 2008; 36: 610–617. doi: 10.1097/01.CCM.0B013E3181611F552.
22. *Zhang L, Yang J, Eastwood GM, Zhu G, Tanaka A, Bellomo R.* Extended daily dialysis versus continuous renal replacement therapy for acute kidney injury: a meta-analysis. *Am J Kidney Dis.* 2015; 66: 322–330. doi: 10.1053/j.ajkd.2015.02.328.
23. *Liang KV, Sileanu FE, Clermont G, Murugan R, Pike F, Palevsky PM, Kellum JA.* Modality of RRT and recovery of kidney function after AKI in patients surviving to hospital discharge. *Clin J Am Soc Nephrol*. 2016; 11: 30–38. doi: 10.2215/CJN.01290215.
24. *Schneider AG, Bellomo R, Bagshaw SM, Glassford NJ, Lo S, Jun M et al*. Choice of renal replacement therapy modality and dialysis dependence after acute kidney injury: A systematic review and meta-analysis. *Intensive Care Med.* 2013; 39: 987–997. doi: 10.1007/s00134-013-2864-5.
25. *Wald R, Shariff SZ, Adhikari NKJ, Bagshaw SM, Burns KEA, Friedrich JO et al.* The association between renal replacement therapy modality and long-term outcomes among critically ill adults with acute kidney injury: A retrospective cohort study. *Crit Care Med*. 2014; 42: 868–877. doi: 10.1097/CCM.0000000000000042.
26. *Nash DM, Przech S, Wald R, O'Reilly D.* Systematic review and meta-analysis review and meta-analysis of renal replacement therapy modalities for acute kidney injury in the intensive care unit. *J Crit Care*. 2017; 41: 138–144. doi: 10.1016/j.jcrc.2017.05.002.
27. *Palevsky PM, Zhang JH, O'Connor TZ, Chertow GM, Crowley ST, Choudhury D et al.* Intensity of renal support in critically ill patients with acute kidney injury. VA/NIH Acute Renal Failure Trial Network. *N Engl J Med*. 2008; 359: 7–20. doi: 10.1056/NEJMoa0802639.
28. *Bellomo R, Cass A, Cole L, Finfer S, Gallagher M, Lo S et al.* Intensity of continuous renal-replacement therapy in critically ill patients. RENAL Replacement Therapy Study Investigators. *N Engl J Med.* 2009; 361 (17): 1627–1638. doi: 10.1056/NEJMoa0902413.
29. *Bagshaw SM, Chakravarthi MR, Ricci Z, Tolwani A, Neri M, De Rosa S et al.* ADQI Consensus Group. Precision continuous renal replacement therapy and solute control. *Blood Purif*. 2016; 42: 238–247. doi: 10.1159/000448507.
30. *Sutherland SM, Zappitelli M, Alexander SR, Chua AN, Brophy PD, Bunchman TE et al.* Fluid overload and mortality in children receiving continuous renal replacement therapy: the prospective pediatric continuous renal replacement therapy registry. *Am J Kidney Dis.* 2010; 55: 316–325. doi: 10.1053/j.ajkd.2009.10.048.
31. *Teixeira C, Garzotto F, Piccinni P, Brienza N, Iannuzzi M, Gramaticopolo S et al.* Fluid balance and urine volume are independent predictors of mortality in acute kidney injury. *Crit Care*. 2013; 17: R14. doi: 10.1186/cc12484.
32. *Garzotto F, Ostermann M, Martin-Langerwerf D, Sanchez-Sanchez M, Teng J, Robert R et al.* The dose response multicentre investigation on fluid assessment (DoReMIFA) in critically ill patients. *Crit Care*. 2016; 20: 196. doi: 10.1186/s13054-016-1355-9.

33. *De los Reyes VA, Fuertinger DH, Kappel F, Meyring-Wosten A, Thijssen S, Kotanko P.* A physiologically based model of vascular refilling during ultrafiltration in hemodialysis. *J Theor Biol*. 2016; 390: 146–155. doi: 10.1016/j.jtbi.2015.11.012.
34. Sepsis, kidney and multiple organ dysfunction. Proceedings of the Third International Course on Critical Care Nephrology. June 1–4, 2004. Vicenza, Italy *Contrib Nephrol*. 2004; 144: 1–394. PMID: 15295813.
35. *Bai M, Zhou M, He L, Ma F, Li Y, Yu Y et al.* Citrate versus heparin anticoagulation for continuous renal replacement therapy: an updated meta-analysis of RCTs. *Intensive Care Med*. 2015; 41: 2098–2110. doi: 10.1007/s00134-015-4099-0.
36. *Klingele M, Seiler S, Poppleton A, Lepper P, Fliser D, Seidel R*. The gap between calculated and actual calcium substitution during citrate anticoagulation in an immobilised patient on renal replacement therapy reflects the extent of bone loss – a case report. *BMC Nephrol*. 2014; 15: 163. doi: 10.1186/1471-2369-15-163.
37. *Khadzhynov D, Schelter C, Lieker I, Mika A, Staeck O, Neumayer H-H et al*. Incidence and outcome of metabolic disarrangements consistent with citrate accumulation in critically ill patients undergoing continuous venovenous hemodialysis with regional citrate anticoagulation. *J Crit Care*. 2014; 29 (2): 265–271. doi: 10.1016/j.jcrc.2013.10.015.
38. *Poptsov VN.* Pochechnaya funktsiya u bol'nykh, nakhodyashchikhsya na vspomogatel'nom krovoobrashchenii, i retsipientov serdtsa. *Rukovodstvo po ekstrakorporal'nomu ochishcheniyu krovi v intensivnoy terapii*. Pod red. L.A. Bokeriya, M.B. Yarustovskogo. Izdanie 3-e, M.: NTsSSKh im. A.N. Bakuleva MZ RF, 2016. 804.
39. *Tjahjono R, Connellan M, Granger E.* Predictors of Acute Kidney Injury in Cardiac Transplantation. *Transplant Proc*. 2016; 48 (1): 167–172. doi: 10.1016/j.transproceed.2015.12.006.
40. *García-Gigorro R, Renes-Carreño E, Peiretti MAC, López PA, Vela JLP, Rodríguez JG et al.* Incidence, Risk Factors and Outcomes of Early Acute Kidney Injury After Heart Transplantation: An 18-year Experience. *Transplantation*. 2018; 102 (11): 1901–1908. doi: 10.1097/TP.0000000000002293.
41. *Wang T-J, Lin C-H, Wei H-J, Wu M-J.* Long-Term Outcomes and Risk Factors of Renal Failure Requiring Dialysis after Heart Transplantation: A Nationwide Cohort Study. *J Clin Med*. 2020; 9 (8): 2455. https://doi.org/10.3390/jcm9082455.
42. *Wang L, Wang T, Rushton SN, Parry G, Dark JH, Sheerin NS.* The impact of severe acute kidney injury requiring renal replacement therapy on survival and renal function of heart transplant recipients – a UK cohort study. *Transpl Int*. 2020 Jun 16. doi: 10.1111/tri.13675.
43. *Guven G, Brankovic M, Constantinescu AA, Brugts JJ, Hesselink DA.* Preoperative right heart hemodynamics predict postoperative acute kidney injury after heart transplantation. *Intensive Care Med*. 2018; 44: 588–597. doi: 10.1007/s00134-018-5159-z.
44. *Shen B, Xu J, Lv W, Jiang W, Wang Y, Nie Y et al*. Efficacy of Early Goal-Directed Renal Replacement Therapy for the Treatment of Acute Kidney Injury After Heart Transplantation: A Single-Center 10-Year Experience. *J Cardiothorac Vasc Anesth.* 2020; 34 (6): 1534–1541. doi: 10.1053/j.jvca.2019.11.022.
45. *Lund LH, Edwards LB, Dipchand AI, Goldfarb S, Kucheryavaya AY, Levvey BJ et al.* International Society for Heart and Lung Transplantation. The Registry of the International Society for Heart and Lung Transplantation: Thirty-third Adult Heart Transplantation Report – 2016; Focus Theme: Primary Diagnostic Indications for Transplant. *J Heart Lung Transplant*. 2016; 35 (10): 1158–1169. doi: 0.1016/j.healun.2016.08.017.
46. *Ivey-Miranda JB, Flores-Umanzor E, Farrero-Torres M, Santiago E, Cepas-Guillen PL, Perez-Villa F.* Predictors of renal replacement therapy after heart transplantation and its impact on long-term survival. *Clin Transplant. 2*018; 32 (10): e13401. doi: 10.1111/ctr.13401.
47. *Kolsrud O, Karason K, Holmberg E, Ricksten S-E, Felldin M, Samuelsson O, Dellgren G.* Renal function and outcome after heart transplantation. *J Thorac Cardiovasc Surg*. 2018; 155 (4): 1593–1604. doi: 10.1016/j.jtcvs.2017.11.087.
48. *Jokinen JJ, Tikkanen J, Kukkonen S, Hämmäinen P, Lommi J, Sipponen J, Lemström KB.* Natural course and risk factors for impaired renal function during the first year after heart transplantation. *J Heart Lung Transplant*. 2010; 29 (6): 633–640. doi: 10.1016/j.healun.2010.01.004.
49. *Gude E, Andreassen AK, Arora S, Gullestad L, Grov I, Hartmann A et al*. Acute renal failure early after heart transplantation: risk factors and clinical consequences. *Clin Transplant*. 2010; 24 (6): E207–E213. doi: 10.1111/j.1399-0012.2010.01225.x.
50. *Fortrie G, Manintveld OC, Constantinescu AA, van de Woestijne PC, Betjes MGH.* Renal function at 1 year after cardiac transplantation rather than acute kidney injury is highly associated with long-term patient survival and loss of renal function – a retrospective cohort study. *Transpl Int*. 2017; 30 (8): 788–798. doi: 10.1111/tri.12940.
51. *Lund LH, Khush KK, Cherikh WS, Goldfarb S, Kucheryavaya AY, Levvey BJ et al.* The Registry of the International Society for Heart and Lung Transplantation: Thirty-fourth Adult Heart Transplantation Report – 2017; Focus Theme: Allograft ischemic time. *J Heart Lung Transplant*. 2017; 36 (10): 1037–1046. doi: 10.1016/j.healun.2017.07.019.
52. *Puttarajappa CM, Bernardo JF, John A Kellum JA.* Renal Complications Following Lung Transplantation and Heart Transplantation. *Crit Care Clin*. 2019; 35 (1): 61–73. doi: 10.1016/j.ccc.2018.08.009.
53. *El-Husseini A, Aghil A, Ramirez J, Sawaya B, Rajagopalan N, Baz M et al*. Outcome of kidney transplant in primary, repeat, and kidney-after-nonrenal solid-organ transplantation: 15-year analysis of recent UNOS database. *Clin Transplant.* 2017; 31 (11): e13108. doi: 10.1111/ctr.13108.

54. *Cassuto JR, Reese PP, Sonnad S, Bloom RD, Levine MH, Olthoff KM et al*. Wait list death and survival benefit of kidney transplantation among nonrenal transplant recipients. *Am J Transplant*. 2010; 10 (11): 2502–2511. doi: 10.1111/j.1600-6143.2010.03292.x.
55. *Grupper Av, Grupper Ay, Daly RC, Pereira NL, Hathcock MA, Kremers WK et al.* Kidney transplantation as a therapeutic option for end-stage renal disease developing after heart transplantation. *J Heart Lung Transplant*. 2017; 36 (3): 297–304. doi: 10.1016/j.healun.2016.08.004.
56. *Roest S, Hesselink DA, Klimczak-Tomaniak D, Kardys I, Caliskan K, Brugts JJ et al.* Incidence of end-stage renal disease after heart transplantation and effect of its treatment on survival. *ESC Heart Fail*. 2020; 7 (2): 533–541. doi: 10.1002/ehf2.12585.
57. *Vermes E, Grimbert P, Sebbag L, Barrou B, Pouteil-Noble C, Pavie A.* Long-term results of combined heart and kidney transplantation: a French multicenter study. *J Heart Lung Transplant.* 2009; 28 (5): 440–445. doi: 10.1016/j.healun.2009.01.020.
58. *Czer LSC, Ruzza A, Vespignani R, Jordan S, De Robertis MA, Mirocha J et al.* Survival and allograft rejection rates after combined heart and kidney transplantation in comparison with heart transplantation alone. *Transplant Proc*. 2011; 43 (10): 3869–3876. doi: 10.1016/j.transproceed.2011.08.095.
59. *Hermsen JL, Nath DS, del Rio AM, Eickstaedt JB, Wigfield C, Lindsey JD, Edwards NM.* Combined heart-kidney transplantation: the University of Wisconsin experience. *J Heart Lung Transplant.* 2007; 26 (11): 1119–1126. doi: 10.1016/j.healun.2007.08.011.
60. *Pinderski LJ, Kirklin JK, McGiffin D, Brown R, Naftel DC, Young KR Jr et al.* Multi-organ transplantation: is there a protective effect against acute and chronic rejection? *J Heart Lung Transplant*. 2005; 24 (11): 1828–1833. doi: 10.1016/j.healun.2005.03.015.
61. *Rana A, Robles S, Russo MJ, Halazun KJ, Woodland DC, Witkowski P et al*. The combined organ effect: protection against rejection? *Ann Surg.* 2008; 248 (5): 871–879. doi: 10.1097/SLA.0b013e31817fc2b8.
62. *Shevchenko OP, Kurabekova RM, Tsiroulnikova OM.* Biomarkers of immune tolerance in liver transplantation. *Russian Journal of Transplantology and Artificial Organs.* 2016; 18 (3): 137–144. (In Russ.). https://doi.org/10.15825/1995-1191-2016-3-137-144.
63. *Ruzza A, Czer LSC, Trento A, Esmailian F.* Combined heart and kidney transplantation: what is the appropriate surgical sequence? *Interactive CardioVascular and Thoracic Surgery.* 2013; 17: 416–418. doi: 10.1093/icvts/ivt172.
64. *Chacon MM, Roberts EK.* Dilemmas for the Cardiac Anesthesiologist: Managing Conflicting Fluid Management Strategies During Combined Heart-Kidney Transplantation. *J Cardiothorac Vasc Anesth*. 2018; 32 (1): 50–52. doi: 10.1053/j.jvca.2017.10.044.
65. *Awad M, Czera LSC, Esmailian F, Jordan S, De Robertis MA, Mirocha J et al.* Combined Heart and Kidney Transplantation: A 23-Year Experience. *Transplant Proc*. 2017; 49 (2): 348–353. doi: 10.1016/j.transproceed.2016.11.040.
66. *Toinet T, Dominique I, Cholley I, Vanalderwerelt V, Goujon A, Paret F et al.* Renal outcome after simultaneous heart and kidney transplantation. *Clin Transplant*. 2019; 33 (7): e13615. doi: 10.1111/ctr.13615.
67. *Raichlin E, Kushwaha SS, Daly RC, Kremers WK, Frantz RP, Clavell AL et al.* Combined heart and kidney transplantation provides an excellent survival and decreases risk of cardiac cellular rejection and coronary allograft vasculopathy. *Transplant Proc*. 2011; 43 (5): 1871–1876. doi: 10.1016/j.transproceed.2011.01.190.
68. *Karamlou T, Welke KF, McMullan DM, Cohen GA, Gelow J, Tibayan FA et al.* Combined heart-kidney transplant improves post-transplant survival compared with isolated heart transplant in recipients with reduced glomerular filtration rate: Analysis of 593 combined heart-kidney transplants from the United Network Organ Sharing Database. *J Thorac Cardiovasc Surg*. 2014; 147 (1): 456–461. doi: 10.1016/j.jtcvs.2013.09.017.
69. *Ramsingh D, Harvey R, Runyon A, Benggon M.* Anesthesia for Heart Transplantation. *Anesthesiol Clin*. 2017; 35 (3): 453–471. doi: 10.1016/j.anclin.2017.05.002.
70. *Awad MA, Czer LSC, Emerson D, Jordan S, De Robertis MA, Mirocha J et al.* Combined Heart and Kidney Transplantation: Clinical Experience in 100 Consecutive Patients. *J Am Heart Assoc*. 2019; 8 (4): e010570. doi: 10.1161/JAHA.118.010570.
71. *Kilic A, Grimm JC, Whitman GJR, Shah AS, Mandal K, Conte JV, Sciortino CM.* The survival benefit of simultaneous heart-kidney transplantation extends beyond dialysis-dependent patients. *Ann Thorac Surg*. 2015; 99 (4): 1321–1327. doi: 10.1016/j.athoracsur.2014.09.026.
72. *Schaffer JM, Chiu P, Singh SK, Oyer PE, Reitz BA, Mallidi HR*. Heart and Combined Heart–Kidney Transplantation in Patients With Concomitant Renal Insufficiency and End-Stage Heart Failure. *American Journal of Transplantation.* 2014; 14: 384–396. doi: 10.1111/ajt.12522.
73. *Melvinsdottir I, Foley DP, Hess T, Gunnarsson SI, Kohmoto T, Hermsen J et al*. Heart and kidney transplant: should they be combined or subsequent? *ESC Heart Fail*. 2020; 7 (5): 2734–2743. doi: 10.1002/ehf2.12864.
74. *Gallo M, Trivedi JR, Schumer EM, Slaughter MS.* Combined Heart-Kidney Transplant Versus Sequential Kidney Transplant in Heart Transplant Recipients. *J Card Fail*. 2020; 26 (7): 574–579. doi: 10.1016/j.cardfail.2020.03.002.
75. *Poz YL, Strokov AG, Poptsov VN, Kopylova YuV, Kryshin KN.* Kidney injury and renal replacement therapy in heart transplant recipient. *Russian Journal of Transplantology and Artificial Organs.* 2017; 19 (1): 52–56. [In Russ.]. https://doi.org/10.15825/1995-1191-2017-1-52-56.
76. *Poptsov VN.* Combined heart-kidney transplantation. *Russian Journal of Transplantology and Artificial Organs.* 2016; 18 (1): 78–82. [In Russ.]. https://doi.org/10.15825/1995-1191-2016-1-78-82.

The article was submitted to the journal on 23.07.2021

DOI: 10.15825/1995-1191-2021-4-73-78

EVALUATION OF THE EFFICIENCY OF A NEW PULSATILE FLOW-GENERATING CIRCULATORY-ASSIST SYSTEM IN ROTARY BLOOD PUMPS. RESEARCH ON A MATHEMATICAL MODEL

G.P. Itkin[1, 2], A.I. Syrbu[2], A.P. Kyleshov[1], A.S. Buchnev[1], A.A. Drobyshev[1]

[1] Shumakov National Medical Research Center of Transplantology and Artificial Organs, Moscow, Russian Federation

[2] Moscow Institute of Physics and Technology, Moscow, Russian Federation

Objective: to study the effect of a pulsatile flow-generation (PFG) device on the basic hemodynamic parameters of the circulatory system using a mathematical model. **Results.** Modelling and simulation showed that the use of PFG significantly (76%) increases aortic pulse pressure. The proposed mathematical model adequately describes the dynamics of the circulatory system and metabolism (oxygen debt) on physical activity in normal conditions and heart failure, and the use of non-pulsatile and pulsatile circulatory-assist systems. The mathematical model also shows that the use of PFG device blocks the development of rarefaction in the left ventricular cavity associated with a mismatch of blood inflow and outflow in diastolic phase when there is need to increase systemic blood flow by increasing the rotary pump speed.

Keywords: mathematical model, circulatory system, pulsatile rotary blood pump, pulsatile flow generation.

INTRODUCTION

In recent decades, rotary nonpulsatile flow pumps (NFPs) have almost replaced pulsatile flow pumps (PFPs) in clinical practice as a bridge to heart transplantation and targeted therapy, due to the advantage of these pumps in weight-size, energy and performance characteristics. This promoted higher survival among patients with end-stage heart failure (HF) [1–3]. However, prolonged use of NFPs leads to a number of complications associated with low aortic pressure pulsation. These include gastrointestinal bleeding, arteriovenous malformation, aortic valve insufficiency, etc. [4–7]. Besides, these pumps showed low cardiac unloading in comparison with PFPs, which is one of the main factors of native myocardial contractility restoration [8, 9]. A number of works have shown the important role that pulsatile flow plays not only in implantable systems, but also in extracorporeal short-term mechanical circulatory assist systems, including cardiopulmonary bypass systems [10, 11]. Therefore, in the last decade, the attention of researchers has been directed towards the development of various pulsatile flow generation (PFG) methods [12–14].

One of the main directions for effectiveness assessment of these methods is the use of mathematical models (MM) allowing to analyze the operation of assisted circulatory systems (MCAD) more fully in the dynamic range of circulatory system parameter changes (under physical load, myocardial contractility changes, etc.) compared to the studies using hydrodynamic circulatory system simulators. In particular, the use of MM methods will allow for comparative assessment of the efficiency of MCAD techniques using NFPs in standard mode and in PFG mode. In this work, we carried out a comparative analysis of the circulatory system when including left ventricular assist devices (LVADs) using NFPs in standard non-pulsatile mode and in PFG mode [15].

MATERIALS AND METHODS

The basic structure of the mathematical model of the cardiovascular system (CVS) is presented in A.I. Syrbu et al. [16]. This model additionally includes NFP modules, pulse flow generator (PFG) [15], as well as an element simulating the effect of left ventricular (LV) discharge development, occurring at high NFP speeds [17]. This MM is developed in Matlab Simulink environment using electrohydraulic analog method and describes a large circulatory circuit, consisting of the following modules (Fig. 1): left ventricle (LV), left atrium (LA), aortic valve (AV), mitral valve (MV), aortic section (AS), peripheral section (PS), venous section (VS), coronary vessels (CV), and regulation circuits: baroreceptor (B), oxygen debt (O_2) and heart rate (HR). The dashed lines in Fig. 1 highlight the NFP of PFG and the element simulating LV rarefaction (R).

This MM allows for a comparative study of CVS operation with inclusion of NFPs in the standard mode

Corresponding author: George Itkin. Address: 1, Shchukinskaya str., Moscow, 123182, Russian Federation. Phone: (916) 129-78-33. E-mail: georgeitkin@mail.ru

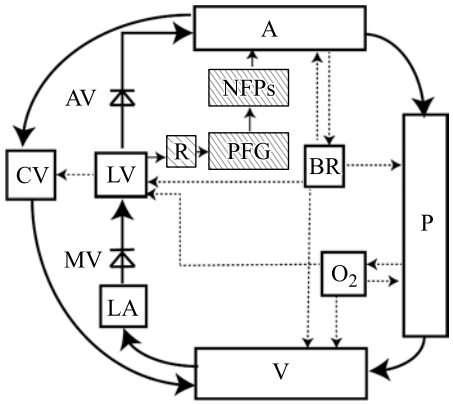

Fig. 1. Block diagram of the mathematical model

and with operation of PFPs with inclusion of PFG. The additional modules included in the CVS mathematical model are described by the following basic relationships.

Blood flow through NFPs is defined by the expression [17]:

$$dQ_{vad}/dt = (P(Q_{vad}) - (P_{ao} - P_{lv}) - R_cQ_{vad}) / L_c,$$

where $P(Q_{vad})$ is the dependence of pressure created by NFPs = on the flow through it, which is determined from the flow-pressure characteristic of NFPs, P_{ao} is aortic pressure, P_{lv} is LV pressure, R_c and L_c are cannula resistance and inertia.

The pressure generated by the NFP is described by the following differential equation [17]:

$$P(Q_{vad}) = aQ_{vad} + bdQ_{vad}/dt + cw^2,$$

where Q_{vad} is blood flow through NFPs; w is pump rotor speed; a, b, c are coefficients; dQ/dt is the time differentiation operator. The coefficients were selected from the flow-pressure characteristic of the HeartWare HVAD centrifugal pump [18].

PFG contains a hydraulic resistance made in the form of connector, in which there is a tube of elastic biocompatible material, hermetically sealed by the ends along the butt ends of the cylinder from its inner side (Fig. 2).

This tube opens fully at a pressure greater than a certain P_2 in the systolic phase and partially closes when the pressure drops below P_1 in the LV diastolic phase, thereby increasing the hydraulic resistance to blood flow.

The following equation was used to describe the PFG device:

$$R_{PFG} = \frac{(P_2 - P_{lv})R_{max}}{P_1 - P_2},\ R_{PFG} \geq 0,$$

where R_{max} is the highest hydraulic resistance in diastole, P_1 is the pressure at which the elastic tube partially collapses, P_2 is the pressure at which the elastic tube opens and resistance is minimal ($R_{min} = 0$).

One of the problems related to NFP operation in elevated rotor speed regime, necessary to normalize systemic blood flow and improve LV unloading, is the danger of developing LV rarefaction related to mismatch of blood inflow and outflow through the pump during diastolic phase. It can lead to tissue damage in the inlet cannula, interventricular septum displacement, deterioration in right ventricular function, arrhythmia, cardiac ischemia, and hemolysis [19].

To describe this effect, we used the following piecewise function [20, 21]:

$$R = \begin{cases} 0;\ P_{lv} \geq P_{th} \\ -3.5P_{lv} + 3.5P_{th};\ P_{lv} < P_{th} \end{cases},$$

where R is additional resistance at the NFP inlet, P_{th} is threshold value.

RESULTS

Fig. 3 shows time dependences of aortic pressure (AP), systemic blood flow, and HR in the simulations: HF (time interval I: 0 to 30 sec), connection of NFPs without PFG (time interval II: 30 to 60 sec), and with PFG connection without change in NFPs (time interval III: 60 to 90 sec) and with increase in NFP speed (time interval IV: 90 to 120 sec).

Analysis of the dependencies shown in Fig. 3, shows the following: NFP connection leads to changes in the main parameters of hemodynamics: increase in mean AP to 114/100 mmHg and blood flow to 4.2 L/min and decrease in HR to 75 beats/min. At the same time, the qualitative nature of the dependencies and the obtained values of hemodynamic parameters correspond to the data given in the literature [22]. In turn, PFG connection at constant NFP rotor speed leads to decreased blood

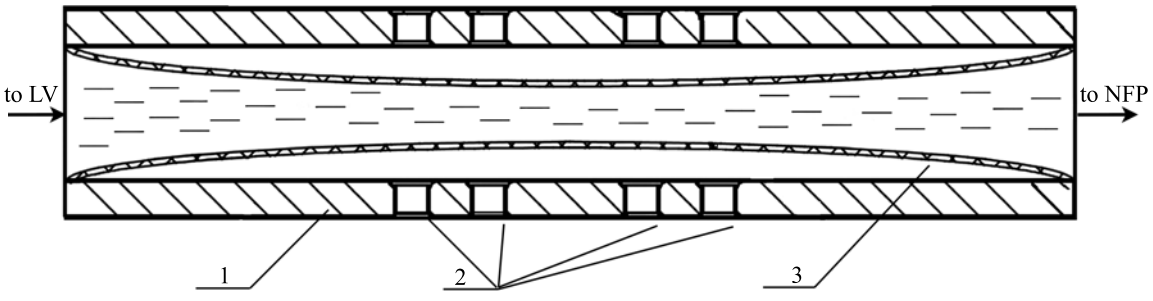

Fig. 2. PFG scheme (1 – connector, 2 – holes with an outlet to the atmosphere or compensation chamber, 3 – elastic tube)

flow and aortic pressure with normalization of the pulsatile nature of blood flow in the aorta. Therefore, to normalize mean AP and systemic blood flow, the NFP rotational speed was increased by 15%. In this case, a concomitant effect is a further increase in pulsatile AP by 76% compared to NFP without PFG.

This model also allows for evaluation of NFPs under physical stress. It was obtained that when PFG was connected, pulse pressure increased from 10 to 24 mmHg, or by 140%.

Fig. 4 shows the time dependences of aortic pressure (AP), systemic blood flow (SBF), HR and oxygen debt (DO) in the simulations: physiological norm (a), HF (b), physical activity in HF conditions (c), physical activity in HF conditions with connected NFP (d) and with PFG with increased NFP turnover (e).

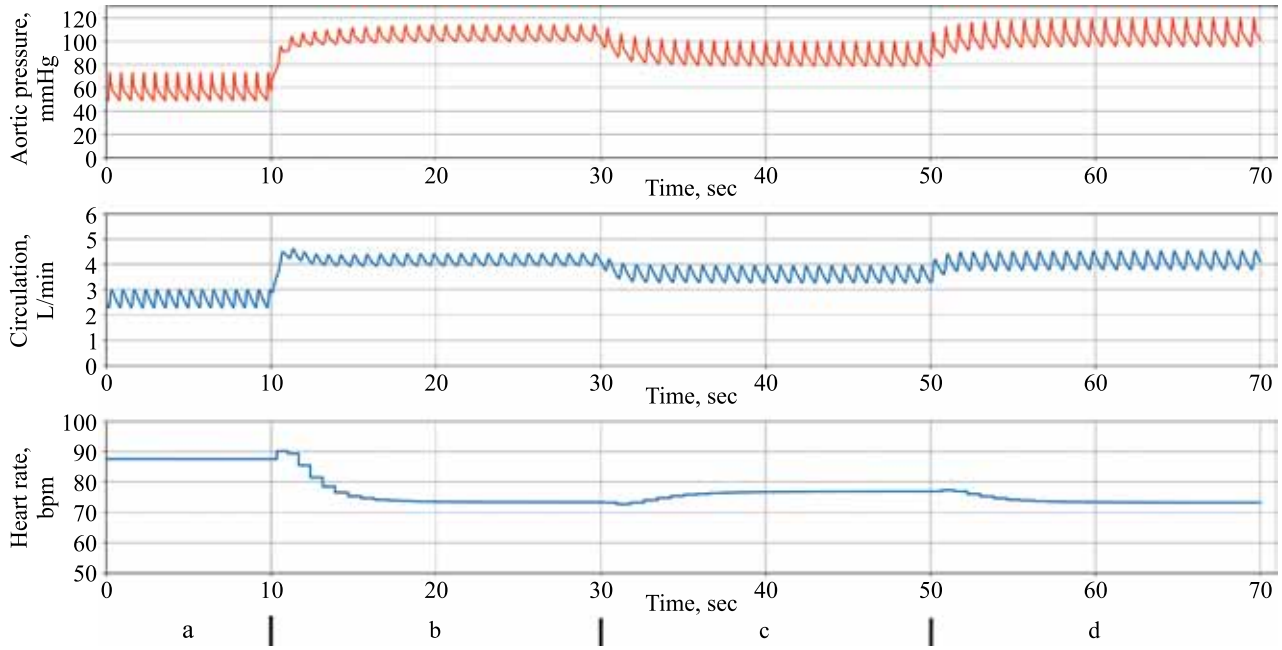

Fig. 3. Dependence of blood pressure, systemic circulation and heart rate on time for simulated states: a, HF; b, NPBP connection; c, NPBP with PFG without increased rotor speed; d, NPBP with PFG with increased rotor speed

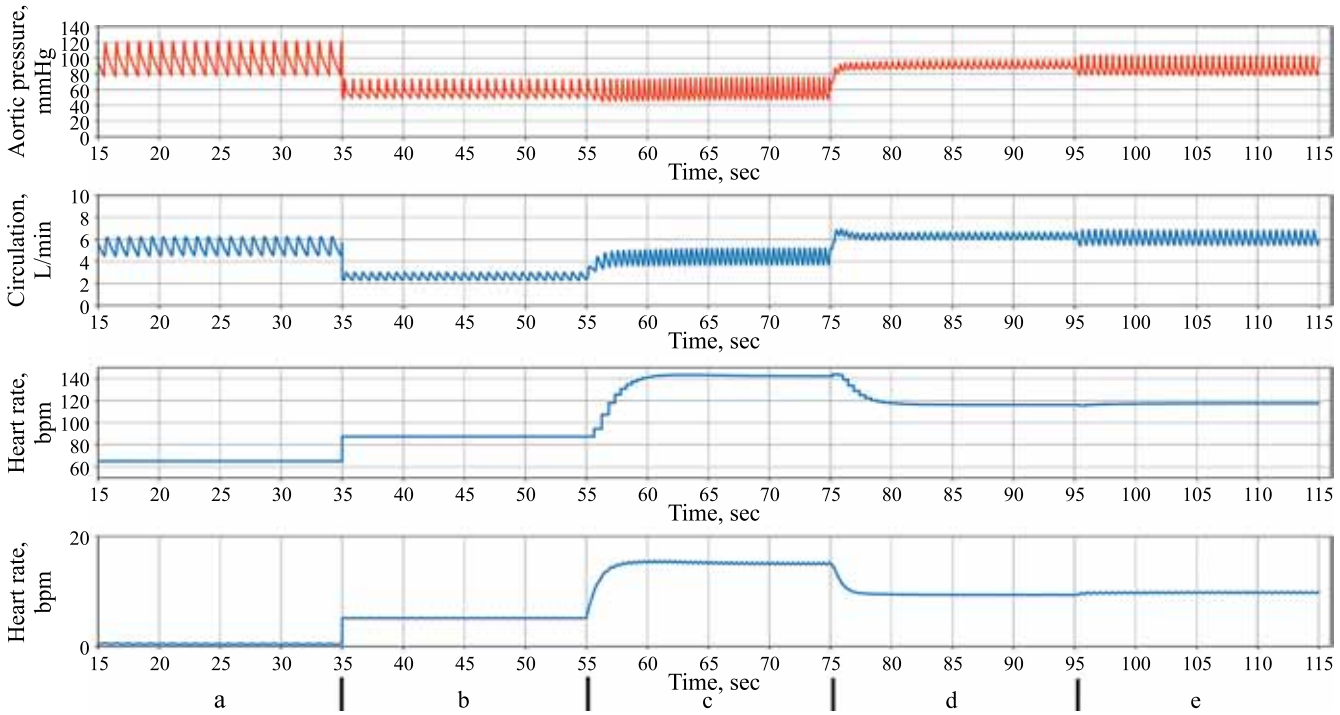

Fig. 4. Dependence of blood pressure, systemic circulation, heart rate and oxygen debt on time in the simulation of physiological norm (a), HF (b), physical activity under HF conditions (c), with connected NPBP (d) and PFG connection (e)

The results obtained are consistent with the experimental data obtained in [22] in the study of physical activity in HF patients with NFPs.

As indicated above, one of the problems of clinical application of PFPs is the effect of development of rarefaction in the diastolic phase of LV when systemic blood flow should be increased by increasing PFP speed [23, 24].

On MM, we evaluated this effect with increased speed of the PFPs (15%) in standard mode and when the PFG is connected (Fig. 5).

The simulation results show that in standard NFP mode, rarefaction reached –58 mmHg, and when PFG was connected, the dangerous effect of LV inlet rarefaction completely disappeared.

Fig. 6 shows the dependence of arterial pressure on LV elasticity in HF modeling with NFP and PFG. The increase in elasticity led to increased mean AP from 90 to 110 mmHg and pulse pressure from 20 to 30 mmHg.

CONCLUSION

The computer MM of human systemic circulation, built on the basis of the model developed earlier by us [16], allows for investigation of the state of the circulatory system in heart failure when MCAD is connected in LVAD mode in standard NFP mode and when PFG is connected. Simulation results show a significant (76% and 140% without and with physical load) increase in pulse pressure in the aorta as well as prevention of rarefaction area in the left ventricle when using variable hydraulic resistance. It has been shown that it is possible to model a new device – PFG, which opens the possibility of optimizing both the parameters of the PFG device itself and combination of PFG and NFP parameters (NFP

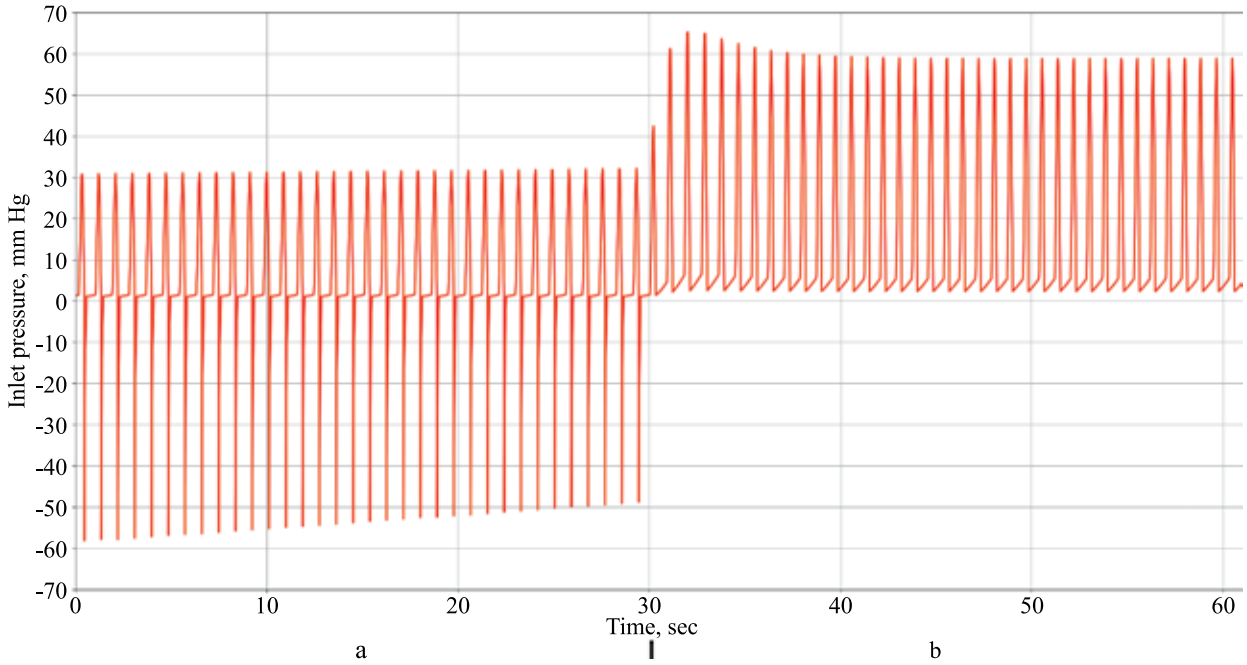

Fig. 5. Dependence of NPBP inlet pressure on high rotor speed without (a) and with PFG (b)

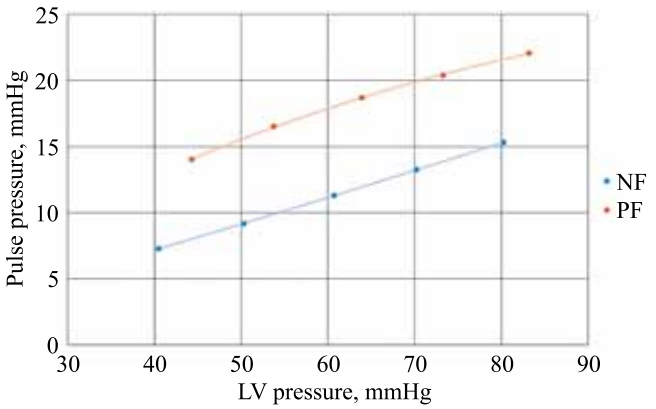

Fig. 6. Changes in pulse pressure with increasing LV pressure in heart failure with NPBP and PFG

operation modes, NFP outlet pressure at different PFG parameters and others). The further direction of research is precisely on addressing the problems of optimizing these devices.

The authors declare no conflict of interest.

REFERENCES

1. *Kirklin JK, Naftel DC, Pagani FD, Kormos RL, Stevenson LW, Blume ED et al.* INTERMACS annual report: 15,000 patients and counting. *J Heart Lung Transplant*. 2015; 34: 1495–1504.
2. *Slaughter SM, Rogers JG, Milano CA, Russell SD, Conte JV et al.* Advanced heart failure treated with con-

tinuous-flow left ventricular assist device. *N Engl J Med*. 2009; 361: 2241–2251.
3. *Rogers JG, Aaronson KD, Boyle AJ, Russell CA, Milano SD, Pagani FD et al.* Continuous flow left ventricular assist device improves functional capacity and quality of life of advanced heart failure patients. *J Am Coll Cardiol*. 2010; 55: 1826–1834.
4. *Saito S, Westaby S, Piggot D, Dudnikov S, Robson D, Catarino PA et al.* End-organ function during chronic nonpulsatile circulation. *Annals of Thoracic Surgery*. 2002; 74: 1080–1085.
5. *Crow S, John R, Boyle A, Shumway S, Liao K, Colvin-Adams M et al.* Gastrointestinal bleeding rates in recipients of nonpulsatile and pulsatile left ventricular assist devices. *Journal of Thoracic and Cardiovascular Surgery*. 2009; 137: 208–215.
6. *Letsou GV, Connelly JH, Delgado RM 3rd, Myers TJ, Gregoric ID, Smart FW et al.* Is native aortic valve commissural fusion in patients with long-term left ventricular assist devices associated with clinically important aortic insufficiency. *Journal of Heart and Lung Transplantation*. 2006; 25: 395–399.
7. *Nishimura T, Tatsumi E, Takaichi S, Taenaka Y, Wakisaka Y, Nakatani T et al.* Prolonged nonpulsatile left heart bypass with reduced systemic pulse pressure causes morphological changes in the aortic wall. *Artificial Organs*. 1998; 22: 405–410.
8. *Birks EJ, George RS, Hedger M, Bahrami T, Wilton P, Bowles CT et al.* Reversal of severe heart failure with a continuous-flow left ventricular assist device and pharmacological therapy: a prospective study. *Circulation*. 2011; 123: 381–390.
9. *Birks EJ, George RS, Firouzi A, Wright G, Bahrami T, Yacoub MH et al.* Long-term outcomes of patients bridged to recovery versus patients bridged to transplantation. *J Thorac Cardiovasc Surg*. 2012; 144: 190–196.
10. *Wang S, Evenson A, Chin BJ, Kunselman AR, Undar A.* Evaluation of conventional non-pulsatile and novel pulsatile ECLS systems in a simulated pediatric ECLS model. *Artificial Organs*. 2015; 39: 1–9.
11. *Wang S, Kunselman AR, Clark JB, Undar A. In vitro* hemodynamic evaluation of a novel pulsatile ECLS system: impact of perfusion modes and circuit components on energy loss. *Artificial Organs*. 2015; 39: 59–66.
12. *Ising MS, Sobieski MA, Slaughter MS, Koenig SC, Giridharan GA*. Feasibility of pump speed modulation for restoring vascular pulsatility with rotary blood pumps. *ASAIO J*. 2015; 61 (5): 526–532.
13. *Vandenberghe S, Segers P, Antaki JF, Meyns B, Verdonck PR.* Rapid Speed Modulation of a Rotary Total Artificial Heart Impeller. *Artificial Organs*. 2016; 40: 824–833.
14. *Soucy KG, Giridharan GA, Choi Y, Sobieski MA, Monreal G, Cheng A. et al.* Rotary pump speed modulation for generating pulsatile flow and phasic left ventricular volume unloading in a bovine model of chronic ischemic heart failure. *J Heart Lung Transplant*. 2015; 34: 122–131.
15. *Itkin GP, Drobyshev AA, Buchnev AS, Kuleshov AP, Nosov MS.* Ustroystvo upravleniya potokom krovi v ekstrakorporal'nykh sistemakh vspomogatel'nogo krovoobrashcheniya. Patent RU 201911. Patentoobladatel': FGBU "NMITs TIO im. ak. V.I. Shumakova" Minzdrava Rossii. 2020. № 201911 ot 21.01.2021 g.
16. *Syrbu AI, Itkin GP, Kuleshov AP, Gayday NA*. Matematicheskaya model' neyrogumoral'noy regulyatsii sistemy krovoobrashcheniya. *Meditsinskaya tekhnika*. 2021; 4: 41–44.
17. *Ferreira A, Chen S, Simaan MA, Boston JR, Antaki JF.* A nonlinear state-space model of a combined cardiovascular system and a rotary pump. *In Proceedings of the 44th IEEE Conference on Decision and Control*. 2005; 15: 897–902.
18. *LaRose JA, Tamez D, Ashenuga M, Reyes C*. Design concepts and principle of operation of the HeartWare ventricular assist system. *ASAIO J*. 2010; 56 (4): 285–289.
19. *Yuhki A, Hatoh E, Nogawa M, Miura M, Shimazaki Y, Takatani S.* Detection of suction and regurgitation of the implantable centrifugal pump based on the motor current waveform analysis and its application to optimization of pump flow. *Artificial Organs*. 1999; 23: 532–537.
20. *Gohean JR, George MJ, Pate TD, Kurusz M, Longoria RG, Smalling RW.* Verification of a computational cardiovascular system model comparing the hemodynamics of a continuous flow to a synchronous valveless pulsatile flow left ventricular assist device. *ASAIO J*. 2013; 59: 107.
21. *Horvath DJ, Horvath DW, Karimov JH, Kuban BD, Miyamoto T, Fukamachi K.* A simulation tool for mechanical circulatory support device interaction with diseased states. *Artificial Organs*. 2020; 14: 1–9.
22. *Hambrecht R, Gielen S, Linke A, Fiehn E, Yu J, Walther C, Schoene N, Schuler G.* Effects of exercise training on left ventricular function and peripheral resistance in patients with chronic heart failure: a randomized trial. *Jama*. 2000; 283 (23): 3095–3101.
23. *Tchantchaleishvili V, Jessica GY, Luc JGY, Cohan CM, Phan K, Hübbert L et al.* Clinical implications of physiological flow adjustment in continuous-flow left ventricular assist devices. *ASAIO J*. 2017; 63: 241–250.
24. *Shumakov VI, Itkin GP, Shtengol'd ESh, Egorov TL.* Issledovanie shuntirovaniya levogo zheludochka serdtsa v usloviyakh dozirovannoy serdechnoy nedostatochnosti na matematicheskoy modeli. *Scripta medica*. 1973; 48: 475–489.

The article was submitted to the journal on 11.10.2021

DOI: 10.15825/1995-1191-2021-4-79-85

DESIGN AND 3D-MODEL OF A DYNAMIC BUBBLE TRAP FOR CARDIOPULMONARY BYPASS

A.P. Kuleshov[1], A.S. Buchnev[1], A.A. Drobyshev[1], G.P. Itkin[1, 2]

[1] Shumakov National Medical Research Center of Transplantology and Artificial Organs, Moscow, Russian Federation

[2] Moscow Institute of Physics and Technology, Moscow, Russian Federation

The use of extracorporeal circulation systems (cardiopulmonary bypass pumps, ECMO) can lead to brain and coronary artery microembolism, which significantly reduces postoperative rehabilitation and often leads to severe complications. Microembolism occurs when oxygen or air microbubbles (MBs) enter the arterial system of patients. Existing CPB pumps come with built-in bubble trap systems but cannot remove bubbles in the circuit. ECMO devices have arterial filters but cannot reliably filter out <40 μm bubbles in a wide flow range. We have proposed an alternative method that involves the use of an efficient dynamic bubble trap (DBT) for both large and small bubbles. The design includes development of two DBT variants for hemodynamic conditions of adult and pediatric patients. The device is installed in the CPB pump and ECMO outlet lines. It provides sufficient bubble separation from the lines in a blood flow of 3.0–5.0 L/min for adults and 0.5–2.0 L/min for children. The developed computer models have shown that MBs smaller than 10 μm can be filtered. The use of this device will greatly reduce the likelihood of air embolism and provide the opportunity to reconsider the concept of expensive arterial filters.

Keywords: cardiopulmonary bypass, microbubbles, ECMO.

INTRODUCTION

Air embolism (AE) is accompanied by blockage of microvessels of vital organs and can occur when using both cardiopulmonary bypass pumps (CPB pumps, heart-lung machines, HL machines) and extracorporeal circulatory support systems. Until now, AE remains a severe problem, the most critical for brain microvessels [1–3].

There are many studies reporting postoperative neuropsychological complications after the use of mechanical circulatory assist devices (MCAD) associated with cerebral microischemia [4, 5]. AE with varying degrees occurs in almost all cardiopulmonary bypass (CPB) surgeries [6]. It is very important to quickly identify and eliminate the cause of air in the circuit, because the patient is often completely dependent on ECMO or CPB. Moreover, the air embolism mechanism is not only associated with microvascular occlusion, but can also be combined with the triggering of thrombosis at the blood-gas interface [7].

The most common cause of air aspiration is the inlet section of venous drainage line at the cannulation site. Unlike the situation when air enters the intake line, where they are trapped by the oxygenator, the presence of air in the return line is a more serious problem. In this case, air is often sucked into the oxygenator, which can occur if the oxygenator capacity exceeds the patient's oxygen requirements, and blood pressure becomes lower than the gas pressure on different sides of the oxygenator membrane [8, 9]. Another reason is reduction in blood level in the venous reservoir below the critical level when using the perfusion technique.

In addition, during open heart surgeries with CPB, errors by perfusionists are not excluded. For example, due to reduction in blood level in the venous reservoir below the critical level, errors during blood sampling for analysis and incomplete air removal when filling the CPB circuits. The highest number of ingress of microbubbles (MBs) into the arterial line is possible during complex surgeries like aortic valve replacement [10]. Also, one should not exclude technical breakdowns in devices leading to circuit line rupture, blood cavitation and microbubble ingress from the venous reservoir into the arterial line due to active blood drainage using suctions.

Despite their small size, MBs are differentiated. Some researchers divide bubbles into: very small (<50 μm), which refers to MBs; small (50–100 mm); medium (100–150 μm); large (150–300 μm); very large (>300 μm) [11]. Others refer to MBs as all objects that can be measured by the current registration systems in the circuit of MCAD machines (from 5–10 μm to 250–500 μm) [12].

Modern MCAD devices provide protection against massive air embolism using arterial filters. These filters provide only limited effectiveness in removing MBs; they do not completely remove 25–40 μm MBs, depend-

Corresponding author: Arkadii Kuleshov. Address: 519, 1, 10, Proizvodstvennaya str., Moscow, 119619, Russian Federation. Phone: (915) 292-47-98. E-mail: ilovemylene@yandex.ru

ing on pore size [8, 13, 14], which can enter the bypass circuit both from the operating field and during perfusion interventions. Reduced size of filtration pores can lead to increased hydrodynamic resistance, damage to blood cells and platelet aggregation [8]. In our studies we consider predominantly 40–50 μm MBs.

In [8], a comprehensive assessment of MBs filtration in different oxygenation systems was carried out. The variation in efficiency of bubble trap systems was from 80% to 99%. It was shown that most of the MBs not captured by the filter ranged from 10 to 30 μm.

Reducing the number of MBs in the circuit of extracorporeal circulatory systems remains an important factor in patient safety, and the development of effective MBs separation devices remains a crucial task.

Fig. 1. Appearance of the DBT for an adult patient and a pediatric patient

MATERIALS AND METHODS

The *aim* of the work is to create an easy-to-use device for maximum separation of >10 μm gas bubbles and significant reduction of <10 μm MBs from MCAD circuit to improve the efficiency of circulatory assist devices. The design of two dynamic bubble trap (DBT) models, which are installed at the outlet of the arterial line by CPB and ECMO (Fig. 1), has been proposed. The devices trap bubbles at 3.0–5.0 L/min flow rates for adults and 0.5–2.0 L/min for pediatric patient.

How the DBT works

The DBT is an elongated cylindrical tube of biocompatible polymer that is connected to the outlet line of a CPB or ECMO machine instead of a filter. The DBT consists of a flow swirl unit, a bubble centering unit and an MBs separation unit (Fig. 2).

I. The flow swirl unit receives and expands blood flow by means of a conical inlet fitting, twisting around the axis with a helix (1).
II. The bubble centering unit is represented by a housing () extending into the outlet fitting (2).
III. The bubble separation unit is represented by a thin separating tube (3) with a small diameter at the separator outlet, positioned exactly along the axis of the device.

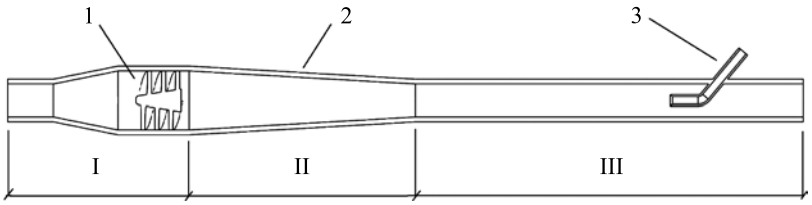

Fig. 2. Schematic diagram of the DBT. I, flow swirl unit; II, bubble centering unit; III, bubble separation chamber. 1, helix; 2, housing, 3, bubble outlet tube

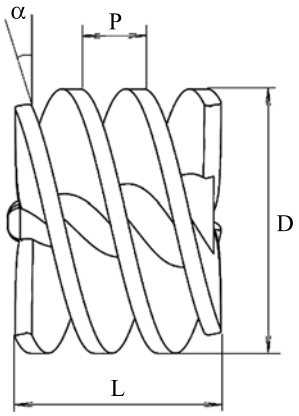

Fig. 3. Sketch of the helix

The *flow swirl unit* is designed for swirling around the axis of the blood flow using an iconic shaped helix in the inlet part of the housing. The helix (Fig. 3) has variable parameters such as inlet angle α, thread pitch P, diameter D and length L, which are calculated for flow parameters.

The blades are designed to convert part of linear flow into radial flow. The conical shape of the central body of the helix, expanding along the flow path, shifts it further away from the DBT axis. At the same time, by reducing the cross-sectional area of the helix channels from inlet to outlet, the velocity, according to partial deduction from Bernoulli's law, increases particle velocity, which

dramatically increases the centrifugal force of flow at the helix outlet. At the helix outlet, the maximum flow rate is reached, and an accelerating flow mode is formed. At the outlet of the helix, in the swirling flow due to centrifugal forces, an axisymmetric area is formed with a pressure drop from the periphery to the axis of the device. Under the generated pressure gradient, the bubbles rush from high pressure zone to low pressure zone, i.e. to the axis of the device, along which they move due to the linear component of the flow velocity. The effect depends on many geometrical factors, both on helix parameters and on angle of the cone-shaped body part.

The bubbles are then captured by a thin-walled, small-diameter tube connected to the venous reservoir and located at the separator outlet exactly along the axis of the device. In this way, a small portion of the blood, together with the micro and macro bubbles collected along the axis, circulates from the DBT to the venous reservoir of the air outlet due to the pressure differential. The operating principle of the design is shown in the fluid flow model (Fig. 4). The blood flow entering the DBT contains bubbles of different diameters. The inlet fitting has a conical expansion of the line. The diameter of this extension corresponds to the diameter of the helix used and allows for sufficient centripetal force in the blood flow. In the figure, it can be noted that the large bubbles are located on the separator axis at the helix outlet, while the MBs are centered some distance from it. This is due to the lower mass of the MBs.

With this in mind, the minimum size of centered MBs is determined by the total length of the block. The main study in this stage of device development comes down to determining the coordinates at which <10 μm bubbles are centered. This will allow the MBs separation tube to be positioned more efficiently.

Computer model of the device and stand

In the adult and pediatric models, according to analytical and mathematical calculations, the helix parameters were: 18 mm diameter, 20 mm length, 1.3 thread pitch, 3 blades and 17° entry angle. The lines were 10 mm and 6 mm in diameters, respectively. The bubble outlet tube has an inner diameter of 2.4 mm, which will allow taking no more than 10–15% of the blood volume. The bubble centering points of different diameters were analyzed on the models. Based on the results of the studies, the optimal distance from the helix where the outlet tube of the bubble outlet is located was chosen to be equal to the MBs centering coordinates to ensure effective operation of the DBT.

For this purpose, a 3D mathematical model of viscous fluid flow in DBT cavities was developed in COMSOL-Multiphysics software. The calculation boundary conditions were 100 mmHg pressure at the DBT outlet and 8 mmHg pressure in the tube, which corresponds to the average venous value. We applied multiphase simulation mode of blood and air flow. The flow rate averaged 5 L/min for adult and 1 L/min for pediatric circulation parameters. A 10^{-4} pressure convergence residual was defined as the convergence criterion. A k-ε turbulence model was used to simulate the flow field. A fairly fine mesh consisting of tetrahedral cells with a total number of 90,000 elements was obtained. An example of a multiphase flow simulation is shown in Fig. 5, where one can see the movement of 50 μm, 10 μm and 5 μm bubbles in the DBT model for a 5 L/min flow rate. As can be seen from the figure, smaller diameter MBs are more likely to pass the tube.

The developed DBT models were produced by 3D printing and examined on the a hydrodynamic stand

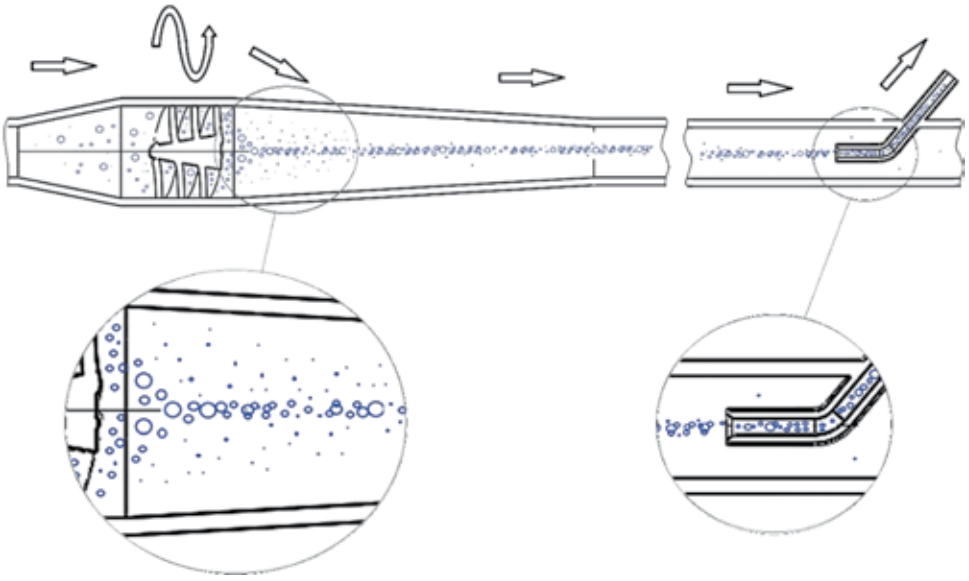

Fig. 4. DBT operating principal. The principle of centering the bubbles and getting them into the tube is shown

shown in Fig. 6. The stand includes a Rotaflow pump (Maquet, Germany), which sets the flow rate recorded by an ultrasonic flow meter (2). Bubbles are discharged from the DBT into a reservoir (8) filled with liquid. Bubbles of different diameters are introduced into the circuit through a port (5), by means of a syringe (6). The bubbles that have not reached the outlet tube are detected by the sensor (9). Pressure is regulated by the system hydraulic resistance (3), and is detected at the DBT inlet and outlet by pressure transducers (4, 10).

Flow rates in the aorta and pump were measured using ultrasonic flowmeter Transonic Systems Inc., USA. Pressure transducers (Edwards Life Sciences, USA). To record hemodynamic parameters, we used multichannel module ANGIOTON (Biosoft-M, Russia) with recording on a personal computer in Pumpax software (Biosoft-M). The stand was filled with 35% glycerol – saline mixture 4.0 ± 0.3 cP to reproduce physiological blood circulation conditions. The studies quantified the presence of MBs without/with the use of DBT.

RESULTS

Computer studies obtained the following data for adult and pediatric model costs.

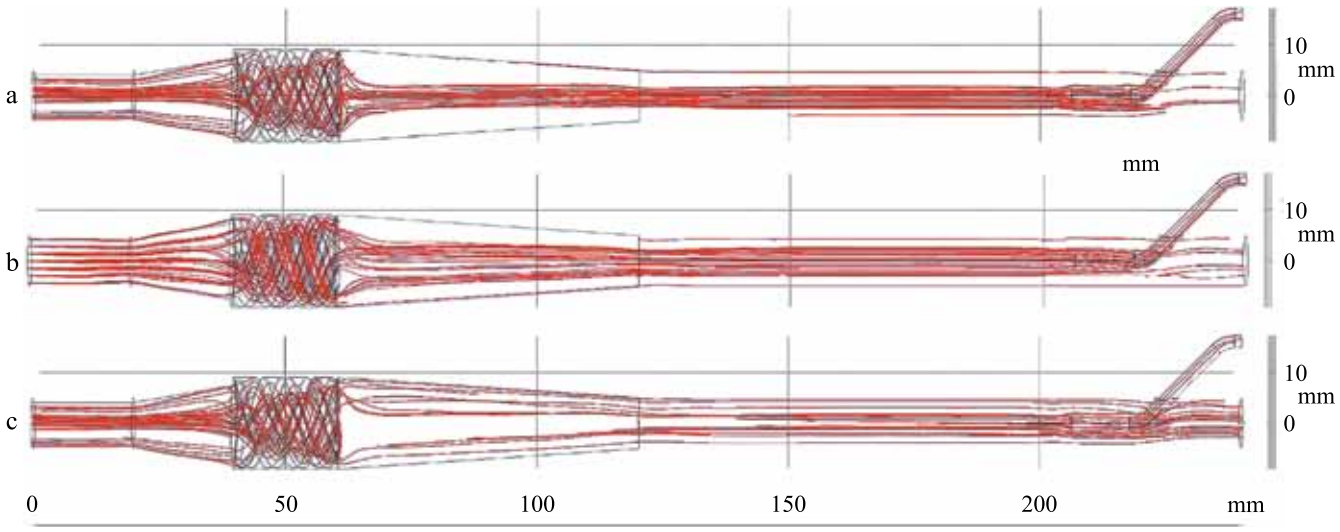

Fig. 5. Simulation of the DBT for a 5 L/min flow rate with 50 μm (a), 25 μm (b), and 5 μm (c) microbubbles

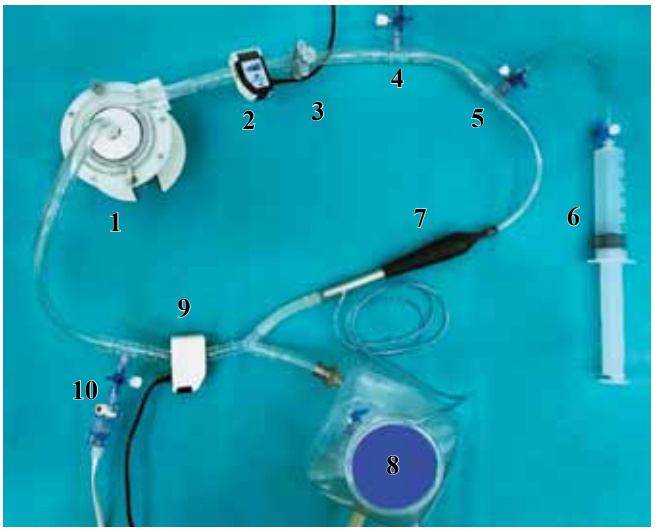

Fig. 6. Hydrodynamic stand for the DBT investigation: 1, Rotaflow pump; 2, flow meter; 3, system hydraulic resistance; 4, pressure transducer at the DBT inlet; 5, bubble input port; 6, bubble generation device; 7, DBT model; 8, bubble intake tank; 9, bubble counting sensor; 10, pressure transducer at the DBT outlet

As can be seen from the figure, MBs are centered much further away from the helix exit. The distance from the helix to the centering of 10 μm MBs for the adult and pediatric versions, were 133 mm and 86 mm, respectively. In view of the values obtained, the distance between the helix and the bubble outlet tube was chosen to be 143 mm and 96 mm, with a 10 mm margin, while the total length of the DBT models was 245 mm and 225 mm for the adult and child versions, respectively. Based on the data obtained from the computer model studies, experimental models of the DBT system were assembled and tested on a hydrodynamic stand.

As a result of studies on the hydrodynamic stand at a low pressure drop (90 mmHg for 3.0–5.0 L/min and 0.5–2.0 L/min blood flow), bubble counts before and after using DBT were obtained as shown in Fig. 8.

For these flow rate ranges in the two models, one can observe a significant decrease (by 3–4-fold) in the total number of MBs and >10 μm bubbles by a factor of 10 or more. There is, however, a decrease in efficiency at the boundaries of the studied flow rates of 0.5, 2.0,

3.0 and 5.0 L/min. Upon reaching the boundary ranges of the study, the number of recorded MBs began to increase. For low flow levels, this was due to a decrease in the pressure gradient and less exposure to MBs. For high flow rates, linear velocity of MBs along the DBT axis increases, which shifts their centering coordinates. There is also a fairly large pressure drop on the DBT (over 100 mmHg, at >5 L/min flow rate in the adult patient model and >2 L/min in the pediatric patient model). Therefore, work was continued to optimize the DBT in terms of reducing pressure drop while maintaining or improving MF separation efficiency.

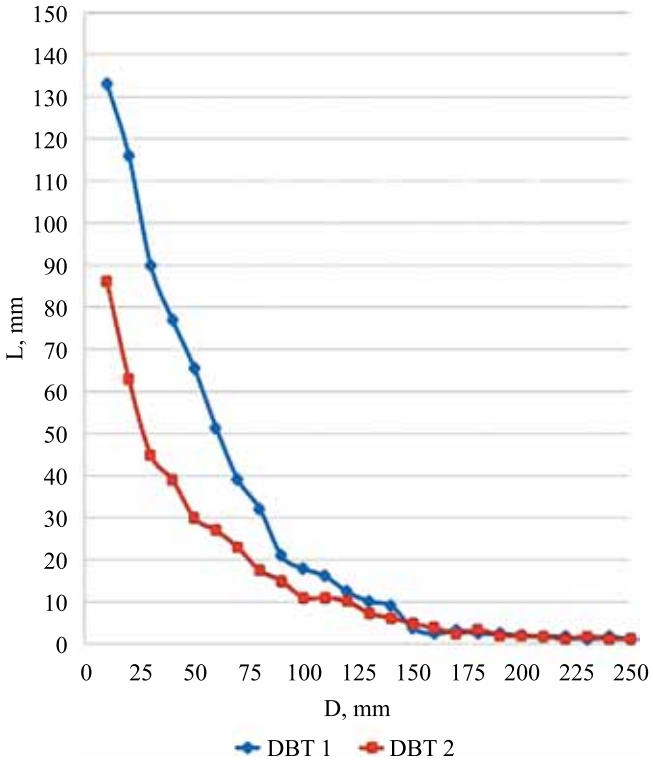

Fig. 7. Dependence of bubble centering distance L on bubble diameter D

CONCLUSION

DBT tests have shown that the use of a DBT reduces the probability of AE by a factor of 3–4 on average. The microbubble separation efficiency depends on the geometric dimensions of the DBT, the flow swirl angle and the outlet cross-section of the helix swirling channels. Adult and pediatric DBT designs were selected based on preliminary studies. Preliminary analysis revealed the directions for further promising improvement of microbubble separation parameters and DBT optimization. The use of this device will reduce the effect of microembolism, make cardiopulmonary bypass safer and provides the opportunity to reconsider the concept of using expensive arterial filters.

The authors declare no conflict of interest.

REFERENCES

1. *Cavayas YA, del Sorbo L, Fan E.* Intracranial hemorrhage in adults on ECMO. *Perfusion.* 2018; 33: 42–50. doi: 10.1177/0267659118766435.

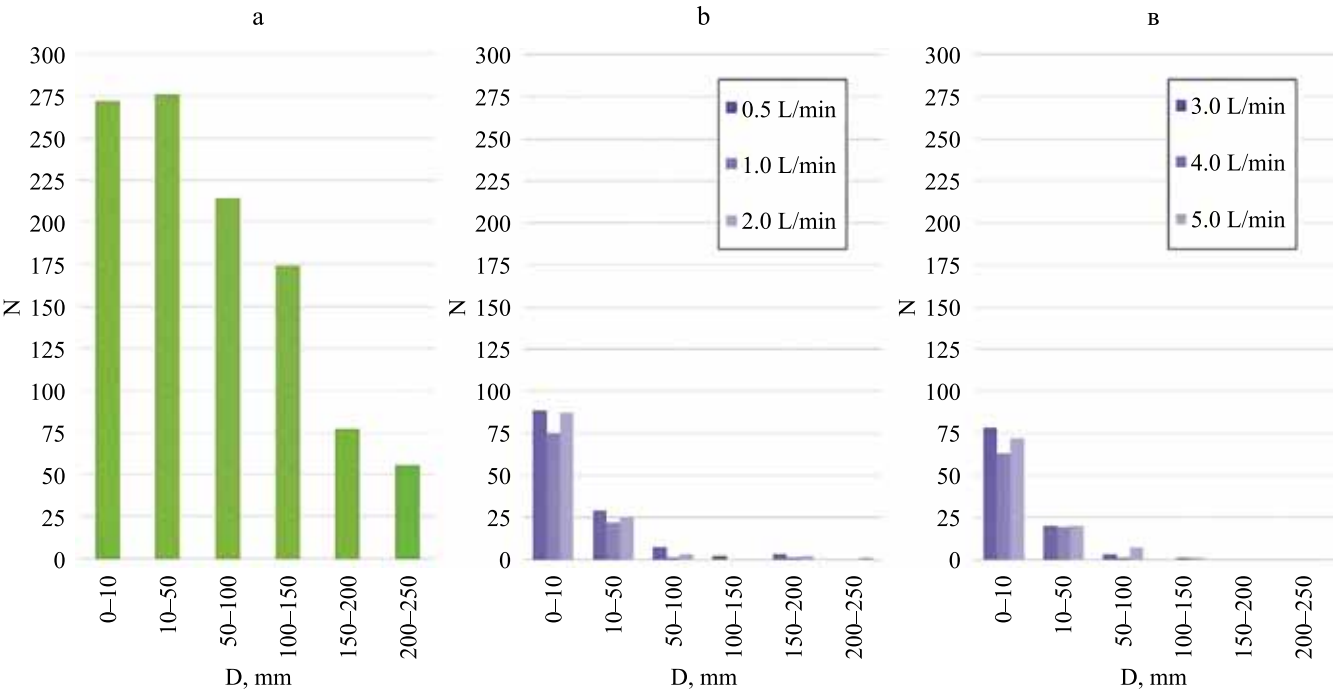

Fig. 8. Separation of bubbles of different diameters at different flow rates for the investigated DBT models: a, composition of bubbles when entering the circuit; b, performance of the pediatric model; c, performance of the adult model

2. *Zanatta P, Forti A, Bosco E et al.* Microembolic signals and strategy to prevent gas embolism during extracorporeal membrane oxygenation. *J Cardiothorac Surg.* 2010; 5: 1–5. doi: 10.1186/1749-8090-5-5.
3. *ClinganS, Schuldes M, Francis S, Hoerr Jr H, Riley J. In vitro* elimination of gaseous microemboli utilizing hypobaric oxygenation in the Terumo FX15 oxygenator. *Perfusion.* 2016; 31 (7): 552–559. doi: 10.1177/0267659116638148.
4. *Honig A, Leker RR.* Cerebral micro-infarcts; the hidden missing link to vascular cognitive decline. *J Neurol Sci.* 2021; 420: 1171–1171. doi: 10.1016/j.jns.2020.117171.
5. *Chen YY, Chen YC, Wu CC, Yen HT, Huang KR, Sheu JJ, Lee FY.* Clinical course and outcome of patients with acute pulmonary embolism rescued by veno-arterial extracorporeal membrane oxygenation: a retrospective review of 21 cases. *Journal of Cardiothoracic Surgery.* 2020; 15 (1). doi: 10.1186/s13019-020-01347-0.
6. *Tingleff J, Jouce FS, Pettersson G.* Intaoperative echocardiographic study of air embolism during cardiac operation. *Ann Thorac Surgery (USA).* 1995; 60 (3): 673–677.
7. *Munakata R, Yamamoto T, Hosokawa Y et al.* Massive pulmonary embolism requiring extracorporeal life support treated with catheterbased interventions. *International heart journal.* 2012; 53: 370–374.
8. *Myers GJ, Voorhees C, Haynes R, Eke B.* Post-arterial filter gaseous microemboli activity of five integral cardiotomy reservoirs during venting: an in vitro studyJECT. *The Journal of Extra Corporeal Technology.* 2009; 41: 20–27.
9. *De Somer F.* Impact of oxygenator characteristics on its capability to remove gaseous microemboli. *J Extra Corpor Technol.* 2007; 39 (4): 271–273.
10. *Nielsen PF, Funder JA, Jensen MØ, Nygaard H.* Influence of venous reservoir level on microbubbles in cardiopulmonary bypass. *Perfusion.* 2008; 23 (6): 347–353. doi: 10.1177/0267659109104954.
11. *Born F, König F, Chen J, Günther S, Hagl C, Thierfelder N.* Generation of microbubbles in extracorporeal life support and assessment of new elimination strategies. *Artificial Organs.* 2020; 44: 268–277. doi: 10.1111/aor.13557.
12. *Born F, Khaladj N, Pichlmaier M, Schramm R, Hagl C.* Potential impact of oxygenators with venous air trap on air embolism in veno-arterial extracorporeal life support. *Technology and Health Care.* 2017; 25 (1): 111–121. doi: 10.3233/THC-161248.
13. *Goritz S, Schelkle H, Rein J-G, Urbanek S.* Dynamic bubble trap can replace an arterial filter during cardiopulmonary bypass surgery. *Perfusion.* 2006; 21: 367–371.
14. *Johagen D, Appelblad M, Svenmarker S.* Can the Oxygenator Screen Filter Reduce Gaseous Microemboli? *J Extra Corpor Technol.* 2014; 46 (1): 60–66.

The article was submitted to the journal on 1.09.2021

DOI: 10.15825/1995-1191-2021-4-86-94

MECHANICAL PROPERTIES OF NATIVE AND DECELLULARIZED AORTIC WALL AFTER LONG-TERM STORAGE IN BIOCIDE SOLUTIONS

M.B. Vasilyeva[1], E.V. Kuznetsova[2], Ya.L. Rusakova[2], E.V. Chepeleva[2], D.S. Sergeevichev[2], I.Yu. Juravleva[2]

[1] Zelman Institute of Medicine and Psychology, Novosibirsk State University, Novosibirsk, Russian Federation

[2] Meshalkin National Medical Research Center, Novosibirsk, Russian Federation

Objective: to determine the optimal method for long-term wet storage of donor material (50 days after collection), with maximum ability to preserve the original mechanical characteristics. **Materials and methods.** Porcine aortic wall fragments were used as objects of study. Half of the original material underwent detergent-based decellularization. The entire material (native and processed) was placed for 50 days in biocidal solutions: complex alcohol solution; ethanol and glycerol mixture; antibiotics mixture. Then the tests for mechanical strength of native and decellularized samples were carried out by the method of uniaxial longitudinal and circumferential stress.

Results. Storage of native material in all media resulted in a significant increase in tensile strength. In the "complex alcohol solution", "ethanol and glycerol mixture", and "antibiotic mixture" group, tensile strength increased by 1.38-, 1.72- and 1.62-fold compared to the native control in circumferential tension. Also, in the "complex alcohol solution" group, the decellularized material was 1.57-fold stronger than the native in circumferential tension. In the "antibiotic mixture" group, the decellularized material was 1.33-fold less strong than the native in longitudinal tension. According to elongation to rupture data, significantly greater plasticity was noted in the "ethanol-glycerol" storage group for the decellularized aortic wall compared to the control group (1.5-fold). Young's modulus did not reliably differ from those of control in all experimental groups regardless of the stress direction. Notably, decellularized specimens clearly tended to be stiffer under circumferential stress. **Conclusion.** Detergent-based decellularization of the porcine aortic wall and subsequent storage of these samples in our chosen experimental solutions for 50 days does not significantly affect the elastic properties of the material. Our proposed treatment methods partially increase the stiffness of the material after storage in alcohol-containing solutions.

Keywords: Young's modulus, tensile strength, xenografts, bioprosthetics.

INTRODUCTION

Currently, one of the widely used methods of surgical treatment of valve and aortic trunk and pulmonary artery conditions is prosthetics with various valve-containing conduits [1–3] aAllogeneic donor material is the gold standard for replacing damaged elements of the cardiovascular system. It has similar hemodynamic characteristics to native valves, low thrombogenicity and is resistant to potential infection [4, 5]. Besides, this type of implants makes re-intervention due to structural degradation less likely [1, 5–7].

Vascular conduits by tissue-engineering methods are widely used to solve allogeneic material deficiency issues. The main types of vascular and valve scaffolds for tissue engineering are natural scaffolds (biologic decellularized tissue and materials) and synthetic structures made of biodegradable polymers [5, 8]. Each type has both advantages and disadvantages. One of the main advantages of decellularized biological matrices is that they preserve the mechanical anisotropy of native valves and the vascular wall structure, can replace the connective tissue scaffold of the affected tissues and promote their recellularization by cells of the recipient itself later [6]. This approach makes it possible to restore the correct structure and adequate function of the replaced element of the cardiovascular system.

Modern approaches to the development of methods for extending the lifespan of donor valves are being implemented in several directions. They include improving the structural characteristics, optimizing preimplantation treatment methods, studying the factors that influence preservation of structural organization of connective tissue scaffold (CTS) and its initial physical and mechanical properties [6, 9].

At the preparatory stage (before implantation in the patient), the allograft is usually either cryopreserved or stored in a solution of antibacterial and fungicidal preparations. However, analysis of the current state of

Corresponding author: Maria Vasilyeva. Address: 1, Pirogova str., Novosibirsk, 630090, Russian Federation. Phone: (913) 930-15-18. E-mail: vasilievam@yandex.ru

the problem shows the lack of a unified approach to the method of long-term preservation of prosthetic material. If the technique of freezing and/or thawing of the material is violated, zones of micro- and macro-damage to the allograft structure may appear, which can be detected only at the surgical stage or will affect the rate of CTS degradation and graft calcification after it has been installed [10–12]. The use of wet storage in an antibiotic cocktail without cryopreservation avoids this type of damage, which helps to reduce the frequency of reoperation associated with early prosthesis damage [7]. However, in practice, wet storage of allografts in an antibiotic solution is used only for a short period of time – 2–14 days [13, 14]. It is also known that residual antibiotics in tissue allografts may be the cause of allergic postimplantation reactions or mask contamination of the allograft by microorganisms in the postoperative period [15].

To date, a universal protocol for long-term storage of allografts has not yet been found. According to global trends, most developers prefer freezing the material [6, 12]. However, coming up with a reliable long-term wet storage method would allow to avoid the negative effects of the processes associated with cryopreservation. As part of the study of this topic, we previously selected biocidal solutions suitable for long-term wet storage of experimental material [16].

The purpose of this work was to evaluate the effect of decellularization and subsequent long-term (50 days) storage in biocidal solutions of different composition on the mechanical properties of aortic tissues.

MATERIALS AND METHODS

Composition of test solutions:

I – Complex alcohol solution (CSR): mixture containing 1,2-octanediol, phenoxyethanol, sorbic acid (1%) and ethanol (20%) [17].

II – Antibiotics mixture (AM): culture medium RPMI-1640 (Biolot, Russia), metronidazole 0.27 mg/ml, gentamicin 0.53 mg/mL, cefazolin 6.66 mg/mL, ampicillin 2.22 mg/ml, oxacillin 1.11 mg/ml, fluconazole 0.027 mg/mL. After the first 48 hours, the solution was replaced with a similar fresh solution.

III – Ethanol and glycerol mixture (E-G): ethanol (10%) and glycerol (20%) in RPMI-1640 culture medium (BioloT, Russia).

Deriving and decellularization of aortic tissues

Porcine aortic wall fragments (arch and descending section), 25–30 cm long, were taken in the slaughterhouse of a meat processing plant. The obtained samples were placed in cooled sterile 0.9% sodium chloride solution and transported to the laboratory.

The aortic wall was cleaned of the remaining surrounding tissues and cut into several 6–7 cm long tubular fragments. Half of the obtained fragments were subjected to detergent-based decellularization.

The entire cycle of cell removal and subsequent washing was performed at 37 °C in an orbital thermoshaker (Heidolf, Germany). The biomaterial was immersed for 24 hours in a sterile phosphate-buffered saline (pH = 7.4) containing 0.5% sodium dodecyl sulfate and 0.5% sodium deoxycholate (Sigma, USA). This was followed by 6-fold washing of the samples for 12 hours in sterile phosphate-buffered saline (pH = 7.4), according to one of the common protocols [18]. The treatment and washing lasted for a total of 4 days, during which the second half of the samples (native samples) was stored at +4–8 °C in sterile 0.9% sodium chloride solution with the addition of an antimicrobial cocktail (metronidazole 0.27 mg/mL, gentamicin 0.53 mg/mL, cefazolin 6.66 mg/mL, ampicillin 2.22 mg/mL, oxacillin 1.11 mg/mL, fluconazole 0.027 mg/mL).

After decellularization, 20 native and decellularized aortic tubular fragments each were used for mechanical tests under uniaxial longitudinal and circumferential stress. The remaining material from each series – native (n = 60) and decellularized (n = 60) – was randomly divided into three groups and stored in the test biocide solutions for 50 days in sterile conditions at +4–8 °C (in AM and E-G solutions), and in CAS solution at room temperature. Eight groups of specimens were examined (Table). Before mechanical testing, the specimens were washed in sterile 0.9% sodium chloride solution for 20 minutes at room temperature.

Table

List of all experimental groups

S/N	Abbreviation	Storage method	Subgroups
1	Contr	Control samples of porcine aorta, fresh material (to determine the basic mechanical properties)	Contr, N – native material without additional treatment
2			Contr, D – decellularized material without additional treatment
3	CAS	Complex alcohol solution (50 days)	CAS, N – CAS native form
4			CAS, D – decellularized form
5	AM	Antibiotics mixture (50 days)	AM, N – AM native form
6			AM, D – AM decellularized form
7	E-G	Ethanol and glycerol mixture (50 days)	E-G, N – E-G native form
8			E-G, D – decellularized form

Study of mechanical properties

Mechanical tests were performed by subjecting the samples to uniaxial stress after 50 days of storage in the test biocidal solutions. To obtain control values, we used porcine aortic wall material from the native group (*Contr, N*) and decellularized material (*Contr, D*) before storage in the appropriate solutions.

Tubular aortic fragments from each of the 8 subgroups were cut lengthwise and test specimens were carved using a standard cutting matrix in the longitudinal (n = 10) and circumferential (n = 10) directions. The width and length of the working part of the specimen corresponded to the matrix dimensions (9 mm and 28 mm, respectively). The sample thickness was measured three times with an electronic digital thickness gauge (Mitutoyo 547-500S, Japan).

The tests were performed on pull tester ESM301 (MARK-10, USA). The tensile speed of the fabric was 30 mm/min. If break occurred at the place where the specimens were fixed in the clamps, the corresponding measurement data was excluded from analysis.

The strength of the materials was evaluated by tensile stress (σ, MPa):

$$\sigma = \frac{F}{h \times w}$$

where F is the force at the moment of break (N), h is the average thickness of the specimen (mm), and w is the width (9 mm) of the specimen.

Deformability was determined by the maximum elongation at break (ε, %):

$$\varepsilon = \frac{\Delta L}{L} \times 100$$

where ΔL is the maximum elongation of the specimen (mm) and L is the initial length of the specimen (mm) equal to the distance between the clamps (28 mm).

Stiffness was determined by the value of Young's modulus (E, MPa):

$$E = \frac{\sigma}{\varepsilon}$$

where E is Young's modulus (MPa), σ is the tensile stress; ε is the elongation of the fragment (mm) at the break of the specimen.

Statistical analysis

Results were processed by variation statistics using the *Statistica 13.0* software (TIBCO Software, USA). Normality of distribution of the obtained data and homogeneity of variance were checked using the Shapiro–Wilk test. Mann–Whitney U Test was used to judge the significance of differences. Data on the graphs are presented as median and interquartile range (25th and 75th percentiles).

RESULTS

Sample thickness

The thickness of fragments of decellularized aorta from the control group was 1.22 times higher than that of native aorta from the control group ($p < 0.01$). Among the decellularized specimens after storage, a lower thickness was found in the alcohol-containing "*CAS, D*" and "*E-G, D*" subgroups by 0.82 and 0.87 times, respectively, compared to the corresponding controls ($p < 0.05$) (Fig. 1).

Stress-strain properties of the biomaterial

The **tensile strength** for non-decellularized (native) specimens increased significantly after storage in all the test solutions in comparison to the control ($p < 0.05$): 1.38 times in the "*CAS, N*" subgroup, 1.72 times in the "*E-G, N*" subgroup and 1.62 times in the "*AM, N*" subgroup. Among the decellularized samples, we observed an insignificant tendency towards increased tensile stress in the "*CAS, D*" subgroup compared to the control. In the "*E-G, D*" subgroup, there was a significant increase in tensile stress by 1.5 times ($p < 0.05$). When comparing the strength of native and decellularized specimens, significant ($p < 0.05$) differences were found in the *Contr* and *CAS* groups, where the decellularized material showed a 1.47- and 1.57-fold higher tensile strength, respectively (Fig. 2, a).

The longitudinal tensile strength for both native and decellularized specimens did not change after storage in all types of solutions compared to the control. When comparing within each experimental group between native and decellularized specimens, a significant difference was found only in the AM group (decellularized material was 1.33 times less strong than native ($p < 0.05$) (Fig. 2, b).

The **elongation at break** for both native and decellularized samples did not change after storage in all types

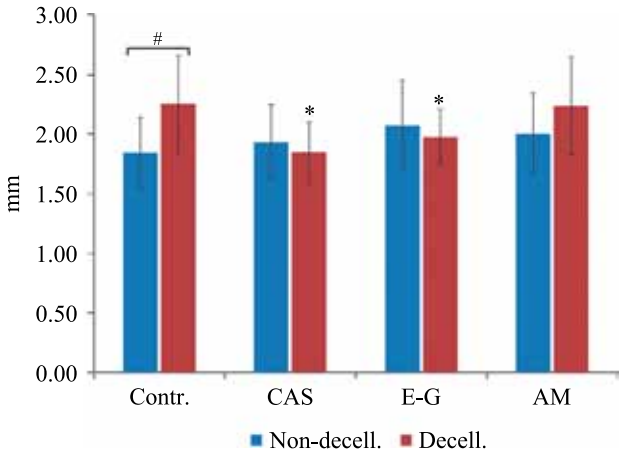

Fig. 1. Thicknesses of the test specimens;
*, $p < 0.05$ in comparison with the corresponding control group; #, $p < 0.05$ in comparison between non-decellularized and decellularized samples within the same group

of solutions compared to the control, regardless of the tension direction (Fig. 3). The exception was the "*E-G, D*" subgroup, where the highest elongation was detected under circumferential stress compared to all other subgroups ("*Contr, D*"/"*E-G, D*" by a factor of 1.5, $p < 0.01$) (Fig. 3, a).

Regardless of the tension direction, there were no significant differences between the **Young's modulus** in native and decellularized tissues both within one group and when compared with the corresponding control values (Fig. 4).

DISCUSSION

Currently, one of the common methods of long-term storage of allogeneic material is cryopreservation, as this method allows creating a bank of cardiac valve allografts for really long storage for subsequent implantation in humans. This method of preservation requires careful compliance with all freezing and thawing stages, increased technical reliability of equipment, and, possibly, search for new cryopreservation media [12, 19].

As the review of specialized literature shows, features and patterns of decellularization, preservation of allograft and xenograft tissues are of considerable research interest [20–22]. Of particular interest is the issue of sufficiently long-term wet storage of obtained donor tissues. In some works, where it was important to preserve cell viability, culture nutrient media were used [23, 24]. In other works, where the principal goal was to preserve connective tissue scaffold without taking into consideration the cellular component, the suitability of saline solution with modifications was investigated [25]. For instance, Wollmann et al. showed that preservation of mechanical and structural properties of the decellularized tissue matrix is not significantly affected during long-term wet storage in sterile saline solution (up to

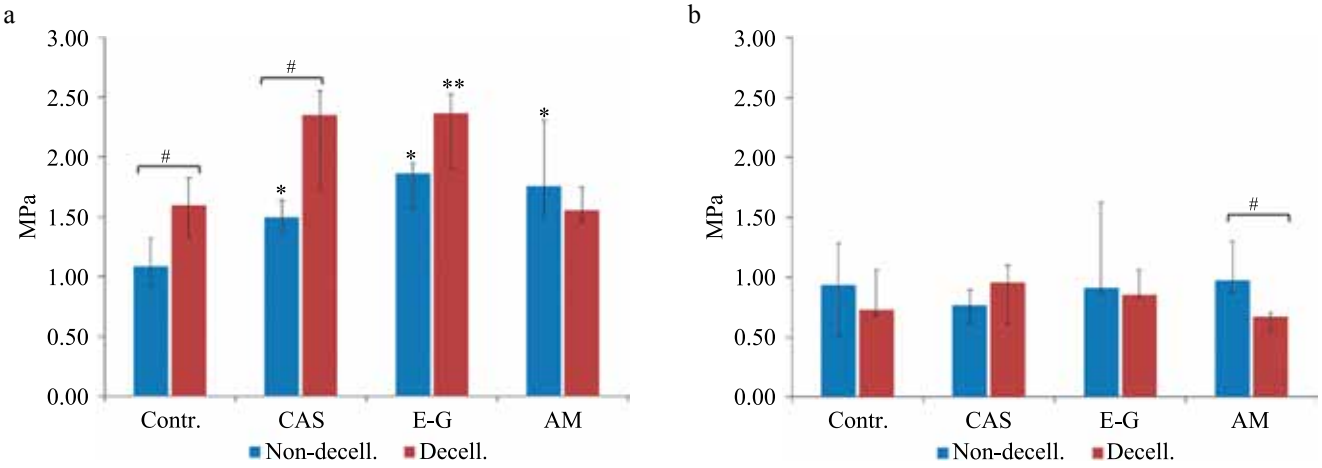

Fig. 2. a) Circumferential tensile strength for the test specimens; b) Longitudinal tensile strength for the test specimens; *, $p < 0.05$ in comparison with native control; **, $p < 0.05$ in comparison with decellularized control; #, $p < 0.05$ compared to non-decellularized and decellularized samples within the same group

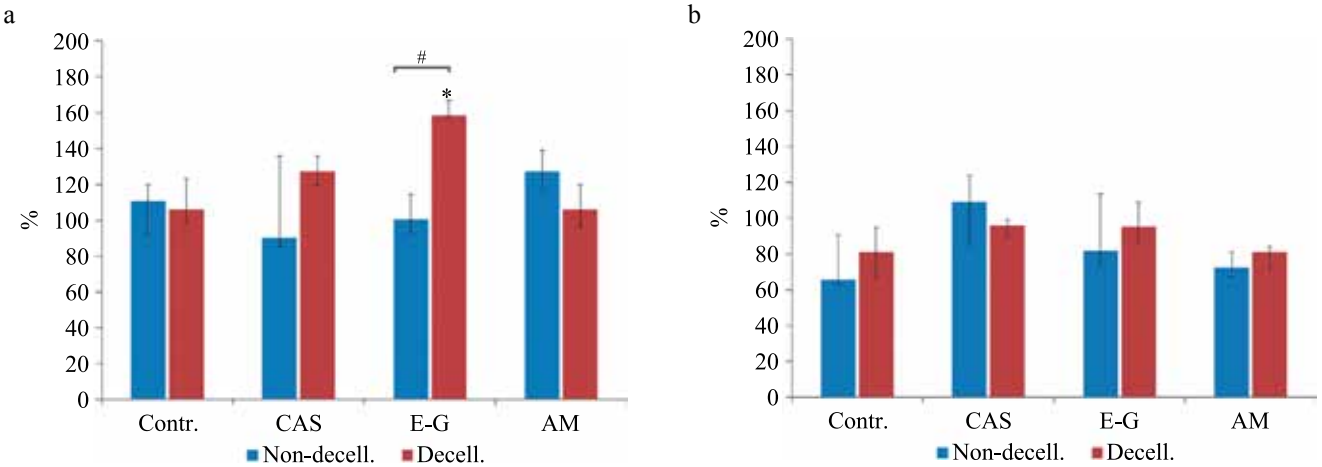

Fig. 3. a) Elongation at break for the test specimens under circumferential stress; b) Elongation at break for the test specimens under stress;
*, $p < 0.05$ in comparison with control; #, $p < 0.05$ in comparison between non-decellularized and decellularized samples within the same group

12 months) [26]. In this experimental work, we chose RPMI-1640 nutrient medium as the basis for storage media II (AM) and III (E-G). The excellent multicomponent buffer medium ensured that the pH of the solutions was maintained throughout the experiment. Performing all manipulations in laminar boxes with abacterial air medium during preparation of working solutions and throughout the experiment allowed us to avoid contaminating the material with microbial and other negative agents.

The success of decellularized heart valve transplantation largely depends on the components of the cell removal method itself (enzymatic, detergent, etc.) and the potential immune response after implantation [27, 28]. The decellularization protocol we used [18] and its variations are also used by other researchers, which testifies to the adequacy of this method for further use in creation of tissue-engineered materials based on donor tissues [20, 21].

Our study found that the thickness of samples in the control group after decellularization increased by 10–30% from the initial state of the native material. This may possibly be due to the appearance of a loosening of the intercellular spaces in the connective-tissue scaffold when the cells were removed and small intercellular molecules (proteoglycans, glucosaminoglycans and other non-collagenous proteins) were partially washed out under the effect of detergents, which were replaced by water molecules [29].

An important property of a deformable material is strength, understood as the ability to resist destruction by external forces. Tensile strength is one of the main indicators characterizing the mechanical properties of a tissue, and a tissue is quantified using tensile stress [30]. We found that decellularization of the aortic material significantly increases circumferential tensile stress. At the same time, the Young's modulus also increases, but without a significant difference from those of the native control group. After long-term storage in alcohol-containing (*CAS* and *E-G*) and alcohol-free (*AM*) solutions, the main changes in the mechanical properties were also evident in the circumferential tensile strength of the aortic wall material. Almost all data on mechanical properties in longitudinal stress remained at the level of the control values of the corresponding subgroups (decellularized and non-decellularized). Such anisotropy of biomechanical properties in the connective tissue scaffold of the aortic wall is down to the peculiarities of three-dimensional orientation of CTS fibers, which provides effective compensation of intravascular fluid pressure for further active blood promotion. It was shown earlier that the main mass of elastin fibers in the aortic wall is located in the media as part of elastin lamellae, which are located predominantly in the circumferential direction. Orientation of collagen fibers in the media is directed to the vessel axis at about 45° angle; the direction is more longitudinal in the intima and adventitia [31–33].

In uniaxial tension tests, we obtained a stress-strain curve for each specimen. The graph of such a curve consists of 3 parts: the low elastic modulus portion, the linear portion, and the yield or break portion. There is a biomechanical interpretation of this phenomenon. The portion with low elasticity modulus occurs due to straightening of spiral collagen fibers according to the direction of the applied force. The linear portion (consisting of two parts) appears as a result of direct stretching of collagen fibrils in the tissue. Breaking area of the stress-strain curve is connected with direct damage to the fibrils [33]. When determining the tensile strength, the maximum applied force, after which the specimen breaks, is initially fixed. In fact, it depends on how many and mainly of what quality collagen are the fibers present in the tissue.

Most likely, the significant increase in the strength of materials during storage in alcohol-containing solutions is associated with a change in the structure of the main CTS proteins – collagen and elastin. It is known that the triple stranded structure of collagen, as well as

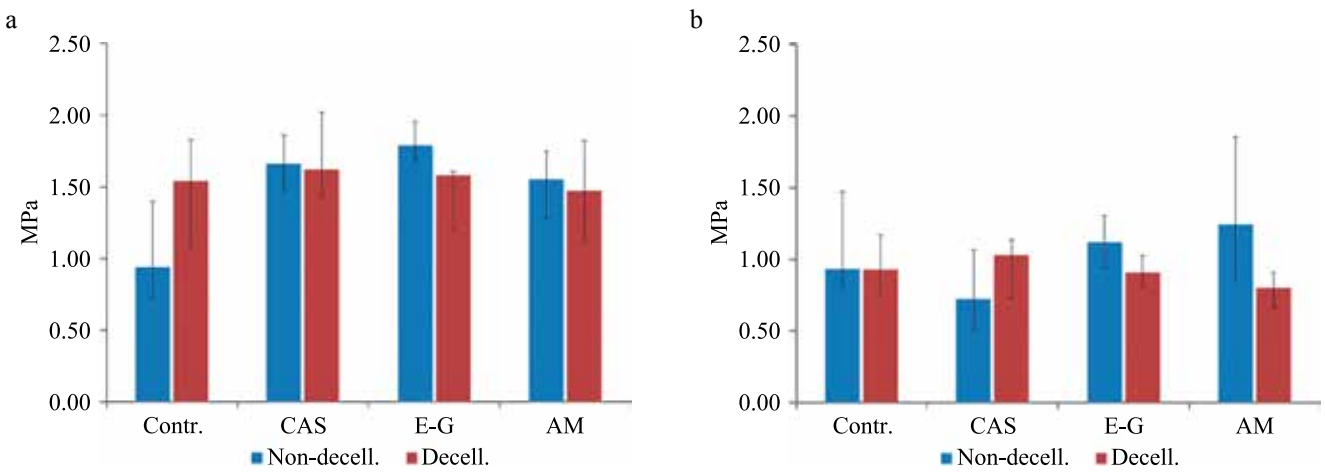

Fig. 4. Young's modulus for the test specimens. a, circumferential stress; b, longitudinal stress

the ratio of hydrophilic and hydrophobic sites of protein molecules, change under the influence of alcohols [34].

The deformation capacity of the material is reflected in the indices of relative elongation during tensile strain. This index is influenced by the structure and fiber composition of the fabric [35]. In our study, it was shown that the circumferential tensile elongation in all experimental groups remains at the level of the control values except for the "*E-G*" subgroup. In this case, the deformation capacity index is 1.58-fold higher than that of the non-decellularized counterpart ("*E-G, N*"). In this situation, we can assume the influence of E-G solution components (glycerol as a plasticizer) on the structural organization of CTS fibers of the aortic wall. Some researchers have noted similar changes in the biomechanics of materials stored in glycerol solutions [36].

Young's modulus characterizes the stiffness of a material [37]. Regardless of the stress direction, the Young's modulus in all experimental groups after storage in the test solutions does not significantly differ from those of native tissue. At the same time, the values have a clear tendency to increase, which indicates increased stiffness. Comparison of Young's modulus values in the circumferential and longitudinal direction within groups with the same type of tissue treatment demonstrates significant differences in average values. This fact is also explained by the specific location of different CTS fibers in the aortic wall [31].

CONCLUSION

Detergent-based decellularization of porcine aortic wall followed by wet storage of the samples in the test solutions for 50 days does not significantly worsen the elastic properties of the material. There is a slight increase in the circumferential tensile stiffness of the test material.

This work was performed within the framework of the state assignment of the Russian Ministry of Health (N: 121031300224-1).

The authors declare no conflict of interest.

REFERENCES

1. *Horke A, Tudorache I, Laufer G, Andreas M, Pomar JL, Pereda D et al.* Early results from a prospective, single-arm European trial on decellularized allografts for aortic valve replacement: the ARISE study and ARISE Registry data. *Eur J Cardiothorac Surg.* 2020; 58 (5): 1045–1053. doi: 10.1093/ejcts/ezaa100. PMID: 32386409; PMCID: PMC7577293.
2. *Arabkhani B, Bekkers JA, Andrinopoulou ER, Roos-Hesselink JW, Takkenberg JJM, Bogers AJJC*. Allografts in aortic position: Insights from a 27-year, single-center prospective study. *J Thorac Cardiovasc Surg*. 2016; 152 (6): 1572–1579. doi: 10.1016/j.jtcvs.2016.08.013; PMID: 27842683.
3. *Demidov DP, Astaspov DA, Bogachev-Prokophiev AV, Zheleznev SI*. Quality of life after aortic valve replacement with biological prostheses in elderly patients. *Patologiya krovoobrashcheniya i kardiokhirurgiya = Circulation Pathology and Cardiac Surgery*. 2017; 21 (3): 40–47. [In Russ, English abstract]. doi: 10.21688/1681-3472-2017-3-40-47.
4. *Spirydonov SV, Odintsov VA, Shchetinko NN, Mozgova EA, Hrynchuk II, Ostrovsky YuP*. Aortic allografts in the world cardiac surgery: historical aspects of clinical implementation, and review of implantation outcomes. *Medical Journal*. 2015; 1: 55–67. [In Russ, English abstract].
5. *Fioretta ES, von Boehmer L, Motta SE, Lintas V, Hoerstrup SP, Emmert MY*. Cardiovascular tissue engineering: From basic science to clinical application. *Exp Gerontol*. 2019; 117: 1–12. doi: 10.1016/j.exger.2018.03.022. PMID: 29604404.
6. *VeDepo MC, Detamore MS, Hopkins RA, Converse GL*. Recellularization of decellularized heart valves: Progress toward the tissue-engineered heart valve. *J Tissue Eng*. 2017 Aug 25; 8: 2041731417726327. doi: 10.1177/2041731417726327. PMID: 28890780; PMCID: PMC5574480.
7. *Cebotari S, Tudorache I, Ciubotaru A, Boethig D, Sarikouch S, Goerler A et al.* Use of fresh decellularized allografts for pulmonary valve replacement may reduce the reoperation rate in children and young adults: Early report. *Circulation*. 2011; 124 (11 SUPPL. 1): 115–124. doi: 10.1161/CIRCULATIONAHA.110.012161. PMID: 21911800.
8. *Argento G, Simonet M, Oomens CW et al.* Multi-scale mechanical characterization of scaffolds for heart valve tissue engineering. *J Biomech.* 2012; 45: 2893–2898.
9. *Odarenko YuN, Rutkovskaya NV, Rogulina NV, Stasev AN, Kokorin SG, Kagan ES, Barbarash LS.* Analysis of 23-year experience epoxy treated xenoaortic bioprosthesis in surgery mitral heart disease. Research factors of recipients by positions of influence on the development of calcium degeneration. *Complex Issues of Cardiovascular Diseases*. 2015; (4): 17–25. [In Russ, English abstract] doi: 10.17802/2306-1278-2015-4-17-25.
10. *Lisy M, Kalender G, Schenke-Layland K, Brockbank KGM, Biermann A, Stock UA*. Allograft Heart Valves: Current Aspects and Future Applications. *Biopreserv Biobank*. 2017; 15 (2): 148–157. doi: 10.1089/bio.2016.0070. PMID: 28151005.
11. *Brockbank KGM, Lightfoot FG, Song YC, Taylor MJ.* Interstitial ice formation in cryopreserved homografts: A possible cause of tissue deterioration and calcification *in vivo*. *J Heart Valve Dis*. 2000; 9 (2): 200–206. PMID: 10772037.
12. *Britikov DV, Lauk-Dubitsky SE, Serov RA. Khugaev GA.* Morphological evaluation of new method of valve and vascular allografts cryopreservation. *Russian Annals of Surgery*. 2019; 24 (1): 16–23. [In Russ, English abstract] doi: 10.24022/1560-9502-2019-24-1-16-23.
13. *Hickey E, Langley SM, Allemby-Smith O, Livesey SA, Monro JL*. Subcoronary allograft aortic valve replacement: parametric risk-hazard outcome analysis to a minimum of 20 years. *Ann Thorac Surg*. 2007; 84 (5):

1564–1570. doi: 10.1016/j.athoracsur.2007.02.100. PMID: 17954063.
14. *Ostrovskij JuP, Judina OA, Muratov RM, Spiridonov SV.* Tehnologija izgotovlenija i metodika ispol'zovanija kriosohranennyh allografтov v hirurgii porokov aortal'nogo klapana. Minsk: Belaruskaja nauka (2016), 229. ISBN 978-985-08-1955-0.
15. *Gatto C, Giurgola L, D'Amato Tothova J*. A suitable and efficient procedure for the removal of decontaminating antibiotics from tissue allografts. *Cell Tissue Bank*. 2013; 14 (1): 107–115. doi: 10.1007/s10561-012-9305-5. PMID: 22407218.
16. *Vasilyeva MB, Krasilnikova AA, Kuznetsova EV, Lunina MV, Samoylova LM, Rusakova YaL et al.* Alternative biocidal solutions for storage of allogeneic vascular grafts used for the replacement of cardiovascular elements. *Patologiya krovoobrashcheniya i kardiokhirurgiya = Circulation Pathology and Cardiac Surgery*. 2018; 22 (4): 95–102. [In Russ, English abstract] doi: 10.21688/1681-3472-2018-4-95-102.
17. *Zhuravleva IYu*. Biotsidnaya kompozitsiya dlya asepticheskogo khraneniya konservirovannogo proteznogo materiala iz tkaney zhivotnogo proiskhozhdeniya. Patent RF na izobretenie RU 2580621C1. Byull. No 10 (ot 10.04.2016).
18. *Lichtenberg A, Tudorache I, Cebotari S, Ringes-Lichtenberg S, Sturz G, Hoeffler K et al. In vitro* re-endothelialization of detergent decellularized heart valves under simulated physiological dynamic conditions. *Biomaterials*. 2006; 27 (23): 4221–4229. doi: 10.1016/j.biomaterials.2006.03.047. PMID: 16620956.
19. *Cheung DT, Weber PA, Grobe AC, Shomura Y, Choo SJ, Luo HH et al.* A new method for the preservation of aortic valve homografts. *J Heart Valve Dis*. 2001; 10 (6): 728–734. PMID: 11767178.
20. *Yao Q, Zheng YW, Lan QH, Kou L, Xu HL, Zhao YZ.* Recent development and biomedical applications of decellularized extracellular matrix biomaterials. *Mater Sci Eng C Mater Biol Appl*. 2019 Nov; 104: 109942. doi: 10.1016/j.msec.2019.109942. PMID: 31499951.
21. *Taylor DA, Sampaio LC, Ferdous Z, Gobin AS, Taite LJ*. Decellularized matrices in regenerative medicine. *Acta Biomater*. 2018 Jul 1; 74: 74–89. doi: 10.1016/j.actbio.2018.04.044. PMID: 29702289.
22. *Theodoridis K, Müller J, Ramm R, Findeisen K, Andrée B, Korossis S et al.* Effects of combined cryopreservation and decellularization on the biomechanical, structural and biochemical properties of porcine pulmonary heart valves. *Acta Biomater*. 2016; 43: 71–77. doi: 10.1016/j.actbio.2016.07.013. PMID: 27422199.
23. *Boekema BKHL, Boekestijn B, Breederveld RS.* Evaluation of saline, RPMI and DMEM/F12 for storage of split-thickness skin grafts. *Burns*. 2015; 41 (4): 848–852. ISSN 0305-4179, https://doi.org/10.1016/j.burns.2014.10.016.
24. *Ranawat AS, Vidal AF, Chen CT, Zelken JA, Turner AS, Williams RJ* 3rd. Material properties of fresh cold-stored allografts for osteochondral defects at 1 year. *Clin Orthop Relat Res*. 2008; 466 (8): 1826–1836. doi: 10.1007/s11999-008-0311-7. PMCID: PMC2584258.
25. *Ziza V, Canaud L, Gandet T, Molinari N, Alonso W, Chastan R, Branchereau P, Picard E.* Outcomes of cold-stored venous allograft for below-knee bypasses in patients with critical limb ischemia. *J Vasc Surg*. 2015; 62 (4): 974–983. doi: 10.1016/j.jvs.2015.04.437. PMID: 26141692.
26. *Wollmann LC, Suss PH, Kraft L, Ribeiro VS, Noronha L, da Costa FDA, Tuon FF*. Histological and Biomechanical Characteristics of Human Decellularized Allograft Heart Valves After Eighteen Months of Storage in Saline Solution. *Biopreserv Biobank*. 2020; 18 (2): 90–101. doi: 10.1089/bio.2019.0106. PMID: 31990593.
27. *Nam J, Choi SY, Sung SC, Lim HG, Park SS, Kim SH, Kim YJ*. Changes of the Structural and Biomechanical Properties of the Bovine Pericardium after the Removal of α-Gal Epitopes by Decellularization and α-Galactosidase Treatment. *Korean J Thorac Cardiovasc Surg*. 2012; 45 (6): 380–389. doi: 10.5090/kjtcs.2012.45.6.380. PMID: 23275920; PMCID: PMC3530722.
28. *Gilbert TW.* Strategies for tissue and organ decellularization. *J Cell Biochem*. 2012; 113: 2217–2222. doi: 10.1002/jcb.24130. PMID: 22415903.
29. *McKee CT, Last JA, Russell P, Murphy CJ*. Indentation versus tensile measurements of Young's modulus for soft biological tissues. *Tissue Eng Part B Rev*. 2011; 17 (3): 155–164. doi: 10.1089/ten.TEB.2010.0520. PMID: 21303220; PMCID: PMC3099446.
30. *Sokolis DP, Kefaloyannis EM, Kouloukoussa M, Marinos E, Boudoulas H, Karayannacos PE*. A structural basis for the aortic stress – strain relation in uniaxial tension, *Journal of Biomechanics*. 2006; 39 (9): 1651–1662. doi: 10.1016/j.jbiomech.2005.05.003.
31. *Yu X, Wang Y, Zhang Y*. Transmural variation in elastin fiber orientation distribution in the arterial wall. *J Mech Behav Biomed Mater*. 2018; 77: 745–753. doi: 10.1016/j.jmbbm.2017.08.002. PMID: 28838859; PMCID: PMC5696052.
32. *Sugita S, Matsumoto T.* Multiphoton microscopy observations of 3D elastin and collagen fiber microstructure changes during pressurization in aortic media. *Biomech Model Mechanobiol*. 2017; 16 (3): 763–773. doi: 10.1007/s10237-016-0851-9. PMID: 27878400.
33. *Silver FH, Horvath I, Foran DJ*. Viscoelasticity of the vessel wall: the role of collagen and elastic fibers. *Crit Rev Biomed Eng*. 2001; 29 (3): 279–301. doi: 10.1615/critrevbiomedeng.v29.i3.10. PMID: 11730097.
34. *Rezvova MA, Kudrjavceva JuA*. Sovremennye podhody k himicheskoj modifikacii belkov v biologicheskih tkanjah, posledstvija i primenenie. *Bioorganicheskaya khimiya / Russian Journal of Bioorganic Chemistry.* 2018; 44 (1): 22–37. doi: 10.7868/S0132342318010025.
35. *Mikhailova IP, Manchenko AA, Byzov DV, Sandomirsky BP*. Fiziko-mehanicheskie svojstva devitalizirovannyh ksenoimplantatov na osnove perikarda, stvorok aortal'nogo klapana i arterij. *Problemy kriobiologii i kriomediciny.* 2015; 25 (4): 311–328.
36. *van Doormaal TP, Sluijs JH, Vink A, Tulleken CA, van der Zwan A.* Comparing five simple vascular storage protocols. *Journal of Surgical Research*, 2014; 192 (Issue 1): 200–205. doi: 10.1016/j.jss.2014.05.001.

The article was submitted to the journal on 6.07.2021

DOI: 10.15825/1995-1191-2021-4-95-109

MODERN PANCREATIC ISLET ENCAPSULATION TECHNOLOGIES FOR THE TREATMENT OF TYPE 1 DIABETES

P.S. Ermakova[1], E.I. Cherkasova[1, 2], N.A. Lenshina[3], A.N. Konev[3], M.A. Batenkin[3], S.A. Chesnokov[3], D.M. Kuchin[4], E.V. Zagainova[1, 2], V.E. Zagainov[1, 4], A.V. Kashina[1]

[1] Privolzhsky Research Medical University, Nizhny Novgorod, Russian Federation
[2] Lobachevsky State University of Nizhny Novgorod, Nizhny Novgorod, Russian Federation
[3] Razuvaev Institute of Organometallic Chemistry, Nizhny Novgorod, Russian Federation
[4] Privolzhsky District Medical Center, Nizhny Novgorod, Russian Federation

The review includes the results of analytical research on the problem of application of pancreatic islet encapsulation technologies for compensation of type 1 diabetes. We present a review of modern encapsulation technologies, approaches to encapsulation strategies, insulin replacement technologies: auto-, allo- and xenotransplantation; prospects for cell therapy for insulin-dependent conditions; modern approaches to β-cell encapsulation, possibilities of optimization of encapsulation biomaterials to increase survival of transplanted cells and reduce adverse consequences for the recipient. The main problems that need to be solved for effective transplantation of encapsulated islets of Langerhans are identified and the main strategies for translating the islet encapsulation technology into medical reality are outlined.

Keywords: pancreas, islets of Langerhans, encapsulation, transplantation, immunosuppression, type 1 diabetes.

INTRODUCTION

Type 1 diabetes mellitus (T1DM) is a multifactorial disease characterised by a relative or absolute deficiency of insulin secretion, leading to chronic hyperglycemia and other metabolic disorders. Diabetes has been shown to develop with over 90% decrease in pancreatic islets, and for a patient with an average body weight, 300,000 viable active islets are enough to control blood sugar [1].

A promising option for the treatment of insulin-dependent carbohydrate metabolic disorders is the use of transplantation of insulin-producing beta cells as part of the islets of Langerhans or a whole organ into the recipient to activate the biological feedback mechanisms of glycemic feedback and insulin production [2].

To reduce the burden of autoimmune disease and increase cell survival, various approaches have been proposed: from the use of steroid-free immunosuppression schemes [3] to transplantation of induced pluripotent stem cells (iPSCs) and mesenchymal stem cells (MSCs), committing to beta cells [4], and the use of immune-independent insulin-producing organoids [5].

Recently, the most promising solution to the problem of immunosuppression is considered encapsulation of transplantable pancreatic islets, also known as islets of Langerhans (IL) to protect them from immunocompetent cells.

ISLET ENCAPSULATION

This paper reviews the main strategies and ways of solving the problems of effective functioning of transplanted IL as part of micro- and macro-units in insulin-dependent disorders in the recipient's body. On the way to the goal set, a whole set of multi-component and interdependent problems, from the chemical structure of the capsule wall to determining the optimal location for transplantation of encapsulated IL, will have to be solved (Fig. 1).

MATERIALS AND CAPSULE DERIVATION

The ideal polymeric capsule for IL encapsulation, according to the literature [6], should meet at least the following criteria:

– let insulin into the blood, and oxygen, glucose, etc. into the cells;
– do not let white blood cells, phagocytes through;
– be compatible with both the encapsulated cells and the recipient's body, so as not to cause immunological and fibrotic reactions;
– have a smooth topography without a rough surface;
– stimulate vascular growth around the capsule (for better supply of the encapsulated cells with nutrition and rapid "drainage" of the released insulin).

In the vast majority of cases, capsules made of hydrogel-forming natural and synthetic polymers have these characteristics [7].

Corresponding author: Polina Ermakova. Address: 1, Meditsinskaya str., Nizhny Novgorod, 603104, Russian Federation. Phone: (987) 750-09-74. E-mail: bardina-polina@mail.ru

Natural polymers

The most commonly used natural polymers for creating IL microcapsules are agarose collagen, chitosan, alginate, cellulose, their mixtures and numerous chemical modifications.

It has been found that the immunoprotective properties of agarose gels [8–9] can be controlled by changing the agarose concentration during gel formation. Typically, 5% agarose is used to create capsules, but by increasing the agarose concentration from 5% to 7.5–10% or by applying other polymers to the capsule surface, the graft survival time in vivo can be increased [11]. To this end, Dupuy et al. [12] coated agarose microcapsules with polyacrylamide; another successful approach was to coat the agarose surface with polybrene and carboxymethyl cellulose (CMC) [13]. To create these capsules, complex mixtures consisting of 5% agarose and 5% polystyrene sulfonic acid incubated with polybrene and CMC were formed.

To stimulate cell growth in the graft system, agarose can be supplemented with other polymers: for example, collagen-agarose macrogranules showed a better effect on rat IL functionality compared to those containing agarose alone. IL encapsulated in these macrogranules were able to maintain normoglycemia for up to 170 days in diabetic mice in a streptozotocin-induced diabetes model [14].

Despite the many studies conducted using agarose and its derivatives, two major drawbacks of agarose capsules for IL confinement can be noted:

1) large scatter of obtained gel balls, 100 to 1000 μm in size. This is related to the capsule derivation method – mainly temperature-induced suspension gelation methods are used.
2) the presence of toxic molecules in the agarose itself due to insufficient purification of natural materials [15].

Alginate is an anionic polysaccharide derived from different species of algae, which significantly affects the physical and chemical properties of alginate microcapsules [16].

To reduce permeability and increase the stability of alginate capsules, the polycationic layer is usually added to the core of the alginate gel as a second layer, followed by an outer layer of alginate. The most commonly used polycation is poly-L-lysine, although other polycations such as poly-L-ornithine can also be used. For example, microcapsules containing alginate-poly-L-ornithine instead of alginate-poly-L-lysine-alginate (APA) provided better graft survival with porcine IL when xenotransplanted to Cynomolgus monkeys [17, 18].

Organization levels	Research targets	Tasks to be solved
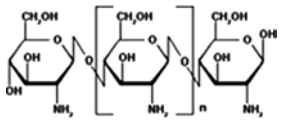	Capsule materials and production	Biopolymers, synthetic polymers, encapsulation with bioactive molecules, capsule formation methods
	Encapsulation strategy (physical parameters of capsules)	Capsule size, permeability (pore size), capsule wall thickness and elasticity
	IL cells in in capsules	Allogeneic, xenogeneic, satellite (supporting) cells, alternative sources of β-cells
	Physiological parameters of capsule environment	Oxygenation, vascularization, fibrosis
	Site of graft insertion into the recipient's body	Abdominal cavity (omental bursa), renal capsule, subcutaneous space

Fig. 1. Multifunctional tasks in the transplantation of encapsulated IL

However, APA microcapsules suffer from a significant drawback: the polycationic coating (PCC) degrades over time and is considered highly immunogenic, making APA capsules unstable in the long term. It has been demonstrated that cross-linking high α-L-guluronic acid alginate with Ba^{2+} ions results in capsules with less permeability to IgG and greater biocompatibility than when cross-linked with Ca^{2+} ions [19].

Animal studies [20, 21] have demonstrated the ability of barium alginate microcapsules to provide long-term immune protection in both allo- and xenotransplantation. However, even in the absence of immunogenic PCC, transplantation of barium alginate microcapsules led to pericapsular fibrotic overgrowth (PFO) [21]. Barium alginate microcapsules and purified alginate [22] do not cause PFO when tested in small animals, such as rodents, but cause severe PFO when transplanted into a large animal such as a baboon.

Chitosan, a basic cationic polysaccharide derived from chitin [23], has not been tested as extensively as alginate or agarose for immunoprotection studies, since chitosan in its salt-free form is insoluble in aqueous solutions except for low molecular weight samples. At the same time, it can be used as an additive in the matrix. It is suggested that the use of chitosan instead of poly-L-lysine can provide higher mechanical strength and stability due to the strong bond between chitosan and the alginate gel [24].

Collagen, a fibrillar protein, is considered one of the most versatile polymers for encapsulating various cell types. To date, 29 types of collagens have been identified and described [25], but nevertheless, type I collagen accounts for 90% of the total and is the most frequently used polymer for encapsulation [26]. Collagen capsules need to form a complex with other polymers or a protective layer for long-term use in biomedical applications [27, 28].

Glutaraldehyde is the most widely used crosslinking agent, including for collagen in model cell systems, but it causes an inflammatory response in the recipient's body [29].

Synthetic polymers

Despite the stability of characteristic properties of synthetic polymers [30], cell encapsulation procedures require the use of toxic solvents [30, 31], which negatively affects biocompatibility of capsules.

Polyethylene glycol (PEG) is most frequently used for cell encapsulation. It is acceptable for encapsulation of a wide range of cells: IL [32], chondrocytes [33], osteoblasts [34], MSCs [35]. PEG is obtained by polymerization of ethylene glycol oligomers in the presence of acid or alkaline catalysts. But when PEG monomers are terminated with methacrylate or acrylate groups, they can undergo rapid crosslinking when exposed to ultraviolet or visible light in the presence of appropriate photoinitiators. Photoinitiators create free radicals that can initiate the formation of photopolymerizable hydrogels [36].

Over the past two decades, many different IL encapsulation procedures using PEG have been applied, but photopolymerization of PEG-diacrylate polymers and gelation based on a combination of physical and chemical cross-linking have become the main methods [37]. Nevertheless, many studies describe the emergence of an immune response to PEG-encapsulated cells. For example, J.Y. Jang et al. noted that PEG grafted onto the collagen capsule can inhibit lymphocyte activation but not macrophages [38]. As an enhancement of immunoprotection, groups of researchers suggest modifying the exosurfaces of PEG capsules with immune cell receptor's such as Fas ligand (FasL) [39] and tumor necrosis factor receptor 1 (TNFR1) [40].

ENCAPSULATION STRATEGIES

IL encapsulation strategies can be divided into three main categories: macroencapsulation, microencapsulation and nanoencapsulation (Fig. 2). The first two are recognized as the most promising.

Macroencapsulation is the encapsulation of several thousand ILs in a macroencapsulation device more than 1000 μm in diameter. Depending on the transplantation site, macroencapsulation devices can be divided into extravascular and intravascular.

Intravascular macroencapsulation usually involves the placement of multiple ILs in hollow semipermeable fibers, which are then directly connected to the host vasculature through anastomoses. Despite promising studies using intravascular devices, researchers have reported severe problems with embolization and blood clot formation. This has prevented the Food and Drug Administration (FDA) from approving these systems for clinical trials [42].

Extravascular macroencapsulation usually involves placing multiple ILs in simple diffusion chambers that do not require intravascular shunts. Such devices are often placed in the abdominal cavity or under the skin, from where they can be retrieved and repaired in case of damage.

Extravascular macrodevices are in the form of tubular or flat diffusion chambers. The tubular device is structurally weak and can break, and requires a large amount of IL for seeding [43]. Flat devices are structurally more stable. For example, the Islet Sheet device from Islet Sheet Medical (USA) has been shown to provide good graft survival in both allogeneic and xenogeneic transplantation [44, 45]. The main disadvantage of the Islet Sheet device is the limited oxygen diffusion leading to hypoxia and necrosis of the central groups, implanted IL.

The problem of limited oxygen diffusion is tackled by several approaches to the design of macrodevices. For example, the TheraCyte™ macroencapsulation device is

equipped with an external membrane that promotes neovascularization [46]. IL encapsulated in TheraCyte™ devices survived for a long period of time in both allo- and xenotransplantation models [47]. A modified version of TheraCyte™ device, namely Encaptra® system (EN250 device), developed by ViaCyte (USA), is currently being tested for safety in a phase II clinical trial [48].

The problem of hypoxia can also be addressed by means of an artificially oxygenated β-Air Bio-artificial Pancreas (BAP) device developed by Beta-O2 Technologies Ltd (Israel) [49]. This device consists of a semi-permeable chamber containing IL immersed in alginate hydrogel, and an additional compartment that provides daily oxygen supply through an external probe system [50]. Preliminary studies with small-sized BAP devices implanted in diabetic pigs showed that the encapsulated allogeneic IL preserved its function and blood glucose levels dropped to normal for several months [51].

In in vitro experiments, perfluorocarbons and calcium peroxide (CaO_2) were added to IL-containing hydrogels to increase the rate of O_2 diffusion in the hydrogel system [52]. This could also be a promising solution for strategies to overcome IL hypoxia in macroencapsulation devices.

Microencapsulation is the incorporation of one or more IL into microcapsules ranging from 200 to 1500 μm in size (Fig. 3).

This technology has several advantages over macroencapsulation. First, the microcapsules are generally spherical in shape, thereby providing a greater surface area to volume ratio and increased transport of oxygen and nutrients required for IL survival. Secondly, microcapsules are mechanically stable and easier to manufacture, giving the freedom to change parameters such as capsule size, permeability and thickness. Thirdly, they can be implanted using a minimally invasive procedure, and the smooth spherical geometry minimizes the immune response to the foreign body. The main disadvantage is the difficulty of extracting microcapsules from the transplant site.

The need to ensure maximum cell survival and preserve their normal viability impose the following restrictions on the conditions of the IL microencapsulation procedure:

– exclusion of organic solvents;
– carrying out the procedure in an aqueous solution isotonic to the cell cytosol (in a phosphate-buffered saline);

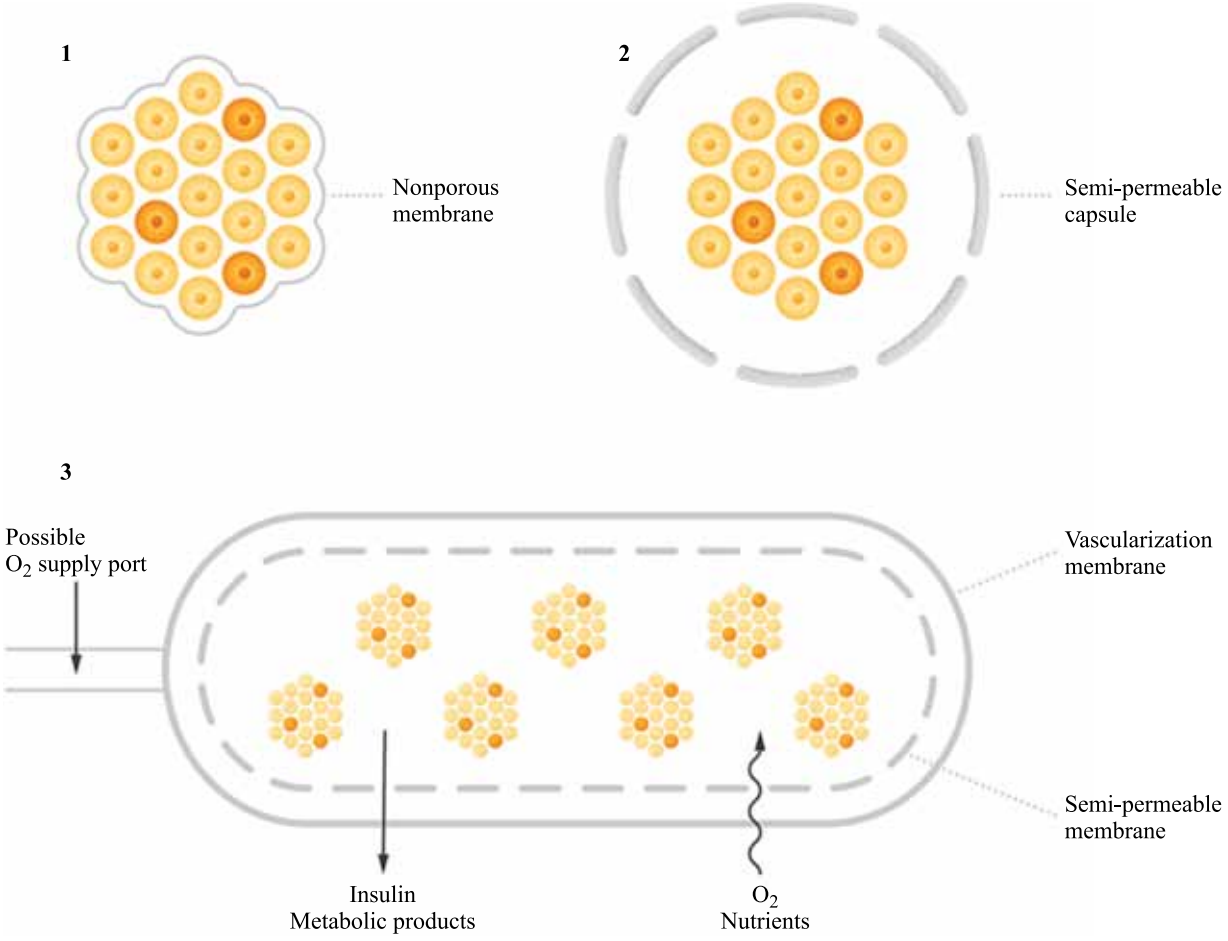

Fig. 2. The main strategies for encapsulation of IL [14]: nanoencapsulation (1), microencapsulation (2), macroencapsulation (3)

– maintaining the pH between 7.2 and 7.5;
– at a temperature between room temperature and 40°C (ideally at 37°C in an atmosphere of 5% carbon dioxide saturated with water vapor);
– the solution should quickly form a gel for even distribution of cells or IL and prevention of sedimentation.

All this significantly narrows the range of materials intended for use, and the above-mentioned conditions correspond well to the polymeric hydrogels discussed above. The most popular natural polymer for IL microencapsulation is sodium alginate, which can form hydrogels quickly in the presence of divalent ions at neutral pH and moderate temperatures [53, 54].

Using sodium alginate as an example, let us consider what the main problems researchers encounter in IL microencapsulation are. The literature identifies several factors that are crucial in the engraftment of microencapsules with IL.

Alginate purity is one of the main factors affecting biocompatibility: alginates obtained from natural sources contain immunogenic contaminants (proteins, polyphenols, endotoxins) [55], which often leads to poor graft survival due to the appearance of PFO [56]. Microcapsules derived from insufficiently purified commercial alginates activate the immune system and induce the release of inflammatory cytokines IL-1β, TNF-α and IL-6 from murine and human monocytes and macrophages [57]. One study aimed to screen for impurities and found that commercial alginate labeled as "ultrapure" still contained impurities such as peptidoglycan and lipoteichoic acid [58]. The same authors proposed the development of a screening assay for identification of pathogen-associated molecular structures in alginate polymers [58].

The composition of alginate also plays an important role in determining biocompatibility, since the G/M ratio strongly influences the physicochemical properties of microcapsules. High-G alginate microcapsules are more stable compared to high-M alginate, whereas high-M alginate microcapsules can provide selective permeability to immunoglobulins and immune cells, thereby providing better immunoprotection [59]. However, some studies have reported that high-M alginate microcapsules are more immunogenic, leading to PFO [60], while other studies have reported the opposite effect [61].

In addition to the G/M ratio, the viscosity and molecular mass (MM) of alginate also play an important role in determining biocompatibility. S. Schneider et al. demonstrated that low-MM alginate microcapsules cause PFO, and stressed the need to remove low molecular mass fractions during the purification procedure to increase biocompatibility [62].

Another important factor is the geometry and size of the capsule. Traditional IL microcapsules are spheres with a fixed diameter of 700–1500 μm. There are several opposing opinions on this issue: small 250–350 μm microcapsules have been shown to be biocompatible and contribute to a smaller PFO compared to traditional ones (500–800 μm) when transplanted into rats [63] and monkeys [64]. On the other hand, O. Veiseh et al. showed that

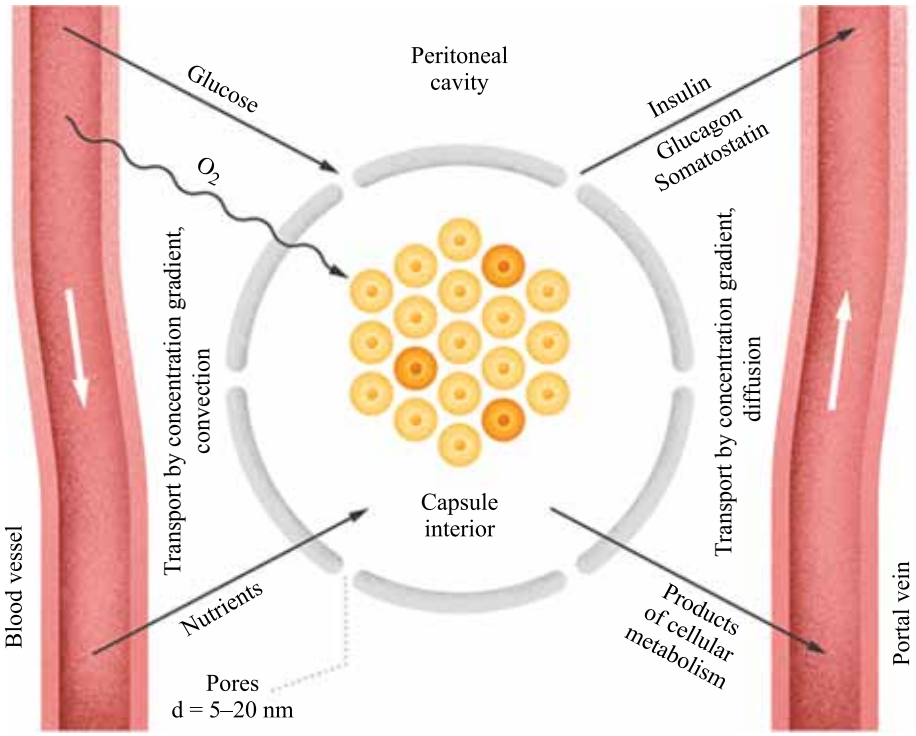

Fig. 3. Model of the structure of microencapsulated IL and its functions

larger 1500 μm alginate microcapsules have better biocompatibility and significantly reduced PFO compared to 500 μm capsules when xenotransplanting both groups into C57BL/6 mice and primates [65]. The authors also demonstrated that ILs encapsulated in larger 1500 μm capsules remained viable, had higher insulin kinetics and provided better glycemic control under xenotransplantation conditions with significantly less PFO compared to smaller microcapsules at 180 days.

Nanoencapsulation is the coating of a single IL with a biopolymer material to form 70–150 μm structures. The most common nanoencapsulation method is layer-by-layer deposition (LbL) of oppositely charged biomaterials on the IL surface (nanoencapsulation).

Various coatings have been developed for LbL with individual physicochemical properties. Haque et al. xenotransplanted primate IL encapsulated by LbL using 3 polymers in immunosuppressed mice. The encapsulation showed uniform nanoscreening of the polymers on IL without loss of cell viability and function [66]. Park et al. transplanted IL with nano-screened heparin to primates, which was shown to reduce instantaneous blood inflammatory reactions using similar nano-screening [67]. Another group used ultra-thin heparin-polymer nanofilm as a platform to incorporate biological mediators to modify the IL surface [68].

PANCREATIC ISLET CELLS IN CAPSULES

In addition to ensuring a high degree of survival of IL cells over a long period of time while maintaining their ability to produce insulin, there is also the problem of shortage of donor healthy, viable beta cells.

Allogeneic IL cells have been successfully used as donor material in the treatment of diabetes since 2000. However, as early as 1994, R. Soon-Shiong et al. [69] conducted the first successful test with microencapsulated IL in alginate-poly-L-lysine: allogeneic IL were transplanted intraperitoneally to a patient with type 1 DM, which reduced blood glucose levels for 9 months. After that, two more groups of researchers, R.C. Calafiore et al. [70] and B.E. Touch et al. [71], made attempts to transplant allogeneic IL microencapsulated in modified alginates, but the fall in glucose levels in both cases was not enough.

Porcine xenogeneic IL cells are a promising source of IL transplantable to humans for any of the following reasons: the similarity of pig and human insulin, high fecundity of pigs, availability of effective and accurate methods of genetic modification of pigs [72].

The most widely used are IL from adult donor females or neonatal islet-like cell clusters (NICC) are most commonly used; experiments with porcine fetal islets, as well as with the buds of the IL from embryos, are known [73].

Currently, there are three main strategies to increase the viability and prolong the functioning of porcine IL in the recipient's body:

1) free porcine IL transplantation according to immunosuppression and tolerance protocols;
2) encapsulation of porcine IL, in which case global immunosuppression is not required;
3) genetic modification of porcine IL and subsequent use with advanced low-toxicity immunosuppression.

However, there are risks of using porcine IL: first of all, porcine endogenous retrovirus (PERV) sequences that can be activated after xenotransplantation [74].

Second, there is a risk of developing a superacute immunological rejection reaction due to human Gal (Galactose-1,3-Galactose) antigens reacting to the porcine cell membrane disaccharide. Binding of antibodies to Gal antigens leads to almost immediate activation of the complement system with subsequent destruction of the graft. Several groups of transgenic pigs have been created to overcome the superacute reaction of immunological rejection:

1) knockout by Gal;
2) with transgenic expression in IL cells of human protein regulating the complement system (hCD46);
3) with transgenic expression of LEA29Y (a high-affinity variant of the T cell co-stimulation inhibitor CTLA-4Ig) under control of porcine insulin gene [75].

It is possible that the dual combination of immunosuppression inhibitors – IL encapsulation from transgenic pigs can provide effective graft protection without the need for strong immunosuppressive agents [76].

Satellite cells are co-cultured in the same macro- or micro-object with IL cells. Sertoli cells have been widely studied as supporting immunomodulatory "companion cells": co-transplantation of unencapsulated IL with Sertoli cells has proven useful for increasing graft survival in allo- [77], xeno- [78] and autotransplantation models [79]. Moreover, co-encapsulation of IL with Sertoli cells secreting immunosuppressive factors improves xenograft survival [80].

The immunomodulatory properties of MSCs are widely known and have been used in several studies to increase IL survival and improve transplant outcomes [81, 82]. In addition, some studies have reported increased insulin secretion as an advantage of co-encapsulating IL with MSCs [83].

Genetically modified cells have also been used to improve IL survival: co-encapsulation of IL with mouse bioengineered Sertoli cells (TM4) producing insulin-like growth factor-II (IGF-II) improves β cell survival and provides better glycemic control [84].

Alternative sources of beta cells. In addition to the above-mentioned sources of donor beta cells, methods for obtaining normally functioning insulin-producing cells from various human cell populations are being actively developed [85] in order to obtain patient-specific cellular products.

Pluripotent stem cells – embryonic stem cells (embryonic SCs or ESCs) and iPSCs – are mainly considered as a product for cell therapy. The use of pancreatic progenitor cells derived from human ESCs to treat patients with type 1 DM is at the experimental stage: the cells are encapsulated in Encaptra® macrosystem [86].

Protocols for iPSCs differentiation with additional steps were developed, optimized by cocktails of inducing factors and chemicals, using 3D cultivation methods, which allowed to obtain cell clusters morphologically and functionally similar to pancreatic islet cells [87].

Mesenchymal stem cells. The use of MSCs in diabetes is possible in two ways: differentiation into insulin-producing cells [88] and direct injection of undifferentiated MSCs [139]. When cultured in media containing fibroblast growth factor, adipose tissue-derived MSCs can express the Isl1 marker, which is necessary for islet cell formation [89]. Human umbilical cord blood-derived MSCs contain the genes required for differentiation into endocrine prostate tissue (Isl1, PDX1, Pax4 and Ngn3) [90], so they release insulin and C-peptide in response to glucose stimulation in vitro and in vivo.

Direct reprogramming for beta cells implies the use of DNA integration (using viral vectors in most cases) into cells of different types, which leads to creation of beta cells, bypassing their return to the pluripotent state. As a starting material for direct reprogramming, pancreatic ductal cells, acinar tissue, alpha cells and others are used.

It has been shown that a combination of three beta cell regulators – NGN3, PDX1 and MAFA – can effectively transform pancreatic adult mouse acinar cells into beta-like cells using an adenoviral vector [91].

Studies have shown that gastrointestinal epithelial cells can also be transformed into beta-like cells. Gastric antrum cells seem to be particularly susceptible to such transformation. In a separate study, conditional removal of Foxo1 from Ngn3+ intestinal endocrine progenitor cells led to formation of insulin-producing cells in the intestine [92].

Other examples of murine cell reprogramming include: cytokine-mediated conversion of acinar cells to insulin-expressing cells, conversion of ductal cells to insulin-expressing cells by FBW7 deletion and conversion of hepatocytes to insulin-producing cells using TGIF2 [93]. Extreme loss of β-cells can spontaneously transform δ- and α-cells of the pancreas into β-cells [94].

PHYSIOLOGICAL PARAMETERS OF THE CAPSULE ENVIRONMENT

There is no formed capillary network in the artificially created system of encapsulating devices, so solving the problem of stable trophism and oxygenation of transplanted cells is essential for their survival. A. Pileggi et al. initiated pre vascularization by simulating the physiological reaction of the body to a foreign body: the catheter was injected subcutaneously and removed after 4 weeks [95]. Pre-vascularization of the transplant site can also be achieved by pre-treating the transplant site with angiogenic factors [96].

Another approach is to embed angiogenic factors into the structure of cell capsules: for example, vascular endothelial growth factor (VEGF) into PEG [97]. G. Marchioli et al. constructed microcapsules from heparinized polycaprolactone, and also observed an increase in angiogenesis in the graft area [98].

Encapsulation of satellite cells together with IL can also lead to increased capsule vascularization. For example, the use of adipose tissue-derived or bone marrow-derived MSCs [99].

In addition, several attempts have been made to improve oxygenation at the capsule transplant site, including generating oxygen near the microcapsules using photosynthesis [100] or an electrochemical generator [101]. Unfortunately, these oxygen generating systems cannot produce enough oxygen required under a clinical setting.

One of the body's defense mechanisms against intrusion is fibrous overgrowth around the foreign object [102]. In microcapsules, the reduced diameter and greater surface area to volume ratio contribute to improved diffusion, which is indirectly confirmed by faster response of microencapsulated islets to changes in glucose in the bloodstream [103].

TRANSPLANTATION SITE IN THE RECIPIENT'S BODY

The ideal site for transplantation should have such features as low immune exposure, ease of extraction of implanted capsules, access to the recipient's vascular network with the possibility of neovascularization of the implanted graft and sufficient space to accommodate the desired number of implanted microcapsules [104]. Non-encapsulated ILs are usually injected into the liver through the portal vein. Portal infusion of microencapsulated IL is not possible due to their size. Microencapsulated ILs are usually injected into the abdominal cavity.

However, there are also negative influences when microcapsules are transplanted into the abdominal cavity: insufficient revascularization, high immunogenicity, chronic hypoxic stress, which makes it necessary to have more encapsulated IL to normalize the glucose levels compared to unencapsulated IL [105]. The advantages of transplantation of encapsulated IL into the surgically created omentum in diabetic rodent models have been shown to result in long-term normoglycemia [106]. Another promising IL transplantation site is the kidney capsule. Studies on large animals showed that in two out of seven Cynomolgus monkeys, C-peptide was detected in the blood 60 days after transplantation of microencapsulated porcine IL under the kidney capsule

[107]. However, the renal capsule is highly vascularized, and the possible space to be used limits the introduction of a large graft volume.

The subcutaneous space is another alternative site that is widely used for transplantation of encapsulated IL.

Studies have shown that xenotransplantation of encapsulated IL into the abdominal cavity of C57BL/6 mice results in strong PFO three weeks after transplantation. However, when the same encapsulated IL were transplanted subcutaneously, PFO was significantly reduced [108]. Thus, subcutaneous transplantation of microencapsulated IL can be adopted as a strategy to reduce PFO and increase IL survival, if the problem of poor oxygen supply proves to be solvable.

GLOBAL CLINICAL TRIALS USING ENCAPSULATED IL

A relatively small number of encapsulation systems have been used in clinical trials. Although all of the systems have been shown to be safe for patients, their efficacy has varied [109–116].

In the creation of IL and β-cell encapsulation systems, researchers use different approaches: micro- and macro devices, transplantation sites and methods, allo- and xenografts.

Initially, clinical trials focused on allogeneic IL, but the selective immune barrier of microcapsules allows the safe use of porcine IL as an alternative cell source as well. Living Cell Technologies (LCT) conducted a large clinical trial using porcine IL encapsulated in alginate-poly-L-ornithine called Diabecell®. Eight patients received different doses of IL (from 5000 to 10,000 IEQ per kg of body weight), and six of them showed reduced exogenous insulin levels for up to eight months [117].

As mentioned earlier, macroencapsulation devices limit oxygen transfusion to cells to a greater extent. Therefore, one of the modifications – the BAP device – is designed to solve this problem by using a built-in reusable oxygen cylinder. A phase I study evaluated the safety and efficacy of implantation of a βAir device containing human allogeneic pancreatic islet in patients with type 1 diabetes mellitus. Four patients were transplanted with 1–2 BAP devices, each containing 1,800–4,600 islet equivalents per kg of body weight and were monitored for 3–6 months with regular oxygen restoration. Although β cells survived in the device, only minute levels of circulating C-peptide were observed without any effect on metabolic control. PFO was observed in the capsule environment, and the recovered devices showed a blunted insulin response and amyloid formation in the endocrine tissue [118].

ViaCyte has developed the Encaptra® macroencapsulation system, which, unlike all competitors, incorporates iPSCs rather than IL. ViaCyte is currently conducting a Phase I/II multicenter clinical trial using macroencapsulation technology and the VC-01™ cell product to evaluate the safety and effectiveness of the system over a 2-year period [114].

Unlike Encaptra®, the Sernova Cell Pouch is not immune-isolating. The specificity of its transplantation is aimed at preliminary vascularization of the subcutaneous area before the introduction of cells through the canal. The canal-forming device is inserted under the skin for 30 days to allow vascular integration with the device. The row of rods is then removed to fill the formed channels with encapsulated IL. It is assumed that such stimulation of the microvasculature can significantly increase the survival rate of encapsulated islets by increasing trophism and gas exchange. However, a 3-year phase I/II clinical trial using this device was discontinued in 2016 after recruiting three patients [110].

Encapsulation of pancreatic islets in thrombin-plasma gel is somewhat different from the encapsulation standards: allogeneic IL is resuspended in autologous plasma and laparoscopically distributed over the omentum surface: it has a dense vascularized surface and is easily accessible. In addition, recombinant clinical-grade human thrombin is used for cell adhesion. This method has been used in one patient with restoration of euglycemia and subsequent insulin independence for 12 months [119].

CONCLUSION

New developments in the field of bioactive IL encapsulation, which will make it possible to avoid transplant immunosuppression and achieve long-term functional activity of islet cells, are now extremely necessary in Russia and the global community. Beta cell and IL encapsulation technologies, including nano-, micro-, and macroencapsulation, are promising strategies to the treatment of type 1 diabetes, as they provide transplantation of cell resources without immunosuppressive agents and allow the use of alternative donor sources.

The main problems that need to be addressed for effective transplantation of encapsulated pancreatic islets are related to graft oxygenation, inflammatory response, biocompatibility of the material, and location and method of optimal transplantation. The long-term success of encapsulation strategies can be hampered by pericapsular fibrotic overgrowth and the limited survival of encapsulated islets, especially after intraperitoneal implantation. In each area of encapsulation, there are still limitations that hinder their wide clinical application: macroencapsulation devices are easily retrievable, but contribute more to pericapsular fibrotic overgrowth and less to normal oxygenation and cell trophism. Micro- and nano-capsules are more difficult to retrieve from the recipient's body, but the cells are in them in more satisfactory conditions.

In addition to the above, there is also the problem of shortage of healthy, viable donor beta cells. Porcine IL xenotransplantation is currently the most advanced

alternative to IL transplantation or allotransplantation in the world, especially since recent advances in genetic engineering have led to a reconsideration of the use of porcine organs. Using the clustered regularly interspaced short palindromic repeats (CRISPR)/CRISPR-associated (Cas) gene technology [120], a pool of 62 known porcine retroviruses can be removed from pig skin cells, which in principle can also be used to obtain iPSCs, and then genetically "pure" pigs can be used as islet cell donors [121]. It should be noted that xenotransplantation is prohibited in Russia.

Overall, advances in biomaterial science, fabrication techniques, safer implantation strategies, angiogenesis stimulation and cell biology, and new alternative sources of pancreatic islets may make beta cell encapsulation technologies become a medical reality.

The work was supported by the Russian Ministry of Health (state assignment No. AAAA20-120022590096-6 on "Creation of pancreatic islet encapsulation technology for compensation of absolute insulin-deficient states").

The authors declare no conflict of interest.

REFERENCES

1. *Rojas J, Bermudez V, Palmar J, Martínez MS, Olivar LC, Nava M, Tomey D et al.* Pancreatic Beta Cell Death: Novel Potential Mechanisms in Diabetes Therapy. *J Diabetes Res*. 2018; 2018: 1–19. doi: 10.1155/2018/9601801.
2. *Aghazadeh Y, Nostro MC.* Cell Therapy for Type 1 Diabetes: Current and Future Strategies. *Curr Diab Rep.* 2017; 17 (6): 37. doi: 10.1007/s11892-017-0863-6.
3. *Primavera R, Razavi M, Kevadiya BD, Wang J, Vykunta A, Mascolo DD, Decuzzi P et al.* Enhancing islet transplantation using a biocompatible collagen-PDMS bioscaffold enriched with dexamethasone-microplates. *Biofabrication.* 2021; 13 (3). doi: 1 10.1088/1758-5090/abdcac.
4. *Peloso A, Citro A, Zoro T, Cobianchi L, Kahler-Quesada A, Bianchi CM et al.* Regenerative Medicine and Diabetes: Targeting the Extracellular Matrix Beyond the Stem Cell Approach and Encapsulation Technology. *Front Endocrinol*. 2018; 9: 445. doi: 10.3389/fendo.2018.00445.
5. *Yoshihara E, O'Connor C, Gasser E.* Immune-evasive human islet-like organoids ameliorate diabetes. *Nature.* 2020; 586 (7830): 606–611. doi: 10.1038/s41586-020-2631-z.
6. *Strand BL, Coron AE, Skjak-Braek G.* Current and future perspectives on alginate encapsulated pancreatic islet. *Stem Cells Transl Med.* 2017; 6 (4): 1053–1058. doi: 10.1002/sctm.16-0116.
7. *Vasile C, Pamfil D, Stoleru E, Baican M.* New Developments in Medical Applications of Hybrid Hydrogels Containing Natural Polymers. *Molecules.* 2020 Mar 27; 25 (7): 1539. doi: 10.3390/molecules25071539.
8. *Hu S, de Vos P.* Polymeric approaches to reduce tissue responses against devices applied for islet-cell encapsulation. *Front Bioeng Biotechnol.* 2019; 7: 134. doi: 10.3389/fbioe.2019.00134.
9. *Gazda LS, Vinerean HV. Laramore MA, Hall RD, Carraway W, Smith BH.* Pravastatin Improves Glucose Regulation and Biocompatibility of Agarose Encapsulated Porcine Islets following Transplantation into Pancreatectomized Dogs. *J Diabetes Res.* 2014; 2014: 405362. doi: 10.1155/2014/405362.
10. *Iwata H, Takagi T, Amemiya H.* Agarose microcapsule applied in islet xenografts (hamster to mouse). *Transplant Proc.* 1992; 24 (3): 952.
11. *Sabatini V, Pellicano L, Farina H, Pargoletti E, Annunziata L, Ortenzi MA et al.* Design of New Polyacrylate Microcapsules to Modify the Water-Soluble Active Substances Release. *Polymers.* 2021; 13 (809). doi: 10.3390/polym13050809.
12. *Dupuy B, Gin H, Baquey C, Ducassou D. In situ* polymerization of a microencapsulating medium round living cells. *J Biomed Mater Res.* 1988; 22 (11): 1061–1070. doi: 10.1002/jbm.820221109.
13. *Tun T, Inoue K, Hayashi H, Aung T, Gua Y-J, Doia R et al.* A newly developed three-layer agarose microcapsule for a promising biohybrid artificial pancreas: rat to mouse xenotransplantation. *Cell Transplant.* 1996; 5 (5 Suppl 1): 59–63. doi: 10.1016/0963-6897(96)00042-5.
14. *Jain K, Yang H, Asina SK, Patel SG, Desai J, Diehl C et al.* Long-term preservation of islets of Langerhans in hydrophilic macrobeads. *Transplantation.* 1996; 61 (4): 532–536. doi: 10.1097/00007890-199602270-00003.
15. *Barkai U, Rotem A, de Vos P.* Survival of encapsulated islets: More than a membrane story. *World J Transplant*. 2016; 6 (1): 69–90. doi: 10.5500/wjt.v6.i1.69.
16. *Basta G, Montanucci P, Calafiore R.* Microencapsulation of cells and molecular therapy of type 1 diabetes mellitus: The actual state and future perspectives between promise and progress. *J Diabetes Investig.* 2020; 12 (3). doi: 10.1111/jdi.13372.
17. *Vaithilingam V, Bal S, Tuch BE.* Encapsulated Islet Transplantation: Where Do We Stand? *Rev Diabet Stud.* 2017; 14 (1): 51–78. doi: 10.1900/RDS.2017.14.51.
18. *Simó G, Fernández-Fernández E, Vila-Crespo J, Ruipérez V, Rodríguez-Nogales JM.* Research progress in coating techniques of alginate gel polymer for cell encapsulation. *Carbohydr Polym*. 2017; 170: 1–14. doi: 10.1016/j.carbpol.2017.04.013.
19. *Ernst AU, Bowers DT, Wang L-H, Shariati K, Plesser MD, Brown NK, Mehrabyan T et al.* Nanotechnology in cell replacement therapies for type 1 diabetes. *Adv Drug Deliv Rev.* 2019; 139: 116–138. doi: 10.1016/j.addr.2019.01.013.
20. *Bochenek MA, Veiseh O, Vegas AJ.* Alginate encapsulation as long-term immune protection of allogeneic pancreatic islet cells transplanted into the omental bursa of macaques. *Nat Biomed Eng.* 2018; 2 (11): 810–821. doi: 10.1038/s41551-018-0275-1.
21. *Vaithilingam V, Kollarikova G, Qi M, Lacik I.* Effect of prolonged gelling time on the intrinsic properties of

barium alginate microcapsules and its biocompatibility. *J Microencapsl*. 2011; 28 (6): 499–507.
22. *Qi M, Lacik I, Kolláriková G, Strand BL, Formo K, Wang Y, Marchese E et al.* A recommended laparoscopic procedure for implantation of microcapsules in the peritoneal cavity of non-human primates. *J Surg Res*. 2011; 168 (1): 117–123. doi: 10.1016/j.jss.2011.01.040.
23. *Ellis CE, Korbutt GS.* Chitosan-based biomaterials for treatment of diabetes. *Chitosan Based Biomaterials*. 2017; 91–113. doi: 10.1016/B978-0-08-100228-5.00004-3.
24. *Kim MJ, Park H-S, Kim J-W, Lee E-Y, Rhee M, You Y-H et al.* Suppression of Fibrotic Reactions of Chitosan-Alginate Microcapsules Containing Porcine Islets by Dexamethasone Surface Coating. *Endocrinol Metab (Seoul)*. 2021; 36 (1): 146–156. doi: 10.3803/EnM.2021.879.
25. *Lin K, Zhang D, Macedo MH, Cui W, Sarmento B, Shen G*. Advanced Collagen-Based Biomaterials for Regenerative Biomedicine. *Advanced Functional Materials*. 2019; 29 (3). doi: 10.1002/adfm.201804943.
26. *Silvipriya KS, Kumar KK, Bhat AR, Kumar D, John A, lakshmanan P.* Collagen: Animal Sources and Biomedical Application. *JAPS*. 2015; 5 (03): 123–127. doi: 10.7324/JAPS.2015.50322.
27. *Lee CH, Singla A, Lee Y.* Biomedical applications of collagen. *Int J Pharm*. 2001; 221 (1–2): 1–22. doi: 10.1016/s0378-5173(01)00691-3.
28. *Yin C, Chia SM. Quek CH, YuH, Zhuo R-X, Leong KW, Maoad H-Q et al.* Microcapsules with improved mechanical stability for hepatocyte culture. *Biomaterials*. 2003; 24 (10): 1771–1780. doi: 10.1016/S0142-9612(02)00580-X.
29. *Marinucci L, Lilli C, Guerra M, Belcastro S, Becchetti E, Stabellini G et al.* Biocompatibility of collagen membranes crosslinked with glutaraldehyde or diphenylphosphoryl azide: an *in vitro* study. *J Biomed Mater Res A*. 2003; 67 (2): 504–509. doi: 10.1002/jbm.a.10082.
30. *Song R, Murphy M, Li C, Ting K, Soo C, Zheng Z.* Current development of biodegradable polymeric materials for biomedical applications. *Drug Des Devel Ther*. 2018; 12: 3117–3145. doi: 10.2147/DDDT.S165440.
31. *Gill I, Ballesteros A*. Bioencapsulation within synthetic polymers (Part 1): sol–gel encapsulated biologicals. *Trends Biotechnol*. 2000; 18 (7): 282–296. doi: 10.1016/s0167-7799(00)01457-8.
32. *Klymiuk N, Ludwig B, Seissler J, Reichart B, Wolf E.* Current Concepts of Using Pigs as a Source for Beta-Cell Replacement Therapy of Type 1 Diabetes. *Curr Mol Biol Rep*. 2016; 2: 73–82. doi: 10.1007/s40610-016-0039-1.
33. *Schneider MC, Barnes CA, Bryant SJ.* Characterization of the chondrocyte secretome in photoclickable poly(ethylene glycol) hydrogels. *Biotechnol Bioeng*. 2017; 114 (9): 2096–2108. doi: 10.1002/bit.26320.
34. *Carles-Carner M, Saleh LS, Bryant SJ.* The effects of hydroxyapatite nanoparticles embedded in a MMP-sensitive photoclickable PEG hydrogel on encapsulated MC3T3-E1 pre-osteoblasts. *Biomed Mater*. 2018; 13 (4). doi: 10.1088/1748-605X/aabb31.
35. *Nachlas ALY, Li S, Jha R.* Human iPSC-derived mesenchymal stem cells encapsulated in PEGDA hydrogels mature into valve interstitial-like cells. *Acta Biomater*. 2018 Apr 15; 71: 235–246. doi: 10.1016/j.actbio.2018.02.025.
36. *Qin X-H, Ovsianikov A, Stampfl J, Liska R.* Additive manufacturing of photosensitive hydrogels for tissue engineering applications. *BioNanoMaterials*. 2014; 15 (3–4): 49–70. doi: 10.1515/bnm-2014-0008.
37. *Cellesi F, Tirelli NA.* New process for cell microencapsulation and other biomaterial applications: thermal gelation and chemical cross-linking in "tandem". *J Mater Sci Mater Med*. 2005; 16 (6): 559–565. doi: 10.1007/s10856-005-0532-1.
38. *Jang JY, Lee DY, Park SJ, Byun Y.* Immune reactions of lymphocytes and macrophages against PEG-grafted pancreatic islets. *Biomaterials*. 2004; 25 (17): 3663–3669. doi: 10.1016/j.biomaterials.2003.10.062.
39. *Cheung CY, Anseth KS.* Synthesis of immunoisolation barriers that provide localized immunosuppression for encapsulated pancreatic islets. *Bioconjug Chem*. 2006; 17 (4): 1036–1042. doi: 10.1021/bc060023o.
40. *Lin CC, Metters AT, Anseth KS.* Functional PEG–peptide hydrogels to modulate local inflammation induced by the pro-inflammatory cytokine TNFalpha. *Biomaterials*. 2009; 30 (28): 4907–4914. doi: 10.1016/j.biomaterials.2009.05.083.
41. *Dimitrioglou N, Kanelli M, Papageorgiou E, Karatzas T, Hatziavramidis D.* Paving the way for successful islet encapsulation. *Drug Discov Today*. 2019; 24 (3): 737–748. doi: 10.1016/j.drudis.2019.01.020.
42. *Hwang PTJ, Shah DK, Garcia JA, Bae CY, Lim D-J, Huiszoon RC at al*. Progress and challenges of the bioartificial pancreas. *Nano Converg*. 2016; 3 (1): 28. doi: 10.1186/s40580-016-0088-4.
43. *Song S, Roy S.* Progress and challenges in macroencapsulation approaches for type 1 diabetes (T1D) treatment: Cells, biomaterials, and devices. *Biotechnol Bioeng*. 2016; 113 (7): 1381–13402. doi: 10.1002/bit.25895.
44. *Gamble A, Pepper AR, Bruni A, Shapiro AMJ.* The journey of islet cell transplantation and future development. *Islets*. 2018; 10 (2): 80–94. doi: 10.1080/19382014.2018.
45. *Lamb M, Storrs R, Li S, Liang O et al.* Function and viability of human islets encapsulated in alginate sheets: *in vitro* and *in vivo* culture. *Transplant Proc*. 2011; 43 (9): 3265–3266. doi: 10.1016/j.transproceed.2011.10.028.
46. *Boettler T, Schneider D, Cheng Y, Kadoya K, Brandon EP, Martinson L et al.* Pancreatic tissue transplanted in theracyte encapsulation devices is protected and prevents hyperglycemia in a mouse model of immunemediated diabetes. *Cell Transplant*. 2016; 25 (3): 609–614. doi: 10.3727/096368915X688939.
47. *Lysy PA, Corritore E, Sokal EM.* New Insights into Diabetes Cell Therapy. Curr *Diab Rep*. 2016; 16: 38. doi: 10.1007/s11892-016-0729-3.
48. *Bartlett ST, Markmann JF, Johnson P, Korsgren O, Hering BJ, Scharp D et al.* Report from IPITA-TTS Opinion Leaders Meeting on the Future of β-Cell Replacement. *Transplantation*. 2016; 100 (Suppl 2): S1–44. doi: 10.1097/TP.0000000000001055.

49. *Cañibano-Hernández A, Burgo LSD, Espona-Noguera A, Ciriza J, Pedraz JL*. Current advanced therapy cell-based medicinal products for type-1-diabetes treatment. *Int J Pharm*. 2018; 543 (1–2): 107–120. doi: 10.1016/j.ijpharm.2018.03.041.
50. *Ludwig B, Rotem A, Schmid J et al*. Improvement of islet function in a bioartificial pancreas by enhanced oxygen supply and growth hormone releasing hormone agonist. *Proc Natl Acad Sci USA*. 2012; 109 (13): 5022–5027. doi: 10.1073/pnas.1201868109.
51. *Neufeld T, Ludwig B, Barkai U et al*. The efficacy of an immunoisolating membrane system for islet xenotransplantation in minipigs. *PLoS One*. 2013; 8 (8). doi: 10.1371/journal.pone.0070150.
52. *Gholipourmalekabadi M, Zhao S, Harrison SB, Mozafari M, Seifalian MA*. Oxygen-generating biomaterials: A new, viable paradigm for tissue engineering? *Trends Biotechnol*. 2016; 34 (12): 1010–1021. doi: 10.1016/j.tibtech.2016.05.012.
53. *Rausa RA, Nawawi FWMW, Nasaruddin RR*. Alginate and alginate composites for biomedical applications. *AJPCR*. 2021; 16 (3): 280–306. doi: 10.1016/j.ajps.2020.10.001.
54. *Pandolfi V, Pereira U, Dufresne M, Legallais C*. Alginate-Based Cell Microencapsulation for Tissue Engineering and Regenerative Medicine. *Curr Pharm Des*. 2017; 23 (26): 3833–3844. doi: 10.2174/1381612823666170609084016.
55. *Fernando IPS, Lee WW, Han EJ, Ahn G*. Alginate-based nanomaterials: Fabrication techniques, properties, and applications. *Chemical Engineering Journal*. 2020; 391. doi: 10.1016/j.cej.2019.123823.
56. *Mallett AG, Korbutt GS*. Alginate modification improves long-term survival and function of transplanted encapsulated islets. *Tissue Eng Part A*. 2009; 15 (6): 1301–1309. doi: 10.1089/ten.tea.2008.0118.
57. *Ashimova A, Yegorov S, Negmetzhanov B, Hortelano G*. Cell Encapsulation Within Alginate Microcapsules: Immunological Challenges and Outlook. *Front Bioeng Biotechnol*. 2019; 7: 380. doi: 10.3389/fbioe.2019.00380.
58. *Paredes-Juarez GA, de Haan BJ, Faas MM, de Vos PA*. Technology platform to test the efficacy of purification of alginate. *Materials (Basel)*. 2014; 7 (3): 2087–2103. doi: 10.3390/ma7032087.
59. *De Groot M, Schuurs TA, van Schilfgaarde R*. Causes of limited survival of microencapsulated pancreatic islet grafts. *J Surg Res*. 2004; 121 (1): 141–150. doi: 10.1016/j.jss.2004.02.018.
60. *Mitchell A, Johnson B*. Reactive polymers and microcapsules. *McMaster*: 2020.
61. *De Vos P, de Haan B, van Schilfgaarde R*. Effect of the alginate composition on the biocompatibility of alginatepolylysine microcapsules. *Biomaterials*. 1997; 18 (3): 273–278. doi: 10.1016/s0142-9612(96)00135-4.
62. *Schneider S, Feilen PJ, Kraus O, Haase T, Sagban TA, Lehr H-A et al*. Biocompatibility of alginates for grafting: impact of alginate molecular weight. *Artif Cells Blood Substit Immobil Biotechnol*. 2003; 31 (4): 383–394. doi: 10.1081/bio-120025409.
63. *Robitaille R, Pariseau JF, Leblond FA, Lamoureux M, Lepage Y, Hallé JP*. Studies on small (<350 microm) alginate-poly-L-lysine microcapsules. III. Biocompatibility Of smaller versus standard microcapsules. *J Biomed Mater Res*. 1999; 44 (1): 116–120. doi: 10.1002/(sici)1097-4636(199901)44:1<116::aid-jbm13>3.0.co;2-9.
64. *Lum ZP, Krestow M, Tai IT, Vacek I, Sun AM*. Xenografts of rat islets into diabetic mice. An evaluation of new smaller capsules. *Transplantation*. 1992; 53 (6): 1180–1183. doi: 10.1097/00007890-199206000-00002.
65. *Veiseh O, Doloff JC, Ma M, Vegas AJ, Tam HH, Bader AR et al*. Size- and shape-dependent foreign body immune response to materials implanted in rodents and non-human primates. *Nat Mater*. 2015; 14 (6): 643–651. doi: 10.1038/nmat4290.
66. *Haque MR, Kim J, Park H, Lee HS, Lee KW, Al-Hilal TA et al*. Xenotransplantation of layer-by-layer encapsulated nonhuman primate islets with a specified immunosuppressive drug protocol. *J Control Release*. 2017; 258: 10–21. doi: 10.1016/j.jconrel.2017.04.021.
67. *Park H, Haque MR, Park JB, Lee KW, Lee S, Kwon Y et al*. Polymeric nano-shielded islets with heparin-polyethylene glycol in a non-human primate model. *Biomaterials*. 2018; 171: 164–177. doi: 10.1016/j.biomaterials.2018.04.028.
68. *Lou S, Zhang X, Zhang J, Deng J, Kong D, Li C*. Pancreatic islet surface bioengineering with a heparinincorporated starPEG nanofilm. *Mater Sci Eng C Mater Biol Appl*. 2017; 78: 24–31. doi: 10.1016/j.msec.2017.03.295.
69. *Soon-Shiong P, Heintz RE, Merideth N, Yao QX, Yao Z, Zheng T et al*. Insulin independence in a type 1 diabetic patient after encapsulated islet transplantation. *Lancet*. 1994; 343 (8903): 950–951. doi: 10.1016/s0140-6736(94)90067-1.
70. *Calafiore R, Basta G, Luca G, Lemmi A, Montanucci MP, Calabrese G et al*. Microencapsulated pancreatic islet allografts into nonimmunosuppressed patients with type 1 diabetes: First two cases. *Diabetes Care*. 2006; 29 (1): 137–138. doi: 10.2337/diacare.29.1.137.
71. *Touch BE, Keogh GW, Williams LJ, Wu W, Foster JL, Vaithilingam V et al*. Safety and viability of microencapsulated human islets transplanted into diabetic humans. *Diabetes Care*. 2009; 32 (10): 1887–1889. doi: 10.2337/dc09-0744.
72. *Graham ML, Schuurman H-J*. Pancreatic islet xenotransplantation. *Drug Discovery Today: Disease Models*. 2017; 23: 43–50. doi: 10.1016/j.ddmod.2017.11.004.
73. *Nagaraju S, Bottino R Wijkstrom M, Trucco M, Cooper DKC*. Islet xenotransplantation: what is the optimal age of the islet-source pig? *Xenotransplantation*. 2015; 22 (1): 7–19. doi: 10.1111/xen.12130.
74. *Pellegrini C, Sordi B, Piemonti L*. Pancreatic β-cell replacement in diabetes mellitus. *Diabetes*. 2013; (3): 11–20.
75. *Klymiuk N, van Buerck L, Bahr A, Offers M, Kessler B, Wuensch A et al*. Xenografted islet cell clusters from INSLEA29Y transgenic pigs rescue diabetes and prevent immune rejection in humanized mice. *Diabetes*. 2012; 61 (6): 1527–15232. doi: 10.2337/db11-1325.

76. *Ludwig B, Ludwig S.* Transplantable bioartificial pancreas devices: current status and future prospects. *Langenbecks Arch Surg.* 2015; 400 (5): 531–540. doi: 10.1007/s00423-015-1314-y.
77. *Korbutt GS, Elliott JF, Rajotte RV.* Co-transplantation of allogeneic islets with allogeneic testicular cell aggregates allows long-term graft survival without systemic immunosuppression. *Diabetes.* 1997; 46 (2): 317–322. doi: 10.2337/diab.46.2.317.
78. *Dufour JM, Rajotte RV, Kin T, Korbutt GS.* Immunoprotection of rat islet xenografts by cotransplantation with sertoli cells and a single injection of antilymphocyte serum. *Transplantation.* 2003; 75 (9): 1594–1596. doi: 10.1097/01.TP.0000058748.00707.88.
79. *Korbutt GS, Suarez-Pinzon WL, Power RF, Rajotte RV, Rabinovitch A.* Testicular Sertoli cells exert both protective and destructive effects on syngeneic islet grafts in non-obese diabetic mice. *Diabetologia.* 2000; 43 (4): 474–480. doi: 10.1007/s001250051331.
80. *Luca G, Calafiore R, Basta G, Ricci M, Calvitti M, Neri L et al.* Improved function of rat islets upon comicroencapsulation with Sertoli's cells in alginate/poly-Lornithine. *AAPS PharmSciTech*. 2001; 2 (3). doi: 10.1208/pt020315.
81. *Rasmusson I.* Immune modulation by mesenchymal stem cells. *Exp Cell Res.* 2006; 312 (12): 2169–2179. doi: 10.1016/j.yexcr.2006.03.019.
82. *Longoni B, Szilagyi E, Quaranta P, Paoli GT, Tripodi S, Urbani S et al.* Mesenchymal stem cells prevent acute rejection and prolong graft function in pancreatic islet transplantation. *Diabetes Technol Ther.* 2010; 12 (6): 435–446. doi: 10.1089/dia.2009.0154.
83. *Kerby A, Jones ES, Jones PM, King AJ.* Cotransplantation of islets with mesenchymal stem cells in microcapsules demonstrates graft outcome can be improved in an isolated-graft model of islet transplantation in mice. *Cytotherapy.* 2013; 15 (2): 192–200. doi: 10.1016/j.jcyt.2012.10.018.
84. *Jourdan G, Dusseault J, Benhamou PY.* Co-encapsulation of bioengineered IGF-II-producing cells and pancreatic islets: effect on beta-cell survival. *Gene Therapy*. 2011; 18: 539–545. doi: 10.1038/gt.2010.166.
85. *Babiker NE, Gassoum A, Abdelraheem NE, Arbab MA, ALDeaf SAH, El-Sheikh MAA et al.* The progress of stem cells in the treatment of diabetes mellitus type 1. *Progress in Stem Cell.* 2017; 1: 175–188.
86. *Ilic D, Devito L, Miere C, Codognotto S.* Human embryonic and induced pluripotent stem cells in clinical trials. *Br Med Bull.* 2015; 116: 19–27. doi: 10.1093/bmb/ldv045.
87. *Zhou Q, Melton DA.* Pancreas regeneration. *Nature.* 2018; 557 (7705): 351–358. doi: 10.1038/s41586-018-0088-0.
88. *Dang LT-T, Bui AN-T, Pham VM, Phan NK, Pham PV.* Production of islet-like insulin-producing cell clusters *in vitro* from adiposederived stem cells. Biomedical Research and *Therapy.* 2015; 2 (1): 184–192. doi: 10.7603/s40730-015-0003-3.
89. *Borisov MA, Petrakova OS, Gvazava IG, Kalistratova EN, Vasiliev AV.* Cellular approaches to the treatment of insulin-dependent diabetes. *Acta Nature (Russian version)*. 2016; 8 (3): 34–48.
90. *Hashemian SJ, Kouhnavard M, Nasli-Esfahani E.* Mesenchymal stem cells: rising concerns over their application in treatment of type one diabetes mellitus. *J Diabetes Res.* 2015; 2015: 675103. doi: 10.1155/2015/675103.
91. *Li W, Cavelti-Weder C, Zhang Y, Clement K, Donovan S, Gonzalez G et al.* Long-term persistence and development of induced pancreatic β cells generated by lineage conversion of acinar cells. *Nat Biotechnol.* 2014; 32 (12): 1223–1230. doi: 10.1038/nbt.3082.
92. *Ariyachet C, Tovaglieri A, Xiang G, Lu J, Shah MS, Richmond CA et al.* Reprogrammed stomach tissue as a renewable source of functional β cells for blood glucose regulation. *Cell Stem Cell.* 2016; 18 (3): 410–421. doi: 10.1016/j.stem.2016.01.003.
93. *Cerda-Esteban N, Naumann H, Ruzittu S, Mah N, Pongrac IM, Cozzitorto C et al.* Stepwise reprogramming of liver cells to a pancreas progenitor state by the transcriptional regulator Tgif2. *Nature Communications.* 2017; 8: 14127. doi: 10.1038/ncomms14127.
94. *Chera S, Baronnier D, Ghila L, Cigliola V, Jensen JN, Gu G et al.* Diabetes recovery by age-dependent conversion of pancreatic δ-cells into insulin producer. *Nature.* 2014; 514 (7523): 503–507. doi: 10.1038/nature13633.
95. *Pileggi A, Molano RD, Ricordi C, Zahr E, Collins J, Valdes R et al.* Reversal of diabetes by pancreatic islet transplantation into a subcutaneous, neovascularized device. *Transplantation*. 2006; 81 (9): 1318–1324. doi: 10.1038/nature13633.
96. *Pepper AR. Gala-Lopez B, Pawlick R, Merani S, Kin T, Shapiro AMJ.* A prevascularized subcutaneous deviceless site for islet and cellular transplantation. *Nat Biotechnol.* 2015; 33 (5): 518–523. doi: 10.1038/nbt.3211.
97. *Phelps EA, Templeman KL, Thule PM, García AJ.* Engineered VEGF-releasing PEG-MAL hydrogel for pancreatic islet vascularization. *Drug Deliv Transl Res.* 2015; 5 (2): 125–136. doi: 10.1007/s13346-013-0142-2.
98. *Marchioli G, Luca AD, Koning E.* Hybrid polycaprolactone/alginate scaffolds functionalized with VEGF to promote de novo vessel formation for the transplantation of islets of Langerhans. *Adv Healthc Mater.* 2016; 5 (13): 1606–1616. doi: 10.1002/adhm.201600058.
99. *Phelps EA, Headen DM, Taylor WR.* Vasculogenic biosynthetic hydrogel for enhancement of pancreatic islet engraftment and function in type 1 diabetes. *Biomaterials.* 2013; 34 (19): 4602–4611. doi: 10.1016/j.biomaterials.2013.03.012.
100. *Veriter, S. Gianello P, Igarashi Y, Beaurin G, GhyselinckA, Aouassar N et al.* Improvement of subcutaneous bioartificial pancreas vascularization and function by coencapsulation of pig islets and mesenchymal stem cells in primates. *Cell Transplant.* 2014; 23 (11): 1349–1364. doi: 10.3727/096368913X663550.
101. *Bloch K, Papismedov E, Yavriyants K. Vorobeychik M, Beer S, Vardi P.* Photosynthetic oxygen generator for bioartificial pancreas. *Tissue Eng.* 2006; 12 (2): 337–344. doi: 10.1089/ten.2006.12.337.
102. *Barkai U, Weir GC, Colton CK, Ludwig B, Bornstein SR, Brendel MD et al.* Enhanced oxygen supply im-

proves islet viability in a new bioartificial pancreas. *Cell Transplant.* 2013; 22 (8): 1463–1476. doi: 10.3727/096368912X657341.
103. *Thevenot P, Hu W, Tang L.* Surface chemistry influences implant biocompatibility. *Curr Top Med Chem*. 2008; 8 (4): 270–280. doi: 10.2174/156802608783790901.
104. *Zhu H, Li W, Liu Z, Li W, Chen N, Lu L et al.* Selection of Implantation Sites for Transplantation of Encapsulated Pancreatic Islets. *Tissue Eng Part B Rev.* 2018; 24 (3): 191–214. doi: 10.1089/ten.TEB.2017.0311.
105. *Desai T, Shea LD.* Advances in islet encapsulation technologies. *Nat Rev Drug Discov.* 2017; 16 (5): 338–350. doi: 10.1038/nrd.2016.232.
106. *Muthyala S, Safley S, Gordan K, Barber G, Weber C, Sambanis A.* The effect of hypoxia on free and encapsulated adult porcine islets-an *in vitro* study. *Xenotransplantation.* 2017; 24 (1). doi: 10.1111/xen.12275.
107. *Dufrane D, Goebbels RM., Saliez A, Guiot Y, Gianello P.* Six-month survival of microencapsulated pig islets and alginate biocompatibility in primates: proof of concept. *Transplantation.* 2006; 81 (9): 1345–1353. doi: 10.1097/01.tp.0000208610.75997.20.
108. *Vaithilingam V, Evans MD, Rowe A, Bean PA, Tuch BE.* Co-encapsulation of Target Effector Cells With Mesenchymal Stem Cells Reduces Pericapsular Fibrosis and Improves Graft Survival in a Xenotransplanted Animal Model. *Cell Transplant.* 2016; 25 (7): 1299–1317. doi: 10.3727/096368915X688975.
109. *Yang HK, Yoon KH.* Current status of encapsulated islet transplantation. *J Diabetes Complications.* 2015; 29 (5): 737–743. doi: 10.1016/j.jdiacomp.2015.03.017.
110. US National Library of Medicine. ClinicalTrials.gov. [Internet] A Phase I/II Study of the Safety and Efficacy of Sernova's Cell PouchTM for Therapeutic Islet Transplantation. Available from: https://clinicaltrials.gov/ct2/show/NCT01652911.
111. US National Library of Medicine. ClinicalTrials.gov [Internet]. Open-label Investigation of the Safety and Effectiveness of DIABECELL® in Patients With Type 1 Diabetes Mellitus. Available from: https://clinicaltrials.gov/ct2/show/NCT01739829.
112. US National Library of Medicine. ClinicalTrials.gov [Internet] Safety and Efficacy Study of Encapsulated Human Islets Allotransplantation to Treat Type 1 Diabetes. Available from: https://www.clinicaltrials.gov/ct2/show/NCT00790257.
113. US National Library of Medicine. ClinicalTrials.gov https://clinicaltrials.gov/ct2/show/NCT01379729(2013).
114. US National Library of Medicine. ClinicalTrials.gov [Internet] A Safety, Tolerability, and Efficacy Study of VC-01™ Combination Product in Subjects With Type I Diabetes Mellitus. Available from: https://clinicaltrials.gov/ct2/show/NCT02239354.
115. US National Library of Medicine. ClinicalTrials.gov [Internet] An Open Label, Pilot Investigation, to Assess the Safety and Efficacy of Transplantation of Macroencapsulated Human Islets Within the Bioartificial Pancreas Beta-Air in Patients With Type 1 Diabetes Mellitus. Available from: https://clinicaltrials.gov/ct2/show/NCT02064309.
116. US National Library of Medicine. ClinicalTrials.gov [Internet] Allogeneic Islet Cells Transplanted Onto the Omentum. Available from: https://clinicaltrials.gov/ct2/show/NCT02213003.
117. *Tan PL.* Company profile: Tissue regeneration for diabetes and neurological diseases at living cell technologies. *Regen Med.* 2010; 5 (2): 181–187. doi: 10.2217/rme.10.4.
118. *Carlsson P-O, Espes D, Sedigh A*. Transplantation of macroencapsulated human islets within the bioartificial pancreas βAir to patients with type 1 diabetes mellitus. *Am J Transplant.* 2018; 18 (7): 1735–1744. doi: 10.1111/ajt.14642.
119. *Baidal DA, Ricordi C, Berman DM, Alvarez A, Padilla N, Ciancio et al.* Bioengineering of an intraabdominal endocrine pancreas. *N Engl J Med.* 2017; 376 (19): 1887–1889. doi: 10.1056/NEJMc1613959.
120. *Niu D, Wei HJ, Lin L, George H, Wang T, Lee I-H.* Inactivation of porcine endogenous retrovirus in pigs using CRISPR–Cas9. *Science.* 2017; 357 (6357): 1303–1307. doi: 10.1126/science.aan4187.
121. *Yang L, Güell M, Niu D, George H, Lesha E, Grishin D et al.* Genome-wide inactivation of porcine endogenous retroviruses (PERVs). *Science.* 2015; 350 (6264): 1101–1004. doi: 10.1126/science.aad1191.

The article was submitted to the journal on 13.07.2021

DOI: 10.15825/1995-1191-2021-4-110-118

THE ROLE OF APOPTOTIC BONE MARROW CELLS IN ACTIVATION OF LIVER REGENERATION

N.A. Onishchenko[1], A.O. Nikolskaya[1], Z.Z. Gonikova[1], L.A. Kirsanova[1], M.Yu. Shagidulin[1, 2], V.I. Sevastianov[1]

[1] Shumakov National Medical Research Center of Transplantology and Artificial Organs, Moscow, Russian Federation

[2] Sechenov University, Moscow, Russian Federation

Objective: using an adoptive transfer model to study the cellular mechanisms involved in the formation of the initial stage of liver regeneration during intraperitoneal injection of a healthy recipient with apoptotic bone marrow-derived mononuclear cells (BM-MNCs) from a donor after extended liver resection. **Materials and methods.** Male Wistar rats (n = 40) were used to create a model of adoptive transfer of apoptotic BM-MNCs (a-BM-MNCs) taken from the donor after extended liver resection to a healthy recipient. During the experiments, the animals were divided into five groups. Four experimental groups with intraperitoneal injection of the same doses to the recipient: freshly isolated BM-MNCs (group 1); BM-MNCs subjected to apoptosis for 48 hours by storage at t = 4–6 °C in phosphate-buffered saline (PBS) (group 2) or in a Custodiol HTK solution (group 3). In group 4, the animals were injected with PBS after storing BM-MNCs in it. The control animals were animals injected with saline (group 5). For selection of effective modes of apoptosis induction, BM-MNCs stained with 7AAD after incubation in solutions were analyzed by flow cytometry. Targeted transfer of regenerative signals to the recipient was assessed by the mitotic activity of hepatocytes in the liver and tubular epithelium in the kidneys, as well as by the intensity of microstructural changes in the liver 24, 48 and 72 hours after injection of the studied material. **Results.** BMC incubation in PBS and HTK for 48 hours at t = 4–6 °C provides the most effective accumulation of a-BM-MNCs in early apoptosis. It was shown that a-BM-MNCs retain the ability to target-focused transmission of regulatory signals to the liver supported by autophagy process during adoptive transfer. It was established that a-BM-MNCs (groups 2 and 3) in comparison to native BM-MNCs (group 1) at adoptive transfer increased the regenerative potential of the liver due to pronounced increase in the activity of autophagy processes and directed infiltration of immunomodulatory mononuclear cells in the liver. **Conclusion.** a-BM-MNCs create a stronger basis for development and implementation of a targeted and effective regeneration program by enhancing autophagy processes and immunomodulatory effect on mononuclear cells, which are regenerative signal carriers.

Keywords: apoptosis, autophagy, bone marrow cells, liver, resection, regeneration.

INTRODUCTION

Organ and tissue damage through autoregulation mechanisms involves evolutionarily developed regeneration processes in the body. Targeted transport of regenerative signals to the damaged tissues is facilitated by mononuclear immunoregulatory blood cells and primarily by lymphocytes [1–3]. Hematopoietic and bone marrow-derived mesenchymal stem/stromal cells (BM-MNCs) also have a high regenerative potential. However, the effect of clinical application of BM-MNCs turned out to be not so pronounced and not always reproducible [4, 5], which made researchers turn to the study of how the regenerative processes of BM-MNCs are activated in order to increase their regulatory role.

The initial opinion about the influence of the processes of transdifferentiation or fusion of bone marrow-derived stem/progenitor cells with differentiated cells on the regeneration of damaged tissue/organ was not confirmed [6–9]. Activation of regenerative processes under the influence of BM-MNCs, as well as the supernatant obtained after their cultivation, was attributed to the action of paracrine factors secreted by these cells [10–13].

Further study of alternative mechanisms of induction of regenerative processes by bone marrow cells [14], allowed Thum et al. to put forward a hypothesis [15], which states that cells producing paracrine factors in the state of apoptosis, whose content in the BM-MNCs pool varies from 5 to 25%, are responsible for enhancement of regenerative processes during therapy with these cells.

At first glance, the opinion that dying apoptotic cells can increase the survival of other cells seems absurd, but at the same time, such a view contains an evolutionary justification and rationalism used by living organisms to

Corresponding author: Zalina Gonikova. Address: 1, Shchukinskaya str., Moscow, 123182, Russian Federation. Phone: (966) 188-33-33. E-mail: zalina3392@gmail.com

maintain their vital activity [16–19] and protect against the development of pathological conditions [20–22].

It is known that it is the apoptotic cells that release growth-stimulating signals in the form of nanovesicles [23], lipids in exosomes [24], microRNA and proteins [25], which not only accelerate repair processes in the body, but also have immunomodulatory effects, blocking inflammatory reactions, which, being an integral part of any damage, prevent regeneration.

To date, the hypothesis that apoptotic bone marrow-derived cells play a determining regulatory role in regenerative processes has been proven [26] and has been repeatedly confirmed by preclinical studies on cell suspensions and in experiments on animals with simulation of various pathological processes [27].

Meanwhile, early changes in damaged organs arising in response to induction effect of apoptotic bone marrow-derived mononuclear cells (a-BM-MNCs) regulating regenerative processes more efficiently have not been the subject of special studies.

The aim of this study is to investigate the cellular mechanisms of formation of the early stage of regenerative processes in the liver during intraperitoneal injection of healthy recipient with a-BM-MNCs of donor after extended liver resection (ELR) on an adoptive transfer model.

MATERIALS AND METHODS

The work was performed on male Wistar rats weighing 250–300 g (n = 40). The ability of a-BM-MNCs to regulate and target regenerative signals to the damaged organ (liver) tissue was studied by adoptive transfer method [1]. For this purpose, created in the donor was an experimental ELR model -70–75%, which is known to be accompanied by activation of hypertrophic regeneration mechanisms with pronounced mitotic activity in the remaining part of the organ [28]. Rats with ELR constituted the donor group (n = 15). Bone marrow was harvested from donor rats 12 hours after liver resection (the specified interval is necessary for appearance of morphogenetically active cells in bone marrow) and a mononuclear (hematopoietic) fraction of BM-MNCs was obtained for subsequent single intraperitoneal administration of these cells to intact (unoperated) recipient rats (n = 20) in 4 experimental groups that differed by apoptosis activation method.

Freshly isolated unsorted donor BM-MNCs at a dose of 3.0–3.5 × 10^7 cells per rat (group 1, n = 5), as well as a-BM-MNCs at the same dose activated by incubation were used, in PBS (group 2, n = 5) or in preserving ion-balanced Custodiol HTK solution (group 3, n = 5) at temperature t = 4–6 °C for 48 hours.

In group 4 we used conditioned medium – PBS – after storing BM-MNCs in it for 48 hours (n = 5). Intact rats injected with 1 mL of saline served as the control group (group 5, n = 5).

To select the modes and timing of apoptosis activation of BM-MNCs, we performed a comparative study of the dynamics of reversible and irreversible BM-MNC apoptosis during incubation in PBS by Paneco (Russia) and in preservation solution Custodiol (NTK-histidine-tryptophan-ketoglutarate solution) by Dr. Franz Köhler Chemie GmbH (Germany) at different temperatures (t = 18–22 °C and t = 4–6 °C) and different incubation times (6, 18, 24, 48, and 72 hours).

Under the indicated storage times and temperature regimes, BM-MNCs retain viability and maintain their structural and functional homeostasis due to an evolutionarily developed mechanism – autophagy – adaptive structural, functional and energy restructuring of their own metabolic reserves, which is accompanied by a gradual development of early reversible and then late irreversible cell apoptosis.

FITC Annexin V Apoptosis Detection Kit with 7-AAD (BioLegend, USA) was used to detect early apoptosis and late apoptosis/necrosis of BM-MNCs during cell incubation for the indicated periods. Cells were suspended in 100 μL of Annexin V Binding Buffer at 1 × 10^7 cells/mL and mixed with 5 μL of FITC-conjugated Annexin V and 7-AAD (dye 7 aminoactomycin D penetrates only non-viable cell nuclei and intercalates into the DNA double helix). Positively stained, i.e. non-viable mononuclear cells in the BM-MNCs pool used in 7-AAD studies should be no more than 7–10% [29]. After incubation at room temperature for 15 min in the dark, 400 μL of Annexin V Binding Buffer was added to the mixtures. The stained cells were then analyzed using a Beckman Coulter Cytomics FC 500 flow cytometer with appropriate settings.

The ability to enhance targeted (liver) transport of regenerative signals by a-BM-MNCs was assessed by the severity of proliferative activity of hepatocytes in the liver compared to the renal tubular epithelium (control of targeted exposure). The severity of mononuclear cell infiltration of these organs (by macrophages and lymphocytes) in intact recipient rats was also evaluated 24, 36, 48 and 72 hours after administration of donor freshly isolated BM-MNCs and apoptotic BM-MNCs.

The livers and kidneys of recipient rats were dissected on the indicated dates, and histological preparations, stained with hematoxylin and eosin, were prepared from them. Using a Leica DML5 microscope (Germany), we performed histological analysis of the preparations and determined in 30 fields of view the number of mitotically dividing cells, and then calculated the mitotic index (MI) in ppm (‰).

The significance of the differences in the studied indicators in the compared groups was assessed using the parametric Student's t-test at $p < 0.05$.

RESULTS AND DISCUSSION

The results of studies of the effect of the compositions of incubation solutions, the timing and temperature regimes of incubation of BM-MNCs in them on activation of early (reversible) and irreversible apoptosis/necrosis of cells are demonstrated in Figs. 1 and 2. Fig. 1 shows that at room temperature (t = 18–22 °C) of incubation of BM-MNCs in HTK and PBS solutions, the cells in the state of late apoptosis prevail after 18 and 24 hours, exceeding acceptable levels [29].

Meanwhile, storage of BM-MNCs in the same solutions at t = 4–6 °C inhibited the development of late apoptosis in cells and increased during storage (by 48 and 72 hours) the BM-MNCs content in the state of early (reversible) apoptosis, which was significantly more pronounced after 48 and 72 hours for cells in HTK – 44.8 ± 10.9% and 51.84 ± 12.2% solutions versus 29.5 ± 7.1% and 38.6 ± 10.8% in PBS solution (Fig. 2). Since after 48 hours of BM-MNCs storage in HTK and PBS solutions, they showed the highest content of cells in the state of early reversible apoptosis, while the content of BM-MNCs in the state of late apoptosis did not exceed 7–10%, ($p < 0.02$), we studied the regulatory potential of these cells in different groups of experiments when modeling adopting transfer.

There were no significant changes in the mitotic activity of hepatocytes in the liver and tubular epithelium cells in the kidneys (control of tissue-specificity of adoptive

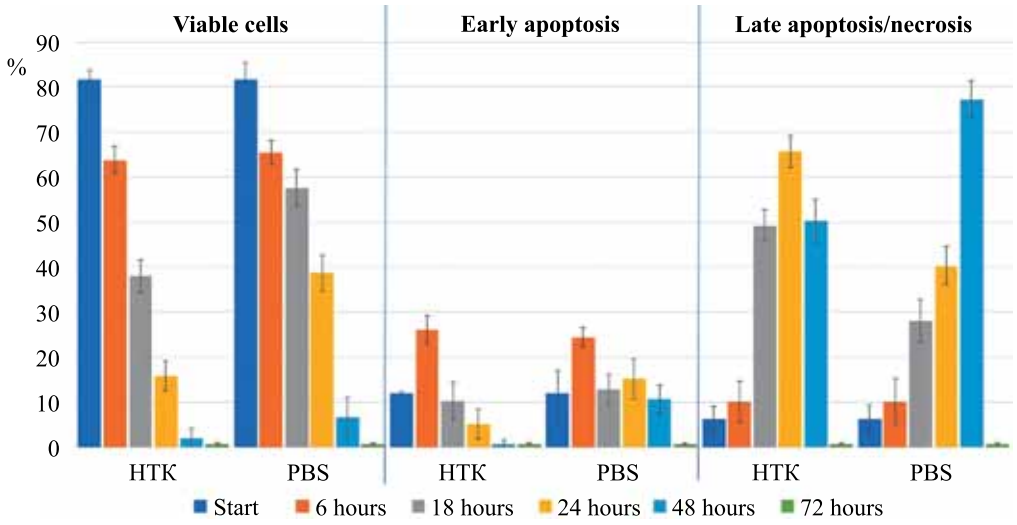

Fig. 1. Dynamics of changes in the content of viable cells, cells in a state of early apoptosis and late apoptosis/necrosis during BMC incubation in PBS and Custodiol (NTC) solutions at t = 18–22 °C

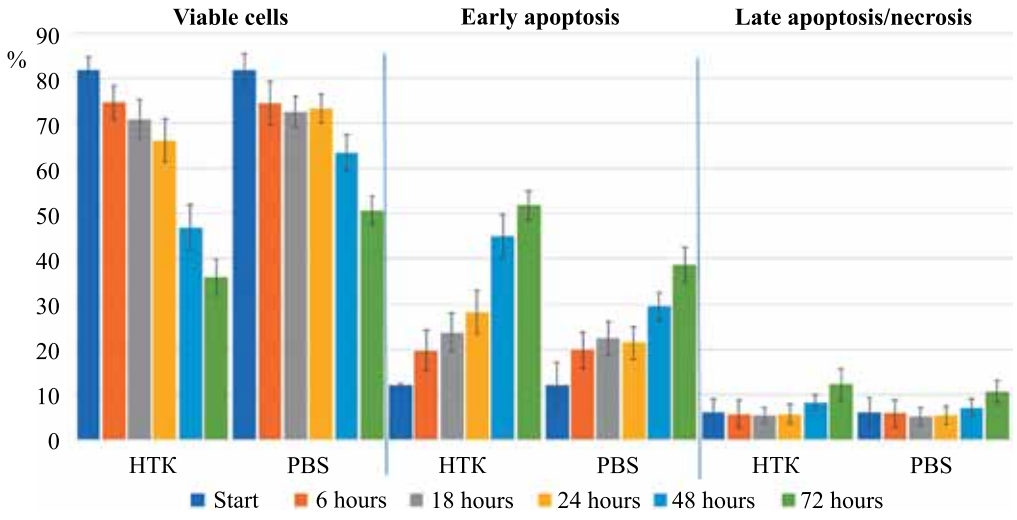

Fig. 2. Dynamics of changes in the content of viable cells, cells in a state of early apoptosis and late apoptosis/necrosis during BMC incubation in PBS and Custodiol (NTC) solutions at t = 4–6 °C

transfer) in all groups and at all time points studied after cell administration to the recipient.

The values of mitotic index (MI) in the liver and kidneys at 36, 48 and 72 hours in groups 1–4 did not exceed 0.02 ± 0.01‰ (0–2 mitoses per 30 fields of view) and did not differ from the initial values, as in group 5. Fig. 3 (a, b, c, d) shows histological picture of the liver tissue of recipient rats at different time points after administration of a-BM-MNCs incubated in Custodiol solution (group 3). One can see from Fig. 3 that the expected rise in mitotic activity of hepatocytes in the livers of recipient rats using apoptotically induced donor material after ELR (at different stages after its administration) was not detected.

At the same time, it is known that after introduction of ELR-activated donor spleen lymphocytes, the mitotic activity of not only hepatocytes but also Kupffer cells in the intact recipient's body significantly increases [1]. In this connection, we expected a similar effect for recipient liver hepatocytes and with the injection of donor a-BM-MNCs after ELR.

Meanwhile, based on the current concepts of regeneration, the result we obtained (absence of mitoses) is not surprising. In the early stages after exposure to damage, directed mobilization of the energy and metabolic reserves of cells with the development of their autophagy, which predetermines the efficiency of subsequent regenerative process, occurs in the surviving cells of the damaged organ to trigger the regenerative process [30–33].

Earlier, we also showed by morphocytometry that in the rat liver tissue at the earliest stages (up to 48 hours) after ELR, there is mobilization increase in cell density, decrease in liver weight, decrease in the areas of hepatocytes, their nuclei and cytoplasm [34], and these facts confirm the important induction role of autophagy and early reversible apoptosis in triggering an an effective regenerative process.

In experiments on the model of adoptive transfer, we obtained only indirect evidence that apoptotic BM-MNCs, in contrast to freshly isolated BM-MNCs, further enhance the autophagy process of liver cells at early

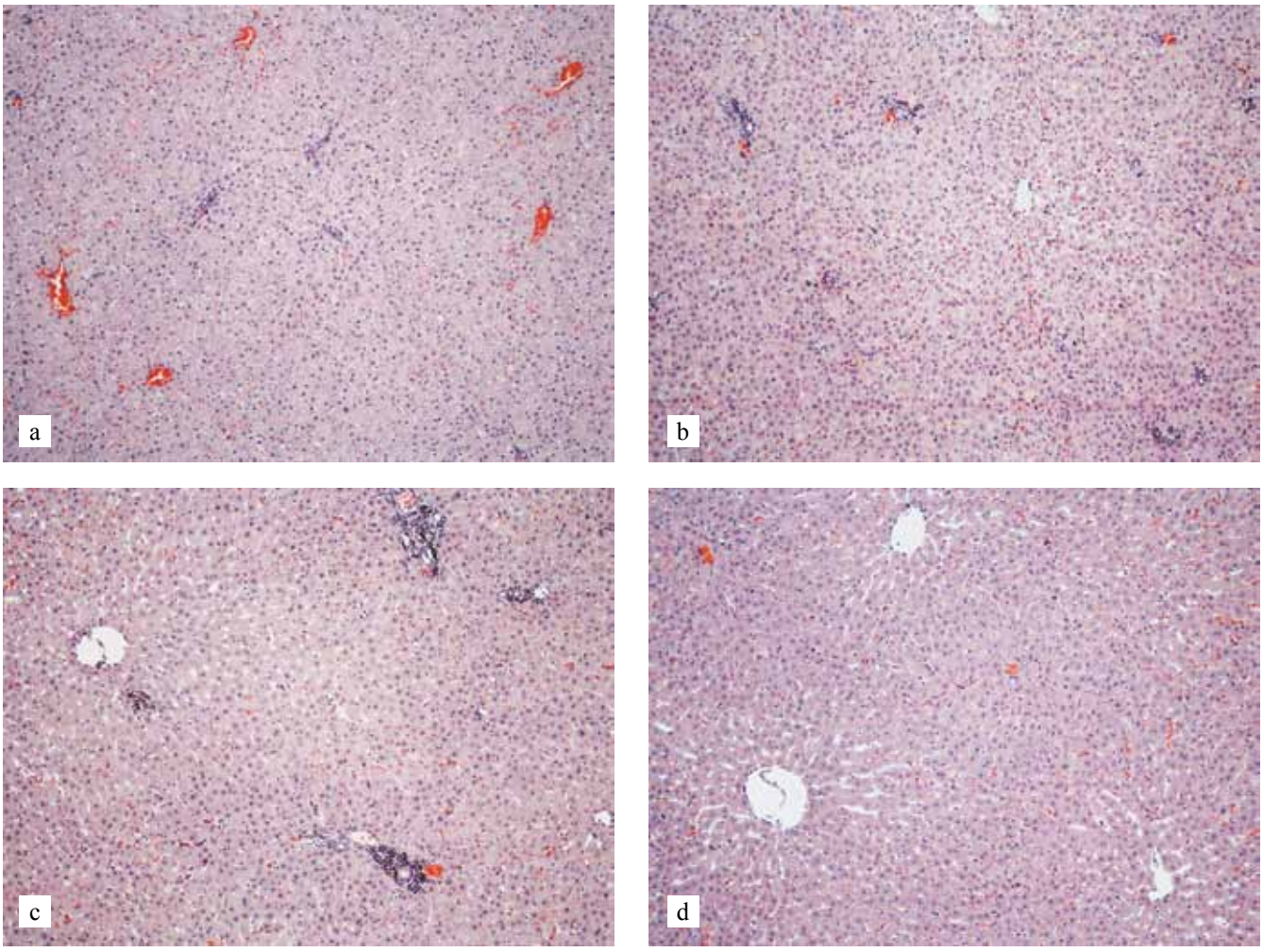

Fig. 3. Histological structure of liver tissue at different periods after a-BM-MNC injection (group 3); H&E stain, 100× magnification. a, 24 hours; b, 36 hours; c, 48 hours; d, 72 hours. No mitotic activity of hepatocytes was observed at all periods of observation

stages. It is known that autophagy is also assigned the role of a cellular autonomous defense system, which in the process of degradation of altered cellular proteins, releases receptors, including its own damage-associated molecular patterns (DAMPS), which manifests as increased tissue immunogenicity and more pronounced enhancement of its cell infiltration, which we observed in our work (see below).

We know from the literature about the appearance of pronounced mitotic activity of hepatocytes in the liver of rat recipients after introduction of donor spleen lymphocytes. We attribute the absence of a similar effect in our experiments after administration of BM-MNCs in recipient rats to cell specialization existing in the body. It is expressed in the fact that during formation of the regeneration process, BM-MNCs seem to play the role of accumulator and transducer of regeneration signals, while mature actively migrating informed lymphocytes of the peripheral immune system – lymphocytes from lymph nodes and spleen, but not BM-MNCs – are already the executors of this process [1–4].

Analysis of histological preparations of recipient liver and kidney samples (Fig. 4, a, b, c) allowed us to ascertain the appearance of cellular infiltration, which was most pronounced in the groups with a-BM-MNCs introduction (groups 2 and 3), especially in the group using cells stored in Custodiol (NTC) solution (group 3) in all groups of experiments at 36 and 48 hours only in liver but not in kidneys. The most pronounced cellular infiltration of the liver tissue in group 3 as compared to group 2 indicated both a dose-dependent regulatory effect of a-BM-MNCs and powerful enhancement of autophagy and early apoptosis processes when exposed to a-BM-MNCs.

When a-BM-MNCs incubated in Custodiol solution were injected after 36 and 48 hours, the liver of a healthy recipient showed signs characteristic of an inflammatory process: infiltration of portal tracts and sinusoids with cells as well as diffuse activation of sinusoid cells were observed, indicating, apparently, reticuloendothelial system activation (Fig. 4, a, b). It should also be noted that mononuclear cells (predominantly lymphocytes)

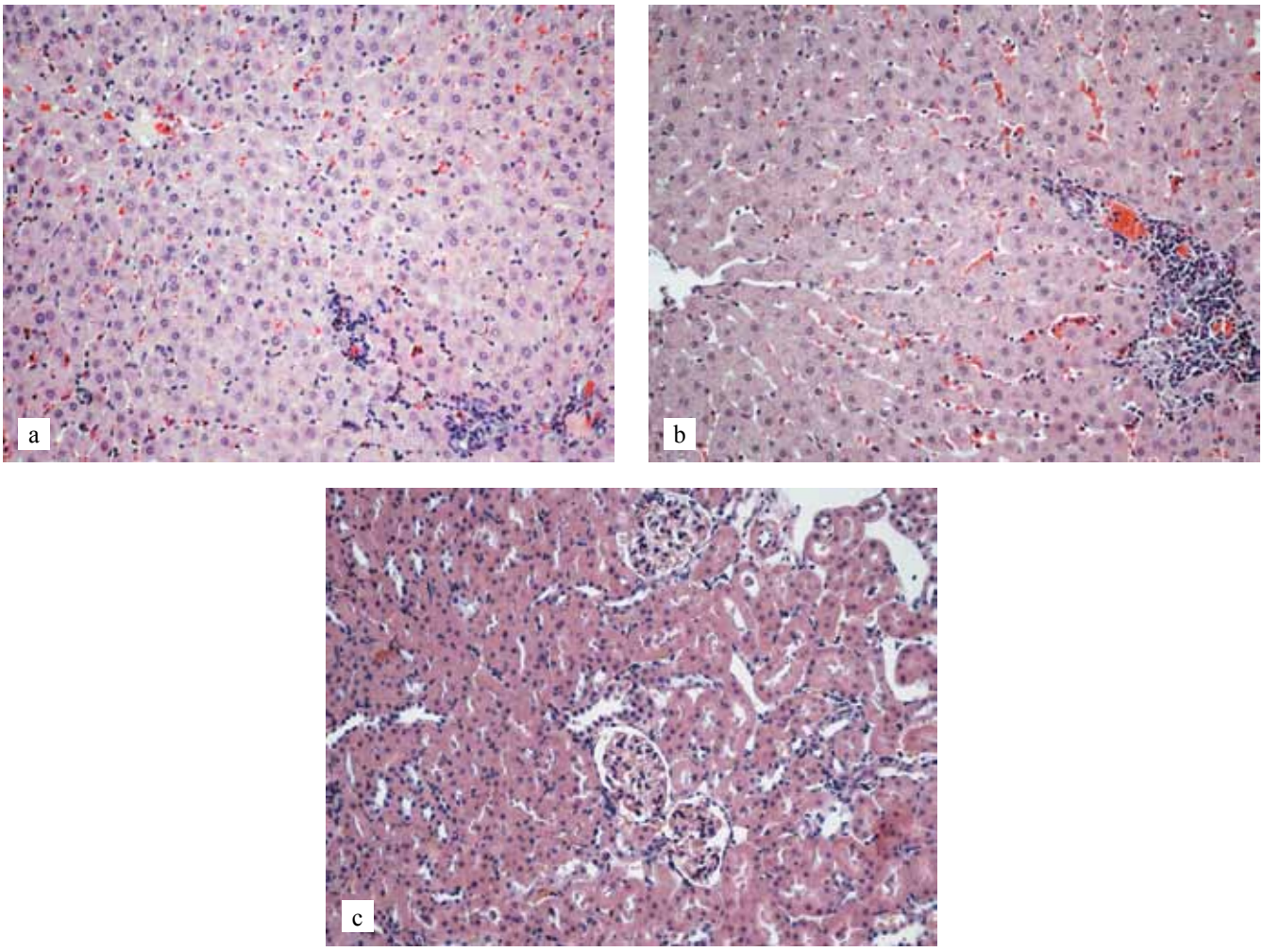

Fig. 4. Histological structure of liver tissue (a, b) and kidney (c) at different periods after a-BM-MNC injection (group 3). a, 36 hours; b, 48 hours; c, 48 hours; H&E stain, 200× magnification. a, b, pronounced infiltration of mononuclear cells in the liver; c, no cellular infiltration in the kidney tissue

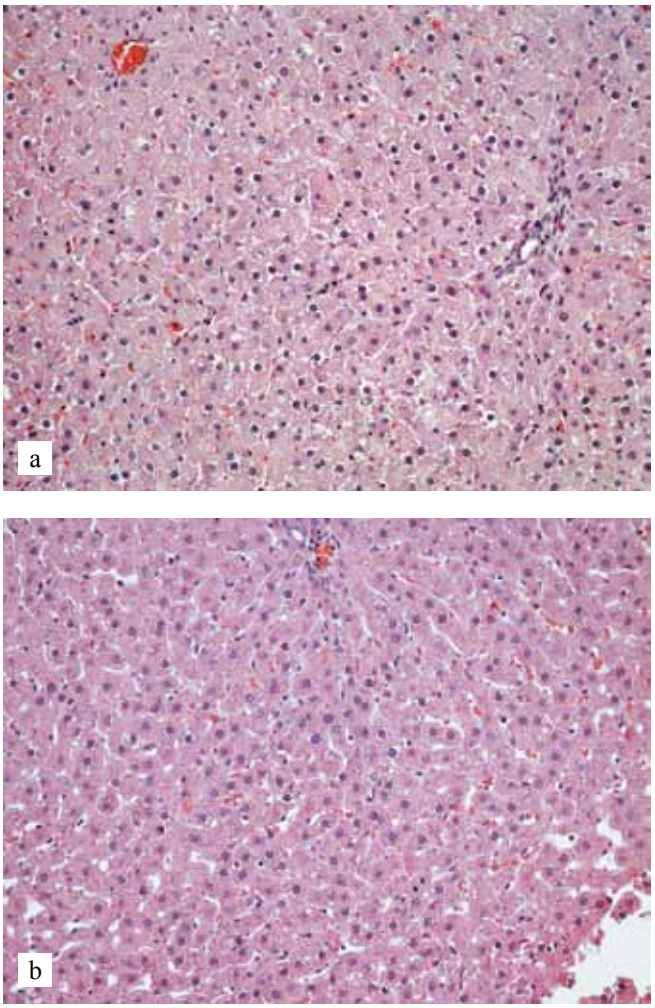

Fig. 5. Histological structure of liver tissue (a, b) at different periods after a-BM-MNC injection (group 3). a, 24 hours; b, 72 hours; H&E stain, 200× magnification. a, b, there is practically no infiltration of mononuclear cells in the liver

predominated among the inflammation cells, abundantly filling the lumen of sinusoids. In 24 and 72 hours after administration of a-BM-MNCs stored in ion-balanced Custodiol solution, there were no effects in the livers of recipients determined at the light-optical level, and the histological pattern of the liver parenchyma, in general, did not differ from that of the intact animal (Fig. 5, a, b), which in our opinion is evidence of the pulse nature of the regulatory effect of a-BM-MNCs on regenerative processes. The absence of cellular infiltration in the recipient kidneys at all time points studied after BM-MNC injection confirms the targeted (tissue-specific) nature of the regulatory effect of freshly isolated BM-MNCs and apoptotic BM-MNCs.

From earlier studies [35], it is known that apoptosis-induced mononuclear cells have not proinflammatory but immunomodulatory effects, releasing immune mediators into the blood directly or indirectly through activation of macrophages and dendritic cells. Administration of apoptotic cells has also been shown to attenuate inflammatory responses after their use, including in the liver in fulminant hepatitis [22], by enhancing the production of anti-inflammatory cytokines (TGF-β, IL-10) by macrophages and inhibiting proinflammatory cytokine production (TGF-β, TNF-α) in the body [20, 21, 36]. In addition, the existence of a relationship between progressive proinflammatory IL-1β/TNF-α-dependent liver damage [37, 38] and reduced ability of liver cells to autophagy, as well as the existence of the possibility of increasing the efficiency of the regenerative process in the liver due to medication activation of autophagy processes in it [30, 31, 39, 40] have all been proven.

CONCLUSION

From the results obtained, the following conclusions are made:

- Incubation of BM-MNCs in PBS and in ion-balanced Custodiol (NTC) solution for 48 hours at t = 4–6 °C optimizes accumulation of a-BM-MNCs in an early apoptosis state;
- Apoptosis-induced and intact BM-MNCs in the adoptive transfer model at early stages after administration do not induce mitotic activity in liver cells;
- in the adoptive transfer model, a-BM-MNCs increase the regenerative potential of liver cells by enhancing the processes of autophagy and directed infiltration of immunomodulatory (mononuclear) cells – carriers of regenerative signals;
- a-BM-MNCs retain the ability for targeted (tissue-specific) transmission of regulatory signals supported in the body by the autophagy process.

All of the above gives us grounds to believe that a-BM-MNCs, unlike intact BM-MNCs, create a stronger foundation in the body for the development and implementation of a targeted and efficient regeneration program. Particularly, after ELR, a-BM-MNCs contribute to targeted and more powerful activation of autophagy process in the liver (due to their stronger regulatory stress-induced potential), a universal mechanism for regulating adaptation processes. By enhancing autophagy, apoptotic bone marrow-derived mononuclear cells exert a more pronounced immunomodulatory effect on immunoregulatory cells, promoting their production of anti-inflammatory cytokines and formation of an effective regenerative response in the damaged liver.

The authors declare no conflict of interest.

REFERENCES

1. *Babaeva AG, Gevorkyan NM, Zotikov E*A. Rol' limfocitov v operativnom izmenenii programmy' razvitiya tkanej. M.: Izd. RAMN, 2009. 107.
2. *Babaeva AG, Tishevskaya NV, Gevorkyan NM*. O morfogeneticheskikh svojstvakh RNK limfoidnykh i stvolovykh kletok pri vosstanovitel'nykh processax. M.: Ros.

akad. nauk, Nauch.-issled. in-t morfologii cheloveka, 2016. 272.
3. *Tishevskaya NV, Babaeva AG, Gevorkyan NM*. Rol' limfocitarnykh RNK v mezhkletochnom informacionnom obmene i regulyacii regenerativnykh processov. *Ross fiziol zhurnal im. I.M. Sechenova*. 2016; 102 (11): 1280–1301.
4. *Carvalho AB Quintannilha LF, Dias AS et al*. Bone marrow multipotent mesenchymal stem cells do not reduce fibrosis or improve function in a rat model of severe chronic liver injury. *Stem Cells*. 2008; 26: 1307–1314.
5. *Dai LJ, Li HY et al*. The therapeutic potential of bone marrow-derived mesenchymal stem cells on hepatic cirrhosis. *Stem Cell Res*. 2009; 2 (1): 16–25.
6. *Hodgkinson CP, Bareja A, Gomez JA, Dzau VJ*. Emerging concepts in paracrine mechanisms in regenerative cardiovascular medicine and biology. *Circ Res*. 2016; 118: 95–107.
7. *Mansour S, Roy DC, Bouchard V et al.* COMPARE-AMI trial: comparison of intracoronary injection of CD133+ bone marrow stem cells to placebo in patients after acute myocardial infarction and left ventricular dysfunction: study rationale and design. *J Cardiovasc Transl Res*. 2010; 3: 153–159.
8. *Chen SL, Fang WW, Ye F et al.* Effect on left ventricular function of intracoronary transplantation of autologous bone marrow mesenchymal stem cell in patients with acute myocardial infarction. *Am J Cardiol*. 2004; 94: 92–95.
9. *Murry CE, Soonpaa MH, Reinecke H et al.* Haematopoietic stem cells do not transdifferentiate into cardiac myocytes in myocardial infarcts. *Nature*. 2004; 428: 664–668.
10. *Mirotsou M, Zhang Z, Deb A et al.* Secreted frizzled related protein 2 (Sfrp2) is the key Akt-mesenchymal stem cell-released paracrine factor mediating myocardial survival and repair. *Proc Natl Acad Sci*. 2007; 104: 1643–1648.
11. *Gnecchi M, Zhang Z, Ni A, Dzau VJ*. Paracrine mechanisms in adult stem cell signaling and therapy. *Circ Res*. 2008; 103: 1204–1219.
12. *Gnecchi M, Danieli P, Malpasso G, Ciuffreda MC*. Paracrine mechanisms of mesenchymal stem cells in tissue repair. *Methods Mol Biol*. 2016; 1416: 123–146.
13. *Korf-Klingebiel M, Kempf T, Sauer T et al.* Bone marrow cells are a rich source of growth factors and cytokines: implications for cell therapy trials after myocardial infarction. *Eur Heart J*. 2008; 29: 2851–2858.
14. *Fadok VA, Bratton DL, Konowal A, Freed PW, Westcott JY, Henson PM*. Macrophages that have ingested apoptotic cells *in vitro* inhibit proinflammatory cytokine production through autocrine/paracrine mechanisms involving TGF-beta, PGE2, and PAF. *J Clin Invest*. 1998; 101: 890–898.
15. *Thum T, Bauersachs J, Poole-Wilson PA, Volk HD, Anker SD*. The dying stem cell hypothesis: immune odulation as a novel mechanism for progenitor cell therapy in cardiac muscle. *J Am Coll Cardiol*. 2005; 46: 1799–1802.
16. *Kerr JF, Wyllie AH, Currie AR*. Apoptosis: a basic biological phenomenon with wide-ranging implications in tissue kinetics. *Br J Cancer*. 1972; 26: 239–257.
17. *Stark MA, Huo Y, Burcin TL, Morris MA, Olson TS, Ley K*. Phagocytosis of apoptotic neutrophils regulates granulopoiesis via IL-23 and IL-17. *Immunity*. 2005; 22: 285–294.
18. *Erwig LP, Henson PM*. Immunological consequences of apoptotic cell phagocytosis. *Am J Pathol*. 2007; 171: 2–8.
19. *Palmer E*. Negative selection – clearing out the bad apples from the T-cell repertoire. *Nat Rev Immunol*. 2003; 3: 383–391.
20. *Ren Y, Xie Y, Jiang G et al.* Apoptotic cells protect mice against lipopolysaccharide-induced shock. J Immunol. 2008; 180: 4978–4985.
21. *Gray M, Miles K, Salter D, Gray D, Savill J*. Apoptotic cells protect mice from autoimmune inflammation by the induction of regulatory B cells. *Proc Natl Acad Sci USA*. 2007; 104: 14080–14085.
22. *Zhang M, Xu S, Han Y, Cao X*. Apoptotic cells attenuate fulminant hepatitis by priming Kupffer cells to produce interleukin-10 through membrane-bound TGF-β. *Hepatology*. 2011; 53: 306–316.
23. *Sirois I, Raymond MA, Brassard N et al.* Caspase-3-dependent export of TCTP: a novel pathway for antiapoptotic intercellular communication. *Cell Death Differ*. 2011; 18: 549–562.
24. *Huang Q, Li F, Liu X et al.* Caspase 3-mediated stimulation of tumor cell repopulation during cancer radiotherapy. *Nat Med*. 2011; 17: 860–866.
25. *Beer L, Zimmermann M, Mitterbauer A et al.* Analysis of the secretome of apoptotic peripheral blood mononuclear cells: impact of released proteins and exosomes for tissue regeneration. *Sci Rep*. 2015; 5: 16662.
26. *Ankersmit HJ, Hoetzenecker K, Dietl W et al.* Irradiated cultured apoptotic peripheral blood mononuclear cells regenerate infarcted myocardium. *Eur J Clin Invest*. 2009; 39: 445–456.
27. *Beer L, Mildner M, Gyöngyösi M, Ankersmit HJ.* Peripheral blood mononuclear cell secretome for tissue repair Apoptosis. 2016; 21: 1336–1353. doi 10.1007/s10495-016-1292-8.
28. *Yel'chaninov AV, Fatkhudinov TKh*. Regeneratsiya pecheni mlekopitayushchikh: Mezhkletochnyye vzaimodeystviya. M.: Nauka, 2020. 126.
29. *Mougel F, Bonnefoy F, Kury-Paulin S et al.* Intravenous infusion of donor apoptotic leukocytes before transplantation delays allogeneic islet graft rejection through regulatory T cells. *Diabetes Metab*. 2012; 38: 531–537.
30. *Lin CW, Chen YS, Lin CC, Chen YJ, Lee PH, Kuo PL et al.* Amiodarone as an autophagy promoter reduces liver injury and enhances liver regeneration and survival in mice after partial hepatectomy. *Sci Rep*. 2015 Oct 30; 5: 15807. doi: 10.1038/srep15807.

31. *Cheng Y, Wang B, Zhou H, Dang S, Jin M, Shi Y et al*. Autophagy is required for maintenance of liver progenitor cell functionality. *Cell Physiol Biochem*. 2015; 36 (3): 1163–1174.
32. *Gazizov IM, Gumerova AA, Kiyasov AP*. Apoptosis in regenerative histogenesis of the liver after partial hepatectomy in rats. *Genes and cells*. 2015; 10 (3): 22–26.
33. *Mongolov KhP, Plekhanov AN*. Interrelation of apoptosis and liver regeneration in hepatic insufficiency after partial hepatectomy in an experiment. *Acta Biomedica Scientifica*. 2009; 3: 203–206.
34. *Onishchenko NA, Fomenko YeV, Nikol'skaya AO, Gonikova ZZ, Shagidulin MYu, Balyasin MV i dr*. K mekhanizmu aktivatsii vosstanovitel'nykh protsessov v pecheni pri ispol'zovanii obshchey RNK kletok kostnogo mozga. *Vestnik transplantologii i iskusstvennykh organov*. 2020; XXII (3): 134–142.
35. *Saas P, Daguindau E, Perruche S.* Concise review: apoptotic cell-based therapies-rationale, preclinical results and future clinical developments. *Stem Cells*. 2016; 34 (6): 1464–1473.
36. *Notley CA, Brown MA, Wright GP, Ehrenstein MR*. Natural IgM is required for suppression of inflammatory arthritis by apoptotic cells. *J Immunol*. 2011; 186: 4967–4972.
37. *Ruart M, Chavarria L, Campreciós G, Suárez-Herrera N, Montironi C, Guixé-Muntet S et al.* Impaired endothelial autophagy promotes liver fibrosis by aggravating the oxidative stress response during acute liver injury. *J Hepatol*. 2019 Mar; 70 (3): 458–469. doi: 10.1016/j.jhep.2018.10.015.
38. *Shen Y, Malik SA, Amir M, Kumar P, Cingolani F, Wen J et al.* Decreased Hepatocyte Autophagy Leads to Synergistic IL-1β and TNF Mouse Liver Injury and Inflammation. *Hepatology*. 2020 Aug; 72 (2): 595–608. doi: 10.1002/hep.31209.
39. *Xue R, Yang J, Jia L, Zhu X, Wu J, Zhu Y, Meng Q*. Mitofusin2, as a Protective Target in the Liver, Controls the Balance of Apoptosis and Autophagy in Acute-on-Chronic Liver Failure. *Front Pharmacol*. 2019 May 31; 10: 601. doi: 10.3389/fphar.2019.00601.
40. *Lv H, Fan X, Wang L, Feng H, Ci X.* Daphnetin alleviates lipopolysaccharide/d-galactosamine-induced acute liver failure via the inhibition of NLRP3, MAPK and NF-κB, and the induction of autophagy. *Int J Biol Macromol*. 2018 Nov; 119: 240–248. doi: 10.1016/j.ijbiomac.2018.07.101.

The article was submitted to the journal on 23.07.2021

DOI: 10.15825/1995-1191-2021-4-119-131

BIOACTIVE COATING FOR TISSUE-ENGINEERED SMALL-DIAMETER VASCULAR GRAFTS

V.A. Surguchenko[1], E.A. Nemets[1], V.Yu. Belov[1, 2], V.I. Sevastianov[1]

[1] Shumakov National Medical Research Center of Transplantology and Artificial Organs, Moscow, Russian Federation

[2] Institute of Biomedical Research and Technology, Moscow, Russian Federation

Objective: to develop a method for modifying composite small-diameter porous tubular biopolymer scaffolds based on bacterial copolymer poly(3-hydroxybutyrate-co-3-hydroxyvalerate) and gelatin modified with a double-layered bioactive coating based on heparin (Hp) and platelet lysate (PL) that promote adhesion and proliferation of cell cultures. **Materials and methods.** Composite porous tubular biopolymer scaffolds with 4 mm internal diameter were made by electrospinning from a 1 : 2 (by volume) mixture of a 10% solution of poly(3-hydroxybutyrate-co-3-hydroxyvalerate) copolymer, commonly known as PHBV, and a 10% solution of gelatin, respectively, in hexafluoro-2-propanol. The structure of the scaffolds was stabilized with glutaraldehyde vapor. The scaffolds were modified with a bioactive Hp + PL-based coating. The surface morphology of the samples was analyzed using scanning electron microscopy. Biological safety of the modified scaffolds *in vitro* (hemolysis, cytotoxicity) was evaluated based on the GOST ISO 10993 standard. Interaction with cultures of human endothelial cell line (EA.hy926) and human adipose-derived mesenchymal stem cells (hADMSCs) was studied using vital dyes. **Results.** We developed a method for modifying small-diameter composite porous tubular biopolymer scaffolds obtained by electrospinning from a mixture of PHBV and gelatin modified with double-layered bioactive coating based on covalently immobilized Hp and human PL. The modified scaffold was shown to have no cytotoxicity and hemolytic activity *in vitro*. It was also demonstrated that the developed coating promotes hADMSC adhesion and proliferation on the external surface and EA.hy926 on the internal surface of the composite porous tubular biopolymer scaffolds *in vitro*. **Conclusion.** The developed coating can be used for the formation of *in vivo* tissue-engineered small-diameter vascular grafts.

Keywords: heparin, platelet lysate, biopolymer matrix, gelatin, poly(3-hydroxybutyrate-co-3-hydroxyvalerate), electrospinning, small-diameter vascular grafts, biological safety.

INTRODUCTION

Minimization of thrombosis and intimal hyperplasia processes is one of the key tasks for successful development and application of small-diameter vascular grafts (sdVGs) [1–3]. Endothelialization is considered the most preferable option for optimization of the internal surface of vascular grafts [4–6]. The monolayer of functionally active endothelium, similar to that present in native blood vessels, increases thromboresistance and long-term patency of the prosthesis due to ability of endothelial cells to synthesize a wide range of bioactive factors preventing platelet aggregation, regulating excessive proliferation, migration and contractile activity of smooth muscle cells, homeostasis, and inflammation [7–9].

In order to increase the specificity of interaction with endothelial cells (ECs), endothelial progenitor cells (EPCs) and other cell types responsible for blood vessel regeneration, as well as to achieve rapid endothelization, various approaches for modifying sdVGs surface are used [10–15]. A widely used modification method is the use of coatings based on extracellular matrix proteins, such as collagen, its partially hydrolyzed form gelatin, elastin, fibronectin [12, 14, 16] or immobilization on the surface of peptides simulating adhesion sites. The best known of the family of such synthesized compounds is RGD peptide (Arg-Gly-Asp), which repeats the adhesive fragment of the fibronectin molecule [8, 17, 18]. Incorporation of bioactive compounds, such as antibodies or growth factors, into the structure of sdVGs can help to attract EPCs and mature ECs in situ. CD34 and vascular endothelial growth factor receptor 2 (VEGFR-2, CD309) are present on the surface of circulating EPCs. CD31 and VEGFR-2 antibodies are used to bind ECs [11, 18]. Factors such as stromal cell-derived factor-1 (SDF-1) and granulocyte colony-stimulating factor (G-CSF) have been found to enhance EPC mobilization from bone marrow [11, 18–21]. Basic fibroblast growth factor (bFGF)

Corresponding author: Valentina Surguchenko. Address: 1, Shchukinskaya str., Moscow, 123182, Russian Federation. Phone: (499) 196-26-61. E-mail: valent.egorova@gmail.com

can stimulate resting ECs, causing their proliferation and organization into tubular structures [11, 22].

The most frequently used vascular endothelial growth factor (VEGF) is a cytokine that is highly specific to ECs and EPCs, activating and supporting their migration and proliferation [22–24]. One of the significant disadvantages of using growth factors, particularly VEGF, is the rapid loss of biological activity and high cost [22]. Immobilization of growth factors such as bFGF, transforming growth factor beta 2 (TGF-β2) or VEGF through the heparin-binding domain has been shown to increase resistance to denaturation and enzymatic cleavage under physiological conditions, prolonging their bioactivity [18, 25].

Heparin (HP), a glycosaminoglycan with well-studied and characterized anticoagulant properties, is also often used to functionalize biomaterials and matrices intended for contact with blood in order to increase their thromboresistance [26]. HP also plays an important role in endothelial cell adhesion and homeostasis, it improves attachment to the matrix, providing trophic and differentiation cell signaling, while inhibiting the proliferative activity of smooth muscle cells [1]. Joint immobilization of heparin and angiogenic growth factors can simultaneously suppress thrombosis and stimulate endothelization [2] At the same time, platelet lysate (PL) obtained from platelet-rich plasma (PRP) can serve as a promising, accessible, and inexpensive source of growth factors (bFGF, TGF-β2, VEGF) [27–30]. PL can become an alternative to the widely used recombinant growth factors, which lead to a significant increase in the cost of the resulting products and can also provoke immunogenic reactions [29].

We have previously developed composite small-diameter porous tubular biopolymer scaffolds based on bacterial copolymer poly(3-hydroxybutyrate-co-3-hydroxyvalerate) (PHBV) and gelatin with adjustable resorption rate, possessing the necessary complex of physical and mechanical properties characteristic of native small-diameter blood vessels [31]. However, stabilization of the scaffold structure using glutaraldehyde vapor resulted in increased cytotoxicity. Taking into account both the properties of HP and the rich set of growth factors, including VEGF and bFGF contained in PL, we made an assumption that biofunctionalization of the surface of the tubular scaffolds we developed earlier by immobilizing HP in combination with a PL-based bioactive coating may help to eliminate cytotoxicity and impart adhesion to the scaffold both high hemocompatibility, including thromboresistance, and specific affinity for endothelial cell.

The aim of this work was to develop a method for modifying PHBV- and gelatin-based small-diameter composite porous tubular biopolymer scaffolds with a two-layer bioactive heparin and platelet lysate coating that promotes surface endothelization.

MATERIALS AND METHODS

Fabrication of composite porous tubular biopolymer scaffolds

Composite porous tubular biopolymer scaffolds (CPTB scaffolds) with 4 mm internal diameter were made by electrospinning from a 1:2 (by volume) mixture of 10% PHBV copolymer solution (PHBV, Sigma-Aldrich, USA) and a 10% acidic gelatin solution (Gelatin from porcine skin Type A, Sigma-Aldrich, USA) respectively in 1,1,1,3,3,3-hexafluoro-2-propanol (HFIP, P&M-Invest, Russia) on electrospinning machine NANON-01A (MECC CO, Japan) at 25 kV voltage between electrodes, 2 mL/h solution feed rate, 100 mm distance to the collector, 1000 rpm rotation speed of the substrate rod, using a 27G needle. After the end of the solution application process, the sample scaffolds were dried in the thermostat at 37 °C for 2 hours followed by vacuuming at 10–20 mmHg residual pressure and 37 °C temperature for 24 hours.

Stabilization of CPTB scaffold structure

The structure of CPTB scaffolds was stabilized with glutaraldehyde (GA) vapor in a closed container without direct contact of the samples with 25% GA solution at room temperature for 48 hours. After the fixation process, the samples were washed thoroughly in three changes of distilled water and dried for 24 hours at room temperature.

Application of the bioactive coating

Immobilization of heparin (HP) (Sigma-Aldrich, USA) was performed by incubating the CPTB scaffold samples in an aqueous anticoagulant solution with 1 mg/ml (150–200 units/ml) concentration for 2 hours at room temperature, resulting in covalent binding of HP amino groups to unreacted GA aldehyde groups. The unbound HP was removed by washing three times in distilled water. The resulting heparinized scaffolds were sterilized by gamma-irradiation at 1.5 MiRad dose.

The required volume of human platelet lysate solution (hPL, Renam, Russia) was obtained by diluting dry (lyophilized) hPL in a 1:9 ratio with Hanks' solution containing no Ca^{2+} and Mg^{2+} ions (HBSS, Gibco® by Life Technologies™, UK). The lysate solution was sterilized by filtration through a 0.22 μm membrane filter, 0.22 μm

pore size. Sterile heparinized samples were treated with hPL solution under aseptic conditions for 1 hour at 37 °C immediately before the experiment. Binding of positively charged growth factors contained in hPL to negatively charged HP was polyionic.

Surface morphology of CPTB scaffolds

The surface structure of the modified CPTB scaffold samples was analyzed using a JSM-6360LA scanning electron microscope (SEM) (JEOL, Japan) at 5 kV accelerating voltage and 100×–1000× magnification. Gold was sputtered to create a conductive coating.

Cell cultures

Cultures of mouse embryonic fibroblast cell line NIH/3T3 cells (ATCC®CRL-1658™) and human umbilical vein endothelial cell line EA.hy926 ATCC®CRL-2922™) from the ATCC (American Type Culture Collection) were stored in liquid nitrogen at –196 °C before use. After thawing, NIH/3T3 fibroblasts and EA.hy926 ECs were seeded into 25 cm^2 or 75 cm^2 standard culture vials (CELLSTAR® Greiner Bio-One, Germany) and cultured in appropriate complete growth medium DMEM, high glucose (4.5 g/L, DMEM high glucose with HEPES, PanEco, Russia) supplemented with 10% calf serum (CS, Biosera, Germany) or fetal calf serum (FCS, HyClone, USA), respectively, antibiotic and antimycotic Anti-Anti (Gibco® by Life Technologies™, UK) and 2 mM alanyl-glutamine (PanEco, Russia) in a CO_2 incubator under standard conditions: 37 °C, in a humid atmosphere containing (5 ± 1) % CO_2. Before the experiment, cells were removed from the surface of the culture plate using TrypLE™ Express Enzyme dissociation reagent (Gibco® by Life Technologies™, UK) and a suspension with the required concentration of cells was prepared.

A culture of human adipose-derived mesenchymal stem cells (hADMSCs) was obtained at the department of biomedical technologies and tissue engineering, Shumakov National Medical Research Center of Transplantology and Artificial Organs, Moscow according to the previously developed technique [32]. Prior to use, MSCs were stored in liquid nitrogen at –196 °C. After thawing, the hADMSCs were seeded into 75 cm^2 standard culture vials (CELLSTAR® Greiner Bio-One, Germany) and cultured in DMEM/F12 complete growth medium (CGM) (PanEco, Russia) with 10% fetal calf serum added (FCS, HyClone, USA), 10 μg/ml human basic fibroblast growth factor (FGF-2, Peprotech, AF-100-18B, USA), antibiotic and antimycotic Anti-Anti (Gibco® by Life Technologies™, UK), 1 mM HEPES (Gibco® by Life Technologies™, UK) and 2 mM alanyl-glutamine (PanEco, Russia) in CO_2 incubator under standard conditions: 37 °C, in a humid atmosphere containing (5 ± 1) % CO_2. Before the experiment, cells were removed from the surface of the culture plate using TrypLE™ Express Enzyme dissociating reagent (Gibco® by Life Technologies™, UK) and a suspension with the required concentration of cells was prepared. Cells of passages V–VI were used in the experiments. Various authors have shown that hADMSCs are used as an independent cellular component in the development of tissue-engineered small-diameter vascular grafts [33, 34]; also, hADMSCs maintain viability of ECs and promote vascularization of tissue-engineered small-diameter vascular constructs in vivo [35], which was the reason for using this cell culture in our work.

The initial number of cells in the suspension was determined on an automated cell counter (TC20™ Automated Cell Counter, BIORAD, Singapore) with simultaneous viability analysis by trypan blue dye exclusion (BIORAD, #145-0013, Singapore).

Hemolysis

The hemolytic action of the modified CPTB scaffolds was investigated on extracts from samples using rabbit red blood cell mass according to interstate standard GOST ISO 10993-4-2011 [36]. The extracts were prepared according to GOST ISO 10993-1-2011 guidelines [37]. A 0.9% sodium chloride solution was used as the extractant (model medium), the extraction time was 72 hours at 37 °C. The negative control sample was 0.9% sodium chloride solution, the positive control sample causing 100% hemolysis was distilled water. Blood from three rabbits was used to evaluate the hemolytic effect of one sample.

Blood containing 3.8% sodium citrate (1:9 ratio) obtained from chinchilla rabbits in compliance with the bioethical principles of animal handling approved by the European Convention for the Protection of Vertebrate Animals used for Experimental and other Scientific Purposes (2005) and in accordance with the Rules of Laboratory Practice, approved by Order #708 of the Russian Ministry of Health on 23 August 2010 on experimental animals, centrifuged at 900 rpm for 10 minutes to obtain erythrocytic mass. A 10% suspension of erythrocytes, obtained by dilution of the washed red blood cell mass three times (1:9 with 0.9% sodium chloride solution), was added to the test extracts from the modified CPTB scaffold samples, as well as to the negative control sample and positive control sample and incubated for 1 hour at (37 ± 2) °C, then centrifuged for 20 minutes at 2000 rpm.

The supernatant was separated, and the optical density was measured using a Stat Fax 4500 spectrophotometer (Awareness Technology, USA) at 540 nm wavelength. The percentage of hemolysis was calculated using formula (1):

$$\frac{E_{op} - E_c}{E_{100}} \times 100, \quad (1)$$

where E_{op} is the optical density of the test sample, E_c is the optical density of negative control sample, E_{100} is the optical density of the sample with 100% hemolysis.

Hemolysis in all blood samples should be less than 2%.

Cytotoxicity

The cytotoxicity of the fragments of modified CPTB in vitro was assessed according to the GOST ISO 10993-5-2011 interstate standard on NIH/3T3 mouse fibroblast cell line by direct contact method [38]. The surface of a culture plate (CP, CELLSTAR® Greiner Bio-One, Germany) served as a negative control sample, while a single-element aqueous zinc standard 10 mg/ml (Sigma-Aldrich, USA) served as the positive control sample. All procedures were performed under aseptic conditions.

To study the cytotoxic effect, fibroblasts were seeded in 24-well flat-bottom culture plates (CELLSTAR® Greiner Bio-One, Germany) at a concentration of 7–12 × 10^4 cells per well and incubated for 24 hours at 37 °C in a humid atmosphere containing (5 ± 1)% CO_2, until the formation of (80 ± 10)% monolayer, after which the studied fragments of matrices were placed directly on the fibroblast monolayer surface. The culture was visually assessed using a binocular fluorescence inverted microscope Nikon Eclipse TS100 (Japan).

The metabolic activity of fibroblasts after contact with matrix fragments was assessed after 24 hours using PrestoBlue™ HS Cell Viability Reagent (Invitrogen™ by Thermo Fisher Scientific, USA) according to the protocol recommended by the manufacturer. 10% PrestoBlue™ Viability Reagent was added to the wells containing the test samples, negative control and positive control samples, after which the plate was incubated for 3 hours at 37 °C in a humid atmosphere containing (5 ± 1) % CO_2. PrestoBlue™ is a vital dye containing redox indicator resazurin. Viable proliferating cells reduce resazurin with the participation of mitochondrial dehydrogenases, cytochromes and dehydrogenases located in the cell cytoplasm to resafurin [39], resulting in a color change from indigo to pink. Changes in medium absorbance were recorded using a Spark 10M microplate reader (Tecan, Austria) with Spark Control™ Magellan V1.2.20 software at 570 nm and 600 nm wavelengths. The percentage of reduced PrestoBlue™ characterizes the metabolic activity of the cells. The relative percentage difference between the metabolic activity of cells in the negative control sample and after contact with the test samples characterizes the cytotoxicity of the test sample and is calculated by formula (2):

$$\frac{117.216 \times A_{570\ Samp.} - 80.586 \times A_{600\ Samp.}}{117.216 \times A^0_{570} - 80.586 \times A^0_{600}} \times 100\%, \quad (2)$$

where 117.216 and 80.586 are molar extinction coefficients for the oxidized form of PrestoBlue™ Vital Reagent at 600 nm and 570 nm wavelengths, respectively; $A_{570\ Samp.}$ and $A_{600\ Samp.}$ are absorbance of the test sample at 570 nm and 600 nm wavelengths, respectively; A^0_{570} and A^0_{600} are absorbance of the negative control sample at 570 nm and 600 nm wavelengths, respectively.

The results were analyzed using a grading scale of the degree of cell response after direct contact with the samples according to GOST ISO 10993-5-2011 (Table 1).

Table 1

Cell response rate

Cytotoxicity grading scale	Interpretation of result
0	No cytotoxicity
1	Mild cytotoxicity
2	Moderate cytotoxicity
3	Severe cytotoxicity

The negative control sample should correspond to response grade 0 (no cytotoxicity), while the positive control sample should correspond to response grade 3 (severe cytotoxicity, almost completely destroyed monolayer). The degree of response of the test specimen should correspond to response grade 0.

Cultivation of EA.hy926 and hADMSCs on the surface of CPTB scaffolds

Sterile samples of modified CPTB scaffolds were precut lengthwise, straightened out, placed on the bottom of a flat-bottom 24-well culture plate (CELLSTAR® Greiner Bio-One, Germany) with the appropriate side (inner or outer), and fixed with sterile silicone rings. EA.hy926 and hADMSCs were seeded under aseptic conditions on the inner and outer sides of the samples, respectively. The initial seeding density on the test samples and controls was 4×10^4 kL/cm^2 for EA.hy926 culture and 3×10^4 kL/cm^2 for hADMSCs culture. Since the test samples were obtained by electrospinning and are three-dimensional, it would be incorrect to use a two-dimensional CP surface as a control sample. In these experiments, the CP surface was used to control the morphology and adequate growth of the cell cultures under study. After seeding, 24-well

plates with the samples were cultured in a CO_2 incubator under standard conditions for 24 hours and 96 hours or 24 hours, 96 hours, and 168 hours, after which appropriate studies were performed.

Viability assessment

The Live/Dead® Viability/Cytotoxicity Kit (Molecular Probes® by Life Technologies™, USA) was used to assess the viability and visualize the number of EA.hy926 and hADMSCs on the surface of modified CPTB scaffolds according to the protocol recommended by the manufacturer. The method consists of double immunofluorescence staining, with simultaneous determination of live and dead cells by binding dyes: ethidium bromide homodimer (EthD-1) and calcein acetoxymethyl (calcein AM). EthD-1 is a marker of dead cells, penetrating the damaged plasma membrane and binding to nucleic acids, giving a bright red fluorescent glow (excitation/emission ~495 nm/~635 nm). Calcein AM penetrating into viable cells is exposed to intracellular esterases, transforming into calcein, which gives a bright green homogeneous fluorescent glow (excitation/emission ~495 nm/~515 nm). Dulbecco's phosphate-buffered saline containing 2 μM calcein AM and 4 μM EthD-1 was added to the test wells, and after 15 minutes, the staining results were visualized using a Nikon Eclipse TS100 binocular inverted fluorescence microscope (Japan) equipped with a Digital Sight DS-Vil (Nikon, Japan). Photographs of the test and control samples during cultivation of EA.hy926 and hADMSCs were taken 24 hours and 96 hours after seeding.

Assessment of metabolic activity and cell count

The metabolic activity of EA.hy926 and hADMSCs on the surface of matrix samples was assessed after 24, 96 and 168 hours using PrestoBlue™ HS Cell Viability Reagent (Invitrogen™ by Thermo Fisher Scientific, USA) according to the protocol recommended by the manufacturer. 10% of PrestoBlue™ viability reagent was added to wells containing the test samples and a cell-free control sample (CGM containing no cells), after which the plate was incubated for hours at 37 °C in a humid atmosphere containing (5 ± 1) % CO_2. Changes in media absorbance were recorded using a microplate reader as previously, described at 570 nm and 600 nm

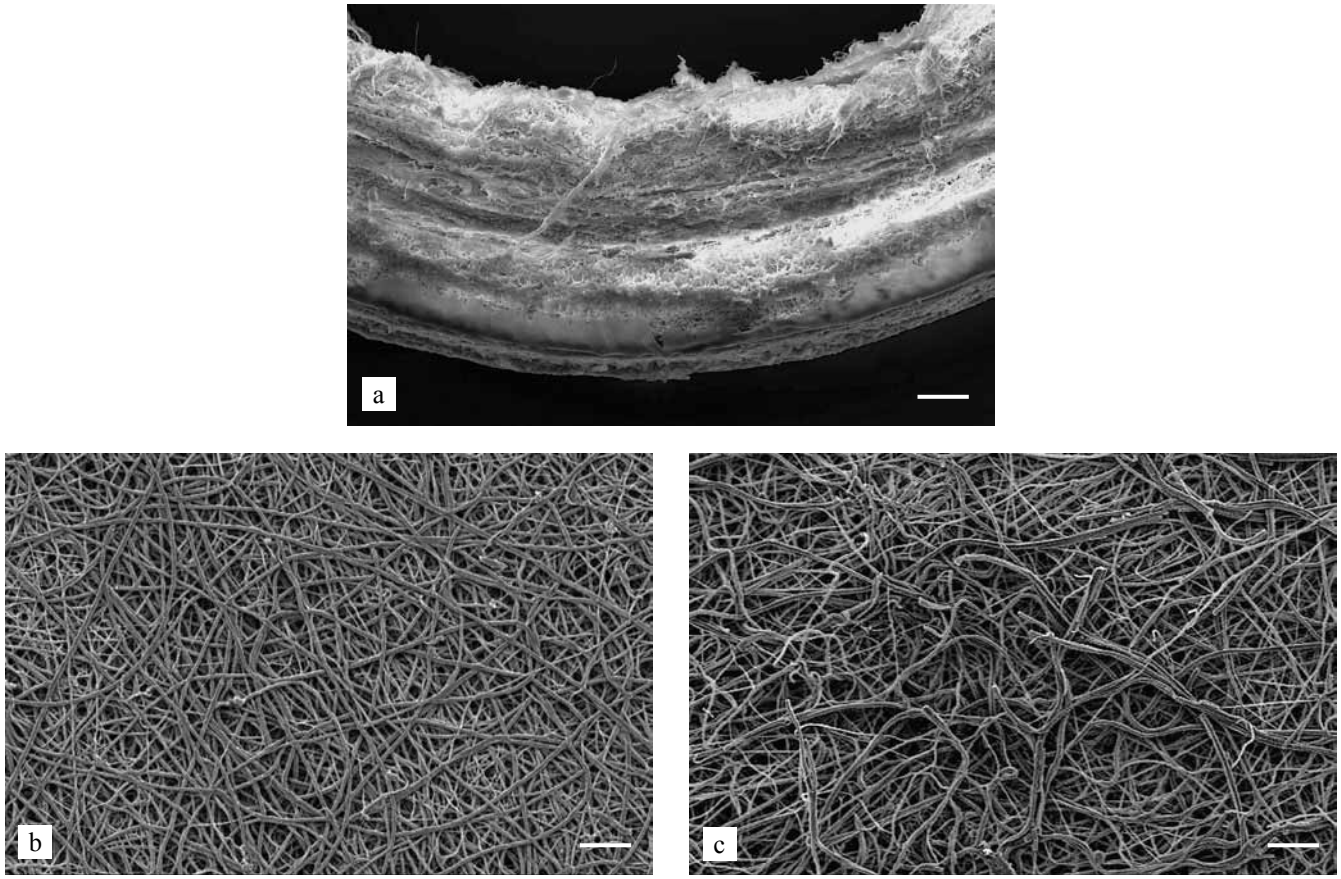

Fig. 1. Structure of CPTB scaffold modified with double-layered coating, d = 4 mm; a, cross-section (100× magnification, Bar 100 μm); b, inner surface (1000× magnification, Bar 10 μm); c, outer surface (1000× magnification, Bar 10 μm)

Table 2

Percentage of viable NIH/3T3 fibroblast cell line relative to a negative control sample after contact with the modified samples of CPTB scaffolds

Sample	% of viable cells relative to negative control sample	Cell response rate
Modified (HP)	95.55 ± 2.06	0
Modified (double-layer bioactive coating HP + hPL)	97.83 ± 1.67	0
Positive control sample	9.87 ± 0.73	3

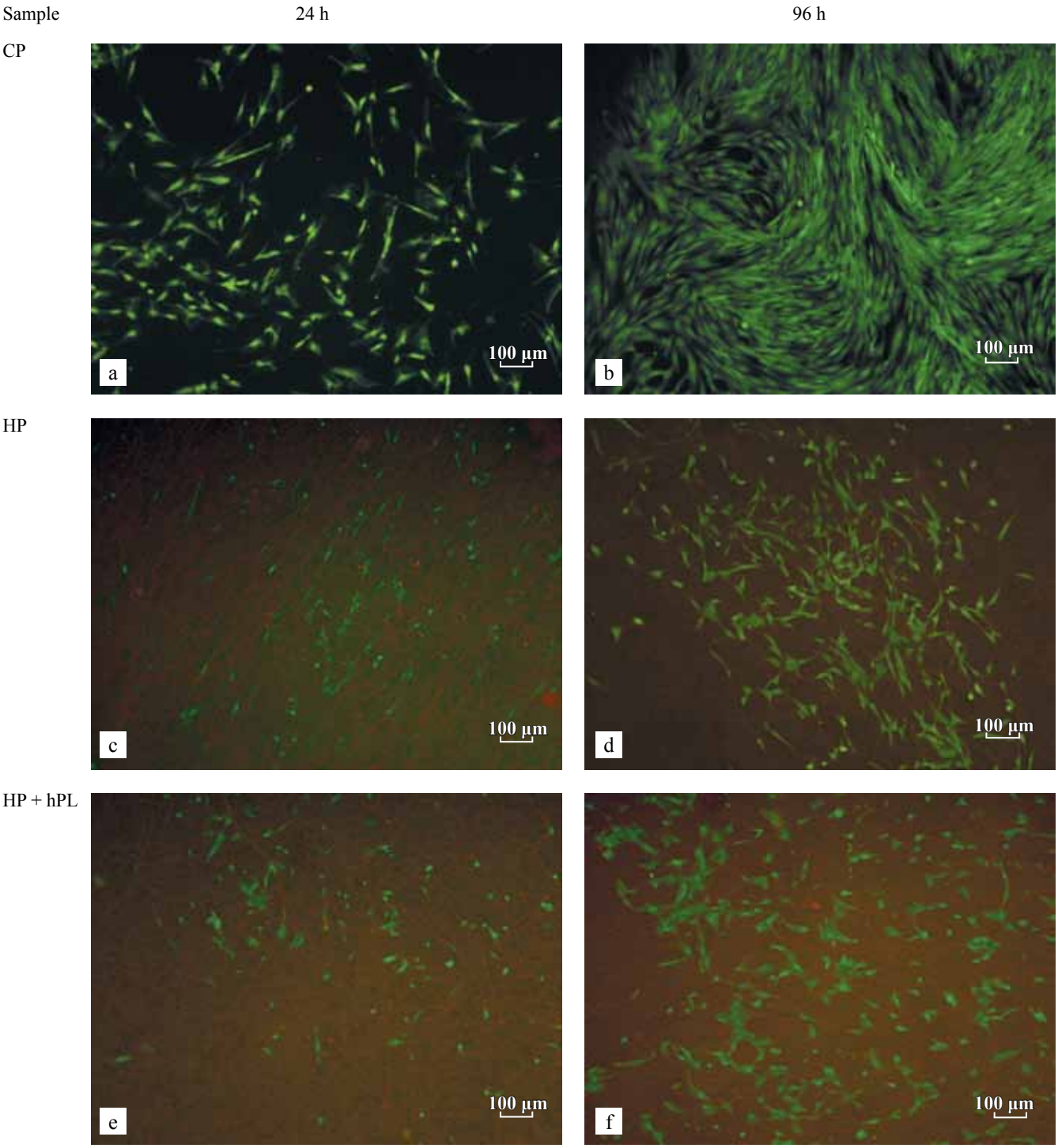

Fig. 2. hADMSCs culture (passage 6) on the outer surface of modified CPTB scaffolds; a, b, culture plate, 24 h and 96 h, respectively; c, d, scaffolds with modifying covalently immobilized HP coating, 24 h and 96 h, respectively; e, f, scaffolds with modifying human platelet lysate coating, 24 h and 96 h, respectively. Live/Dead® Viability/Cytotoxicity Kit staining. 10× magnification, Bar 100 µm

wavelengths. The percentage of reduced PrestoBlue™ characterizes the metabolic activity of cells and is calculated by formula (3):

$$\frac{117.216 \times A_{570\ Samp.} - 80.586 \times A_{600\ Samp.}}{155.677 \times A'_{600} - 14.652 \times A'_{570}} \times 100\%, \quad (3)$$

where 117.216 and 80.586 are molar extinction coefficients for the oxidized form of PrestoBlue™ Vital Reagent at 600 nm and 570 nm wavelengths, respectively; 155.677 and 14.652 are molar extinction coefficients for the reduced form of PrestoBlue™ Vital Reagent at 570 nm and 600 nm wavelengths, respectively; $A_{570\ Samp.}$ and $A_{600\ Samp.}$ are absorbance of the test sample at 570 nm and 600 nm wavelengths, respectively; A'_{570} and A'_{600} are absorbance of the cell-free control sample at 570 nm and 600 nm wavelengths, respectively.

The number of EA.hy926 and hADMSCs on the surface of scaffold samples was estimated using calibration curves, linear in semi-logarithmic coordinates to a 0.8×10^5 cell concentration in the case of EA.hy926 and 1×10^5 in the case of hADMSCs (VI passage). To construct a calibration curve, the selected cell type was seeded into flat-bottomed 24-well culture plates (CELLSTAR® Greiner Bio-One, Germany) at a seeding density of $1–20 \times 10^4$ kL/cm^2. After 24 hours, PrestoBlue™ vital reagent was added to the wells containing the required number of cells and a cell-free control sample, the plate was incubated for 3 hours at 37 °C in a humid atmosphere containing (5 ± 1) % CO_2 and changes in medium uptake were recorded. The percentage of reduced PrestoBlue™ determined by formula (3) was plotted on the graph on the Y axis, and the corresponding number of cells was plotted on the X axis.

Statistical processing

Quantitative and statistical processing of the obtained data was done using Microsoft Excel 2007. All results were presented as mean ± standard deviation. Differences were considered reliable at $p < 0.05$ with the number of samples (n) from 3 to 5.

RESULTS AND DISCUSSION

Fig. 1 shows the structure of the CPTB scaffold. The cross section (Fig. 1, a) shows a pronounced highly porous structure. The wall thickness is ~500 μm. The inner and outer layers of the scaffold (see Figs. 2, b, c) are similarly organized from disordered fibers with predominantly 0.8 to 2.0 μm thickness, 10–25 μm pore size.

Data from the performed hemolytic activity study allow us to conclude that the tested samples of modified bioactive HP and hPL coating for CPTB scaffolds have no hemolytic effect (hemolysis percentage 0.07%) and correspond to acceptable values (hemolysis percentage less than 2%), satisfying the requirements for medical products according to the GOST ISO 10993-4-2011 standard.

Table 2 shows the values characterizing the metabolic activity of the NIH-3T3 mouse fibroblasts after direct contact with samples of the modified CPTB scaffold relative to the negative (non-cytotoxic) control sample (CP). The sample has no cytotoxic effect if the metabolic activity of the fibroblasts relative to the negative control sample remains above 90%. As can be seen from Table 3, after cells come into contact with samples modified with HP or HP + hPL, the relative metabolic activity of fibroblasts is above 90%, indicating the absence of cytotoxic action. We have previously shown that PHBV- and gelatin-based CPTB scaffolds stabilized in GA vapor without additional treatment exhibit significant cytotoxicity (response rate 3) [31].

Fig. 2 shows photographs of hADMSC culture (passage VI) on the surface of CP and the outer surface of the modified CPTB scaffolds 24 and 96 hours after seeding.

After 24 hours, comparable numbers of adhered and melted hADMSCs were observed on the surface of all modified CPTB scaffolds. After 96 hours of cultivation, hADMSCs form a monolayer on the CP surface. On the test samples, the number of hADMSCs increases markedly, but does not reach the monolayer; all cells are viable and fused, which also confirms the previously obtained data that the modified samples have no cytotoxicity. Fig. 3 shows the results of hADMSCs proliferation on the outer surface of the modified CPTB scaffolds. After 24 hours, the number of hADMSCs on the outer surface of HP-modified and HP + hPL-coated samples differed only slightly ($11.8 \pm 0.6 \times 10^3$ kL and 15.1 ±

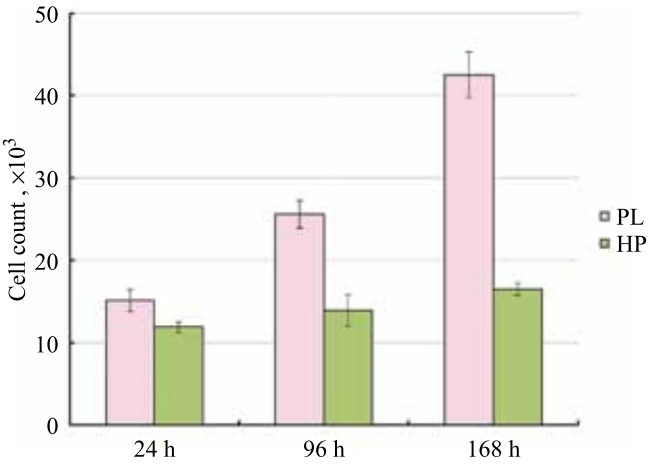

Fig. 3. hADMSCs proliferation (passage 6) on the outer surface of CPTB scaffolds modified with covalently immobilized heparin and heparin with human platelet lysate coatings

1.3×10^3 kL, respectively). By the end of the cultivation period, after 168 hours, the number of hADMSCs on the external surface of the test samples with the modifying HP + hPL-based coating increases 3-fold ($42.5 \pm 2.8 \times 10^3$ kL), while the number of hADMSCs on the external surface of heparinized matrices increases only 1.3-fold ($16.5 \pm 0.7 \times 10^3$ kL). Thus, the modifying platelet lysate-based coating promotes adhesion and proliferation of hADMSCs on the external surface of CPTB scaffolds. A modifying coating based on covalently immobilized HP alone in relation to the culture of hADMSCs promotes adhesion rather than proliferation of this cell type.

Figs. 4 and 5 show the results of the interaction of the modified inner surface of CPTB scaffolds with a

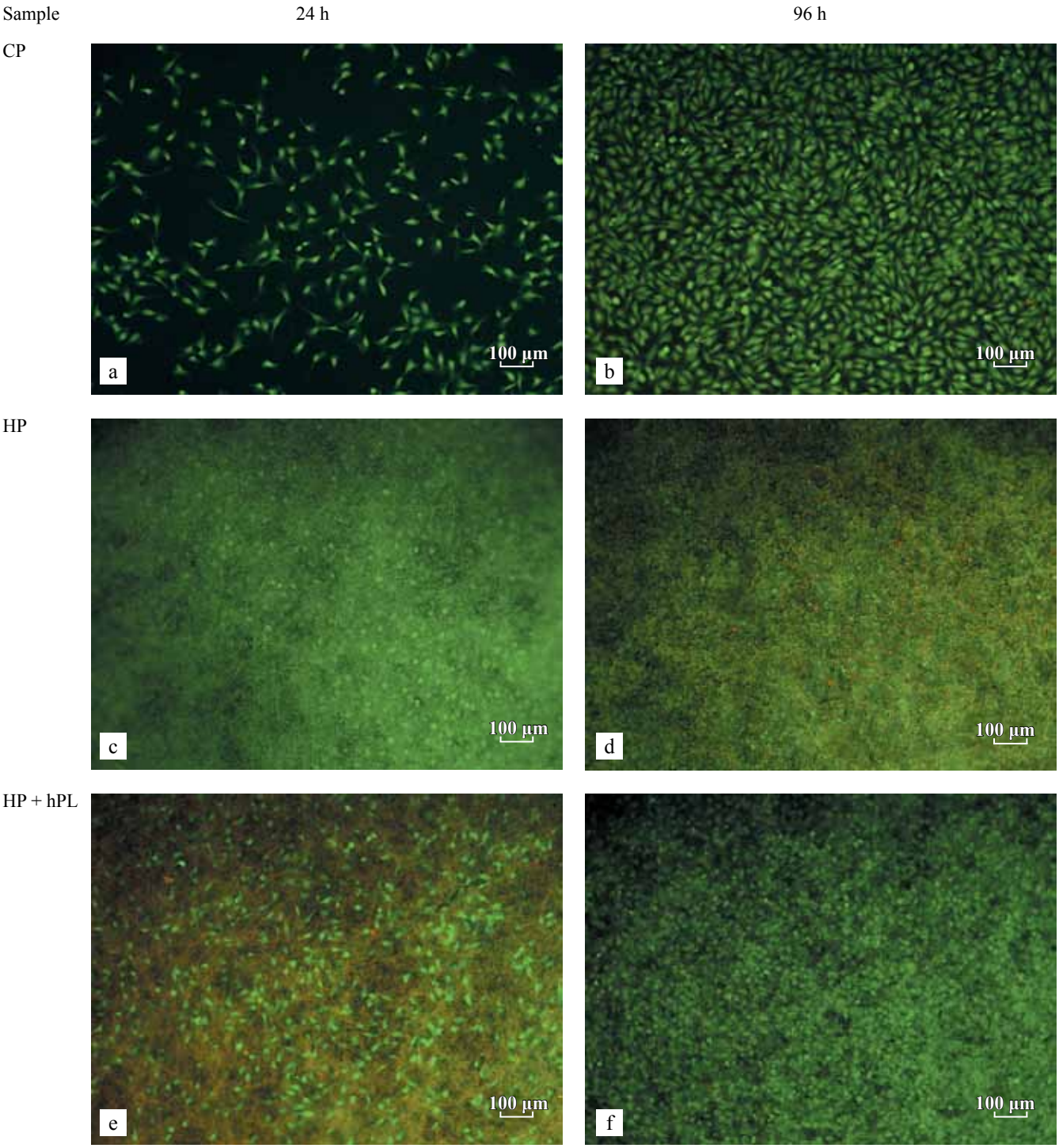

Fig. 4. EA.hy926 culture on the inner surface of modified CPTB scaffolds; a, b, culture plate, 24 h and 96 h, respectively; c, d, scaffolds with modifying covalently immobilized HP coating, 24 h and 96 h, respectively; e, f, scaffolds with modifying heparin and human platelet lysate coating, 24 h and 96 h, respectively. Live/Dead® Viability/Cytotoxicity Kit staining. 10× magnification, Bar 100 µm

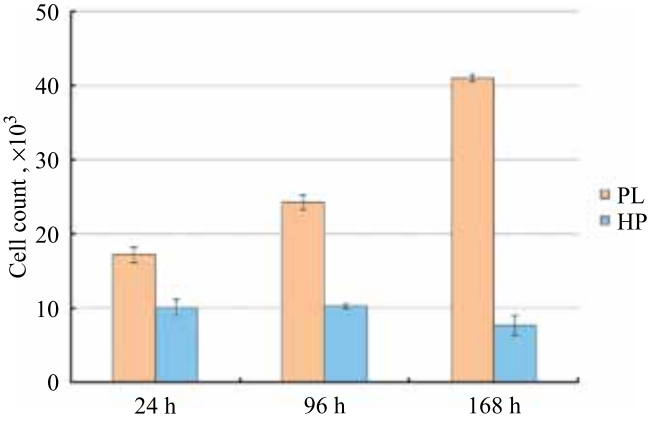

Fig. 5. EA.hy926 proliferation on the inner surface of modified CPTB scaffolds

culture of human endothelial cell line EA.hy926 24 and 96 hours after seeding. After 24 hours, a greater number of adherent and molten endothelial cells were observed on the surface of HP + hPL-modified scaffolds compared to samples modified with HP alone. After 96 hours of cultivation, no proliferation and a significant number of nonviable cells were observed in the HP-modified sample. At the same time, a monolayer of viable cells was formed on the samples modified with a two-layer coating. Note that a similar effect is observed for the CP. Fig. 5 shows that the modifying bioactive coating based on immobilized HP and hPL promotes adhesion, spreading and stimulates proliferation of EA.hy926 in vitro on the inner surface of CPTB scaffolds, due to a fairly high content of growth factors contained in platelet lysate, including VEGF: the number of ECs after 168 hours increases 2.4-fold. Our results are indirectly confirmed by data available in the literature. SM Oliveira et al. showed that PL-based nanocoating activates endothelial cells and promotes angiogenesis (microtubule formation) in the presence of sulfated polysaccharides in a three-dimensional matrix [29].

Probably, surface heparinization, under the conditions of this experiment, does not contribute to endothelialization in vitro. This, in our opinion, is due to the fact that although heparin is able to bind growth factors present in the serum component of the medium, their concentration is clearly insufficient to support endothelial cell proliferation. Despite the fact that HP plays an important role in endothelial cell adhesion and homeostasis [1], RJ Smith Jr et al. showed that when implanting cell-free prosthetic blood vessels modified with HP and with HP + VEGF into murine aorta, the samples although were completely endothelialized after 4 weeks of implantation, the composition of the prosthetic wall for samples with different coating differed significantly [40]. In the grafts modified only by HP, the endothelial and smooth muscle cell layers were not pronounced and were not formed typically for native vessels. But in the HP + VEGF-modified samples, there were clearly separated inner and middle layers, similar in structure to native vessels. and there was also a functioning endothelium. It means that modifying the prosthesis with HP alone is not sufficient to obtain an adequately functioning tissue-engineered graft.

CONCLUSION

So, for the surface of small-diameter CPTB scaffolds obtained by electrospinning from a PHBV and gelatin mixture, we developed a method of modification involving a two-layer bioactive coating based on covalently immobilized HP and hPL, whose components form polyionic complexes with HP. The modified CPTB scaffold samples were shown to have no cytotoxicity and hemolytic activity in vitro. It was also demonstrated that the developed bioactive coating promotes adhesion and proliferation of human adipose-derived mesenchymal stem cells on the outer surface of CPTB scaffolds and human umbilical vein endothelial cell on the inner surface of CPTB scaffolds in vitro.

The results obtained show that the developed coating can be used to form in vivo tissue-engineered constructs of small-diameter vascular grafts.

The authors declare no conflict of interest.

REFERENCES

1. *Matsuzaki Y, Ulziibayar A, Shoji T, Shinoka T.* Heparin-eluting tissue-engineered bioabsorbable vascular grafts. *Appl Sci.* 2021; 11: 4563–4575. https://doi.org/10.3390/app11104563.
2. *Henry JJD, Yu J, Wang A, Lee R, Fang J, Li S.* Engineering the mechanical and biological properties of nanofibrous vascular grafts for *in situ* vascular tissue engineering. *Biofabrication*. 2017; 9 (3): 035007. doi: 10.1088/1758-5090/aa834b. PMID: 28817384; PMCID: PMC5847368.
3. *Pashneh-Tala S, MacNeil S, Claeyssens F.* The Tissue-Engineered Vascular Graft-Past, Present, and Future. *Tissue Eng Part B Rev*. 2016; 22 (1): 68–100. doi: 10.1089/ten.teb.2015.0100. Epub 2015 Oct 8. PMID: 26447530; PMCID: PMC4753638.
4. *Ren X, Feng Y, Guo J, Wang H, Li Q, Yang J et al.* Surface modification and endothelialization of biomaterials as potential scaffolds for vascular tissue engineering applications. *Chem Soc Rev.* 2015; 44 (15): 5680–5742. doi: 10.1039/c4cs00483c. PMID: 26023741.
5. *Cai Q, Liao W, Xue F, Wang X, Zhou W, Li Y et al.* Selection of different endothelialization modes and different seed cells for tissue-engineered vascular graft.

Bioact Mater. 2021; 6 (8): 2557–2568. doi: 10.1016/j.bioactmat.2020.12.021. PMID: 33665496; PMCID: PMC7887299.

6. *Hasan A, Memic A, Annabi N, Hossain M, Paul A, Dokmeci MR et al.* Electrospun Scaffolds for Tissue Engineering of Vascular Grafts. *Acta Biomater.* 2014; 10 (1): 11–25. doi: 10.1016/j.actbio.2013.08.022.
7. *Smith RJ, Nasiri B, Kann J, Yergeau D, Bard JE, Swartz DD et al.* Endothelialization of arterial vascular grafts by circulating monocytes. *Nat Commun.* 2020; 11: 1622–1638. https://doi.org/10.1038/s41467-020-15361-2.
8. *Neufurth M, Wang X, Tolba E, Dorweiler B, Schröder HC, Link T et al.* Modular Small Diameter Vascular Grafts with Bioactive Functionalities. *PLoS One.* 2015; 10 (7): e0133632. doi: 10.1371/journal.pone.0133632. PMID: 26204529; PMCID: PMC4512703.
9. *Matsuzaki Y, John K, Shoji T, Shinoka T*. The evolution of tissue engineered vascular graft technologies: from preclinical trials to advancing patient care. Appl Sci (Basel). 2019; 9 (7): 1274–1295. doi: 10.3390/app9071274.
10. *Ardila DC, Liou JJ, Maestas D, Slepian MJ, Badowski M, Wagner WR et al.* Surface Modification of Electrospun Scaffolds for Endothelialization of Tissue-Engineered Vascular Grafts Using Human Cord Blood-Derived Endothelial Cells. *J Clin Med.* 2019; 8 (2): 185. doi: 10.3390/jcm8020185. PMID: 30720769; PMCID: PMC6416564.
11. *Melchiorri AJ, Hibino N, Fisher JP.* Strategies and techniques to enhance the *in situ* endothelialization of small-diameter biodegradable polymeric vascular grafts. *Tissue Eng Part B Rev.* 2013; 19 (4): 292–307. doi: 10.1089/ten.TEB.2012.0577. PMID: 23252992; PMCID: PMC3690089.
12. *Chen FM, Liu X.* Advancing biomaterials of human origin for tissue engineering. *Prog Polym Sci.* 2016 Feb 1; 53: 86–168. doi: 10.1016/j.progpolymsci.2015.02.004. PMID: 27022202; PMCID: PMC4808059.
13. *Mota C, Puppi D, Chiellini F, Chiellini E.* Additive manufacturing techniques for the production of tissue engineering constructs. *J Tissue Eng Regen Med.* 2015; 9 (3): 174–190. doi: 10.1002/term.1635. PMID: 23172792.
14. *Schmedlen RH, Elnjeirami WM, Gobin AS, West JL.* Tissue engineered vascular grafts. *Tissue engineering: principles and practices.* ed. by JP Fisher, AG Mikos, JD Bronzino, DR Peterson. 1st ed. USA: CRC Press Taylor & Francis Group; 2013: 1–9.
15. *Mallis P, Kostakis A, Stavropoulos-Giokas C, Michalopoulos E*. Future Perspectives in Small-Diameter Vascular Graft Engineering. *Bioengineering*. 2020; 7 (4): 160–200. https://doi.org/10.3390/bioengineering7040160.
16. *Han F, Jia X, Dai D, Yang X, Zhao J, Zhao Y et al.* Performance of a multilayered small-diameter vascular scaffold dual-loaded with VEGF and PDGF. *Biomaterials*. 2013; 34 (30): 7302–7313. doi: 10.1016/j.biomaterials.2013.06.006. PMID: 23830580.
17. *Kuwabara F, Narita Y, Yamawaki-Ogata A, Kanie K, Kato R, Satake M et al.* Novel small-caliber vascular grafts with trimeric peptide for acceleration of endothelialization. *Ann Thorac Surg.* 2012; 93 (1): 156–163; doi: 10.1016/j.athoracsur.2011.07.055. PMID: 22054652.
18. *Antonova LV, Silnikov VN, Khanova MYu, Koroleva LS, Serpokrilova IYu, Velikanova EA et al.* Adhesion, proliferation and viability of human umbilical vein endothelial cells cultured on the surface of biodegradable non-woven matrices modified with RGD peptides. *Russian Journal of Transplantology and Artificial Organs*. 2019; 21 (1): 142–152. (In Russ.). https://doi.org/10.15825/1995-1191-2018-1-96-109.
19. *Smith RJ, Koobatian MT, Shahini A, Swartz DD, Andreadis ST.* Capture of endothelial cells under flow using immobilized vascular endothelial growth factor. *Biomaterials*. 2015 May; 51: 303–312. doi: 10.1016/j.biomaterials.2015.02.025.
20. *Wang K, Chen X, Pan Y, Cui Y, Zhou X, Kong D et al.* Enhanced vascularization in hybrid PCL/gelatin fibrous scaffolds with sustained release of VEGF. *Biomed Res Int.* 2015; 2015: 865076. doi: 10.1155/2015/865076. PMID: 25883978; PMCID: PMC4390103.
21. *Lee KW, Johnson NR, Gao J, Wang Y.* Human progenitor cell recruitment via SDF-1α coacervate-laden PGS vascular grafts. *Biomaterials.* 2013; 34 (38): 9877–9885. doi: 10.1016/j.biomaterials.2013.08.082. PMID: 24060423; PMCID: PMC3882008.
22. *Antonova LV, Sevostyanova VV, Kutikhin AG, Velikanova EA, Matveeva VG et al.* Influence of bFGF, SDF-1α, or VEGF incorporated into tubular polymer scaffolds on the formation of small-diameter tissue-engineered blood vessel *in vivo*. *Russian Journal of Transplantology and Artificial Organs.* 2018; 20 (1): 96–109. (In Russ.). https://doi.org/10.15825/1995-1191-2018-1-96-109.
23. *Wan X, Li P, Jin X, Su F, Shen J, Yuan J.* Poly(ε-caprolactone)/keratin/heparin/VEGF biocomposite mats for vascular tissue engineering. *J Biomed Mater Res A.* 2020; 108 (2): 292–300. doi: 10.1002/jbm.a.36815. PMID: 31606923.
24. *Emechebe GA, Obiweluozor FO, Jeong IS, Park J-K, Park CH et al.* Merging 3D printing with electrospun biodegradable small-caliber vascular grafts immobilized with VEGF. *Nanomedicine: NBM* 2020; 30: 102306, https://doi.org/10.1016/j.nano.2020.102306.
25. *Spadaccio C, Nappi F, De Marco F, Sedati P, Sutherland FW, Chello M et al.* Preliminary *in vivo* evaluation of a hybrid armored vascular graft combining electrospinning and additive manufacturing techniques. *Drug Target Insights.* 2016; 10 (Suppl 1): 1–7. doi: 10.4137/DTI.S35202. PMID: 26949333; PMCID: PMC4772909.

26. *Wight TN.* Cell biology of arterial proteoglycans. *Arteriosclerosis.* 1989; 9 (1): 1–20. doi: 10.1161/01.atv.9.1.1. PMID: 2643420.
27. *Santos SCNDS, Sigurjonsson ÓE, Custódio CA, Mano JFCDL.* Blood plasma derivatives for tissue engineering and regenerative medicine therapies. *Tissue Eng Part B Rev.* 2018; 24 (6): 454–462. doi: 10.1089/ten.TEB.2018.0008. PMID: 29737237; PMCID: PMC6443031.
28. *Giusti I, D'Ascenzo S, Macchiarelli G, Dolo V. In vitro* evidence supporting applications of platelet derivatives in regenerative medicine. *Blood Transfus.* 2020; 18 (2): 117–129. doi: 10.2450/2019.0164-19. PMID: 31657710; PMCID: PMC7141937.
29. *Oliveira SM, Pirraco RP, Marques AP, Santo VE, Gomes ME, Reis RL et al.* Platelet lysate-based pro-angiogenic nanocoatings. *Acta Biomater.* 2016; 32: 129–137. doi: 10.1016/j.actbio.2015.12.028. PMID: 26708711.
30. *Shanskij YD, Sergeeva NS, Sviridova IK, Kirakozov MS, Kirsanova VA, Ahmedova SA et al.* Issledovanie lizata trombocitov cheloveka kak perspektivnoj rostovoj dobavki dlja kul'tivirovanija stvolovyh i drugih tipov kletok. *Kletochnye tehnologii v biologii i medicine.* 2013; 3: 153–158. (In Russ).
31. *Nemets EA, Belov VYu, Ilina TS, Surguchenko VA, Pankina AP, Sevastianov VI.* Composite porous tubular biopolymer matrix of small diameter. *Perspektivnye materialy.* 2018; 9: 49–59. (In Russ.). doi: 10.30791/1028-978X-2018-9-49-59.
32. *Egorova VA, Ponomareva AS, Bogdanova NB, Abramov VYu, Sevastianov VI.* Characterization of human adipose-derived stem cells phenotype by flow cytometry method. *Tehnologii zhivyh system.* 2009; 6 (5): 40–46. (In Russ.).
33. *Heydarkhan-Hagvall S, Schenke-Layland K, Yang JQ, Heydarkhan S, Xu Y, Zuk PA et al.* Human adipose stem cells: a potential cell source for cardiovascular tissue engineering. *Cells Tissues Organs.* 2008; 187 (4): 263–274. doi: 10.1159/000113407. PMID: 18196894.
34. *Zhang X, Simmons CA, Paul Santerre J.* Paracrine signalling from monocytes enables desirable extracellular matrix accumulation and temporally appropriate phenotype of vascular smooth muscle cell-like cells derived from adipose stromal cells. *Acta Biomater.* 2020; 103: 129–141. doi: 10.1016/j.actbio.2019.12.006. PMID: 31821896.
35. *Ciucurel EC, Sefton MV.* Del-1 overexpression in endothelial cells increases vascular density in tissue-engineered implants containing endothelial cells and adipose-derived mesenchymal stromal cells. *Tissue Eng Part A.* 2014; 20 (7–8): 1235–1252. doi: 10.1089/ten.TEA.2013.0242. PMID: 24151812; PMCID: PMC3993021.
36. GOST ISO 10993-4-2020 Izdelija medicinskie. Ocenka biologicheskogo dejstvija medicinskih izdelij. Chast' 4. Issledovanija izdelij, vzaimodejstvujushhih s krov'ju. Data vvedenija 2021-03-01. M.: Standartinform, 2020.
37. GOST ISO 10993-12-2011 Izdelija medicinskie. Ocenka biologicheskogo dejstvija medicinskih izdelij. Chast' 12. Prigotovlenie prob i kontrol'nye obrazcy. Data vvedenija 2013-01-01. M.: Standartinform, 2014.
38. GOST ISO 10993-5-2011 Izdelija medicinskie. Ocenka biologicheskogo dejstvija medicinskih izdelij. Chast' 5. Issledovanija na citotoksichnost': metody *in vitro*. Data vvedenija 2013-01-01. M.: Standartinform, 2014.
39. *Rampersad SN.* Multiple applications of alamar blue as an indicator of metabolic function and cellular health in cell viability bioassays. *Sensors.* 2012; 12 (9): 12347–12360. doi: 10.3390/s120912347.
40. *Smith RJ Jr, Yi T, Nasiri B, Breuer CK, Andreadis ST.* Implantation of VEGF-functionalized cell-free vascular grafts: regenerative and immunological response. *FASEB J.* 2019; 33 (4): 5089–5100. doi: 10.1096/fj.201801856R. PMID: 30629890; PMCID: PMC6436645.

The article was submitted to the journal on 8.10.2021

DOI: 10.15825/1995-1191-2021-4-132-142

COMPUTER MODELING OF DIFFERENT SHAPED PATCHES IN CLASSICAL CAROTID ENDARTERECTOMY

V.G. Borisov[1, 2], Yu.N. Zakharov[1, 2], A.N. Kazantsev[3], Yu.I. Shokin[1, 2], A.V. Evtushenko[4], L.S. Barbarash[4], P.S. Onishchenko[2, 4], K.Yu. Klyshnikov[4], E.A. Ovcharenko[4]

[1] Kemerovo State University, Kemerovo, Russian Federation
[2] Federal Research Center for Information and Computational Technologies, Novosibirsk, Russian Federation
[3] City Alexandrovskaya Hospital, St. Petersburg, Russian Federation
[4] Research Institute for Complex Problems of Cardiovascular Diseases, Kemerovo, Russian Federation

Objective: to construct geometric models of carotid bifurcation and build a computer modeling for carotid endarterectomy (CEA) operations with patches of various configurations. **Materials and methods.** The method uses reconstructed models of a healthy blood vessel obtained from a preoperative computed tomography (CT) study of the affected blood vessel of a particular patient. Flow in the vessel is simulated by computational fluid dynamics using data from the patient's ultrasonic Doppler velocimetry and CT angiography. Risk factors are assessed by hemodynamic indices at the vessel wall associated with Wall Shear Stress (WSS). **Results.** We used the proposed method to study the hemodynamic results of 10 virtual CEA operations with patches of various shapes on a reconstructed healthy artery of a particular patient. The reason for patch implantation was to ensure that the vessel lumen is not narrowed as a result of the surgery, since closing the incision without a patch can reduce the vessel lumen circumference by 4–5 mm, which adversely affects blood flow. On the other hand, too wide a patch creates aneurysmorphic deformation of the internal carotid artery (ICA) mouth, which is not optimal due to formation of a large recirculation zone. In this case, it was found that the implanted patch width of about 3 mm provides an optimal hemodynamic outcome. Deviations from this median value, both upward and downward, impair hemodynamics. The absence of a patch gives the worst of the results considered. **Conclusion:** The proposed computer modeling technique is able to provide a personalized patch selection for classical CEA with low risk of restenosis in the long-term follow-up.

Keywords: classical carotid endarterectomy, computer modeling, patch.

INTRODUCTION

Acute cerebrovascular accident due to hemodynamically significant stenosis of the internal carotid artery (ICA) is one of the main causes of death and long-term disability [1, 2].

Classical carotid endarterectomy (CEA) is one of the most common treatment options for this patient cohort [1, 2]. However, as a result of patch implantation during this intervention, local deformation of the vessel may occur, leading to changes in flow hemodynamics.

The study of hemodynamic characteristics of blood flow on the vessel wall is extremely difficult in vitro, and even more so in vivo.

Therefore, computational methods of hydrodynamics are widely used to assess hemodynamic effects in vessels of a personally-specific shape [3, 4].

The aim of the work is to identify the zones of the highest risk of restenosis in the constructed computer models during classical CEA.

MATERIALS AND METHODS

Initial mathematical modeling data

The initial geometric model of the vessel was reconstructed based on preoperative computed tomography (CT) of the affected left carotid bifurcation of a particular patient. Fig. 1 (a) shows the affected part of the vessel flow area (the carotid artery is in the foreground). The segment of the curve in Fig. 1 (a) shows the presumed position of the vessel wall beneath the atherosclerotic plaque. The dotted line marks the inner surface of the plaque in the depicted projection.

The initial flow modeling data are the results of postoperative ultrasound Doppler velocimetry (UDV) of the patient. The dependence of inlet flow velocity on time was plotted on the basis of UDV study of the common carotid artery (CCA). The ratio of flow rates through the internal carotid artery (ICA) and external carotid artery (ECA) was calculated using their cross-sectional areas

Corresponding author: Anton Kazantsev. Address: 4, Solidarity Avenue, St. Petersburg, 193312, Russian Federation. Phone: (908) 947-47-57. E-mail: dr.antonio.kazantsev@mail.ru

and time-averaged peak velocity (TAPV), which were also derived from UDV data.

Building geometric models

A reconstructed 3D model of a healthy vessel was built using SimVascular Updegrove (2016) and Salome Salome (2007) software. SimVascular was used to construct vessel segments (see Fig. 1 (b–d)). Using a Python script of our own design, these segments were then imported into Salome to build the geometric model and grids. The reconstructed 3D model of the vessel is shown in Fig. 1 (e). This model is referred to hereafter as the base model and is denoted by m0. The black line on the vessel wall in Fig. 1 (e) indicates the incision line for subsequent simulation of patch implantation.

The above script was also used to visually model the result of CEA surgery. It can be used to visually draw the incision line and the patch contours on the vessel segmentation contours (see Fig. 2). Information about the drawn lines is exported by the script to a data file as a list of patch width values at its intersections with segmentation contours. The script then uses this data to change the geometric shape of the base model, simulating the patch implantation result.

The modified models, which are the results of virtual CEA, were constructed by increasing (or decreasing) the perimeters of all model segments m0 that intersect the incision line. This allows to simulate any shape of the patch or incision closure without a patch. Perimeters were changed by scaling the segments relative to their geometric centers according to the values recorded in the data file. The default scaling factor is assumed to be equal to the value of the relative perimeter increment stored in the file, divided by 2π. For segments close to ellipses

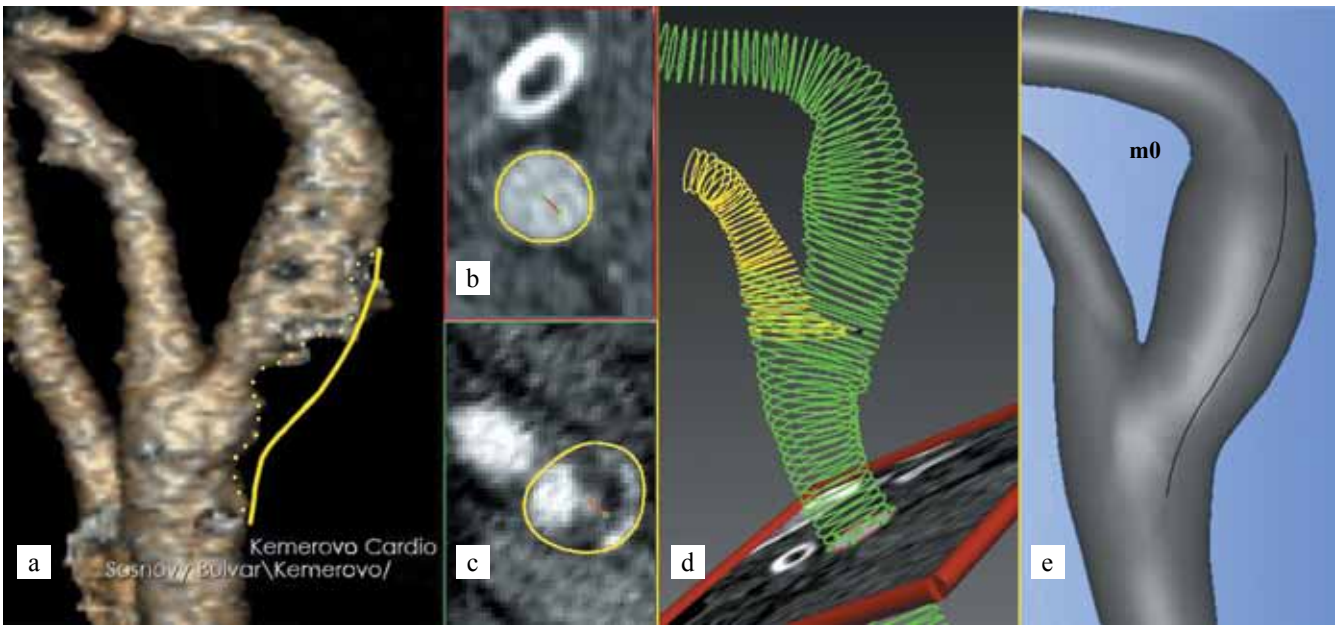

Fig. 1. CT angiography of preoperative flow area in carotid arteries (vessel in the foreground). (a) Segmentation contour in the healthy part of the CCA. (b) Segmentation contour in the affected part of the ICA near the bifurcation. (c) CCA-ICA and ECA segmentations. (d) Geometric shape of the base model m0 with an incision line (e)

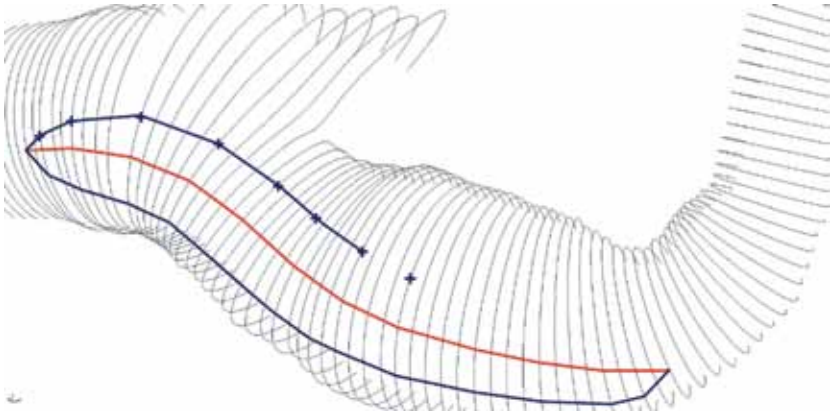

Fig. 2. The process of visual construction of the patch shape on the CCA-ICA segmentation contours

with small eccentricity, this choice is accurate enough. For irregularly shaped segments, the scaling factor can be adjusted manually if desired. Due to scaling, the upper (in Fig. 2) parts of the ICA proximal contours were shifted upwards and began to intersect with the ECA proximal contours. To correct this, a slight parallel shift of all ECA contours was performed along the major axis of the distal CCA contour. After that, a geometric model of the vessel and the computational grids on it were constructed. The grids were then exported to OpenFoam for numerical calculations.

For comparative analysis, geometric models m1–m10 were constructed using the method described above. Models m1–m9 simulate the results of CEA surgery on model m0 with p1–p9 patch implantation, respectively (Fig. 3). Model m10 (not shown in Fig. 3) simulates incision closure without patch implantation.

Data on patch shapes are given in Table 1, which contains the values of patch widths in their cross sections along the incision line. Point 0 in the "Distance..." column of the table corresponds to the proximal end of the incision line, point 3.9 to the distal end. The incision line shown in Fig. 1 (e) is the same for all models. Both its length 3.9 cm and location are same with the actual incision made during the classical CEA. The m10 model was constructed by reducing the circumference of the vessel lumen along the incision line. This is indicated by the negative values of the virtual patch width p10 in Table 1.

Note that Table 1 shows the incremental perimeter of the vessel after implantation, while the width of the patch itself before implantation should be somewhat greater.

Flow modeling

Flow velocity U and pressure p in the constructed geometric models were described using three-dimensional unsteady Navier-Stokes equations for a viscous incompressible fluid:

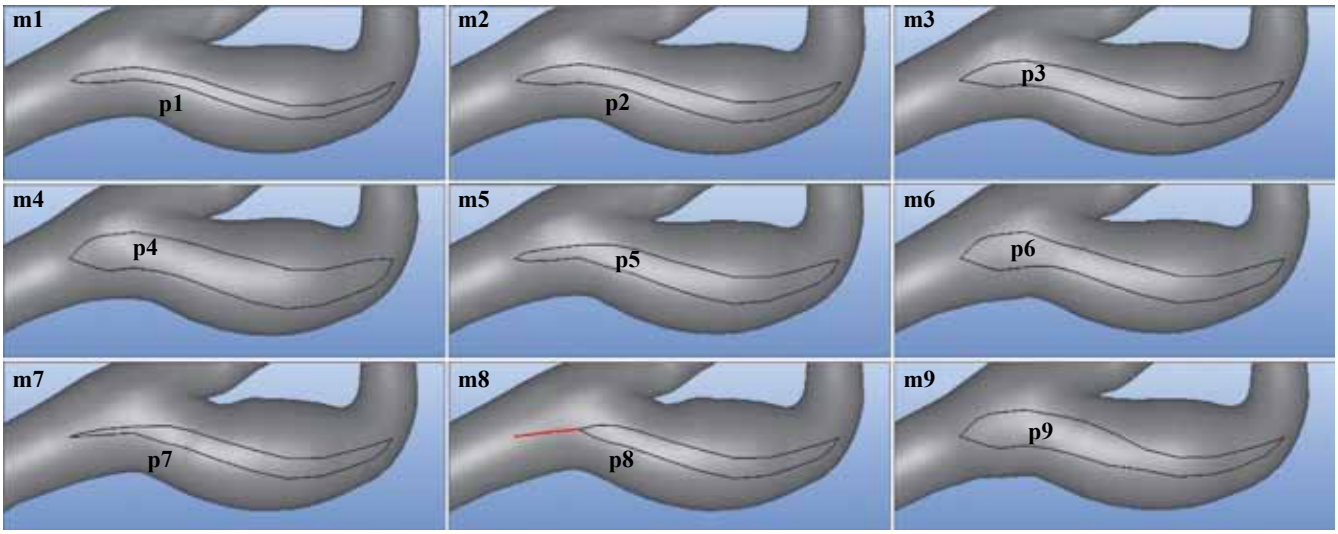

Fig. 3. Shapes of patches and vessels after virtual carotid endarterectomy

Table 1

The width (cm) of patches p1–p10 (cm) along the incision line

Distance along the cut (cm)	p1	p2	p3	p4	p5	p6	p7	p8	p9	p10
0.00	0.00	0.00	0.00	0.00	0.00	0.00	0.00	0.00	0.00	–0.00
0.29	0.12	0.16	0.19	0.34	0.13	0.35	0.05	–0.10	0.34	–0.26
0.72	0.14	0.21	0.28	0.42	0.14	0.42	0.07	0.00	0.42	–0.22
1.16	0.13	0.20	0.27	0.39	0.25	0.29	0.18	0.19	0.39	–0.22
1.59	0.14	0.20	0.27	0.40	0.27	0.27	0.20	0.20	0.38	–0.22
2.02	0.15	0.22	0.29	0.43	0.29	0.29	0.22	0.22	0.33	–0.24
2.46	0.16	0.24	0.33	0.47	0.33	0.33	0.24	0.24	0.24	–0.26
2.89	0.15	0.23	0.32	0.45	0.32	0.32	0.23	0.23	0.23	–0.26
3.32	0.13	0.20	0.27	0.39	0.27	0.27	0.20	0.20	0.20	–0.22
3.61	0.12	0.17	0.23	0.34	0.23	0.23	0.17	0.17	0.15	–0.14
3.90	0.00	0.00	0.00	0.00	0.00	0.00	0.00	0.00	0.00	0.00

$$\rho\left(\frac{\partial U}{\partial t}+(U\cdot\nabla)U\right)=-\nabla p+\nabla\tau,$$
$$\nabla U=0, \quad (1)$$

with constant density $\rho = 1050$ kg/m^3 and dynamic viscosity $\mu = 3.675 \times 10^{-3}$ Pa·s, where τ is shear stress tensor. The no-flow boundary condition was not set for U at the lateral surface of the flow area, but for parallel flow conditions at the inlet and outlet. The boundaries of the flow region were considered rigid. The initial velocity was chosen to be a constant 0.15 m/s. A periodically varying pressure difference was set as the boundary conditions for p at the inlet and outlets, which created a periodic flow corresponding to the patient's postoperative UDV data:

– T = 1.06 sec, cardiocycle period;
– Q = 6.9 mL/s, CCA volumetric flow rate;
– r = 1.72, ratio of CCA volumetric flow rate to ECA volumetric flow rate.

The method of constructing boundary conditions was as follows. First, a numerical calculation was performed in which both outputs were set to zero pressure, and a suitable pressure curve was plotted at the inlet step by step at 10 ms time intervals. During this calculation, the pressure increments at each time step were manually selected such that the resulting inlet velocity curve (see 4 (a)) corresponded to the UDV spectral envelope in the patient's CCA. Based on the results of this calculation, an *r* value was calculated that turned out to be different from the target value 1.72. Further, to correct the *r* value, a variable pressure, instead of zero, was set at the outputs. Namely, the same pressure curve was set at the ECA output as for CCA, only decreased in amplitude with coefficient $k = 0.1$ and with a slight phase lag. At the ICA output, the same pressure curve as at ECA was set, only inverted with respect to the x-axis. Thus, the ECA volumetric flow rate decreased, and ICA volumetric flow rate increased, while the CCA volumetric flow rate remained virtually unchanged. Then, with another series of auxiliary calculations, parameter *k* (and the shape of the pressure curve, if necessary) was corrected such that *Q* and *r* became close to their target values.

Numerical calculations and post-processing

Numerical calculations were performed in OpenFoam using the finite-volume method using the PISO algorithm, which along with commercial software such as Ansys Fluent, OpenFoam is a common tool for performing hydrodynamic calculations and simulating flow in blood vessels [4]. In the described preliminary numerical calculations performed to obtain a flow consistent with UDV data, coarse computational grids were used. After satisfactory results were obtained from preliminary calculations, final calculations on fine grids were carried out. The calculations yielded dynamic fields of pressure, velocity, and velocity gradient in the flow region for several cardiac cycles with time discretization in 10^{-2} s increments. Information about flow parameters and its derived characteristics was extracted from the calculation results by post-processing performed in ParaView Ayachit.

To verify these results, we investigated their independence on mesh pitch. It was found that the results do not change significantly when grids with a number of nodes greater than 5×10^5 are used. The grid cell size on the lateral surface was set equal to half the size of the cell inside the computational domain. This was done to increase the accuracy of calculation of hemodynamic indices, which are expressed through the velocity gradient on the vessel wall. Stabilization of periodic oscillations was also studied. As it turned out, the process of pulse oscillations can be considered stable starting from the second cardiac cycle [5]. In this connection, it is further assumed that time t = 0 corresponds to the beginning of the systolic increase in flow velocity in the second cardiac cycle.

Parietal shear stress and hemodynamic indices

The wall shear stress index (WSS) indicator was calculated as the tangential component t_w of shear stress tensor τ exerted on the vessel wall. The time average WSS (TAWSS), oscillatory shear stress (OSI) and relative residence time (RRT) indices were calculated according to formulas (2) through the averaged t_w value for one cardiac cycle [24]:

$$TAWSS=\frac{1}{T}\int_0^T\tau_w\,dt, \quad OSI=\frac{1}{2}\cdot\left(1-\frac{\left|\int_0^T\tau_w\,dt\right|}{\int_0^T|\tau_w|\,dt}\right),$$
$$RRT=\frac{T}{(1-2\cdot OSI)\cdot\int_0^T|\tau_w|\,dt}. \quad (2)$$

Here *T* is cardiac cycle duration, and $|t_w|$ is the Euclidean norm of vector t_w. To quantitatively compare the indices in some zone σ on the vessel wall, their average values were calculated according to the formulas:

$$RRT_\sigma=\frac{1}{s}\int_\sigma RRT\,d\sigma, \quad OSI_\sigma=\frac{1}{s}\int_\sigma OSI\,d\sigma,$$
$$TAWSS_\sigma=\frac{1}{s}\int_\sigma|TAWSS|\,d\sigma, \quad (3)$$

where S is the area of the zone σ. We also used the dimensionless mean I_RRT and logarithmic maximum M_RRT values of the RRT index for the zone σ, which were calculated using the formulas:

$$I\_RRT = TAWSS_{CCA} \cdot RRT_{\sigma},$$
$$M\_RRT = \max_{\sigma}(\ln(RRT \cdot TAWSS_{CCA} + 1)). \quad (4)$$

Here, $TAWSS_{CCA}$ is the averaged TAWSS value in the cylindrical part of the CCA at a distance of three CCA radii from the branching point of the vessel [24].

The TAWSS < 0.4 Pa and OSI > 0.3 inequalities given in Harrison (2014) [6] were used to assess pathological RRT values. In this case, formula (2) gives the corresponding critical value of RRT = 6.25 Pa^{-1}. Further, RRT values exceeding the critical value will be considered pathological.

RESULTS

Basic model flow results

The results of velocity field and hemodynamic calculations for baseline model *m*0 were analyzed. Fig. 4 shows some visualizations for the following parameter values: T = 1.06 s, Q = 6.9 mL/s, r = 1.72. Fig. 4 (a) shows a plot of the velocity vector modulus at the center of the CCA proximal cross section.

Table 2

Flow parameters T (s), Q (mL/s), r (dimensionless) in calculations a–d

	T	Q	r
a	1.06	6.90	1.72
b	1.06	6.00	1.78
c	0.7	7.76	1.77
d	0.8	10.65	1.72

Fig. 4 (b–d) respectively shows the current lines at time points t = 0.06 s, 0.14 s, and 0.6 s, which are marked with dots in Fig. 4 (a). The color changes along the current line reflect the velocity of the blood particles according to the scale provided.

We also studied the effect of pulse frequency and amplitude on distribution of hemodynamic indices on the vessel wall in the area of its atherosclerotic lesion. Table 2 shows the values of T, Q, and r for the four calculation variants, designated by letters a–d.

Fig. 5 (a–d) shows the RRT level lines on a selected section of the vessel wall corresponding to the same-name parameter sets from Table 2. Level 0 lines correspond to the critical value of RRT = 6.25 Pa^{-1}. Level 1–3 lines correspond to RRT values 2, 4 and 8 times greater, respectively, than the critical value. The color indicates the ln(RRT + 1) value between 0 and 8 according to the supplied scale. Fig. 7 shows the location of the selected site on the vessel wall. Fig. 5 (a–d) demonstrates that there is no significant qualitative change in the distribution of the RRT parameter when the flow parameters given in Table 2 are varied.

Fig. 6 shows a slightly enlarged view of the area of local maximums of the RRT index from Fig. 5 (a) in combination with the phase portrait of the TAWSS vector field.

The arrows in the figure indicate the local direction of the TAWSS field; the color reflects the ln(RRT + 1) value in the range [0, 8]. The black dots are fixed points of the TAWSS field, the bold lines are the separatrices of two saddle points 2 and 4, and the thin lines represent regular trajectories.

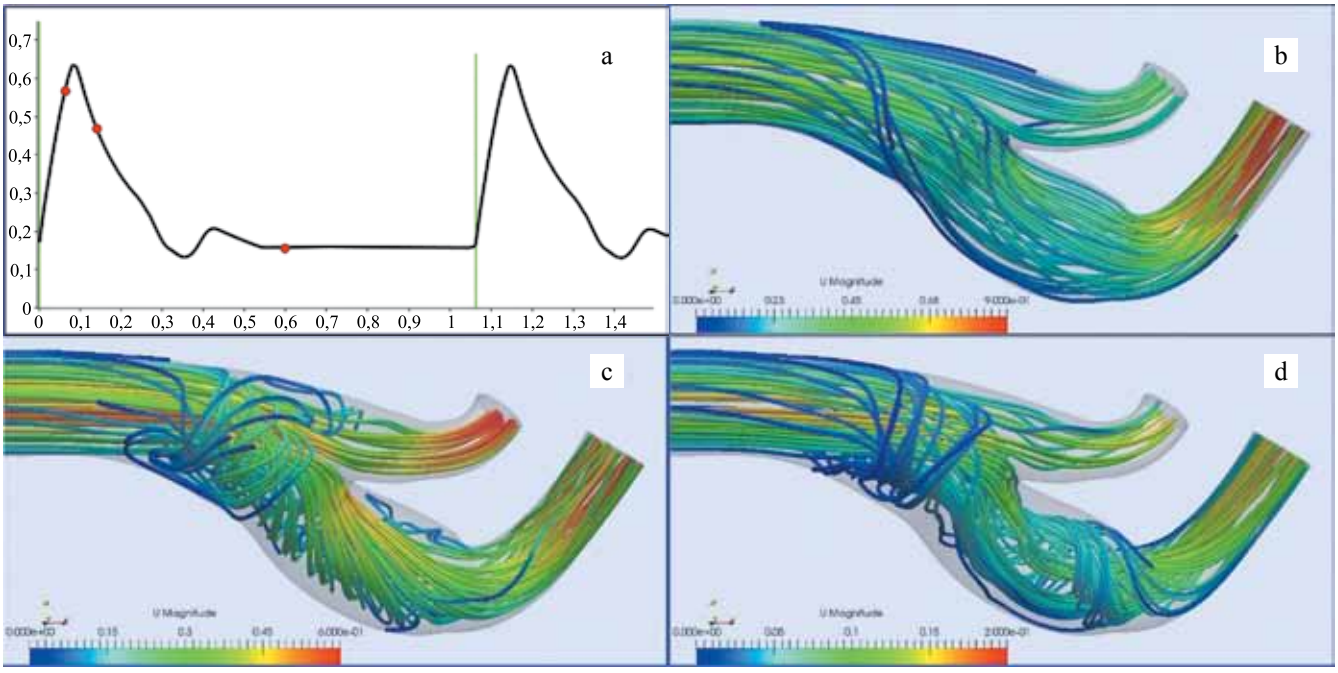

Fig. 4. Velocity plot for CCA (a). Streamlines at: t = 0.06 s (b), t = 0.14 s (c), t = 0.6 s (d)

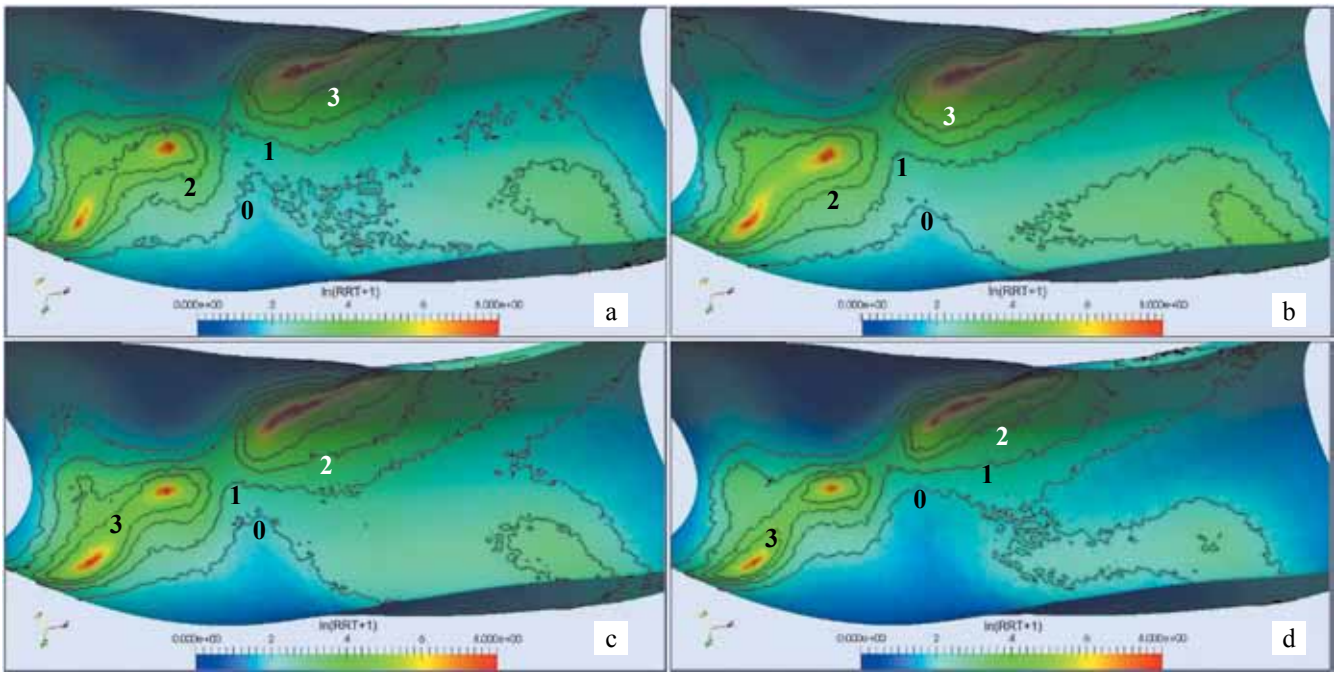

Fig. 5. RRT level lines (Pa^{-1}) and ln(RRT + 1) distribution for parameter sets a–d in Table 2

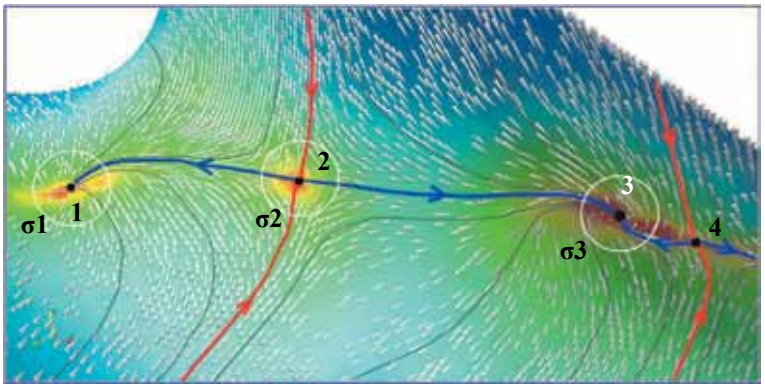

Fig. 6. Topological structure of the TAWSS field in the vicinity of its rest points (points 1–4)

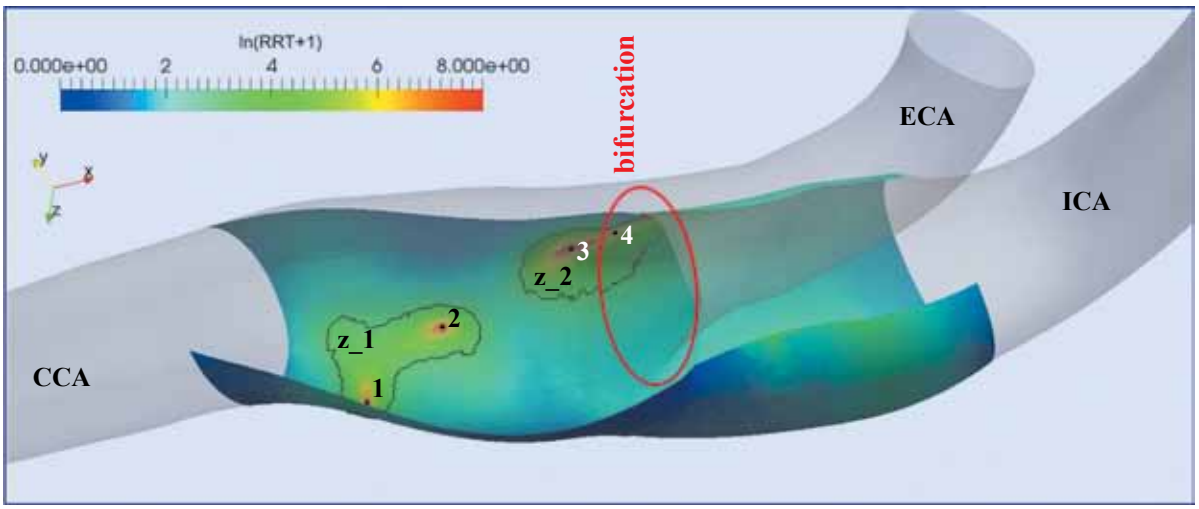

Fig. 7. z_1 and z_2 zones and stationary points 1–4 of the TAWSS field for the baseline model

Three zones σ1–σ3 (see Fig. 6) with equal areas *S* were chosen for comparative quantification of the integral RRT values. The centers of these zones are stationary points 1–3 of the TAWSS field. The average values of the indices calculated for each zone using formulas (3) are given in Table 3.

Hemodynamic indices for m0–m10 models

The results of numerical calculations with flow parameters *Q* and *r* differing by no more than 0.7% from calculation result "a" for the basic model (see Table 2) were obtained for models *m*1–*m*10. Changes in the geometric shape of the vessel caused by the virtual patch implantation causes changes (within 10%) in the calculated values of *Q* and *r* under unchanged boundary conditions. For this reason, auxiliary calculations were performed for each of the *m*1–*m*10 models in order to fit within the interval [–0.7%, 0.7%] of changes in *Q* and *r* parameters.

In order to obtain comparative quantitative characteristics of hemodynamic indices, regions were selected in each model where both criteria TAWSS < 0.4 Pa and OSI > 0.3 were simultaneously satisfied. These regions for all models consisted of two zones *z*_1 and *z*_2, the first containing stationary points 1, 2, and the second containing stationary points 3, 4 of the TAWSS field. Fig. 7 depicts these zones for the basic model. The I_RRT and M_RRT values in zones *z*_1 and *z*_2 calculated by formulas (4) for each model are shown in Table 4. The table rows show the I_RRT and M_RRT values for *m*0–*m*10 models as a percentage of the corresponding values for the baseline model m0.

Table 3

Average index values in zones

	RRT_σ (Pa^{-1})	$\ln(RRT_\sigma + 1)$	OSI_σ	$TAWSS_\sigma$ (Pa)
σ_1	287	5.66	0.409	0.047
σ_2	739	6.61	0.428	0.049
σ_3	974	6.88	0.453	0.031

Table 4

Comparison of I_RRT and M_RRT for m0–m10 models

	I_RRT_1	I_RRT_2	M_RRT_1	M_RRT_2
m0	100%	100%	100%	100%
m1	88.8%	97.8%	78.7%	98.7%
m2	78.6%	94.7%	75.9%	95.8%
m3	71.8%	92.9%	70.0%	96.1%
m4	76.1%	96.5%	74.3%	96.8%
m5	76.3%	96.8%	75.2%	98.3%
m6	75.4%	98.1%	82.5%	97.3%
m7	75.9%	97.3%	74.9%	99.8%
m8	75.7%	97.0%	74.2%	99.9%
m9	77.0%	95.7%	74.6%	98.3%
m10	82.0%	110.0%	81.9%	105.9%

DISCUSSION

Building geometric models

Our task was to reconstruct the segmentation of the original healthy vessel by computed tomography from angiography of the affected vessel. In intact vessel sections (Fig. 1 (b)), the lumen boundaries coincide with its inner wall, and segmentation in SimVascular can be performed automatically. However, in the areas of atherosclerotic lesions (Fig. 1 (c)) there is no such coincidence, so each contour was built using manual correction followed by Fourier smoothing. For example, the right side of the contour in Fig. 1 (c) was built on the outer border of the radiopaque calcified plaque. In addition, due to the limited resolution of the equipment, the vessel lumen boundary is blurred, hence, there is some scaling uncertainty when recognizing it. Therefore, the areas of some recognized cross sections were compared with the areas of the same cross sections obtained by UDV tools, a correction factor was calculated, and then all contours were scaled according to this factor. As a result, the CCA-ICA and ECA segmentations were obtained (Fig. 1 (d)), from which the baseline model *m*0 (Fig. 1 (e)) was constructed.

Flow modeling

Flow modeling was performed under the assumption that blood is a Newtonian fluid. It has long been established that non-Newtonian rheology manifests itself mainly in small-diameter vessels and capillaries. Therefore, Newtonian rheology is usually used to simulate flow in the carotid artery [7].

The assumption of a stiff vessel wall was accepted in this work for several reasons. First, a healthy carotid artery is located in a bed of elastic and pliable structures of connective and fatty tissue, within which its wall moves. With the appearance of calcified atherosclerotic plaque, pulse movements of the vessel wall in its area stop due to lack of flexibility. Plaque removal followed by patch implantation, however, does not fully restore the flexibility of the vessel wall, since the pliable surrounding structures are replaced by rigid connective tissue due to surgical trauma. Note that the absence of vascular wall movements in response to pressure changes inside the vessel from the medical point of view is the most unfavorable hemodynamic option, which was chosen in the work as the model with the worst prognosis. Secondly, the investigated sections of the vessel are much shorter than the pressure pulse wavelength. So, in the case of an elastic wall, we can assume that they expand and contract almost synchronously. Therefore, if we estimate the pulsation amplitude of the vessel diameter at 5%, the amplitude of oscillations of the peak WSS value will not exceed 15% [8]. However, for integral indices (2), this peak systolic value is averaged over the entire cardiocycle period and its effect on the indices will be

several times less. Finally, the introduction of additional input data required for calculations with a deformable wall, such as its mechanical properties and thickness into the model, require their accurate assessment. Otherwise, the assumed errors in these data may introduce uncontrollable uncertainty into the calculation results [8]. For these reasons, the assumption of wall stiffness is fairly common for the carotid artery.

Analysis of results for the m0 model

It is known that the flow in a carotid bifurcation has a complex structure; it always contains time-varying recirculation and stagnation zones [9]. In our case, the qualitative behavior of the streamlines depicted in Fig. 4 (b–d) corresponds to the published results.

To determine the probable position of atherosclerotic plaque initiation zones and their dependence on blood flow parameters, we obtained the distribution of hemodynamic indices (Fig. 5) for four calculation variants (Table 2). Fig. 5 shows that the location of the zones with high RRT values is almost independent of the changes in T and Q parameters.

Fig. 6 shows the phase portrait of the TAWSS vector field corresponding to the parameter set "a" from Table 2. In the considered area, the TAWSS field has four stationary points, marked in Fig. 6 by numbers 1–4. Points 1 and 3 are stable nodes, points 2 and 4 are saddle points (unstable). The arrows in Fig. 6 correspond to the direction of shear stress action on endothelial cells. The phase trajectories of the TAWSS field correspond to the transport pathways of blood components and chemicals along the vessel wall. Calculations performed also for the b–d parameter sets from Table 2 showed that the topological structure of the TAWSS vector field in the considered area is identical for all four a–d variants. This fact, together with the results shown in Fig. 5, allows us to conclude that changes in flow parameters have less influence on the configuration of the risk zones compared to changes in the geometric shape of the vessel.

Table 3 shows that in terms of worsening values of hemodynamic indices, the σ1–σ3 zones are arranged in the order of their numbering. Note that the location of the real atherosclerotic plaque in Fig. 1 (a), correlates with the location of risk zones σ1–σ3 in Fig. 6. Occurrence of the plaque changes the local hemodynamics, which leads to the spread of pathological areas and its further growth. Thus, it can be assumed that plaque formation in a healthy m0 vessel started from the special points of the TAWSS field. The vicinity of σ3, according to Table 3, all other things being equal, has the highest probability of pathological phenomena.

Comparative analysis of results for m0–m10 models

Comparative results of calculating I_RRT and M_RRT in z_1 and z_2 zones for all models are shown in Table 4. Zones z_1 and z_2 are the zones of the most likely occurrence of atherosclerotic phenomena; larger values of the indices in them mean a greater risk of restenosis. According to Table 1, p1–p4 patches have an approximately constant width along their entire length, except for the ends. These patches are the most commonly used by practicing surgeons, leaving the choice of patch width up to them. The world literature does not reveal any rules for the patch width in any particular case. However, the choice between patch implantation and incision closure without patch implantation is also discussed [10]. The data in Table 4 suggest that, in terms of risk of restenosis in both z_1 and z_2 zones, p3 is preferable among p1–p4 patches. The preference for using a patch before direct closure of the incision in our case is confirmed by the data in Table 4 for the m10 model simulating such an operation.

In this work, in contrast to those mentioned above, patches of unequal width were also investigated. As shown in Table 1, patches p5 and p6 were derived from patch p3 by narrowing and widening it proximally, respectively. Both variants lead to worser values in Table 4.

Patches p7 and p8 were derived from p2. The p7 patch is a p2 narrowed at its proximal end. The p8 is a p2 shortened by 0.7 cm, implanted in the incision, with direct closure of the incision in the proximal part with a 0.1 cm decrease in the vascular lumen circumference. In both cases, there was a slight improvement in the z_1 zone and deterioration in the z_2 zone compared to the p2 patch.

The p9 patch is derived from p4 by narrowing it distally, and this does not lead to any significant changes in the values in Table 4.

Thus, in our case, the best results are obtained with medium-width patches without narrowing or widening at the ends. The best option is to choose the p3 patch, and the worst option is to close the incision without a patch.

In summary, we should note the high prospect of the presented computer modeling method in personalized selection of an optimal patch for implantation into the arteriotomy. As previous studies have shown, this method makes it possible not only to calculate the deformation of hemodynamic indices in the carotid bifurcation, but also to predict the probability of restenosis development in a particular area [11–13]. In the future, the demonstrated method can become the basis for individual approach in choosing the patch size and shape, which will reduce the number of adverse cardiovascular events due to prevention of vessel lumen loss and recurrent strokes.

CONCLUSION

In the case under consideration, it was found that the width of the implanted patch, approximately equal to 3 mm, provides an optimal hemodynamic outcome. Deviations from this median value, either upward and downward, impair hemodynamics, and the absence of the patch gives the worst of the results considered. The proposed technique may assist in experimental selection of a patch.

The authors declare no conflict of interest.

REFERENCES

1. *Kazantsev AN, Tarasov RS, Burkov NN, Shabaev AR, Leader RYu, Mironov AV.* Carotid endarterectomy: three-year follow-up in a single-center registry. *Angiology and vascular surgery.* 2018; 24 (3): 101–108. [In Russ, English abstract].
2. *Kazantsev AN, Tarasov RS, Burkov NN, Volkov AN, Grachev KI, Yakhnis EYa et al.* Hospital results of percutaneous coronary intervention and carotid endarterectomy in hybrid and phased modes. *Angiology and vascular surgery.* 2019; 25 (1): 101–107. [In Russ, English abstract]. doi: 10.33529/angio2019114.
3. *Zhong L, Zhang JM, Su B et al.* Application of Patient-Specific Computational Fluid Dynamics in Coronary and Intra-Cardiac Flow Simulations: Challenges and Opportunities. *Front Physiol.* 2018; 9: 742. doi: 10.3389/fphys.2018.00742.
4. *Gijsen F, Katagiri Y, Barlis P et al.* Expert recommendations on the assessment of wall shear stress in human coronary arteries: existing methodologies, technical considerations, and clinical applications. *Eur Heart J.* 2019; 40 (41): 3421–3433. doi: 10.1093/eurheartj/ehz551.
5. *Borisov VG, Zakharov YN, Shokin YI et al.* Numerical Method for Predicting Hemodynamic Effects in Vascular Prostheses. *Numer Analys.* 2019; 12: 326–337. doi: 10.1134/S1995423919040025.
6. *Harrison GJ, How TV, Poole RJ, Brennan JA, Naik JB, Vallabhaneni SR, Fisher RK.* Closure technique after carotid endarterectomy influences local hemodynamics. *J Vasc Surg*. 2014; 60 (2): 418–427. doi: 10.1016/j.jvs.2014.01.069.
7. *Geers AJ, Morales HG, Larrabide I, Butakoff C, Bijlenga P, Frangi AF.* Wall shear stress at the initiation site of cerebral aneurysms. *Biomech Model Mechanobiol*. 2017; 16 (1): 97–115. doi: 10.1007/s10237-016-0804-3.
8. *Steinman DA.* Image-based computational fluid dynamics modeling in realistic arterial geometries. *Ann Biomed Eng.* 2002; 30 (4): 483–497. doi: 10.1114/1.1467679.
9. *Hoskins PR, Hardman D.* Three-dimensional imaging and computational modelling for estimation of wall stresses in arteries. *Br J Radiol.* 2009 Jan; 82 Spec No 1: S3–17. doi: 10.1259/bjr/96847348.
10. *Avrahami I, Raz D, Bash O.* Biomechanical Aspects of Closing Approaches in Postcarotid Endarterectomy. *Comput Math Methods Med.* 2018; 2018: 4517652. doi: 10.1155/2018/4517652.
11. *Kazantsev AN, Burkov NN, Zakharov YuN, Borisov VG, Lider RYu, Bayandin MS, Anufriev AI.* Personalized brain revascularization: a method of computer modeling of the reconstruction area for carotid endarterectomy. *Surgery.* 2020; (6): 71–75. [In Russ, English abstract]. doi: 10.17116/hirurgia202006171.
12. *Kazantsev AN, Burkov NN, Borisov VG, Zakharov YN, Sergeeva Tyu, Shabaev AR et al.* Computer modeling of hemodynamic parameters in the bifurcation of the carotid arteries after carotid endarterectomy. *Angiology and Vascular Surgery.* 2019; 25 (3): 107–112. [In Russ, English abstract]. doi: 10.33529/ANGIO2019311.
13. *Kazantsev AN, Vinogradov RA, Zakharov YN, Borisov VG, Chernyavsky MA, Kravchuk VN et al.* Prediction of restenosis after carotid endarterectomy by computer simulation. *Emergency medical care. Journal them. N.V. Sklifosovsky.* 2021; 10 (2): 401–407.doi: 10.23934/2223-9022-2021-10-2-401-407.

The article was submitted to the journal on 25.05.2020

DOI: 10.15825/1995-1191-2021-4-143-150

SURGICAL TREATMENT OF BIATRIAL MYXOMA

A.S. Ivanov, N.P. Mozheiko, G.A. Akopov, M.K. Lugovskiy, O.O. Shelest

Shumakov National Medical Research Center of Transplantology and Artificial Organs, Moscow, Russian Federation

Cardiac myxoma is a primary tumor histologically formed by multipotent subendocardial mesenchymal cells. Myxomas account for approximately 50% of all cardiac tumors in adults. Myxomas are most commonly located in the left atrium. Very rarely, myxomas can be located in several heart chambers. Only about 100 cases of patients with myxomatous lesions of both atria have been described in the literature. In this paper, we present a successful clinical case of a young patient with biatrial myxomas.

Keywords: cardiac myxoma, cardiac neoplasm, cardiac tumor, biatrial myxoma, atrial myxoma, familial myxoma, Carney complex, myxoma diagnosis, history of heart tumor surgery.

The first description of cardiac tumors was made by Italian Renaissance anatomist and surgeon Matteo Realdo Colombo. In his book "De re anatomica", published in 1559 by his pupils after his death, the following description is given: "In Cardinali Gambaro Brixiano tumorem praedurum, et ad ovi magnitudinem in sinistro cordis ventricolo Romae vidi, ubi illum in affinium gratiam dissecarem". The literal translation of the quotation reads, "In Rome I saw a solid tumor, large like an egg, in the left ventricle of Cardinal Gambaro of whom I was committed by the Pope to make autopsy.") [1].

For centuries, cardiac tumors have been incidental findings in autopsies of deceased patients. In a 1951 article reviewing 150 cases of cardiac tumors detected at autopsy, Richard Prichard wrote that the most common tumor, the myxoma, has never been diagnosed in a living patient [2].

In the same year, Goldberg and colleagues were the first to diagnose left atrial myxoma in vivo. The patient was a 3.5-year-old boy with residual weakness in the right side of the body after incoming hemiparesis. By the time of angioventriculography and tumor imaging, the patient had already undergone 4 hospitalizations. In addition to weakness in the limbs, physical examination of the patient revealed a distinct systolic murmur at the apex of the heart. Surgical treatment of the child was postponed due to high risk and waiting for completion of the tweaking of the heart-lung machine. Nevertheless, 7 months later, the child with clinical signs of pulmonary edema was operated on for emergency indications. The operation was unsuccessful, histological picture of the resected tumor was consistent with cardiac myxoma [3]. Angiocardiography was not the technique of choice for diagnosing cardiac tumors because of a number of significant drawbacks. This diagnostic procedure was performed only in large medical centers, was highly invasive, painful and inaccessible to the general population. In 1959, the first echocardiographic imaging of an intracardiac tumor was obtained, which was certainly a breakthrough in treatment, greatly simplifying the diagnosis of this disease [4]. The first successful operations to resect heart and pericardial tumors were performed on a working heart. In 1936, S. Beck resected an intrapericardial teratoma [5]. In 1951, E. Maeur reported a successful resection of an epicardial lipoma [6]. All attempts to resect tumors localized inside the heart chambers ended in the death of the patient. The most successful attempt was made in 1952 by Bahnson. The operation was performed under hypothermic conditions. The surgeon performed a right atriotomy, isolating the blood flow of the vena cava from the right atrium, which allowed to remove a large right atrial myxoma. Unfortunately, the patient died 24 days later from transfusion complications [7]. The use of a heart-lung machine was a clear breakthrough. It allowed to obtain the necessary tumor resection time under direct visual control. One of the pioneers of world cardiac surgery, Clarence Crafoord, performed the first successful tumor resection under artificial circulation. In 1954, a woman with atypical mitral stenosis was referred to him. She complained of dizziness and transient ischemic attacks, but she had preserved sinus rhythm, which surprised the professor. The patient underwent transthoracic puncture of the left atrial posterior wall with an 18-cm needle. Dr. Bjork describes his memories of the diagnostic procedure as follows: "*We got a very clear image of the myxoma fixed to the interatrial septum. During diastole, it fell downward, blocking the mitral valve opening. This case taught us how to conduct differential diagnosis of myxoma in the presence of mitral stenosis and preserved sinus rhythm*." The operation to remove

Corresponding author: Maksim Lugovskiy. Address: 1, Shchukinskaya str., Moscow, 123182, Russian Federation. Phone: (926) 590-62-05. E-mail: livertranspl@mail.ru

this myxoma was the first case of the use of a heart-lung machine in Sweden. It was performed when the patient was cooled to 28 °C, on a fibrillating heart through a left lateral thoracotomy access. After performing atriotomy, the tumor was divided into three parts and removed. The patient remained on the operating table until the next morning. Thirty-eight years later, she described her condition as excellent [8]. For a long time, surgical procedures under artificial circulation, hypothermia, on a fibrillating heart were the gold standard of cardiac surgery. Sometime after this operation, many publications on successful resections of intracardiac tumors began to appear. In the Soviet Union, the first operation to remove a right atrial myxoma under artificial circulation was performed by Soviet surgeon Ivan Kolesnikov in 1962 [9]. A little later, Yipintsoi et al. described the first case of successful removal of a biatrial myxoma, in 1967 [10].

Myxomas are the most common primary cardiac tumor in the adult patient population with about 0.0017% prevalence in the general population. Among all cardiac tumors, myxomas account for 50% in the older age group and 15% in the younger age group [11]. The peak diagnostic incidence is in the 30–40 year age group [12]. The formation usually attaches to the interatrial septum on the left atrial side (60–88%). Right atrial myxomas are 3–4 times less common (4–28%). Myxomas of several anatomical localizations account for 5% of all observations, and bi-atrial localization is only 2.5% [13]. Biatrial myxomas are usually attached by a stalk in the area of the oval fossa of the interatrial septum and grow towards the cavities of both atria [14]. Cases of localization of myxomas on the inner wall of the pulmonary artery, ventricles, vena cava, and atrio-ventricular valves have also been described in the literature [15, 16]. About 5% of patients have a familial form of the disease – multifocal tumor complex with autosomal dominant mode of inheritance. Patients in this group have an abnormal chromosomal DNA genotype. They are usually young [17]. In the familial form, there is no correlation between male and female gender. Myxomatous lesions of several chambers of the heart are significantly more common in these patients than in the sporadic form. Despite the identical histology, the recurrence rate after surgical resection in the familial form is higher, and is seen in 21 to 67% of cases. There is a familial syndrome inherited in an autosomal X-linked mode of inheritance, named after Irish physician J Aiden Carney. This complex includes recurrent myxoma of the heart, proliferative pathology of endocrine organs, skin lesions: nevi, pigmented spots, or skin myxomas. Endocrine disorders are variable, usually represented by one of the following proliferative disorders: adrenal cortical tumor, breast fibroadenoma, pituitary adenoma, thyroid tumors, Sertoli cells of the testes in men, or a combination of these [18, 19]. The diagnosis of Carney disease is most likely reliable when there are two or more diagnostic findings. Biatrial myxoma may be part of Carney disease, so a patient with this diagnosis needs consultation with an endocrinologist and a dermatologist [20].

The size of myxoma, on average, varies from 1 to 12 cm in diameter, and the mass ranges from 0.6 to 80 g. The average mass often varies between 50–60 g. The macroscopic picture of myxomas is varied. Zuckerman et al. (1999) distinguish three types of myxomas depending on the tumor shape: 1) ovoid dense formations (oval, ovoid, spherical); 2) lobular formations consisting of several large lobes; 3) villous formations (aciniform) resembling a bunch of grapes in appearance. According to the literature, myxomas are more often oval in shape with a lobular or smooth structure. The color of a tumor varies from white, yellowish to dark brown. The outside of a tumor is often covered with thrombotic masses. Tumor mobility depends on the place and area of its attachment, as well as the amount of intercellular matrix collagen in the body and stalk of the mass. Most tumors have a short, wide stalk; myxomas on a wide base are less common [21]. Histologically, myxomas are represented by mesenchymal multipotent subendocardial progenitor cells of various shapes located in isolation in the intercellular matrix containing reticular and collagen fibers, mucopolysaccharides [11]. In addition to myxoma cells, smooth muscle cells, reticulocytes and blood cells can also be found in the neoplasia. In 10% of cases, calcium deposits and glandular structures can be found in myxoma [22]. At the base of myxoma, there are vessels that connect the tumor to cardiac subendocardium [23]. Myxomas usually exhibit exophytic growth [24].

Early diagnosis of intracardiac tumors is very difficult due to the frequent absence of symptoms, or their nonspecificity [25, 26].

Findings on clinical examination of a patient with myxoma depend on the size, location, and mobility of the tumor. In biatrial myxoma, episodes of embolism by tumor fragments or by thrombotic masses layered on its surface may occur in both circulatory circuits. Small circle embolization can be accompanied by lung infarction with cough, hemoptysis and other characteristic symptoms. Patients with embolization of the large circulatory circle have neurological symptoms or may complain of muscle or joint pain in the limbs, usually of ischemic etiology. On auscultation of patients with a mobile tumor, a third heart tone may be heard, caused by the tumor striking or sliding against the atrio-ventricular valve leaflets. Large masses obstructing the lumen of the right heart can mimic the clinical picture of superior vena cava syndrome. Left atrioventricular orifice tumor obstruction is usually accompanied by the clinical picture of transient ischemic attacks, acute pulmonary edema, and can also lead to sudden cardiac death [27]. Some patients present with immunoconstitutional symptoms: fever, weight loss, obesity, weakness, myalgia and arthralgia. These symptoms are accompanied by changes

in the general blood count: erythrocytosis, leukocytosis or, conversely, hemolytic anemia, thrombocytopenia, as well as increased erythrocyte sedimentation rate, hypergammaglobulinemia. IL-6 production by tumor cells or its metastases can be the cause [28–30].

The most widespread method of detecting cardiac tumors is echocardiography, which has 100% sensitivity in diagnosing a myxoma in heart chambers. Transesophageal echocardiography provides the most accurate information on tumor size, location of tumor attachment, and mobility. Transesophageal cardiography can detect tumors that were not detected during transthoracic examination, the smallest tumors with a diameter of 1 to 3 mm [31]. Computed tomography and magnetic resonance imaging should be performed in all patients with detected cardiac tumors if possible. The data obtained helped to estimate the structure of a tumor, its density and the degree of invasion into surrounding tissues, which is important for differential diagnostics of myxoma with other cardiac tumors. Despite the fact that echocardiography has now supplanted contrast-enhanced cardiac X-ray, it is mandatory for all patients over 40 years of age to diagnose coronary lesions.

CLINICAL CASE

After a routine check-up at her place of residence, the 33-year-old patient was referred to Shumakov National Medical Research Center of Transplantology and Artificial Organs in Moscow. She led an active lifestyle, worked as a senior nurse, and had no complaints about her well-being. Physical examination and auscultation did not reveal any diagnostic findings. After echocardiography, two intracardiac tumors attached to the interatrial septum were detected. Both tumors were mobile, prolapsed into the ventricles through locally appropriate atrio-ventricular valves during cardiac diastole. Computed tomography of the chest and abdomen was performed to exclude secondary tumor genesis and to detect metastases. It showed negative results. Taking into account the mobility of the detected tumor and probability of embolization by fragments, the patient underwent urgent surgery. Before the operation, transesophageal echocardiography was performed to establish a clear localization, clarify the information on the tumor attachment site and its size (Fig. 1a and b). In this case, the tumor was localized biatrically, attached to the interatrial septum in the oval fossa. The size of the part located in the right atrium was 63 × 49 mm. The left part of the tumor was 35 × 24 mm in size. Complete median sternotomy was chosen as the surgical access to the heart. After connecting the CPB pump according to the vena cava-aorta scheme, infusion of one portion of blood cardioplegia into the aortic root according to Calafiori protocol, right atriotomy in the tumor projection was performed (Fig. 2). Part of the tumor located in the right atrium was a multilobular dark brown mass of gelatinous consistency, covered with thrombotic masses, which was attached by a 1 cm^2 stalk to the interatrial septum in the oval fossa. Due to the large size of the tumor and its consistency, we decided to resect the tumor in two stages. The first stage was a precision resection of the right tumor component with thrombotic masses. Then the interatrial septum was dissected with an arched incision 5 mm away from the stalk. Together with its part, the left tumor component was dissected (Fig. 3). After the tumor was removed, the chambers were thoroughly inspected for the remaining fragments and other foci of tumor localization. Atria and ventricles were repeatedly flushed with cold saline to prevent embolism. The main stage of the operation was completed by interatrial septum plasty with a xenogeneic pericardium patch. After removal of the clamp from the aorta, the heart restored sinus rhythm on its own. Transesophageal echocardiographic examination performed after disconnection of the CPB pump showed the absence of regurgitation on the atrio-ventricular valves and blood discharge at the level of interatrial septum. Circulatory time was 42 minutes, myocardial ischemia lasted for 28 minutes. The resected tumor masses were sent for histological study. The result corresponded to the histopathological structure of cardiac myxoma (Fig. 4). The main mass of the tumor consisted of myxoma satellite cells, inflammatory cells, and a large amount of surrounding myxomatous stroma. In the area of myxoma base, native vessels feeding the tumor were detected (Fig. 5). The right atrial myxoma was covered by thrombotic masses (Fig. 6).

The results obtained during transthoracic echocardiography corresponded to the control transesophageal study. The postoperative period was uneventful. The patient was discharged from the hospital on day 7 after operation.

Myxoma of both atria is a very rare clinical case. Currently, about 100 cases are available in the literature. The purpose of this paper is to describe our own experience with surgical treatment of a patient with myxoma of such localization. It should be noted that the frequency of embolization by tumor fragments or thrombotic masses in myxomatous lesions of the heart chambers according to the literature reaches 40% [30]. For this reason, patients with an established diagnosis should be examined as soon as possible and operated on urgently.

Multiple myxomas of the heart chambers are more often an inherited condition. If it is detected, the patient needs to consult an endocrinologist and a dermatologist. Examination of the patient's immediate family may be required to rule out any suspicion of familial myxoma.

Despite precision removal of tumor masses, recurrence rates reported for cardiac myxomas are 4% to 7% for sporadic cases and 10% to 21% for familial cases [32]. The recurrence rate is significantly higher in younger patients. Typically, tumor recurrence occurs

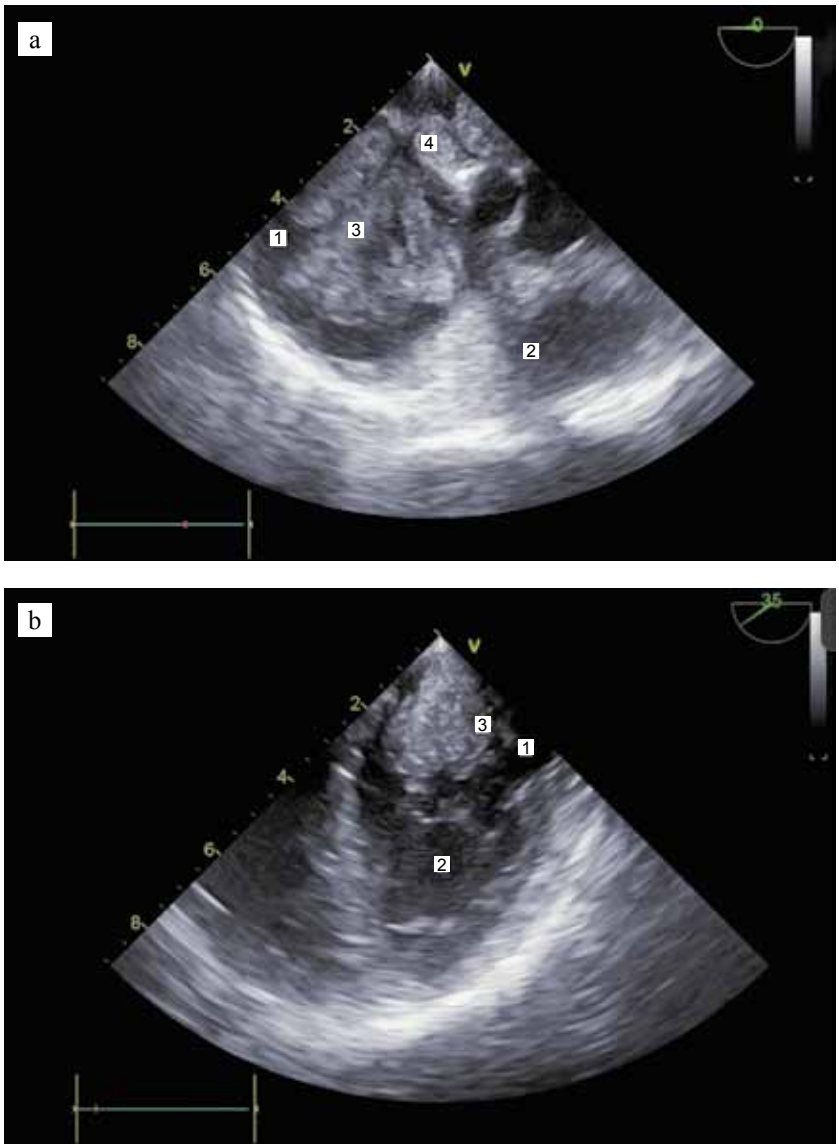

Fig. 1. Transesophageal echocardiography: a, right heart chambers (1, right atrial cavity; 2, right ventricular cavity; 3, tumor masses; 4, tumor stalk); b, left heart chambers (1, left atrial cavity; 2, left ventricular cavity; 3, tumor masses)

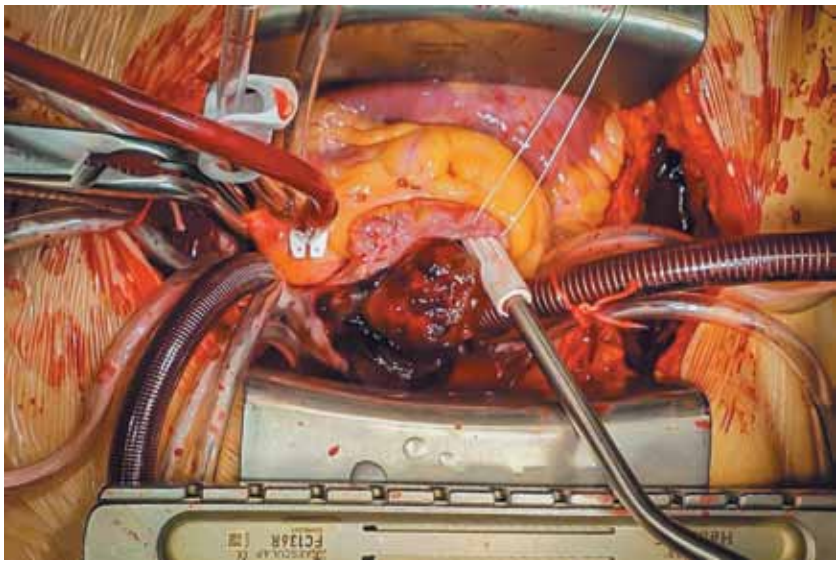

Fig. 2. Intraoperative photograph of myxomatous masses with thrombotic overlays, taken during right atriotomy

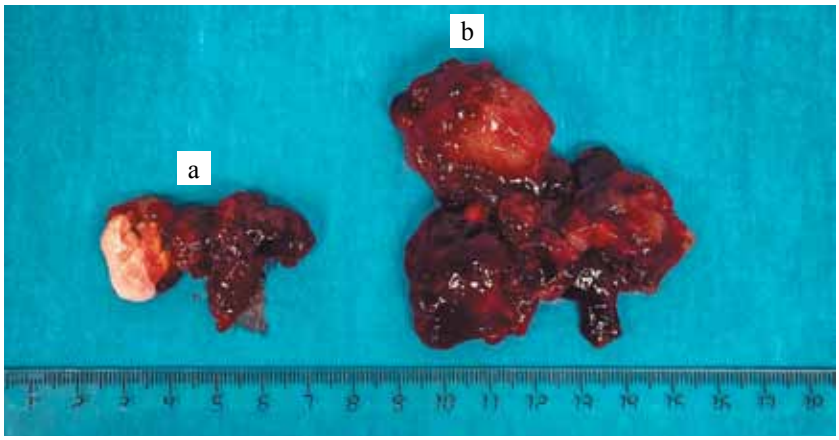

Fig. 3. Intraoperative photograph of excised fragments of the biatrial myxoma: a: left atrial fragment with pedicle; b: right atrial fragment with thrombotic masses

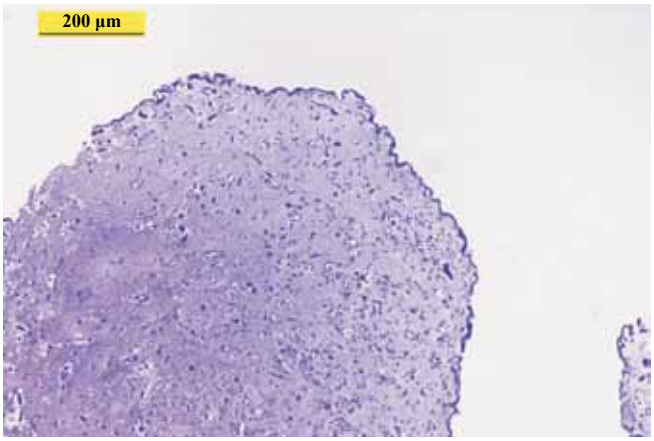

Fig. 4. Myxoma parenchyma. A papillary-type formation consisting of elongated spinous cells with large oval and spindle-shaped, fusiform hyperchromatic nuclei, as well as the surrounding myxoid matrix. Masson's trichrome stain, 200 µm scale, 20× magnification

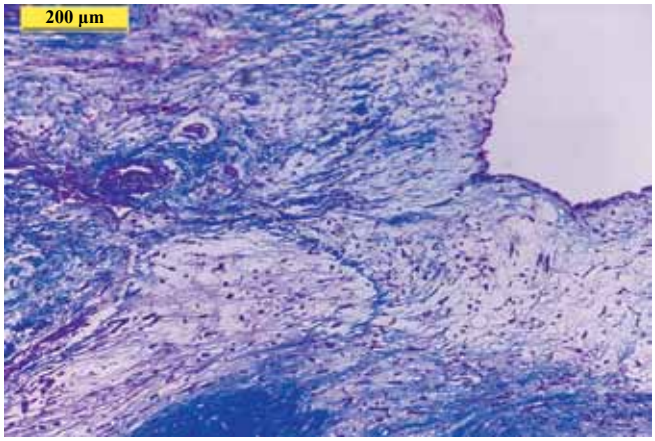

Fig. 5. Base of myxoma. Vessels surrounded by solid structures and unilayer complexes consisting of rounded, stellate, and spindle-shaped cells with weakly basophilic nuclei are seen at the base of the stalk. Scattered mononuclear cells, large focal clusters of erythrocytes, fibrin filaments with admixture of hemosiderin grains were visualized in all fields. Masson's trichrome stain, 200 µm scale, 20× magnification

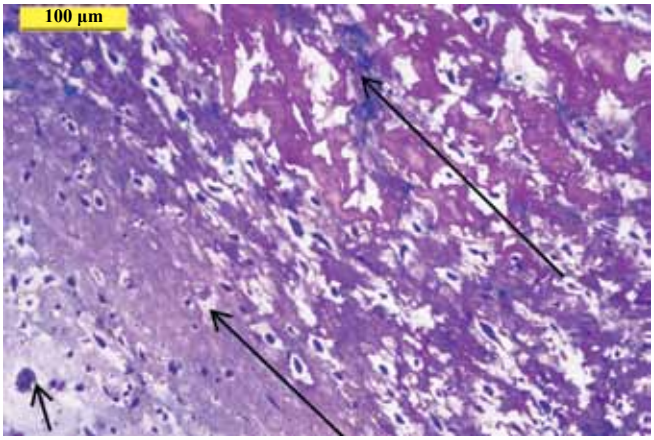

Fig. 6. Boundary of thrombus adherence to myxoma. The border of adhering thrombotic masses consisting of fibrin, unchanged and lysed red blood cells, leukocytes is traced between the arrows. Masson's trichrome stain, 100 µm scale, 40× magnification

within 5 years after the first resection surgery [33]. For these reasons, patients with cardiac myxoma of any localization should undergo periodic examination with echocardiography at least once a year in the long-term postoperative period.

The authors declare no conflict of interest.

REFERENCES

1. *Columbus M.R.* De Re Anatomica, Libri XV. Venice: N Bevilacque, 1559: 269.
2. *Prichard RW.* Tumors of the heart: review of the subject and report of 150 cases. *AMA Arch Pathol.* United States, 1951; 51 (1): 98–128 PMID 14789340.
3. *Goldberg BHP, Glenn F, Dotter CT.* Myxoma of the Left Atrium Diagnosis Made during Life with Operative and Post-mortem Findings. 2015; VI: 762–767. PMID: 12988355. doi: 10.1161/01.cir.6.5.762.

4. *Effert S, Domanig E*. Diagnosis of intra-auricular tumors & large thrombi with the aid of ultrasonic echography. *Dtsch Med Wochenschr.* Germany, 1959; 84 (1): 6–8. PMID: 13619382. doi: 10.1055/s-0028-1113531.
5. *Beck CS*. An Intrapericardial Teratoma and a Tumor of the Heart: Both Removed Operatively. *Ann Surg*. 1942; 116 (2): 161–174. PMID: 17858078. doi: 10.1097/00000658-194208000-00001.
6. *Maurer ER*. Successful removal of tumor of the heart. *J Thorac Surg.* United States, 1952; 23 (5): 479–485. PMID: 14928267.
7. *Bahnson HT, Newman EV*. Diagnosis and surgical removal of intracavitary myxoma of the right atrium. *Bull Johns Hopkins Hosp.* United States, 1953; 93 (3): 150–163. PMID: 13094264.
8. *Chitwood WR*. Clarence Crafoord and the first successful resection of a cardiac myxoma. *Ann Thorac Surg*. 1992; 54 (5): 997–998. PMID: 1417305. doi: 10.1016/0003-4975(92)90676-u.
9. *Pryhodko VP, Nyjdin MD*. Primary cardiac tumors: history of development and methods of surgical treatment. *Patologiya krovoobrashcheniya i kardiokhirurgiya*. 2011; 4: 65–70. URL: https://cyberleninka.ru/article/n/pervichnye-opuholi-serdtsa-istoriya-razvitiya-sovremennye-printsipy-i-metody-hirurgicheskogo-lecheniya.
10. *Yipintsoi T et al*. Bilateral atrial myxoma with successful removal. Report of a case. *Dis Chest*. 1967; 52 (6): 828–834. PMID: 6064988. doi: 10.1378/chest.52.6.828.
11. *Reynen K*. Cardiac myxomas. *N Engl J Med*. United States, 1995; 333 (24): 1610–1617. PMID: 7477198. doi: 10.1056/NEJM199512143332407.
12. *Carney JA*. Differences between nonfamilial and familial cardiac myxoma. *American Journal of Surgical Pathology*. 1985; 9 (1): 53–55. PMID: 3970298. doi: 10.1097/00000478-198501000-00009.
13. *Peachell JL et al*. Biatrial myxoma: A rare cardiac tumor. *Ann Thorac Surg*. 1998; 65 (6): 1768–1769. PMID: 9647099. doi: 10.1016/s0003-4975(98)00206-9.
14. *Imperio J et al*. The Distribution Patterns of Biatrial Myxomas. *Ann Thorac Surg*. The Society of Thoracic Surgeons, 1980; 29 (5): 469–473. PMID: 7377889. doi: 10.1016/s0003-4975(10)61682-7.
15. *Bortolotti U et al*. Right atrial myxoma originating from the inferior vena cava. *Ann Thorac Surg*. The Society of Thoracic Surgeons, 1990; 49 (6): 1000–1002. PMID: 2196010. doi: 10.1016/0003-4975(90)90889-e.
16. *Croti UA et al*. Right ventricle and tricuspid valve myxoma. *Brazilian J Cardiovasc Surg*. 2008; 23 (1): 142–144. PMID: 18719845. doi: 10.1590/s0102-76382008000100026.
17. *Van Gelder HM et al*. Familial cardiac myxoma. *Ann Thorac Surg*. The Society of Thoracic Surgeons, 1992; 53 (3): 419–424. PMID: 1540058. doi: 10.1016/0003-4975(92)90261-2.
18. *Havrankova E et al*. Carney complex with biatrial cardiac myxoma. *Ann Thorac Cardiovasc Surg*. 2014; 20: 890–892. PMID: 24088910. doi: 10.5761/atcs.cr.13-00121.
19. *Stratakis CA, Kirschner LS, Carney JA*. Clinical and Molecular Features of the Carney Complex: Diagnostic Criteria and Recommendations for Patient Evaluation. *J Clin Endocrinol Metab*. 2001; 86 (9): 4041–4046. PMID: 11549623. doi: 10.1210/jcem.86.9.7903.
20. *Bennett WS, Skelton TN, Lehan PH*. The complex of myxomas, pigmentation and endocrine overactivity. *Am J Cardiol*. 1990; 65 (5): 399–400. PMID: 4010501. doi: 10.1097/00005792-198507000-00007.
21. *Lygovskiy MK*. Myxomas of the heart: surgical treatment results and clinical and morphological characteristics. Federal Research Center of Tranplantology and Artificial Organs, Ministry of health of the RF. 2017: 23–24.
22. *McAllister HA Jr.* Primary tumors and cysts of the heart and pericardium. *Curr Probl Cardiol*. 1979 May; 4 (2): 1–51. PMID: 230012. doi: 10.1016/0146-2806(79)90008-2.
23. *Ferrans VJ, Pk D, Roberts WC*. Structural features of cardiac myxomas: Histology, Histochemistry, and Electron Microscopy. *Hum Pathol*. 1973 Mar; 4 (1): 111–146. PMID: 4713680. doi: 10.1016/s0046-8177(73)80051-6.
24. *Krikler DM et al*. Atrial myxoma: a tumour in search of its origins isra. *Br Heart J*. 1992; 5: 89–91. PMID: 1531423. doi: 10.1136/hrt.67.1.89.
25. *Xiao Z et al*. A Typical Bilateral Atrial Myxoma: A Case Report. *Case Reports Cardiol*. 2012; 2012 (Figure 3): 1–3. PMID: 24826252. doi: 10.1155/2012/460268.
26. *Kuon E et al.* The challenge presented by right atrial myxoma. *Herz*. 2004; 29 (7): 702–709. PMID: 15580325. doi: 10.1007/s00059-004-2571-7.
27. *Vijan V, Vupputuri A, Chandrasekharan Nair R*. An Unusual Case of Biatrial Myxoma in a Young Female. *Case Reports Cardiol*. 2016; 2016: 1–3. PMID: 26881142. doi: 10.1155/2016/3545480.
28. *Saji T et al.* Increased serum interleukin-6 in cardiac myxoma. *Am Heart J*. United States, 1991; 122 (2): 579–580. PMID: 1858647. doi: 10.1016/0002-8703(91)91022-f.
29. *Kuroki MK et al*. Increased interleukin-6 activity in cardiac myxoma with serum interleukin-6 in cardiac myxoma with mediastinal lymphadenopathy. 2010; 34 (1): 31–38. PMID: 1286228. doi: 10.2169/internalmedicine.31.1207.
30. *Guhathakurta S, Riordan JP.* Surgical treatment of right atrial myxoma. *Texas Hear Inst J*. 2000; 27 (1): 61–63. PMID: 10830633.
31. *Samdarshi TE et al*. Transesophageal echocardiographic diagnosis of multicentric left ventricular myxomas mimicking a left atrial tumor. *J Thorac Cardiovasc Surg*. American Association for Thoracic Surgery, 1992; 103 (3): 471–474. PMID: 1545546.
32. *Turhan S et al*. Second recurrence of familial cardiac myxomas in atypical locations. *Can J Cardiol*. Elsevier, 2008; 24 (9): 715–716. PMID: 18787723. doi: 10.1016/s0828-282x(08)70671-8.
33. *Perek B et al*. Early and long-term outcome of surgery for cardiac myxoma: Experience of a single cardiac surgical centre. *Kardiol Pol*. 2011; 69 (6): 558–564. PMID: 21678290.

The article was submitted to the journal on 2.08.2021

INSTRUCTIONS TO AUTHORS

Articles should contain original information that has not been previously published and is not considered for publication in other editions. Fee for publication of manuscripts will not be charged.

The manuscript should be presented in Microsoft Word format A4, 1.5 spacing, and Times New Roman font size 12. Submit your article to the online submission system in accordance with the instructions on the journal's website https://journal.transpl.ru.

Structure of the article

The Title page should include:

- Initials (first name and patronymic) of the authors of the article should be specified before their respective last names.
- Full official name of the institution, city and country.
- If authors from different institutions participated in writing of the manuscript, it is necessary to correlate those with the names of the authors by adding a digital index uppercase after last name, and right before the name of the institution.

Information about the authors

For each author fully specify the last and the first name, patronymic and position in the relevant department/institution.

For correspondence

Fully specify the last and the first name, patronymic of the author, who will be holding correspondence, address (including postal code), telephone, fax number, e-mail.

Abstract

Each article must be accompanied by an abstract. The amount of text for the abstract of the original article should be of no more than 300 words, for a literature review, clinical observation – no more than 200 words. The abstract must fully comply with the content of the work. The abstract should not use abbreviations without prior expansion.

Abstract of ***the original article*** should contain the following sections: ***Objective***, ***Materials and methods***, ***Results***, ***Conclusion***. The abstract should present the most important results of the research.

Do not write: "*A comparative analysis of the sensitivity and specificity was conducted …*"

Should write: "*The sensitivity was ... % and ...%, p = , specificity, respectively ...% and ...%, p =* ".

Keywords

At the end of the abstract keywords must be given. To select the keywords a thesaurus of U.S. National Library of Medicine should be used – Medical Subject Headings (MeSH) at http://www.ncbi.nlm.nih.gov/mesh.

Conflict of interest

The author should inform the editor about the factual or potential conflict of interest have included the information about such conflict into the respective section of an article.

If there is no conflict of interest, the author should say so in the form like the following: "Author declares unawareness of the conflict of interest".

This information is supposed to be placed before the article text.

Text of article

Original article should include the following sections:

- Introduction
- Materials and methods
- Results
- Discussion
- Conclusion
- References

Review article should include an analysis of the literature with the presentation of modern sources (mainly in the last 5 years).

Clinical observation should be well illustrated (to reflect the essence of the problem) and include discussion with the use of literature data.

References in the text are indicated by number in square brackets: [1], [2, 5], [14–18] and ***in the references section are presented in order of their appearance in the text.*** All values given in the article should be expressed or duplicated in **SI** units.

References

The author is solely responsible for the accuracy of the data included in the references section of the article. References to unpublished papers or papers in print works are not allowed.

References are presented on a separate page.

The names of journals can be contracted in accordance with an embodiment of reduction adopted by the specific journal.

If the article quoted has DOI (a digital object identifier) or/and PMID (Pub Med identifier) they must be specified after the description of the article. To compile descriptions in References section NLM bibliographic reference citation standard is used – U.S. National Lib-

rary of Medicine (http://www.nlm.nih.gov/bsd/uniform_requirements.html). If the number of authors does not exceed 6, the bibliographic description includes all the authors. If the number of authors is more, only the first six authors should be indicated and then add et al.

Requirements for tables and figures

Tables should be placed into the text; they should have numbered heading and clearly labeled graphs, convenient and simple to read. Table's data must comply with the numbers in the text, but should not duplicate the information therein. Table references in the text are required.

Illustrations and drawings should be submitted in electronic format (JPEG or TIFF format with a resolution of at least 300 dpi and no smaller than 6 × 9 cm), in a volume of close to 1 MB. Drawings must include all copyright symbols – arrows, numbers, signs, etc. Figure captions should be submitted in a separate file with the extension *.doc. First, the name is given, then all arithmetic and alphabetical symbols (lettering) are explained.

Articles should be addressed to the Editor at:
Russian Journal of Transplantology and Artificial Organs
Shumakov National Medical Research Center of Transplantology and Artificial Organs
1, Shchukinskaya ul., Moscow 123182, Russian Federation
E-mail: **vestniktranspl@gmail.com**

Издание зарегистрировано в Госкомпечати РФ, № 018616 от 23.03.99 г.

Подписано к печати 30.12.21.

Тираж 1000 экз.

ООО «Издательство «Триада».
ИД № 06059 от 16.10.01 г.
170034, г. Тверь, пр. Чайковского, 9, оф. 514,
тел./факс: (4822) 42-90-22, 35-41-30
E-mail: triadatver@yandex.ru
http://www.triada.tver.ru

Отпечатано в ООО «Тверская фабрика печати».
170006, г. Тверь, Беляковский пер., 46.

Заказ 0072